Characterization of an associated protein kinase of the BMP type II receptor

im Fachbereich Biologie, Chemie, Pharmazie
der Freien Universität Berlin eingereichte Dissertation

vorgelegt von Raphaela Schwappacher

Berlin 2008

Characterization of an associated protein kinase of the BMP type II receptor

im Fachbereich Biologie, Chemie, Pharmazie
der Freien Universität Berlin eingereichte Dissertation

vorgelegt von Raphaela Schwappacher

Berlin 2008

1. Gutachter: Prof. Dr. Petra Knaus

2. Gutachter: Prof. Dr. Otmar Huber

Promotionskolloquium: 17. Oktober 2008

Meinen Eltern

Table of Contents

1 Introduction 1

1.1 Signal transduction via cytokines of the transforming growth factor β (TGFβ) superfamily... 1

1.2 Bone Morphogenetic Proteins (BMPs) 4

1.2.1 Ligand synthesis, structure and functions of BMP 4

1.2.2 BMP/receptor binding 7

1.2.3 Regulation of BMPs 8

1.3 BMP receptors 12

1.3.1 Receptor structure, activation and function 13

1.3.2 Receptor oligomerization and localization 16

1.3.3 Co-receptors of BMP signaling 18

1.3.4 Intracellular regulatory proteins of the receptors 19

1.4 Smad pathway 23

1.4.1 Smad structure, regulation and modification 23

1.4.2 Smad nucleocytoplasmic shuttling 32

1.4.3 Smad transcriptional complexes and Smad-dependent transcription 33

1.5 Non-Smad signaling 37

1.6 BMP signaling in cell- and tissue-specific context 39

1.7 Diseases related to BMP signaling and its components 44

1.8 Nitric oxide (NO)/ cyclic guanosine 3',5'- monophosphate (cGMP) signal transduction via cGMP-dependent protein kinases 48

1.9 NO synthases and NO 48

1.10 cGMP and its effectors 50

1.10.1 Generation and degradation of cGMP and target molecules of cGMP 50

1.11 cGMP-dependent protein kinases 55

1.11.1 cGMP-dependent protein kinase I (cGKI): Structure, activation and regulation 55

1.11.2 Target proteins regulated by NO/cGMP/cGKI and the phyiological role 60

1.11.3 Genes regulated by NO/cGMP/cGKI signaling and their physiological role 65

1.11.4 cGMP-dependent protein kinase II (cGKII):Structure, activation and regulation 69

1.12 cGMP signaling in health and disease 71

1.13 Aim of the project 73

2 Material and solutions 74

2.1 Chemicals and materials 74

2.2 Technical devices 75

2.3 Kits 76

2.4 Enzymes and substrates 77

2.4.1 Kinases 77

2.4.2 Restriction endonucleases 77

2.4.3 DNA- and RNA-modifying enzymes 77

2.4.4 Substrates ... 77
2.5 Oligonucleotides ... 78
2.6 Standards ... 78
2.6.1 DNA standards ... 78
2.6.2 Protein standards ... 78
2.7 Bacterial strains ... 79
2.8 Expression vectors ... 80
2.8.1 Prokaryotic expression vectors ... 80
2.8.2 Eukaryotic expression vectors ... 81
2.9 Constructs ... 83
2.9.1 Prokaryotic expression constructs ... 83
2.9.2 Eukaryotic expression constructs ... 83
2.10 Cell lines ... 85
2.11 Growth media and reagents for cell culture ... 85
2.12 Growth factors ... 87
2.13 Antibodies ... 87
2.13.1 Primary antibodies ... 87
2.13.2 Secondary antibodies ... 89

3 Methods ... 91
3.1 Microbiological methods ... 91
3.1.1 Sterilization and disinfection ... 91
3.1.2 Bacterial growth media ... 92
3.1.3 Cultivation and conservation of *E. coli* strains ... 93
3.1.4 Preparation of competent *E. coli* strains ... 93
3.1.5 Transformation of competent *E. coli* strains ... 95
3.2 Molecular biological methods ... 96
3.2.1 Amplification and isolation of plasmid DNA from transformed bacteria ... 96
3.2.2 Determination of nucleic acid concentrations ... 96
3.2.3 Sequencing of DNA ... 97
3.2.4 Digestion of DNA via restriction endonucleases ... 97
3.2.5 Isolation of RNA and semi-quantitative polymerase chain reaction ... 97
3.2.6 Agarose gelelectrophoresis ... 99
3.2.7 Knockdown of gene expression via shRNA ... 100
3.2.8 Chromatin immunoprecipitation ... 101
3.3 Cell biological methods ... 102
3.3.1 Cultivation and cryo-conservation of cells ... 102
3.3.2 Determination of cell number ... 103
3.3.3 Transfection of eukaryotic cells ... 103
3.3.4 Determination of transfection efficiency ... 108
3.3.5 Treatment of cells with growth factors and protein activators/inhibitors ... 109
3.3.6 Cellular assays for BMP-2 functionality ... 109

3.3.7 Immunofluorescence microscopy ... 114
3.3.8 Analysis of subcellular protein localization ... 116
3.3.9 *in vivo* kinase assay ... 119
3.3.10 Proliferation assay ... 119
3.4 Protein chemical methods ... 120
3.4.1 Amplification and purification of recombinant proteins ... 120
3.4.2 *in vitro* kinase assay ... 121
3.4.3 Preparation of cell lysates ... 122
3.4.4 Determination of protein content using BCA assay (according to Redinbaugh) ... 123
3.4.5 Precipitation of proteins using TCA/acetone ... 124
3.4.6 Covalent antibody linking to sepharose ... 124
3.4.7 Protein pulldown via GST-fused bait proteins ... 125
3.4.8 *in vitro* binding ... 126
3.4.9 Co-immunoprecipitation ... 127
3.4.10 SDS polyacrylamide gelelectrophoresis ... 128
3.4.11 Coomassie-G stain of proteins ... 129
3.4.12 Western blot and detection of proteins via enhanced chemiluminescence ... 130

4 Results ... 133
4.1 Characterization of cGKI/BRII interaction ... 133
4.1.1 Identification of cGKI as BRII-associated protein ... 133
4.1.2 Mapping of BRII and cGKI interaction sites ... 136
4.1.3 Impact of cGKI association on BRII ... 141
4.1.4 Influence of BMP-2 on BRII/cGKI interaction ... 146
4.1.5 Subcellular distribution of cGKI upon stimulation with BMP-2 and 8-Br-cGMP ... 147
4.2 Interaction of cGKI with BRI ... 149
4.3 Characterization of cGKI/Smad interaction ... 150
4.3.1 Interaction of cGKI with R-Smad1 and 5 ... 151
4.3.2 Mapping of cGKI and Smad1 interaction sites ... 153
4.3.3 Association with co-Smad4 ... 154
4.3.4 Mapping of cGKI and Smad4 interaction sites ... 155
4.3.5 Interaction of cGKI on Smads in different cellular compartments ... 156
4.4 Functional relevance of cGKI for BMP-2-induced Smad pathway ... 161
4.4.1 Effect of cGKI knockdown on R-Smad phosphorylation ... 161
4.4.2 Effect of cGKI expression and activation on R-Smad phosphorylation ... 164
4.4.3 Effect of cGKI on Smad1 *in vitro* ... 166
4.4.4 Effect of cGKI knockdown on BMP-2-induced nuclear translocation of R-Smads ... 167
4.4.5 Effect of cGKI knockdown on the activity of a BMP-2-responsive reporter gene ... 169
4.4.6 Effect of cGKI expression on the activity of a BMP-2-responsive reporter gene ... 171
4.4.7 Effect of overexpression of cGKI on *Id1* expression ... 172
4.4.8 Effect of cGKI activation on the activity on the BMP target gene expression ... 173

4.4.9 Effect of a cGKI NLS mutant on R-Smad phosphorylation and on the activity of a BMP-responsive reporter gene ... 174
4.5 Functional relevance of cGKI for BMP-2-induced non-Smad pathway ... 177
4.5.1 Effect of cGKI on p38-MAPK phosphorylation ... 177
4.5.2 Effect of cGKI expression on alkaline phosphatase expression/activation ... 178
4.6 Relevance of cGKI/TFII-I association for BMP-2-induced Smad pathway ... 179
4.6.1 Characterization of TFII-I/Smad interaction ... 179
4.6.2 Subcellular distribution and co-localization of TFII-I and R-Smad1 ... 181
4.6.3 Effect of TFII-I expression on the activity of a BMP-2-responsive reporter gene ... 183
4.7 Impact of BMP-2 signaling on the expression of cGKI and TFII-I ... 186
4.8 Integration of cGKI in defective BMP signaling caused by a pulmonary hypertension mutant of BRII ... 187
4.8.1 Effect of cGKI expression on signaling arising from PAH BRII mutants ... 187
4.8.2 Effect of cGKI and PAH BRII mutants on the proliferation of VSMCs ... 189

5 Discussion ... 192
5.1 Interaction of cGKI with BMP receptors and cGKI-mediated modulation of the receptor complex ... 192
5.2 Interaction of cGKI with Smad proteins and impact of cGKI on BMP/Smad signaling ... 197
5.3 Evidence for cGKI/TFII-I cooperation in BMP-2-induced Smad pathway ... 207
5.4 The impact of cGKI in the non-Smad pathway ... 211
5.5 Integration of cGMP/cGKI signaling into pulmonary arterial hypertension caused by BRII mutants ... 213
5.6 Current model of the impact of cGKI on Smad BMP signaling ... 215

6 Summary - Zusammenfassung ... 217

7 Other projects ... 219
7.1 Impact of different GDF-5 mutants on GDF-5-induced signaling ... 219
7.2 Impact of the phosphatase PP2A as a Smad linker phosphatase on BMP-2-induced signaling pathways ... 220

8 References ... 221

9 Appendix ... 244
Abbreviations ... 244
Sequences ... 247
Acknowledgement - Danksagung ... 250
Curriculum vitae - Lebenslauf ... 251
Publication list - Schriftenverzeichnis ... 252
Declaration - Erklärung ... 254

Index of Figures

Figure 1.1 Protein components of the TGFβ superfamily.. 2
Figure 1.2 Schematic presentation of the most common combinatorial binding modes of TGFβ receptors which determine the signaling response and the canonical Smad pathway initiated by TGFβ growth factors. 3
Figure 1.3 Butterfly-shape of BMP-2 (Ribbon model). 5
Figure 1.4 View of BMP-2 along the two-fold axis (Ribbon model) 7
Figure 1.5 The different oligomerization modes of the BMP receptors.. 17
Figure 1.6 The interactome of the BMP receptor complex at the cell surface.. 23
Figure 1.7 Structure of the Smad protein. 25
Figure 1.8 The linker region of Smad1/5/8. 27
Figure 1.9 A Smad transcriptional complex at the DNA 34
Figure 1.10 Non-Smad signaling activated by BMP 39
Figure 1.11 PAH exhibits characteristic histological features. 44
Figure 1.12 Extensive heterotropic bone formation of the back of a FOP patient 46
Figure 1.13 The conversion from GTP to cGMP 50
Figure 1.14 Structural and functional characteristics of homodimeric cGKI 56
Figure 1.15 Associated proteins and substrates of cGKI 65
Figure 1.16 Genes controlled by cGMP signaling and the cellular outcome. 69
Figure 4.1 Identification of cGKI as a BRII-tail-associated protein 133
Figure 4.2 Protein sequence analysis of murine cGKI isoforms.. 134
Figure 4.3 Interaction of cGKI isoforms with BRII-LF 135
Figure 4.4 Endogenous binding of cGKI and BRII. 135
Figure 4.5 Co-localization of cGKIβ and BRII. 136
Figure 4.6 Mapping of cGKIβ binding site on BRII.. 137
Figure 4.7 Analysis of the protein amount and purity of recombinant BRII GST fusion proteins and MBP-cGKIβ. 138
Figure 4.8 Interaction of cGKI isoforms and BRII in a pulldown analysis. 139
Figure 4.9 *In vitro* binding of cGKIβ and BRII-tail in a pulldown analysis. 140
Figure 4.10 Mapping of BRII-LF binding site on cGKI. 141
Figure 4.11 Interaction of cGKIβ-D516A, a kinase-dead mutant, with BRII-LF. 142
Figure 4.12 Phosphorylation study of cGKI and BRII-SF or BRII-tail *in vitro*. 143
Figure 4.13 Phosphorylation study of cGKI and BRII-SF or BRII-SF-K230R *in vitro*. 144
Figure 4.14 Phosphorylation study of cGKIβ and BRII *in vivo*. 145
Figure 4.15 Interaction of cGKIβ and BRII-LF upon BMP-2 stimulation. 146
Figure 4.16 Localization of cGKI in C2C12 cells after treatment with 8-Br-cGMP or BMP-2 147
Figure 4.17 Analysis of the subcellular distribution of cGKIβ in HEK293T cells 148
Figure 4.18 Interaction of endogenous cGKI with BRII and BRIa in C2C12 cells. 149
Figure 4.19 Interaction of cGKIβ and BRIb after stimulation with BMP-2. 150
Figure 4.20 Interaction of cGKI isoforms with Smad1 151
Figure 4.21 Interaction of cGKIβ and BMP R-Smads upon BMP-2 stimulation 152
Figure 4.22 Mapping of the Smad1 binding site on cGKI. 153
Figure 4.23 Interaction of cGKIβ with co-Smad4 154
Figure 4.24 Mapping of the Smad4 binding site on cGKI. 155
Figure 4.25 Interaction of endogenous cGKI and BMP R-Smads in C2C12 cells in different cellular compartments 156
Figure 4.26 Co-localization of endogenous cGKI and Smad1 or co-Smad4 in C2C12 cells after BMP-2 stimulation. 158
Figure 4.27 Binding of endogenous cGKI and Smad1 to the *Id1* promoter in BMP-2-treated C2C12 cells 159

Figure 4.28 BMP-2-induced co-localization of endogenous cGKI and Smad1 at the *Id1* promoter in C2C12 cells. 160
Figure 4.29 Analysis of the protein knockdown of endogenous cGKI in C2C12 cells using a cGKI-specific shRNA 161
Figure 4.30 Phosphorylation study of BMP R-Smads in C2C12 cells after cGKI knockdown 162
Figure 4.31 Phosphorylation study of BRIa and R-Smads in C2C12 cells after cGKI knockdown 163
Figure 4.32 Phosphorylation study of Smad1 *in vivo* under the influence of cGKIβ variants 164
Figure 4.33 Phosphorylation study of Smad1/5/8 and VASP in C2C12 cells upon stimulation with 8-Br-cGMP 165
Figure 4.34 Analysis of protein amount and purity of recombinant Smad1 MBP fusion protein 166
Figure 4.35 Phosphorylation study of cGKI and Smad1 *in vitro* 167
Figure 4.36 Nuclear translocation study of Smad1 in cGKI knockdown C2C12 cells 168
Figure 4.37 Endogenous complex formation of Smad1/co-Smad4 upon BMP-2 stimulation in cGKI knockdown C2C12 cells. 168
Figure 4.38 Effect of cGKI knockdown on the BMP-2-induced transcriptional activity in C2C12 cells using the *BRE*-luciferase reporter gene 170
Figure 4.39 Effect of cGKI variants on the BMP-2-induced transcriptional activity in C2C12 cells using the *BRE* luciferase reporter gene 171
Figure 4.40 Effect of cGKIβ on the expression of *Id1* 172
Figure 4.41 Effect of 8-Br-cGMP on the BMP target gene activity in C2C12 cells using an Id1 expression assay and the *BRE* luciferase reporter gene 173
Figure 4.42 Phosphorylation study of Smad1 *in vivo* under the influence of cGKI variants 175
Figure 4.43 Effect of cGKI variants on the BMP-2-induced transcriptional activity in C2C12 cells using the *BRE* luciferase reporter gene 176
Figure 4.44 Phosphorylation study of p38-MAPK *in vivo* under the influence of cGKI 177
Figure 4.45 Analysis of ALP expression and activation in C2C12 cells under the influence of cGKI 178
Figure 4.46 Interaction of endogenous TFII-I with cGKIβ and Smads in C2C12 cells 180
Figure 4.47 Interaction of TFII-I and Smad1 upon BMP-2 stimulation 181
Figure 4.48 Co-localization of TFII-I and Smad1 in BMP-2-induced C2C12 cells 182
Figure 4.49 Co-localization of endogenous TFII-I and Smad1 at the *Id1* promoter C2C12 cells after BMP-2 stimulation 183
Figure 4.50 Effect of TFII-I on the BMP-2-induced transcriptional activity in C2C12 cells using the *BRE*-luciferase reporter gene 184
Figure 4.51 Effect of TFII-I and cGKIβ variants on the BMP-2-induced transcriptional activity in C2C12 cells using the *BRE*-luciferase reporter gene. 185
Figure 4.52 Effect of BMP-2 signaling on the expression of *cGKI* and *TFII-I* in C2C12 cells 186
Figure 4.53 Effect of cGKI on the BMP-2-induced transcriptional activity triggered by a PAH BRII mutant using the *BRE*-luciferase reporter gene 188
Figure 4.54 Summary of the activating effect of cGKI variant on signaling induced by different BRII PAH mutants 189
Figure 4.55 Proliferation study of VSMCs expressing a BRII PAH mutant and cGKI upon stimulation with PDGF 190
Figure 5.1 Phosphorylation of BRII-tail by cGKI 195
Figure 5.2 Dissociation of cGKI from BRII upon BMP-2 stimulation 197
Figure 5.3 Redistribution of cGKI/Smad complexes to the nucleus and binding of cGKI and Smad1 to the promoter region of the BMP target gene *Id1* after BMP-2 stimulation 203
Figure 5.4 Schema of TFII-I action in a resting cell 208
Figure 5.5 BMP-induced complex formation of activated Smads, cGKI and TFII-I at the *Id1* promoter 209
Figure 5.6 Schema of the structure of TFII-I 210

Figure 5.7 Possible effects of cGKI on BMP signaling caused by PAH BRII mutants 214
Figure 5.8 The dual role of cGKI in BMP signaling 216

Index of Tables

Table 1.1 The BMP ligands and their biological properties 6
Table 1.2 The BMP agonists and antagonists and their biological characteristics 10
Table 1.3 The BMP receptors and their biological properties. 13
Table 1.4 The Smad proteins and their biological properties 24
Table 1.5 The activating and inhibiting compounds for cGKs 57
Table 2.1 Manufacturer information about used chemicals and material. 75
Table 2.2 Information about used technical devices. 76
Table 2.3 Information about used prokaryotic expression constructs to generate recombinant proteins 83
Table 2.4 Information about eukaryotic expression constructs for overexpression studies in mammalian cells. 84
Table 2.5 Information about used primary antibodies. 89
Table 2.6 Information about used secondary antibodies. 90
Table 3.1 Information about cell numbers, transfection solution volumes and DNA amounts for calcium-phosphate transfection of HEK293T cells. 104
Table 3.2 Information about cell numbers, transfection solution volumes and DNA amounts for Lipofectamine™/2000 transfection of C2C12 cells. 105
Table 3.3 Information about cell numbers, transfection solution volumes and DNA amounts for PEI transfection of HEK293T cells and C2C12 cells 106
Table 3.4 Information about cell numbers, transfection solution volumes and DNA amounts for Fugene HD of VSMCs. 107
Table 3.5 Pre-treatment and ligand stimulation necessary for the cellular assays. 109
Table 3.6 Information about the DNA amounts of the reporter constructs used for reporter gene analysis in C2C12 cells. 112
Table 3.7 Information about the volume of lysis buffer used against the sown cell number 122
Table 3.8 Pipetting scheme for one mini gel for the Mini Protean gelelectrophoresis systems 128

1 Introduction

1.1 Signal transduction via cytokines of the transforming growth factor β (TGFβ) superfamily

Signaling of ligands of the transforming growth factor β (TGFβ) superfamily, a family of multifunctional cytokines, controls diverse cellular processes in the developing as well as in the adult organism - from worms and fruit fly to humans. TGFβ superfamily ligands regulate cell fate determination during the establishment of the body plan and tissue differentiation through controlling cell proliferation, differentiation, migration, adhesion and apoptosis. Dysfunctions in TGFβ signaling are involved in severe human diseases such as cancer and fibrosis, impaired wound-healing or hereditary disorders as pulmonary arterial hypertension. The TGFβ superfamily ligands are divided into two branches, the TGFβ/Activin/Nodal subfamily and the Bone Morphogenetic Protein (BMP)/Growth and Differentiation Factor (GDF)/anti-Muellerian Hormone (AMH) subfamily. Up to now more than 60 members have been identified. Signaling specificity is not only accomplished by the diversity of the ligands, but also through combinatorial binding of the ligands to specific receptors. These receptors can match and mix as homo- and heteromeric receptor complexes differing in their affinities for the ligands which increase the signaling complexity. More signaling diversity is achieved by receptor-mediated activation of different intracellular signaling effectors, the Smads. The diverse TGFβ superfamily ligands, receptors and receptor-regulated intracellular mediators are displayed in **Figure 1.1**:

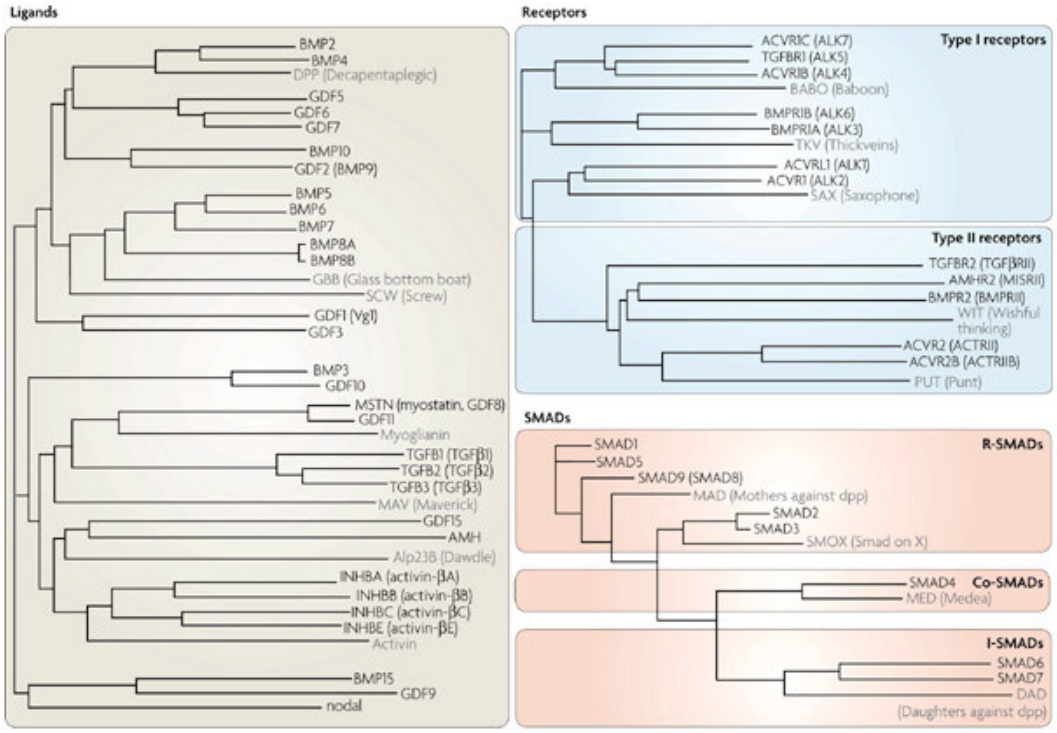

Figure 1.1 Protein components of the TGFβ superfamily. Phylogenetic trees received from protein alignment of the mature proteins of TGFβ superfamily ligands, receptors and Smads in humans and *Drosophila melanogaster*. Human proteins are depicted in black, *Drosophila* proteins in grey. The proteins are denoted with synonymical names in parenthesis. BMP, bone morphogenetic protein; GDF, growth and differentiation factor; TGFβ, transforming growth factor β; INHB, Inhibin; ACVR, Activin receptor; ALK, Activin receptor-like kinase; AMHR, AMH receptor; BMPR, BMP receptor; TGFBR, TGFβ receptor; R-Smad, receptor-regulated Smad; I-Smad, inhibitory Smad [1].

At least 30 genes for TGFβ ligands are encodes by the human genome, including three TGFβ isoforms, four Activin β-chains (correspond to the monomers), Nodal, ten BMP proteins and eleven GDFs [1-3]. The TGFβ cytokines have a common characteristic; they form homo- and heterodimers which are stabilized by disulfide bridging and hydrophobic interaction. The receptors are divided into type I and type II receptor, which are encoded by five and seven genes in humans, respectively. The receptors bear an extracellular domain, a single-pass transmembrane region and a conserved intracellular serine/threonine kinase domain. Downstream of the receptors, three functional classes of Smad proteins can be distinguished: receptor-regulated Smads (R-Smads), inhibitory Smads (I-Smads) and common mediator Smad (co-Smad) [1-3]. **Figure 1.2** illustrates the different signal responses resulting from receptor mixing and matching and shows the classical signaling pathway of TGFβ cytokines:

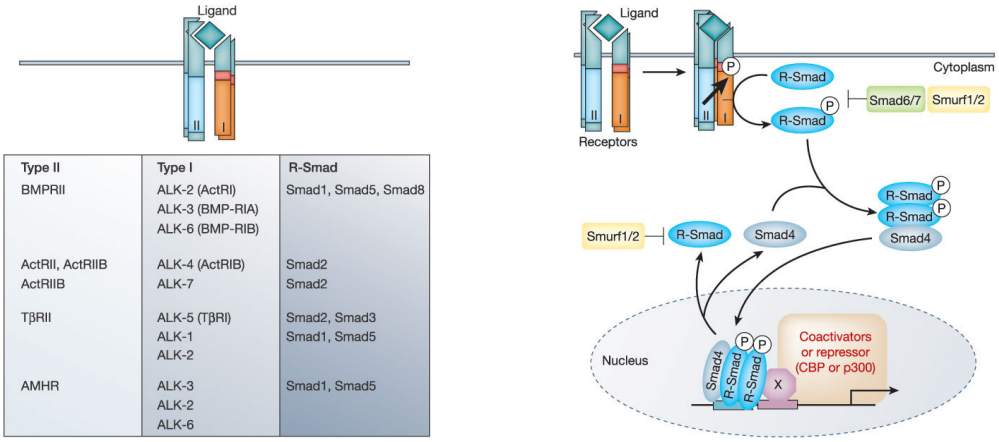

Figure 1.2 Schematic presentation of (left) the most common combinatorial binding modes of TGFβ receptors which determine the signaling response and (right) the canonical Smad pathway initiated by TGFβ growth factors. (Left) The combinatorial interactions of type II and type I receptors define the activation of specific subsets of R-Smads, TGFβ/Activin R-Smads, Smad2 and 3, and the BMP/GDF/AMH R-Smads, Smad1, 5 and 8. **(Right)** TGFβ signaling starts after binding of the ligand to a heterotetrameric type I/type II receptor complex at the cell surface. Activated receptors transduce the signal to the intracellular Smad proteins, which, after phosphorylation, hetero-oligomerize with co-Smad4 to migrate to the nucleus. After binding of the Smads to specific DNA sequences and assembly of a transcriptional complex, target gene transcription is controlled. Inhibition of the pathway occurs via inhibitory Smads (I-Smads) and the Smad ubiquitination regulatory factors (Smurfs), which are E3 ubiquitin ligases and recruited via I-Smads [4].

The members of the TGFβ superfamliy ligands bind with high specificity to a set of type I and type II transmembrane serine/threonine kinase receptors. The diverse heterotetrameric receptor complexes get activated through ligand binding and the signal is propagated by phosphorylation of specific intracellular messenger molecules, the Smad proteins. The Smads mediate signal transduction between the cytoplasm and the nucleus. After heteromeric complex formation of R-Smads and the co-Smad4, the activated Smad complexes translocate into the nucleus to regulate target gene transcription in cooperation with other nuclear co-factors.

BMPs were originally identified by their ability to induce ectopic bone and cartilage formation at extraskeletal sites *in vivo* [5]. The most important BMP, BMP-2, was cloned in 1988 by Wozney and co-workers [6]. Nowadays it is known, that BMPs regulate a plethora of cellular processes in embryonic and mature tissue. BMPs are synthesized in skeletal cells to regulate bone and joint homeostasis [7, 8]. BMP ligands also exhibit extraskeletal functions by directing mesenchymal stem cells to chondrogenic and osteoblastic lineage and furthermore, by functioning disparately in the stem cell biology of embryonic stem cells compared to neural crest stem cells [7, 9]. Moreover, in development BMPs are essential for dorsoventral patterning of the embryo [10]. The signal transduction of BMP ligands is strictly regulated at each step

of the signaling cascade - like for other TGFβ ligands - starting from availability of the extracellular ligand up to the nuclear factors regulating the transcriptional response. The importance of this precise regulation is reflected by the appearance of developmental disorders and dysfunctions in vertebrates and humans such as severe bone and cartilage diseases, cancer or vascular disorders as arterial pulmonary hypertension, in which specific components of the BMP pathway are defective [11-13].

1.2 Bone Morphogenetic Proteins (BMPs)

1.2.1 Ligand synthesis, structure and functions of BMP

Like all TGFβ-related growth factors, BMP is secreated as a large precursor protein. An N-terminal signal sequence marks the protein for the secretory path. The prodomain in the N-terminus is responsible for the right folding and activity of the signaling molecule. It is cleaved off after the sequence -R-X-X-R- by proprotein convertases such as furin, as shown for BMP-4 [14, 15]. An additional cleavage of BMP-4 at a non-consensus furin site positively regulates the activity and signaling range of the mature protein [16, 17]. However, the C-terminal mature protein (110-140 aa) is released and forms after dimerization the active signaling molecule. Normally, the monomers homodimerize, but also heterodimerization of different BMP proteins is known. Heterodimers of BMP-4/BMP-7 and BMP-2/BMP-7 are even more potent than the homomeric protein in inducing cartligage and bone *in vivo* [18, 19]. Furthermore, heteromeric BMP-4/BMP-7 has a strong ventralizing ability in *Xenopus* [20, 21]. In 2003, Butler and Dodd reported that BMP-7/GDF-7 heterodimers regulate the trajectory of commissural axons *in vivo* more efficiently than BMP-7 homodimers [22]. Additionally, an approach with “heteromeric” BMP-2, i.e. wildtype BMP-2 paired with BMP-2 mutated in the receptor binding sites, resulted in impaired BMP signaling [23].

The crystal structure of human mature BMP-2 was resolved by X-ray analysis at 2.7 Å resolution [24] (**Figure 1.3**).

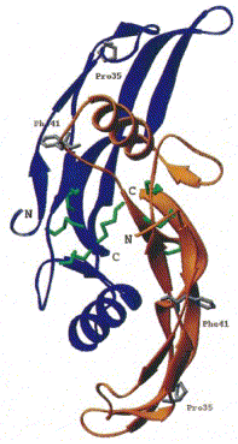

Figure 1.3 Butterfly-shape of BMP-2 (Ribbon model) [24]. Dimeric BMP-2 is formed by two monomers (coloured in blue and orange). The cysteine bridge connecting the monomers is depicted in green.

The dimensions of the dimer are 70 Å x 35 Å x 30 Å [24], and each monomer contains a cysteine-knot motif, characteristic for the so-called cysteine-knot growth factor family. This family includes besides the TGFβ superfamily ligands also the platelet-derived growth factor (PDGF) and nerve growth factor (NGF) [25]. The cystine-knot in BMP-2, highly conserved among TGFβ family members, is built by six cysteines which form three intramolecular bridges; four of these cysteine residues shape an eight-membered macrocycle which is wide enough that a disulfide bridge formed by the two other cysteines can pass through. This rigid cystine-knot scaffold is necessary to stabilize the entire structure of the BMP-2 dimer. A seventh cysteine builds an intermolecular disulfide bridge connecting the monomers and further stabilizing the dimer [24].

Up to now ten BMPs are identified with different functions in the adult organism and during development. The expression patterns of the BMP ligands in the embryo as well as in the adult organism already give an idea of their physiological function. BMP-2 is strongly expressed in embryonal limb buds, heart whisker follicle cells, tooth buds as well as in diverse cells in the adult such as mesenchymal cells and osteoblasts. Expression of BMP-4 is found in the dorsal centre of the embryo, in the embryonic limbs and the heart as well as in adult osteoblastic cells. BMP7- is also highly epressed in the dorsal centre of the embryo as well as in adult eye, epidermal and kidney tissue, and the limbs. Several studies on *bmp* knockout mice allow to learn more about the role of BMPs in early development. *bmp-2*-deficient mice have amnion/chorion abnormalities and defects in cardiac development and die during

embryonic development [26]. Genetic ablation of *bmp-4* in mice lead to malfunctions in extraembryonic and mesoderm formation; this knockout is also lethal in an early embryonic stage [27]. A null mutation in the *bmp-7* gene resulted in polydactyly and skeletal and eye defects; the mice die shortly after birth [28, 29]. These studies explored that BMPs have a broader range of biological activities.

Table 1.1 depicts the so far known BMP ligands, their nature and functions:

name/ synonym	**function**	**bound receptors**	**knockout mouse and phenotypical abnormalities**
BMP-2 [6, 30-32] BMP2a	key role in embryogenesis; induction of osteogenesis; ventralizing factor	BRIa, BRIb, ActRI; BRII, ActRII, ActRIIB	*bmp-2*$^{-/-}$: early embryonic lethality due to defects amnion and heart development [26]
BMP-3 [6, 33-35] osteogenin	inhibitor of BMPs dorsalizing factor [36, 37]	unknown	*bmp-3*$^{-/-}$: increase in bone mineral density and in trabecular bone volume [38]
BMP-4 [39-42] BMP-2b	ventralizing factor; neuragenesis and orgaanogenesis	BRIa, BRIb, ActRI; BRII, ActRII, ActRIIB	*bmp-4*$^{-/-}$: early embryonic lethality due to defects in gastrulation and mesoderm formation [27] *bmp-4*$^{+/-}$: defects in craniofacial, eye, kidney and limb development [43] *bmp-4*$^{+/-}$*/bmp-7*$^{+/-}$: defects in rib cage and distal parts of the ribs [44]
BMP-5 [45, 46]	skeletogenesis	unknown	*bmp-5*$^{-/-}$: recessive *short ear* mouse; abnormalities in skull and axial parts of the skeleton; lung, liver, uterus, bladder and intestine tissue anomalies [46-48] *bmp-5*$^{-/-}$*/gdf-5*$^{-/-}$: abnormal formation of the sternum and the connecting joints to the ribs [49]
BMP-6 [30, 50] vegetal related-1	proliferation and differentiation of the epidermis; osteogenesis	BRIa, BRIb, ActRI; BRII, ActRII	*bmp-6*$^{-/-}$: mild phenotype with defects in sternum ossification [51] *bmp-6*$^{-/-}$: impaired growth plate function [52] *transgenic* (keratin-10 promoter): severe repression of cell proliferation in embryonic and perinatal epidermis [53]
BMP-7 [54-56] osteogenic protein-1 (OP-1)	ventralizing factor; embryonic organ development	BRIa, BRIb, ActRI; BRII, ActRII, ActRIIB	*bmp-7*$^{-/-}$: die shortly after birth, show renal failure and defects in eye development, and polydaktyly [28, 29, 57]
BMP-8a [58, 59] osteogenic protein-2 (OP-2)	spermatogenesis and reproduction	unknown	*bmp-8a*$^{-/-}$: germ cell degeneration in male mice [59]
BMP-8b [60] osteogenic protein-3 (OP-3)	spermatogenesis and reproduction	unknown	*bmp-8b*$^{-/-}$: germ cells show defects in proliferation and apoptosis [60]
BMP-10 [61, 62]	cardiac development	ALK1	*bmp-10*$^{-/-}$: dramatic reduction in proliferative activity in cardiomyocytes during embryogenesis [63]
BMP-15 [64-66]	growth and function of ovarian follicles	BRIa, BRIb, ActRI; BRII, ActRII	*bmp-15*$^{-/-}$: null mutation in this X-linked gene, female mice are subfertile with decreased ovulation and fertilization rates [67]

Table 1.1 The BMP ligands and their biological properties. The mammalian proteins are described. The information is based on [2, 68-70] and the indicated references. The non-listed BMPs are with the nowadays knowledge regrouped to the related GDF proteins (with alternative names). BMP-1 is a metalloproteinase that is unrelated to other BMPs and is described in chapter 1.2.3.

1.2.2 BMP/receptor binding

Ligand/receptor binding in the TGFβ superfamily is highly promiscuous since a large number of ligands binds to an accordingly small number of receptors. BMPs and GDFs bind with high affinity the type I receptor, and with low affinity the type II receptor. In the case of BMP-2/4, BMP-6 and BMP-7, the bound type I receptors are BRIa (ALK3), BRIb (ALK6) and Activin receptor type I (ActRI; ALK2). The recruited type II receptors are ActRII, ActRIIB or BRII [2, 71-76] (see Table 1.1). Furthermore, several co-receptors of BMP ligands are known, which will be discussed in chapter 1.3.3.

In 2000, Kirsch and co-workers resolved the crystal structure of dimeric BMP-2 in complex with the high-affinity BMP receptor type Ia [77]. The receptor binds to a distinct, but discontinous epitope of BMP-2 comprising residues from both BMP-2 monomers [77]. A second, juxtaposed epitope in the dimeric BMP-2 protein is involved in binding of BRII and is constituted by residues of only one monomer [78]. Homomeric BMP-2 has a two-fold symmetry resulting in two pairs of epitope 1 and 2. Not only two type I receptor chains (BRIa), but also two type II receptor ones (ActRII) are found in a ternary crystallized receptor complex around BMP-2. However, no contacts exist between the single extracellular receptor domains [77, 79]. TGFβ superfamily ligands can be compared to an open hand [80], with the central α-helix (α3) at the wrist of the hand, two aligned two-stranded β-sheets as the fingers and the N-terminal segment at the position of the thumb. Due to their location within the BMP-2 molecule, the type I receptor binding epitope is called the “wrist epitope” and the binding interface for the type II receptor “knuckle epitope” [78] (**Figure 1.4**):

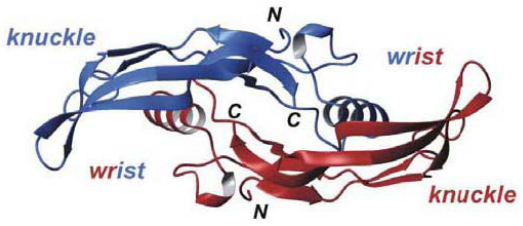

Figure 1.4 View of BMP-2 along the two-fold axis (Ribbon model) [78]. The location of the specific receptor binding interfaces inside the BMP-2 dimer (monomers coloured in blue and red) is shown. The “wrist epitope” binds the BMP type I receptor with high-affinity, whereas the “knuckle epitope” is the low-affinity binding site for the BMP type II receptor.

Both epitopes are hydrophobic. Ten hydrogen bonds are formed in one BRIa/BMP-2 interface. One main chain hydrogen bond (Leu51 in BMP-2 to Gln86 in BRIa) is a hot spot in ligand/receptor recognition. Leu51 is invariant inside the BMP subfamilies; thus, this residue probably plays a very important role in the type I receptor specificity of the ligand [81]. Hydrophobic interactions dominate in low-affinity binding of BMP-2, i.e. the binding of the ligand to type II receptors. Interestingly, a hydrogen bond in the ligand/receptor interface of the BMP-2/ActRII complex can be mutationally activated which resulted in a BMP-2 variant with high-affinity for ActRIIb [82]. All up to now performed studies hint towards that signaling specificity is not only achieved by ligand/receptor pair identity, but also by the mode of cooperative assembly of receptors and ligands in a membrane-restricted manner [79].

1.2.3 Regulation of BMPs

It was found in *Xenopus* and *Drosophila* that during embryogenesis an activity gradient of BMPs is formed which influences dorsal-ventral axis formation of the embryo and thus cell fate determination. The BMP proteins are so called morphogens since they spread from one region, the ventral centre of a *Xenopus* gastrula, and form a concentration gradient across the developing embryo. The BMP morphogens are controlled by extracellular modulators. In *Xenopus* early embryos, several of these regulators are concentrated and secreted from the dorsal centre, the Spemann organizer, to inhibit the function of BMPs [68, 70]. Signals from the Spemann organizer can directly induce neural tissue from ectoderm and can dorsalize ventral mesoderm for muscle formation [83]. An increasing number of these BMP antagonists has been also identified in vertebrates; these proteins interfere with binding of the BMP ligand to its receptors and hence, with BMP-dependent developmental processes.

The antagonists exhibit a cystine-knot motif which are classed as the following: the Noggin/Chordin family (ten-membered cysteine ring), twisted gastrulation (nine-membered cysteine ring) and the DAN/Cerberus family (eight-membered cysteine ring) [84]. This motif is similar to the members of the TGFβ superfamily; thus, ligand and antagonist seem to have evolved from a common ancestral gene. In **Table 1.2** the so far known mammalian agonists and antagonists of

BMP signaling are listed, and in the following some of these are described in more detail.

name/ synonym	**function**	**bound ligands**	**knockout mouse and phenotypical abnormalities**
Noggin [85, 86]	antagonist; dorsalizing and neuralizing factor	BMP-2, -4, -5, -6, -7, GDF-5 and -6	*noggin*$^{-/-}$: lethal, shortened body axis, reduced size of somites and neural tube, malformed limb, excess of bone and cartilage [87, 88] *noggin*$^{-/-}$: retardation of fetal hair-follicle induction [89] transgenic (Msx2 promoter): defective postnatal hair development and limb abnormalities [90]
Chordin [91] short gastrulation (*Drosophila*)	antagonist; dorsalizing and neuralizing factor	BMP-2, -4, -7	*chordin*$^{-/-}$: defects of the inner and outer ear and in vascularization [91] *chordin*$^{-/-}$*noggin*$^{-/-}$: abnormal left to right patterning, disrupted mesoderm, failure of parts of the eyes, forebrain and facial structures [91]
Chordin-like-1 (CHL-1) [92, 93] neuralin-1, ventropin	antagonist	BMP-4, -5, -6	-
CHL-2 [94, 95]	antagonist	BMP-2, -4, -5, -6, -7, GDF-5	-
Follistatin [96]	antagonist	BMP-2, -4, -7, GDF-11; Activin	*follistatin*$^{-/-}$: lethal, reduced size, skeletal anomalities, defects in whisker and tooth development;shiny, taut skin [97]
Follistatin-related proteins (FSRPs) [98]	antagonist	BMP-2, -6, -7; Activin	transgenic (*MT-I* promoter): impaired fertility [98]
Follistatin-related genes (FLRGs) [99]	antagonist	BMP-2; Activin	transgenic *(α-inhibin* promoter): defects in gonadal development [100]
Crossveinless-2 (Cvl-2) [101, 102]	agonist and antagonist	BMP-2, -4, -7, GDF-5	-
Brorin [103]	antagonist	BMP-2, -6	-
nephroblastoma overexpressed (Nov) [104]	antagonist	BMP-2; Wnt-3	-
connective tissue growth factor (CTGF) [105]	antagonist	BMP-4; TGFβ-1	*ctgf*$^{-/-}$: pulmonary hypoplasia [106]
cysteine-rich transmembrane BMP regulator-1 (CRIM-1) [107]	antagonist	BMP-4, -7	*crim-1*(KST264/KST264): perinatal lethality, syndactyly, eye and kidney abnormalities [108]
bone morphogenetic protein (BMP)-binding endothelial cell precursor-derived regulator (BMPER) [109]	antagonist	BMP-2, -4, -6	-
Kielin (KCP) [110] CRIM-2	agonist	BMP-7	*kpc*$^{-7-}$: more susceptible to developing renal interstitial fibrosis and more sensitive to tubular injury [110]
twisted gastrulation (Tsg) [111-113]	agonist and antagonist	BMP-4 in complex with Chordin/sog	*tsg*$^{-/-}$: growth retardation, dwarfism, lymphopenia; death within a month [114] *tsg*$^{-/-}$; smaller size, mild vertebral abnormalities and osteoporosis [115]
DAN [116]	antagonist; dorsalizing and neuralizing factor	BMP-2, -4,-7; GDF-5	*dan*$^{-/-}$: no obvious abnormalities [116]
Cerberus-1 [117] caronte (chicken)	antagonist; head organizer	BMP-2, -4, -7; Activin; Nodal; Wnt	*cer*$^{-/-}$: no obvious abnormalities [118, 119]

name/ synonym	function	bound ligands	knockout mouse and phenotypical abnormalities
Gremlin [120] drm (rodent)	antagonist; limb bud outgrowth and pattering	BMP-2, -4, -7	*gremlin*$^{-/-}$: disruption of metanephric development [121] transgenic (osteocalcin promoter): enhanced bone formation [122]
protein related to DAN and Cerberus (PRDC) [123, 124]	antagonist	BMP-2, -4	-
Dante (Dte) [125]	antagonist	unknown	-
Coco [126]	antagonist; neuralizing factor	BMP-4; Wnt-8; TGFβ	-
Sclerostin [127-130] SOST	negative regulator of bone formation	unknown (BMP-5,-6,-7)	*sclerostin*$^{-/-}$: high bone mass phenotype [131]
Sclerostin-domain containing protein-1 (SOSTDC-1) [132-134] ecodin, USAG-1	negative regulator of BMP activity	unknown (BMP-2, -4, -6, 7)	-
BMP-1 [6, 135-138] mammalian tolloid procollagen C-proteinase tolloid (*Drosophila*) xolloid (*Xenopus*) tolloid-like-1 (TLL-1), tolloid-like-2 (TLL-2)	antagonists of chordin; ventralizing factor	complex of chordin/BMP-4	*bmp-1*$^{-/-}$: reduced skull ossification, die shorly after birth [139] *tll-1*$^{-/-}$: lethal [140]

Table 1.2 The BMP agonists and antagonists and their biological characteristics. The mammalian proteins are described. The information is based on [7, 68] and the indicated references.

Well described factors affecting BMP action are Noggin and Chordin. Noggin was characterized as a component of the Spemann organizer inducing dorsalization and neuralization [85, 86]. In the adult organism it is strongly expressed in chondrocytes and osteoblasts [7]. Noggin shows various affinity for BMP and GDF ligands including high affinity for BMP-2 and BMP-4 [83]. The determination of the crystal structure of the Noggin/BMP-7 complex revealed important insight into the molecular mechanism of the antagonist´s action. It showed that Noggin inhibits BMP signaling by blocking the binding epitopes for both type I and type II receptors [141]. Knockout studies showed that homozygous *noggin*$^{-/-}$ mice (lethal) have a shortened body axis, reduced size of somites and the neural tube, malformed limb, excess of bone and cartilage and dysfunction in the initiation of joint formation [87, 88]. Furthermore, ablation of *noggin* results in retardation of fetal hair-follicle induction [89]. *Msx2-noggin* transgenic mice indicate a phenotype with defective postnatal hair development and limb abnormalities [90]. Heterozygous mutation of the human *noggin* gene causes proximal symphalangism [142, 143] (SYM1, OMIM185800) and multiple synostosis syndrome [142, 144] (SYNS, OMIM186500). Both diseases affect the joints and are characterized by multiple joint fusions. Some cases of fibrodysplasia ossificans

progressiva (FOP, OMIM135100; see chapter 1.7), a severe disease with progressive endochondral ossification of the muscle [145], can also be attributed to mutations in the *noggin* gene [146-149].

Chordin is another factor secreted from the Spemann organizer which dorsalizes the *Xenopus* embryo [136, 150]. Furthermore, this protein is strongly expressed by osteoblasts [7]. The protein contains four characteristic cysteine-rich (CR) domains (also known as von Willebrand Factor type C domain) which mediate the binding of Chordin to BMPs with specificity for BMP-2, BMP-4 and BMP-7 [136]. Chordin inactivation in mice resulted in stillborn pups which in the later development show defects of the inner and outer ear and abnormalities in vascularization [91]. After double-knockout of *chordin* and *noggin*, the mutant mice show abnormal left to right patterning, disrupted mesoderm and lack parts of the eyes, forebrain and facial structures [91]. Secreted metalloproteinases as BMP-1, the mammalian orthologue of *Drosophila* Tolloid and Tolloid-like antagonize the effect of Chordin through proteolytical cleavage of the protein [136, 137].

Twisted gastrulation (Tsg) is a BMP antagonist in for example osteoblasts, which binds Chordin or short gastrulation (sog). The formation of a ternary BMP/Tsg/Chordin complex facilitates the inhibitory effect of Chordin on BMP [111-113]. *Tsg*-deficient mice are born healthy, but neonatal pups often show severe growth retardation shortly after birth and displayed dwarfism with delayed endochondral ossification and lymphopenia. The mice normally die within a month [114]. Furthermore, Tsg negatively regulates BMP-induced gene expression [151]. On the other hand, Tsg exhibits also a pro-BMP function. It can dislodge BMP from proteolytically-cleaved Chordin fragments to reactivate BMP signaling [152]. The metalloproteinase involved is *Drosophila* Tolloid which specifically cleaves and therefore antagonizes Chordin activity [153].

The DAN/Cerberus family is formed by the proteins DAN, Cerberus, Gremlin/drm, Dante (Dte) and Sclerostin (SOST) among others. A very interesting member of this family is Sclerostin [68, 154]. This protein is expressed in bone tissue, kidney, brain and liver [7]. *In vitro* binding of Sclerostin to several BMPs could be demonstrated [7], but the *in vivo* function of Sclerostin is discussed controversially. On the one hand it is suggested that the factor can inhibit BMP action in preosteoblasts [129]; on the other hand a model for sclerostin function assumed that Sclerostin is a negative regulator of bone formation, but not a classical BMP

antagonist as Noggin [128]. Interestingly, serious diseases with a hyperostotic phenotype are associated with mutations inside the *sclerostin* (*SOST*) gene: sclerosteosis (OMIM269500) [154-156] and the van Buchem disease (hyperostosis corticalis generalisata) (OMIM239100) [68, 157]. In both cases, patients suffer from an excessive and abnormal thickening or growth of bone tissue [158].

BMPs not only generate a morphogenetic gradient in the developing embryo but also within tissues. In order to achieve this locally restricted activity, BMP proteins can interact with the cell surface via proteoglycans as heparin and heparin sulphate and the extracellular matrix (ECM). In 1996, Ruppert et al. established the basic N-terminal domains of dimeric BMP-2 as heparin binding sites; these regions are not compulsary for receptor activation but modulate the biological activity of BMP-2 [159]. Heparan sulfate and heparin modulate the activity of BMP-2 by sequestering the ligand on the cell surface and mediate its internalization [160-162]. Furthermore, it is reported that heparin inhibits the osteogenic activity of BMP-2 by binding to both the BMP-2 ligand and the BMP type I and type II receptor [163]. Also BMP-4 can bind to heparan sulfate proteoglycans and thereby its *in vivo* diffusion is restricted [164]. Additionally, the already described BMP antagonists Noggin and Chordin are bound by heparan sulfate proteoglycans which results in modification of BMP activity [160, 165, 166]. However, binding of heparan sulfate to BMP-7 is required for BMP-7 signaling [167]. The ECM is also important for BMP regulation. The proteoglycan Decorin is thought to have a role in BMP-2 signaling since induction of alkaline phosphatase (ALP) activity is diminished in *decorin* null myoblasts compared to wild type cells [168]. *Biglycan* knockout mice resemble osteoporosis and premature arthritis. Moreover, the absence of Biglycan causes less BMP-4 binding to the ECM which reduces the BMP-mediated osteogenetic differentiation [169].

1.3 BMP receptors

Interestingly, for the more than 30 identified ligands of the TGFβ superfamily a comparably small number of specific receptors exist in humans indicating that ligand binding to the receptors is highly promiscuous.

1.3.1 Receptor structure, activation and function

BMPs bind with different affinities to type I and type II receptors that are transmembrane serine/threonine kinase receptors. So far, three high affinity type I receptors for BMPs are known: BRIa (ALK3), BRIb (ALK6) and ActRI (ALK2) [50, 71, 76, 99, 170, 171]. The recruited type II receptors are BRII [72-75] ActRII and ActRIIb [56, 172, 173]. The BMP receptors are specifically used by BMPs, whereas the Activin receptors are shared by BMPs and Activins. The following **Table 1.3** summarizes the role of these receptors inside the body:

name/ synonym	**function**	**bound ligands**	**knockout mouse and phenotypical abnormalities**
BRIa [71, 76, 174-176] ALK3	dorsal-ventral patterning of limbs; in adipogenesis, osteogenesis and chondrogenesis, hair follicle formation, chardiac development	BMP-2, -4, -6, -7, -15, GDF-5	*br1a*$^{-/-}$: early embryonic lethality due to defects in gastrulation and mesoderm formation [177] transgenic (double knockout BRIa/Ib, *Col-2* promoter): cartilage-specific, severe chondrodysplasia, reduced size [178]
BRIb [76, 175, 176, 179] ALK6	osteogenesis and reproduction	BMP-2, -4, -6, -7, -15, GDF-5	*br1b*$^{-/-}$: multiple skeletal defects, female infertility [180, 181]
ActRI [76, 182-184] ALK2	gastrulation, heart development, skeletal development	BMP-2, -4, -6, -7, -15	transgenic: neural crest cell-specific, cardio-vascular defects, multiple craniofacial defects [185, 186]
BRII [72-75]	gastrulation, osteogenesis, vascular tone	BMP-2, -4, -6, -7, -15; GDF-5	*br2*$^{-/-}$: early embryonic lethality due to defects in gastrulation and mesoderm formation [187]
ActRII [172, 188]	embryonic patterning	BMP-2, -4, -6, -7, -15	*actr2*$^{-/-}$/*actr2b*$^{+/--}$: severe disruption of mesoderm formation [189]
ActRIIB [172, 188]	embryonic patterning	BMP-2, -4, -7	*actr2*$^{-/-}$/*actr2b*$^{+/--}$: severe disruption of mesoderm formation [189]

Table 1.3 The BMP receptors and their biological properties. The mammalian proteins are described. The information is based on [2, 7, 89] and the indicated references. TRβIII is a newly identified BMP receptor that is unrelated to the other BMP receptors and is described in chapter 1.2.2. Furthermore, the orphan receptor ALK1 was shown to be a receptor for BMP-10 in endothelial cells [61].

The mammalian type I receptors show a molecular weight of about 50-55 kD (BRIa, 532 aa; BRIb, 502 aa; ActRI, 509 aa). The receptors exhibit an extracellular domain for ligand binding, a single transmembrane region and an intracellular part including the serine/threonine kinase. The C-terminus of the kinase domain harbors another motif that is characteristic for TGFβ type I receptors, the so called NANDOR (non-

activating non-downregulating) box, required for TGFβ signaling and downregulation [190]. The type II receptors are higher glycosylated and have a molecular weight of about 75 kD (ActRII, 513 aa; ActRIIb, 512 aa). An extracellular domain, a region passing the membrane and an intracellular kinase domain structurally organize the type II receptors; the BMP type II receptor is an exception. This receptor occurs in two splice variants, the short form (BRII-SF, 529 aa) and the long form (BRII-LF, 1038 aa, about 130 kD). BRII-LF exhibits a long cytoplasmic tail following the kinase domain encoded by exon 12 [72, 74, 75]. The majority of cells tested for the presence of BRII-SF and BRII-LF express the long receptor variant [191]. As established for TβRII, type II receptors are constitutively active kinases that show autophosphorylation [192, 193].

In response to ligand stimulation the type I receptor undergoes a very fast, type II receptor-mediated phosphorylation that occurs within less than two minutes [193, 194]. Exchange of the critical lysine to arginine at position 230 in BRII (BRII-K230R) inactivates the kinase activity of the receptor and lead to inhibition of BMP signaling [195]. The target site for this phosphorylation is the GS-box, a glycine- and serine-rich domain (-S^{216}-G-S-G-S-G^{221}-, positions according to BRIa) which is located N-terminal of the type I receptor kinase. As shown for the TβRI kinase domain, a smaller N-terminal lobe is involved in ATP binding, and a larger C-terminal lobe is required for substrate recognition [196]. However, BRIa and BRIb activation can be mimicked by mutation at position 233 or 203, respectively, exchanging glutamic acid to aspartic acid, which results in a receptor that transduces its signal without ligand-triggered phosphorylation at the GS-box [197]. Inversely, inactivation of BRI´s kinase activity is achieved by exchanging the critical lysine to arginine (BRIa-K231R, BRIb-K231R) [198, 199]. The GS-box serves as an important regulatory domain for signaling of TGFβ superfamily ligands. Phosphorylation activates the type I receptor by switching the GS-box into a preferred binding site for R-Smads [3]. In this aspect it is known for TβRI, but not for BRI that the immunophilin FKBP12 can associate with the unphosphorylated receptor to lock the catalytic center of the type I receptor in an inhibited conformation [196, 200]. However, for determining the specificity of the ligand signal, the juxtamembrane region including the GS-box and most parts of the kinase domain of the type I receptor are dispensable. The responsiveness of TGFβ superfamily signaling is specified by two distinct regions: the L45 loop within the receptor and the L3 loop within the R-Smad

protein. The L45 loop of the type I receptor is an 8 aa loop between the β-sheet 4 and β-sheet 5 which connects two subdomains of the receptor´s kinase region; the L-45 loop is exposed in the 3D structure of the kinase and offers distinct signaling ability since it is invariant among the receptors [201]. The L3 loop in the C-terminal domain of the Smads is a 17 aa sequence with two critical residues specifying and establishing the recognition of the L45 loop of the respective type I receptor [202, 203]. This allows the type I receptor to phosphorylate R-Smad proteins. In the case of BRIa, BRIb and ActRI (in complex with BRII or ActRII/IIb) these are the BMP R-Smad1, 5 and/or 8. Also ALK1 together with TβRII can phosphorylate BMP R-Smads. TGFβ R-Smads are C-terminally activated by TβRI (ALK5) (in complex with TβRII) or ActRIb (ALK4) or ALK7 (in complex with ActRII/IIb) [2].

In the following, the physiological role of receptors for BMPs focussed on BRIa, Ib and BRII will be described more in detail. BRIa and BRII are ubiquitiously expressed in the developing embryo and are strongly expressed in the adult organism in osteoblasts and chondrocytes. During embryogenesis, BRIb is found in cartilage, muscle and limbs, in the nervous system, in epithelium, ear and eye. In the adult, the Ib receptor is also highly expressed in osteoblasts and chondrocytes. The expression pattern already suggests that BMP receptors are required for limb patterning [204, 205]. Studies of knockout or transgenic mice allowed more insight into the importance of BMP receptors and signaling in the developing organism. *Br1a*$^{-/-}$ knockout mice are lethal in early embryonic development due to defects in gastrulation and mesoderm formation [177]. *Br1b*$^{-/-}$ knockout mice are viable, but suffer from multiple skeletal defects and female infertility [180, 181]. Cartilage-specific double knockout of *br1a/br1b* shows severe chondrodysplasia and a reduced body size [178]. Furthermore, transgenic mice with neural crest-specific *br1a* ablation die before birth from acute heart failure [206]. Additionally, a neural stem cell-specific *br1a* knockout lead to an increased number of blood vessels and defects in formation of blood-brain-barrier [207]. *Br1a* inactivation in the hair follicle resulted in impaired cell differentiation and reduced number of hair follicles [206]. *Xenopus* studies analyzing a truncated type I receptor lacking the intracellular part alters ventral to dorsal mesoderm [208, 209]. Besides embryogenesis, it is known that BMP-2 stimulation inhibits the terminal differentiation of C2C12 myoblasts and converts their differentiation pathway into that of osteoblast lineage cells [210]. Kinase domain-truncation of BRI blocks the BMP-2-induced signal transduction in C2C12 myoblasts

[211], whereas constitutively active BMP type I receptors induce the osteoblastic differentiation marker alkaline phosphatase [198]. Interestingly, studies in the osteoblastic precursor cell line 2T3 discovered that BRIa promotes adipogenic differentiation, while BRIb is more potent in osteoblastic differentiation [175].

Deletion of the *br2* gene in mice is lethal in the early embryogenesis due to defects in gastrulation and mesoderm formation [187], and thus exhibits the same phenotype than null mutation of *br1a*. Moreover, truncated BRII in *Xenopus* embryos induce secondary axial structures and thus is involved in dorsoventral patterning [212]. As mutated BRIa, a kinase-dead BMP type II receptor blocks BMP signaling in C2C12 cells [195].

Interestingly, several mutations in BRII were found in patients with pulmonary arterial hypertension (PAH) [13, 213-215], a rare autosomal dominant disease that will be discussed in detail in chapter 1.7. Pulmonary arterial vascular smooth muscle cells (PAVSMCs) from patients or PAVSMCs from *br2*$^{+/-}$ heterozygous knockout mice showed attenuated BMP signaling [216-218]. All these results indicate that both BRI and BRII are essential for embryonic development and that cell-specific disruption or inactivation of the receptors affects BMP signaling leading to severe dysregulation of cellular processes such as proliferation, apoptosis and differentiation.

1.3.2 Receptor oligomerization and localization

From the TGFβ receptors it is known that TβRII is the high-affinity receptor for TGFβ-1, which after ligand binding recruits the low-affinity receptor TβRI into an active signaling complex [193]. Both, hetero- and homomeric complex formation of TβRI and TβRII appears to be important for efficient signal transduction [219-221] leading to the approved model of the active heterotetrameric receptor complex with two type I and type II receptors [3]. Receptor oligomerization and thus signal induction of the related BMP receptors is different.

The oligomerization pattern of BMP type I (BRI) and type II (BRII) receptors is more flexible and influenceable for ligand modulation [219]. Prior to ligand binding, a significant proportion of BMP receptors are already complexed at the cell surface. These complexes, mainly consisting of BRII and BRI, reside preassembled in the plasmamembrane as so called preformed complexes (PFCs). On the other hand, a

larger population of receptor complexes is formed after ligand binding to the high-affinity receptor BRI, which recruites the low-affinity receptor BRII into a signaling complex. These complexes are called BMP-induced signaling complexes (BISCs). Intriguingly, these two receptor oligomerization patterns induce different BMP-induced signaling pathways: PFCs signal via the canonical Smad pathway (see chapter 1.4) and BISCs start non-Smad signaling via the MAPK p38 which lead to the induction of ALP (see chapter 1.5) [195].

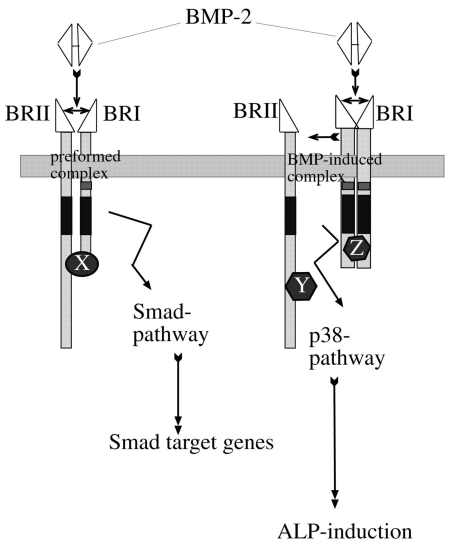

Figure 1.5 The different oligomerization modes of the BMP receptors [195]. BMP-dependent activation of the Smad pathway and the non-Smad pathway via MAPK p38 depends on the formation of preformed receptor complexes or BMP-induced signaling complexes at the cell surface.

Moreover, it is known that the kinase domain and the kinase activity of BRII are required for ligand-independent heterodimerization and clustering with BRI since BRII mutants lacking the kinase domain are unable to oligomerize with BRI [195, 222].

It is known that localization of transmembrane receptors to specific membrane microdomains as well as endocytotic events of these receptors influence signaling. The plasma membrane is a mosaic of different membrane compartments and domains. Among these are the lipid rafts which are cholesterol-rich and detergent-resistant (also known as detergent-resistant membranes DRMs) [223]. A subpopulation of these DRMs contain the protein caveolin-1 (Cav-1) [224]. Two main endocytotic pathways exist in the cell, clathrin-mediated and caveolae-mediated endocytosis. TGFβ receptors reside in Cav-1-positive vesicles as well as clathrin-coated vesicles (CCPs); both receptor endocytosis routes influence TGFβ signaling

[225, 226]. Comparitive studies for BMP signaling revealed that BRII as well as BRI are not only located in Cav-1-positive DRMs but also interact with Cav-1 [227-229]. Furthermore, Hartung and co-workers could show that (1) BMP Smad phosphorylation occurs while the receptors are still at the cell surface, (2) BRII and BRI undergo CCP-mediated endocytosis, while BRII is also internalized via caveolae, (3) Cav-1 inhibits Smad signaling suggesting BRII degradation via the caveolar pathway (supported by [230]), (4) CCP-mediated endocytosis is necessary for the continuation of Smad signaling induced by the preformed receptor complex and (5) that non-Smad signaling resulting in the induction of ALP starts from receptors (BISCs) residing in cholesterol-enriched plasma membrane regions [227]. Interestingly, for some BRII PAH mutant receptors it is suggested that they do not reach the cell surface and are instead retained in in complex with the type I receptor in intracellular compartments; this contributes negatively to the ligand binding ability and thus to activation of BMP signaling [216, 231].

1.3.3 Co-receptors of BMP signaling

BMP receptor activity is modulated by various transmembrane co-receptors; these receptors are discussed in the following: The membrane-anchored glycoprotein Betaglycan was identified as the TGFβ type III receptor that binds all three TGFβ isoforms [232-234]. Betaglycan can act on TGFβ signaling in two ways: as enhancer due to stabilization of ligand/receptor binding and elimination of binding differences of TGFβ isoforms to the receptors or antagonist due to membrane-release; furthermore, it can bind TGFβ in solution [235, 236]. Very recently, it was explored that BMP-2/4, BMP-7 and GDF-5 also bind to Betaglycan facilitating ligand binding to the BMP type I receptor [237].

The related protein Endoglin (CD105) supports in contrast to Betaglycan TGFβ-1 and -3 binding to TβRII receptors [238]. Regarding BMP signaling, Endoglin binds to BMP-7 when complexed with ActRII/IIb, and to BMP-2/BRI complexes adding further binding specificity to these complexes [239]. Moreover, Endoglin enhances the BMP-7/Smad1/Smad5 pathway [240].

The pseudoreceptor BMP and Activin membrane-bound inhibitor (BAMBI) is closely related to TGFβ type I receptors, but lacks the characteristic kinase domain.

BAMBI inhibits besides BMP signaling also TGFβ/Activin signaling by preventing receptor complex formation [241]. During embryogenesis BAMBI is co-expressed with BMP-4 [241, 242]. Surprisingly, genetic ablation of *bambi* in mice does not exhibit a developmental defect [243].

Three members of the repulsive guidance molecule (RGM) family have been implicated in the BMP signaling pathway. Dragon (RGMb) is a GPI-anchored member of this family which binds BMP-2/-4 and associates with BMP type I (ALK2, BRIa and BRIb) and type II receptors (ActRII and ActRIIb) and specifically enhances BMP signaling but not the TGFβ pathway [244, 245]. RGMa interacts with BMP-2/-4 and several BMP-specific receptors, and is similarly involved in BMP signaling [244, 246]. Additionally, RGMa facilitates the use of ActRII by endogenous BMP-2/-4 that prefer signaling via BRII, and thus enhances the BMP signal [247]. Hemojuvelin (RGMc) is also a BMP-2/-4 co-receptor for ActRII, BRII, ALK-2, BRIa and BRIb and stimulates BMP signaling [244, 248, 249]. Hemojuvelin is implicated in the regulation of the iron level as it controls hepcidin expression, a key regulator of iron homeostasis. Interestingly, hemojuvelin mutants associated with hemochromatosis show impaired BMP-2 signaling ability and BMP-2 by itself upregulates hemojuvelin and thus hepcidin expression in hepatocytes [248, 250]. Recently it was published that BMP Smad signaling can be selectively blocked by dorsomorphin (inhibitor of AMP-activated protein kinase; compound C) through inhibition of the type I receptor kinase. This comes along with a normalized expression of hepcidin and an elevated iron level in the liver due to inhibited BMP signaling [251].

The orphan tyrosine kinase receptor Ror2 was shown to bind BRIb and to modulate signaling initiated by this receptor. Interestingly, mutations Ror2, BRIb and the BRIb ligand GDF-5 cause different type of brachydactyly [252].

1.3.4 Intracellular regulatory proteins of the receptors

For the TGFβ system, many interactors of the type I and type II receptors are known yet. But also a lot of work was done in the BMP field in the last years to identify BMP receptor interactors.

In a yeast-two-hybrid screen the BMP receptor-associated molecule 1 (BRAM-1) was identified as a BRIa-binding protein. BRAM-1 is a splice variant of BS69

(adenovirus E1A-associated protein) and negatively regulates the Epstein-Barr virus latent membrane protein. BRAM-1 in BMP signaling links TAB1, an important component of BMP non-Smad signaling (see chapter 1.5), to the type I receptor [253]. Another protein interacting with BMP type I receptors is the X-chromosome-linked inhibitor of apoptosis (XIAP) which is a member of the inhibitor of apoptosis protein (IAP) family. XIAP binds not only to the BMP receptor complex but also interacts with TAB1. It supports TAB-1/TAK-1 (see chapter 1.5) in ventralization of *Xenopus* embryos suggesting that XIAP participates in BMP signaling as a positive regulator by linking the BMP receptors and the TAB-1/TAK-1 apparatus [254, 255].

Watanabe and co-workers identified that a fraction of the splicing factor 3b subunit 4 (SF3b4) interacts with BRIa in the cell membrane specifically inhibiting BMP-mediated osteochondral cell differentiation [256].

The probably best examined BRII-associated protein is LIM kinase I (LIMKI). The kinase phosphorylates and thus inactivates ADF/cofilin, an actin depolymerization factor. LIMKI was originally identified as a BRII-tail interactor by Foletta and co-workers [191]. BRII/LIMKI association decreases LIMKI activity, whereas BMP-4 treatment attenuates this downregulation. Since PAH BRII mutants can not bind LIMKI, the negative regulation of the kinase via BRII is abolished; thus, LIMKI might be involved in the etiology of PAH [191]. Furthermore, LIMKI activity plays a role in BMP-induced dendritogenesis of neurons. Since LIMKI binding is specific for BRII-tail, the tail region seems to be essential for BMP-mediated branching of neurons [257]. Moreover, axon pathfinding of neurons comes along with distinct actin dynamics regulated by an interplay of BMP and ADF/cofilin phosphorylation and dephosphorylation through LIMKI and the phosphatase slingshot [258, 259]. Additionally, in *Drosophila* the interaction between the BMP type II receptor wit and LIMKI is also required for synaptic stability [260].

Another BRII-interacting protein is Tctex-1. Tctex-1 is a light chain of the motor complex dynein that transports protein cargo along the microtubular network. Tctex-1 binds to BRII and BRI within the receptor complex and is selectively phosphorylated by BRII-LF, a function which is disrupted by PAH BRII-LF mutants. This suggests that the phosphorylation might contribute to the pathogenesis of PAH [261]. Interestingly, other dynein light chains, km23/LC7 and Tctex-2β, bind the TGFβ receptor complex and affect not only TGFβ-Smad and non-Smad signaling but also dynein composition [262, 263].

In a yeast-two-hybrid screen for BRII-associated proteins, the tyrosine kinase c-Src was found to bind to BRII-tail [264]. The kinase participates in signaling transduction pathways that influence cell differentiation, proliferation, motility and survival; furthermore, abberant c-Src function is found in many cancers. Wong et al. could show that BMP stimulation decreases phosphorylation of c-Src at Tyr418 and that PAH BRII mutants abolished this effect and disrupted c-Scr/BRII interaction. Therefore, BMP signaling seems to balance the proproliferative function of c-src [264].

A proteomics-based approach for BRII binding partners revealed that Eps15R, a constituent component of clathrin-coated pits (CCPs), does interact with the cytoplasmic domain of BRII [227, 265]. A modest inhibitory effect of Eps15R on BMP Smad signaling is suggested (diploma thesis V. Wenzel, 2005, University of Wuerzburg, Germany). As already described, several studies suggest that the BMP receptor complex associates with Cav-1 resulting in DRM localization [227-229].

The tyrosine kinase receptor c-Kit is besides type I receptors and the described co-receptors another transmembrane protein that interacts with BRII. c-Kit recognizes the stem cell factor (SCF) as a ligand; moreover, c-Kit is a proto-oncogene whose expression is significantly increased in various cancers. Inside BMP signaling, complex formation of c-Kit and BRII lead to phosphorylation of BRII at Ser757 which modulates BRII-dependent signaling [265, 266]. Interestingly, BMP-4 modulates c-Kit expression in specific kidney cells [267].

One further protein interacting with BRII is Tribbles-like protein 3 (Trb-3). It is the mammalian homolog of the *Drosophila* cell cycle-controlling protein Tribbles. Trb-3 is a non-functional kinase that regulates various signaling transducers as the kinase PKB/Akt. Chan and co-workers found Trb-3 associated with BRII-tail in the absence of ligand. However, BMP stimulation lead to dissociation of Trb-3 from the receptor to mediate the degradation of the E3 ubiquitin ligase and Smad inhibitor Smurf1; thus, Trb-3 acts as a promoter of BMP Smad signaling. Furthermore, Trb-3 is essential for the BMP-mediated differentiation of PASMCs pointing to a potential role for this protein in the regulation of pulmonary vasculature [268].

The receptor for activated C-kinase (Rack-1) was identified as a BRII-binding partner in a yeast-two-hybrid screen. Several studies hint towards that Rack-1 functions as a signaling molecule in cytokine signaling cascades. The kinase domain of BRII is the binding region for Rack-1. This protein seems to be important for the

pathology of hypertension diseases since Rack-1 binds weaker to PAH BRII mutants, enhances (the antiproliferative) BMP signaling and is a negative regulator of proliferation [269].

The proto-oncogene TrkC (tropomyosin-related kinase C), necessary for growth and survival of cancer tissue, associates with BRII, prevents BMP receptor complex formation and thus might block the BMP tumor suppressor activity in metastatic cells [270]. Notably, TrkC also binds to TβRII, inhibits TGFβ signaling and TGFβ tumor suppressor activity [271].

An additional and interesting protein that interacts with BRII is Dullard. This factor is involved in neural development. Satow et al. established that Dullard neuralizes *Xenopus* embryos by antagonizing BMP signaling [230]. Dullard associates with BMP receptors, promotes proteasomal degradation of BRII via the caveolae pathway and supports dephosphorylation of BRI due to its phosphatase activity; both functions lead to inhibition of BMP signaling [230].

Further studies on the interactome of the BMP receptor complex will identify more associated proteins and will deliver deeper insight into the complexity of BMP signaling. In this thesis the interaction of the cGMP-dependent protein kinase Iβ (cGKIβ) and BRII will be examined and its impact on the BMP pathway. Another interacting protein, the protein phosphatase 2A (PP2A), was investigated and these results are summarized in chapter 7.2. **Figure 1.6** illustrates the BMP receptor interactome:

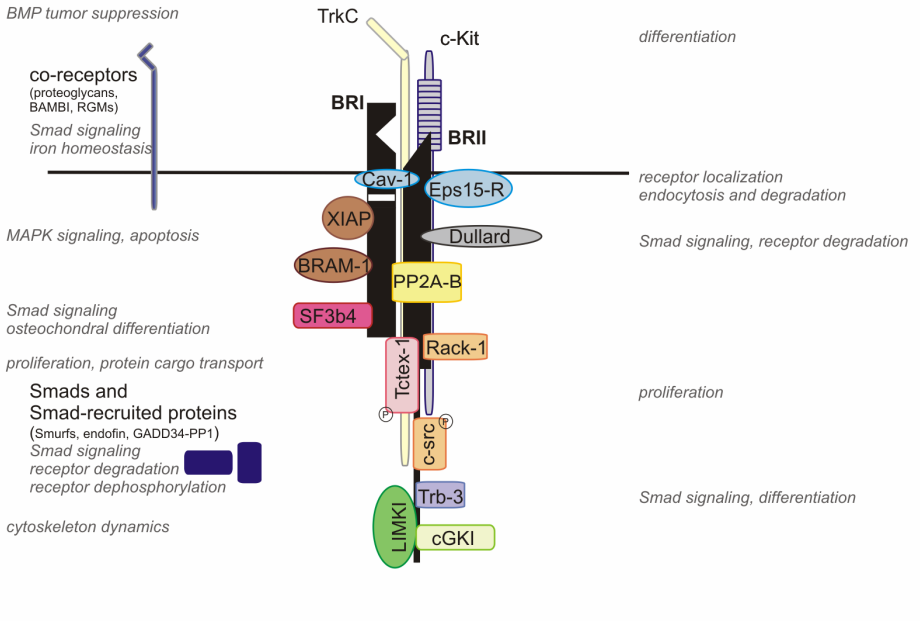

Figure 1.6 The interactome of the BMP receptor complex at the cell surface. The BMP receptors are depicted in black. Associated physiological functions of each interacting protein are depicted.

1.4 Smad pathway

Activation of the receptor complex at the cell surface after ligand binding runs into two major downstream pathways whereby intracellular messenger proteins are activated. The Smad pathway is mediated through R-Smad proteins and the other route, the non-Smad pathway goes primarily via MAPKs and will be discussed in chapter 1.5.

1.4.1 Smad structure, regulation and modification

Mammalian Smad proteins got named due to their orthologs found in *Drosophila* (MAD proteins) and *C. elegans* (Sma proteins). Three subclasses exist: receptor-regulated Smads (R-Smads), common mediator Smad (co-Smad) and inhibitory Smads (I-Smads). **Figure 1.7** summarizes the biological function of the R-Smad proteins and of co-Smad and I-Smad proteins.

name/ synonym	function	knockout mouse and phenotypical abnormalities
R-Smad1 [272] MADH1	ventralizing factor essential role in the development of the germ layer and extraembryonic tissue	*smad1*$^{-/-}$: early embryonic lethality (chorioallantoic fusion and germ cell formation defects) [273, 274] transgenic *(Smad1/Smad5* knockout*)*, in somatic cells: metastatic tumor development [275]
R-Smad5 [276, 277] MADH5	ventralizing factor essential role in early embryonic angiogenesis	*smad5*$^{-/-}$: early embryonic lethality mainly due to severe defects in angiogenesis [278, 279]
R-Smad8 [280, 281] MADH9, Smad9	ventralizing factor	-
co-Smad4 [282-284] DPC4, MADH4	mesoderm inducing factor tumor suppressor	*smad4*$^{-/-}$: early embryonic lethality, no gastrulation [285, 286] *smad4*$^{+/-}$*/Apc*$^{+/-}$: intestinal polyps develope into more malignant tumors than those in the simple Apc$^{+/-}$ heterozygotes [287] *smad4*$^{+/-}$: intestinal inflammatory polyps [288]
I-Smad6 [289, 290] MADH6	inhibition of Smad signaling neuralizing and dorsalizing factor	*smad6*$^{-/-}$: multiple cardiovascular abnormalities [291]
I-Smad7 [292] MADH7	inhibition of Smad signaling dorsalizing and neuralizing factor	*smad7*$^{exon1-/-}$: several changes in B cell responses [293]

Table 1.4 The Smad proteins and their biological properties. The *Xenopus* and mammalian proteins are described. The information is based on the indicated references.

The R-Smad subclass comprises intracellular messenger molecules which are specifically phosphorylated and activated by the receptor complex to translocate into the nucleus for the regulation of target gene transcription. R-Smad2 and 3 respond to TGFβ signaling and R-Smad1, 5 and 8 primarily to BMP signaling [3, 272, 294-296]. Knockout of *smad1* in mice results in early embryonic lethality due to defects in chorioallantoic fusion and germ cell formation [273, 274]. Other studies support this essential role in the development of the germ layer and extra-embryonic tissue [297]. As demonstrated in *Xenopus*, Smad1 and Smad5 are ventralizing factors [21, 272]. Mice with genetic ablation of the *smad5* gene also die in the early embryonic development mainly due to severe defects in angiogenesis and the nervous system [278, 279]. A blood vessel wall-specific inactivation of *smad5* disturbs chardiac contractility [298]. Interestingly, metastatic tumor development is initiated after conditional knockout of both *smad1/smad5* in somatic cells [275]. Moreover, Smad1 can be transactivated by TGFβ in human breast cancer cells [299] as well as in epithelial cells via Ras/MEK [300]. Recently it was published that BMP signaling enhances the invasion of bone metastasis of breast cancer via the Smads [301]. Besides this, Smad1 and Smad5 have specific, but distinct function in hematopoiesis

[302], whereby Smad5 seems to be more important since the protein cooperates with TGFβ signaling in the regulation of human hematopoiesis [303, 304]. Osteoblastic and chondrogenetic signaling initiated by BMP is intracellularly transduced by Smad1 and 5 in C2C12 cells [198, 296, 305].

In 1996, human Smad1 was cloned [272, 294]. R-Smad proteins exhibit around 465 aa (Smad1, 465 aa; Smad5, 465 aa; Smad8, 430 or 467 aa). R-Smads contain two conserved structural domains, the N-terminal MH1 domain and the MH2 domain at the C-terminus, named accordingly to their sequence homology to MAD proteins in the fly (**Figure 1.7**).

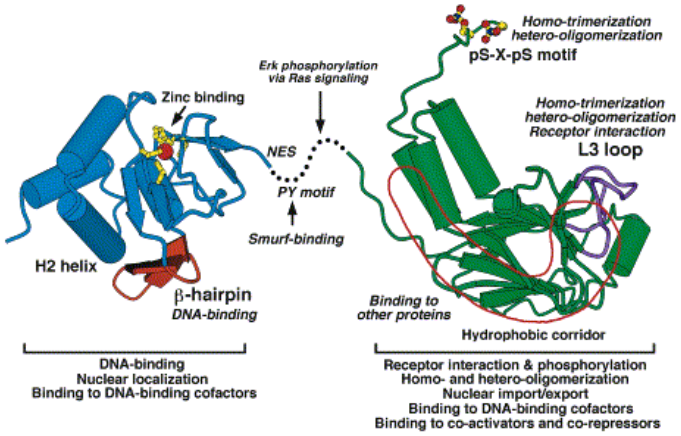

Figure 1.7 Structure of the Smad protein [3]. The MH domains are shown in blue (MH1) and in green (MH2). The linker region connecting the two domains is shown as a dotted line. Structural features are depicted or additionally coloured (red, DNA binding site; magenta, L3 loop; yellow, zinc binding motif and SSXS motif; red encircled, hydrophobic corridor).

The MH1 domain is required for DNA binding and nuclear localization. It also functions as interaction platform for diverse proteins which will be discussed later in this chapter. The MH2 domain is formed by a central β-sheet sandwich with a bundle of three α-helices on the one end and two auxiliary α-helices plus three surface loops on the other end. Responsiveness of TGFβ superfamily signaling is specified by two distinct regions: the L45 loop within the type I receptor and the L3 loop within the R-Smad protein. The L45 loop, already described in chapter 1.3.1, offers distinct signaling ability since it is invariant among the type I receptors [201]. The L3 loop inside the R-Smad1/5 molecule is a 17 aa sequence in length comprising the residues 417 to 433; it protrudes from the C-terminal domain [203]. Two residues - in Smad1 and 5 these are His425 and Asp428 - differ between the BMP and the TGFβ

[202, 203] . These residues are critical for R-Smad specificity and recognition of the L45 loop inside the respective type I receptor [202, 203], and thus for phosphorylation of the R-Smad proteins at the extreme C-terminus [306, 307]. Crystal structure analysis revealed that the unphosphorylated C-terminus of Smad1 is completely disordered and flexible [308]. After phosphorylation, the SSXS motif (-S^{462}-S-V-S^{465} in Smad1 and 5) gets in contact with a basic phospho-serine binding pocket in the MH2 domain of an adjacent Smad1 molecule. The MH2 domain of the phosphorylated molecule undergoes conformational changes [308]; this is in contrast to the TGFβ-activated Smad2 whose MH2 domain excepting the very C-terminus is conformational stable upon phosphorylation [309, 310]. Studies primarily done in the TGFβ system demonstrated that upon phosphorylation, R-Smad proteins form homotrimers [308, 309] as well as heterotrimers with co-Smad4 [308, 311-313]. R-Smad molecules more often heterotrimerize with one co-Smad4 molecule than homotrimerize. Strong electrostatic interactions within the heteromeric interface contribute to this, although the stabilizing C-terminal phosphorylated site in the Smad4 molecule is missing [311, 312]. This heterotrimeric model is supported by the fact that Smad-dependent transcription often requires the presence of co-Smad4 [2]. Additionally, heterodimers of R-Smads and co-Smad4 are reported suggesting a fundamental difference between R-Smad/co-Smad heterodimers and heterotrimers [309, 310, 314]. Inman and Hill indeed could show that the Smad complex formation occurs in a promoter-specific manner [315].

In their inactive state, R-Smad protein activation and thus contact to co-Smad4 are blocked by autoinhibition of the MH2 domain through an intramolecular interaction with the MH1 domain [316]. The linker region connecting the two MH domains is very divergent among the Smad proteins and comprises multiple phosphorylation sites which allow crosstalk with other signaling pathways. In this context, also dephosphorylation events via phosphatases play an interesting role which will be described in the next chapter. Furthermore, the R-Smad linker contains a PY motif. The sequence -P-P-X-Y- (-P^{224}-P-X-Y^{227}- in Smad1 and 5) is a conserved site recognized by WW domains that are found in the HECT E3 ubiquitin ligase family members such as Smad ubiquitin regulatory factor 1 (Smurf1) [317]. Initial analysis revealed that Smurf1 dorsalizes and neuralizes *Xenopus* embryos indicating a BMP antagonistic function [317]. Indeed, Smurf1 interacts with Smad1/5 via the PY motif and induces its ubiquitination and its proteasomal degradation [317-319]. Also

Smurf2 negatively regulates R-Smad activity and degradation [320, 321]. In a *smurf1* transgenic mice with osteoblast-specific ablation, bone formation is significantly reduced [322]. Another E3 ubiquitin ligase, the carboxyl terminus of Hsc70 interacting protein (CHIP), mono- and polyubiquitinates Smad1 and thereby regulates BMP signaling [323, 324]. Intriguingly, a study in *Drosophila* suggests a Smurf-independent regulation of Smad degradation. The eukaryotic translation initiation factor 4A (eIF4A) mediates inhibition of decapentaplegic (DPP)/BMP signaling through degradation of the components Mad and Medea - the *Drosophila* homologs to R-Smad and co-Smad [325]. Also other modifications of the R-Smad molecule are known. Inside the TGFβ pathway, Smad2 and 3 are acetylated at several lysines in the MH2 and MH2 domain by the transcriptional co-activator p300/CREB binding protein (CBP) which has intrinsic acetyltransferase activity. The acetylation induces conformational changes resulting in a stronger DNA binding and/or enhanced nuclear translocation of the R-Smads and thus augmentation of signaling [326-328]. Smad1 is also acetylated by p300/CBP regulating its stability [329]. R-Smad activity is further modulated by a dynamic interplay of kinases and phosphatases. Kretzschmar and co-workers described opposing regulatory input on BMP R-Smads balancing their action. Stimulation with epidermal growth factor (EGF) or hepatocyte growth factor (HGF) activate receptor tyrosine kinases (RTKs) which induce MAPKs. The extracellular signal-regulated kinase (Erk) was found to phosphorylate the linker region of Smad1 counteracting C-terminal phosphorylation through the type I receptor and hence inhibiting nuclear translocation of Smad1 [330]. Because of the neuralizing effect of insulin growth factor (IGF) and fibroblast growth factor (FGF) on *Xenopus* embryos, these factors were also identified to trigger inhibitory linker phosphorylation of Smad1 [331]. Furthermore, Erk2-mediated phosphorylation at Ser187, Ser195, Ser206 (the main site) and Ser214 (**Figure 1.8**) restricts Smad1 activity by enabling Smurf1 binding to the linker [332].

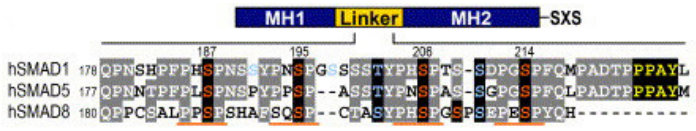

Figure 1.8 The linker region of Smad1/5/8 [332]. The proline-rich linker region contains four conserved MAPK consensus sites (orange, underlayed with black), conserved GSK-3 consensus sites (blue), a PY motif (yellow, underlayed with black) and other sites for proline-directed kinases.

Thereby polyubiquitination and proteasomal degradation of Smad1 are induced as well as contact of Smad1 to the nucleoporin Nup214 (see chapter 1.4.2) is restricted. Moreover, MAPK-induced linker phosphorylation primes Smad1 for glycogen synthase kinase 3 (GSK-3) phosphorylation which further enhances polyubiquitination [332]. Notably, Fuentealba et al. also reported sequential linker phosphorylation of Smad1. GSK-3-mediated phosphorylation on Ser210 (**Figure 1.8**) requires prior MAPK phosphorylation. Modulation through GSK-3 leads to polyubiquitination and to proteasomal degradation of Smad1 at the centrosomes. Furthermore, prolonged BMP signaling is not only achieved by pharmacological inhibition of kinases as Erks and GSK-3, but also by Wnt8 signaling which blocks GSK-3 activity [333]. Several other kinases as c-jun N-terminal kinase (JNK), calmodulin-dependent kinase II (CamKII), cyclin-dependent kinases (CDKs), protein kinase C (PKC) or protein kinase B (PKB/Akt) are reported to regulate TGFβ-specific Smads [2] which likely can be transferred to BMP Smads as well. Consequently, phosphatases are also implicated in the regulation of Smad activity. Pyruvate dehydrogenase phosphatase (PDP) dephosphorylates Smad1 at the SSXS motif resulting in inhibition of signaling. The BMP Smad-specific interaction takes place in the cytoplasm and in the nucleus [334]. Moreover, PPM1A (protein phosphatase 2C (PP2C)) also inhibits BMP and TGFβ signaling through dephosphorylating the C-terminus of Smads. Since PPM1A is predominantly localized in the nucleus, this phosphatase is thought to be the missing piece in the basic regulation of nucleocytoplasmic shuttling of Smads [335, 336] (see chapter 1.4.2). Additionally, small C-terminal domain phosphatases (SCPs) were shown to C-terminally dephosphorylate R-Smads in the nucleus which attenuates signaling. In contrast to this, SCPs can also dephosphorylate Erk-mediated linker phosphorylation. In BMP signaling, SCP action results in resetment of Smad phosphorylation to a basal level, whereas in the TGFβ pathway SCPs enhance signaling because dephosphorylation of the linker overwrites the C-terminal dephosphorylation [337-339].

Despite the already described co-Smad and I-Smad proteins, several other proteins are known to interact with and thereby modulate R-Smads outside the transcriptional complex. The protein endofin, which can bind phospholipids via a FYVE domain, binds Smad1 and facilitates C-terminal phosphorylation of the R-Smad. On the other hand, it balances signaling through recruitment of the regulatory subunit of PP1 (growth arrest and DNA damage-inducible protein (GADD-34)) to BRI

that mediates BRI dephosphorylation [340]. The protein endofin was also shown to enhance TGFβ signaling by supporting complex formation of Smad2 and Smad4 [341]. Interestingly, other FYVE domain proteins also participate in TGFβ superfamily signaling. The Smad anchor for receptor activation (SARA) interacts with TβRI and Smad2/3 in early endosomes and brings the R-Smads in the proximity of the receptors which initiates and enhances signaling [225, 342, 343]. In addition, the FYVE domain protein Hgs (Hrs, HGF-regulated tyrosine kinase substrate) associates with Smad2/3 and promotes TGFβ signaling [344]. CD44, the receptor for the ECM macromolecule hyaluron, intracellularly binds Smad1. Studies in chondrocytes revealed that both truncated CD44 as well as treatment with hyaluronidase inhibits Smad activity [345]. Furthermore, the inner nuclear membrane (INM) protein MAN1 (LEMD3) is a neuralizing factor in *Xenopus* indicating BMP antagonistic action. Indeed, MAN1 interacts with BMP and TGFβ Smads at the INM and inhibits signaling [346-348]. The mechanism causing this behaviour could either be R-Smad/co-Smad complex disruption and/or induction of R-Smad dephosphorylation in the nucleus [349]. Notably, MAN1 and TGFβ signaling cooperate in vascular remodeling and thus during embryonic development [350, 351]. Other proteins of the INM as A-type lamins also participate in the regulation of the phosphorylation status of R-Smads [352].

Human co-Smad4/DPC4 (deletion target in pancreatic carcinoma) was originally identified as a candidate tumor suppressor gene [282] and is inactivated in various carcinoma [353]. Moreover, Smad4 mutations are associated with the appearance of the juvenile polyposis syndrome (JPS, see chapter 1.7), a disease which predisposed the patient for gastrointestinal cancer. Also heterozygous *smad4*$^{+/-}$ mice develop intestinal inflammatory polyps [288] (see Table 1.4). General *smad4* knockout in mice revealed that Smad4 is a mesoderm-inducing factor since the knockout mice die early in embryonic development due to the lack of gastrulation [285, 286].

Smad4 shares high structural homology with the R-Smad proteins and also contains an MH1 and MH2 domain connected via a proline-rich linker. But Smad4 (552 aa) misses the C-terminal SSXS phosphorylation motif and the PY motif [4]. Notably, in *Xenopus* a second Smad4 variant exists, XSmad4β, which differs primarily at the extreme N-terminus and in the linker region [354, 355]. Co-Smad4 is essential for the function of R-Smads in mesoderm induction and patterning in

Xenopus embryos, as well as cellular antimitogenic and transcriptional responses which suggested a partnership between co-Smad4 and R-Smad proteins in TGFβ signaling pathways [283, 284]. Smad4 is the central mediator of Smad function which does not bind the receptors but the R-Smads [283, 284, 295, 305]. As mentioned before, heterotrimeric complex formation of R-Smads/co-Smad4 requires intermolecular interaction between the MH2 domains [308, 311-313]. This is supported by the fact that the transcriptional activity and synergistic effects of Smad4 requires the N-terminal MH2 domain; additionally, a proline-rich sequence, the Smad activation domain (SAD), located N-terminal of the MH2 domain, is necessary for the full transcriptional response [284, 356, 357]. Structural analysis demonstrated that the SAD provides this transcriptional competence by tightening the structural core and the surfaces of the MH2 domain for interaction with transcription partners [357]. Furthermore, Smad4 contains a unique loop (H3/4 loop) in its MH2 domain to preclude oligomerization in the absence of signaling [358].

Also the Smad4 protein can be structurally modified: Erk-2 is suggested to phosphorylate Thr276 within Smad4 which interfered with TGFβ-induced nuclear accumulation of Smad4 and transcriptional activity [359]. Moren et al. demonstrated that Smad4 undergoes ubiquitination. After complex formation with the E3 ubiquitin ligase Smurf and R-Smads or I-Smads, Smad4 is ubiquitinated and degraded via the proteasom [360]. Furthermore, tumorigenic Smad4 mutants are polyubiquitinated and thus targeted for proteasomal degradation [361, 362]. Also other ubiquitin ligases as NEDD4-2 or CHIP can mediate Smad4 decomposition [323, 360]. However, when mono- or oligoubiquitinated, Smad4 is modified and heterooligomerization with R-Smads is facilitated resulting in enhancement of signaling [361]. Sumoylation of proteins is a related process. Smad4 is modified by the small ubiquitin-like modifier 1 (SUMO-1) which is mediated by the E2 enzyme Ubc9 and the protein inhibitor of activated Stats (PIAS), an E3-like SUMO ligase. This protects Smad4 from ubiquitin-mediated degradation and consequently enhances transcriptional responses of Smad4 [363-366]. However, it was also reported that sumoylation represses Smad4 transcriptional response involving the transcriptional co-repressor Daxx [367, 368]. Other cytoplasmic interacting proteins of Smad4 regulating BMP signaling are not known. For example, the Smad4 interaction partner Erbin specifically regulates TGFβ signaling [369].

The I-Smads 6 and 7 downregulate ligand-mediated signaling. *Xenopus* studies showed that I-Smads induce dorsalization and neutralization of the embryo indicating an antagonistic role in BMP signaling [289, 292]. Moreover,s*mad6*$^{-/-}$ knockout mice express multiple cardiovascular abnormalities [291]. Ablation of *smad7* resulted in a normal phenotype, but changes in the B cell response were observed [293] (see Table 1.4). In an autoregulatory loop, gene transcription of both *smad6* and *smad7* is regulated by TGFβ superfamily signaling [370-373]. Intriguingly, *smad7* transcription is induced by Interferonγ/Jak/STAT signaling or by nuclear factor (NF)-κB signaling in response to inflammatory cytokines (tumor necrosis factor α (TNFα) and interleukin-1 (IL-1)) and lipopolysaccharides [2]. I-Smads have an N-terminal N-domain, which is different from the MH1 domain in R- and co-Smads, and a C-terminal MH2 domain with high homology to the C-terminus of other Smads; as co-Smad4, the I-Smads lack the SSXS motif [3]. The MH2 domain is responsible for the inhibitory effect of the I-Smad, whereas the N-domain delivers the specificity and regulates the subcellular distribution [374]. Smad6 (496 aa) specifically inhibits the BMP pathway by competing with Smad4 for binding of the receptor-activated R-Smad [289]. As already described, Smurf1 interferes with BMP signaling by triggering R-Smad degradation [317]. In cooperation with Smad6, Smurf1 additionally mediates BMP type I receptor degradation [375]. Consistent with this, Smad6/Smurf1 overexpression in cartilage causes dwarfism with osteopenia hinting towards a strong depression of BMP signaling by these proteins [376]. Besides its cytoplasmic role, Smad6 acts as a nuclear repressor of BMP-dependent transcription [377, 378]. Smad7 (426 aa), however, affects both the BMP and the TGFβ/Activin pathway [292, 379]. It regulates the signal by recruitment of Smurf1 and 2 (and other ubiquitin ligases) for receptor ubiquitination and degradation [380, 381], by binding to type I receptors preventing R-Smad phosphorylation [382], and by recruitment of the PP1 regulatory subunit GADD-34 to TβRI for receptor dephosphorylation and thus inhibition of signaling [383]. Smad7 itself undergoes an Arkadia-mediated poly-ubiquitination which leads to amplification of BMP and TGFβ signaling [384]. Supporting this, ubiquitination-mediated degradation of Smad7 in the kidney might underlie renal fibrosis [385]. However, acetylation of specific lysines through p300/CBP protects Smad7 from ubiquitination and degradation. Thus, the balance between acetylation, deacetylation and ubiquitination of Smad7 regulates its protein stability [386, 387]. Other proteins without enzymatic activity are also able to regulate

I-Smads. The cytoplasmic protein associated molecule with the SH3 domain of STAM (AMSH) was identified as a direct binding partner of Smad6. AMSH prolonges BMP Smad phosphorylation by disrupting binding of Smad6 to the receptors and the R-Smads [388]. Moreover, Tid1 associates with Smad7 and thereby blocks its dorsalizing, i.e. BMP antagonizing effect in *Xenopus* embryos [389].

1.4.2 Smad nucleocytoplasmic shuttling

Nucleocytoplasmic shuttling of Smads is a central mechanism in TGFβ superfamily signaling. Since little is known about Smad shuttling inside BMP signaling, also TGFβ Smads will be discussed here. The nuclear envelope is perforated by the nuclear pores which are formed by huge nuclear core complexes, each containing more than 50 proteins. Nucleocytoplasmic transport is provided by nuclear transport proteins, the karyopherins that can be divided in two functionally subclasses: the importins and the exportins. The importins bind the protein cargo in the cytoplasm via a nuclear localization sequence (NLS), a short basic sequence rich in lysines and arginines. After passing through the pore, the cargo is released through binding of the GTPase Ran-GTP to the complex. The exportins get in contact with their cargo in the nucleus via a leucine- or isoleucine-rich nuclear export sequence (NES), transport it into the cytoplasm and release the protein cargo upon GTP hydrolysis. Sometimes, an adaptor protein connecting the transporter and the cargo is necessary [1]. R-Smads undergo constant shuttling from the cytoplasm to the nucleus and reverse. In the absence of ligand, R-Smads are mainly cytoplasmic due to a faster nuclear export rate compared to the import. Co-Smad4 also constantly moves between the two compartments leading to an equal distribution. Upon stimulation, R-Smads get phosphorylated and complex with Smad4 leading to trapping of the R-Smad/co-Smad complex in the nucleus due to a fast drop in the export rate [390-393]. The reason for this behaviour is based on the masking of the NES within Smad4 after binding to the phosphorylated R-Smads [394]. Right after dephosphorylation of R-Smads, the components are released from the complex for nuclear export [391].

Smad1 has an NLS in the MH1 domain (-K^{39}-K-L-K-K-K-K^{44}-) [395] and is imported into the nucleus via *Drosophila* Moleskin and its mammalian orthologs importin-7/-8 [396]. Besides this, Smad1 nuclear import needs the contact to the

nucleoporin Can/Nup214 suggesting also a karyopherin-independent transport [332]. Furthermore, a C-terminal NES (-L^{406}-T-K-M-C-T-I-R-M^{414}-) was identified. Since Smad1 accumulates in the nucleus upon leptomycine B treatment, a specific inhibitor for exportin-1 (CRM-1, XPO-1), the nuclear export of Smad1 likely occurs via exportin-1 [395]. Smad2 and 3 also harbor an NLS in the MH1 domain and are imported via direct interaction with importin β and/or importin-7/-8 [396-398]. Additionally, karyopherin-independent transport of Smad2 and 3 is aided by Can/Nup214 and Nup153, likely via the MH2 domain [393, 399]. Export of Smad2 and 3 from the nucleus into the cytoplasm is leptomycin B-insensitive, hence exportin-1 does not play a role here [391]. However, it was demonstrated that Smad3 is transported via exportin-4 and Ran [400]. Smad4 contains a constitutively active NLS in the MH1 domain (aa 37-55) [391]. Another study enlarged it to an extended, bipartite NLS (aa 45-110) which binds to importin α [401]. Nuclear export of Smad4 depends on an NES in the linker (-^{142}D-L-S-G-L-T-L-Q^{149}-) and is blocked by leptomycine B. This suggests a Smad4 export via exportin-1 [391, 394]. On the contrary, the distribution of the I-Smads, likely regulated by the N-domains, is different: Smad7 is predominantly nuclear in the absence of ligand, whereas Smad6 can be found in both compartments [374, 402]. Smad6 and 7 are imported to the cytoplasm upon ligand stimulation as well as through Smurfs [374, 380, 381].

1.4.3 Smad transcriptional complexes and Smad-dependent transcription

After nuclear import, the signal transducers Smads bind to DNA to assemble a transcriptional complex at specific target gene sequences for regulating gene expression. Important BMP target genes are *Id1* [210, 403], *Xvent-2* [404, 405], *smad6* [372], *msx-1/-2* [406, 407] or *peroxisome proliferator-activating receptor γ (pparγ)* [408]. All R-Smads excepting Smad2 as well as co-Smad4 selectively bind to DNA in a sequence-specific manner. The β-hairpin in the MH1 domain of the Smad protein associates with the optimal sequence of 5`-G-T-C-T-3´ and its reverse complement 5`-C-A-G-A-3`, the Smad-binding element (*SBE*) [3, 409, 410]. At these sequences the R-Smad/co-Smad complex cooperates with a multitude of sequence-specific transcription factors. The factors not only bind with high affinity to an adjacent DNA sequence (*XBE*), but also recognize the *SBE* to activate transcription in a

ligand-dependent manner. Both sites are enhancer sequences upstream of the TATA box, the initiation site for transcription, where the basal transcription machinery is formed. Inside this multicomponent complex, Smads interact with co-activators or co-repressors which further define the transcriptional response (**Figure 1.9**).

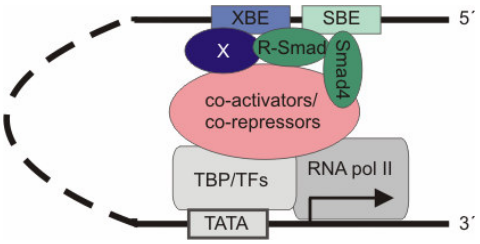

Figure 1.9 A Smad transcriptional complex at the DNA. The complex assembles at specific sequences within the target gene promoter (*SBE*). Other DNA sequences (*XBE*) are important for high-affinity binding of sequence-specific transcription factors (X). A typical complex consists of the R-Smads, the co-Smad, sequence-specific transcription factors, co-activators or -repressors, as well as the basal transcriptional machinery (general transcription factors (TFs), TATA box binding protein (TBP) and RNA polymerase II (RNA pol II)). Drawing adapted from [4].

At the target gene promoter, several sequence-specific transcription factors can associate with the Smads. The transcription factor Runx-2 (Cbfa-1, PEBP2αA, AML-3) of the Runx family is one of the osteogenic master transcription factors that regulates transcription of BMP target genes. Its importance for osteogenic differentiation was first described by Zhang et al. since a truncated Runx-2 protein failed to interact with and respond to R-Smads and thus was unable to induce an osteoblastic phenotype in C2C12 myoblasts in response to BMP-2 [411]. This factor is further described in the context of osteoblast-specific BMP signaling (see chapter 1.6). Furthermore, Smad1 interacts with the homeobox domain protein Hoxc-8 at the *osteopontin* and the *osteoprotegerin* promoter. The interaction with Smad1 prevents Hoxc-8-mediated transcriptional repression and allows transcription in response to BMP [412, 413]. Moreover, Hoxc-9 was found to interact with Smad4 [414]. The homeobox domain protein distal-less 1 (Dlx-1) inhibits Smad4-mediated transcription and blocks BMP, TGFβ and Activin A signaling [415]. Interestingly, Dlx-3 is bound by Smad6 inhibiting the DNA binding of Dlx-3 [416]. Zn finger transcription factors are also implicated in the regulation of BMP- and TGFβ-induced transcription. OAZ interacts with the BMP Smad complex at the *Xvent-2* promoter and enhances signaling [417]. OAZ also complexes with Smad1/4 at the *smad6* promoter to regulate duration and intensity of BMP signaling through Smad6 [418]. Furthermore,

the OAZ-interacting protein poly(ADP ribose) polymerase 1 (Parp1) may serve as a co-activator at these promoters [419]. The Zn finger proteins GATA4, 5 and 6 modulate BMP responses via interaction with Smad1/4 at *smad7* and *nkx2.5* promoters [420, 421]. Moreover, YY1, another Zn finger protein, assembles with Smads and GATAs at the *nkx2.5* promoter to further stimulate BMP signaling [422]. On the other hand, YY1 represses specific BMP and TGFβ gene responses [423]. Schnurri-1 and -2 are Zn finger proteins which are also involved in BMP signaling. *Schnurri-2*-deleted mice show abnormal adipogenesis as well as reduced bone remodeling [424, 425] indicating a connection to BMP signaling. Indeed, Schnurri-2 directly interacts with Smad1/4 at the *pparγ2* promoter finetuning its transcription [424]. Also Schnurri-1 forms a complex with the Smads [426]. Family member of the bZIP proteins are involved in TGFβ superfamily signal transduction [427, 428]. ATF-2 stimulates the *βMHC* promoter activity in a synergistic manner with Smad1/4 and TAK1 and promoted terminal cardiomyocyte differentiation [427]. Other transcription factors as Nanog, an essential regulator of self-renewal on ES cells, blocks the BMP-induced mesoderm differentiation by interacting with Smad1. In mES cells, this leads to inhibition of Smad transcriptional complexes [429], which gives important insight in the regulation of ES cell self-renewal through BMP (see chapter 1.6).

Interestingly, also signaling crosstalk between BMP signaling and other pathways occur at the transcriptional level. Wnt signaling crosstalks to the BMP pathway through interaction of β-catenin with Smad4 at the *msx2* promoter. Inversely, BMP can induce the association of β-catenin, TCF-4 and Smad1 at the *myc* promoter to stimulate its transcription [430, 431]. Furthermore, estrogen signaling is interwoven with BMP signaling. Estrogen induces an interaction of Smad1 and the estrogen receptor that inhibits Smad activity [432]. *Vice versa*, estrogen response is attenuated by binding of Smad4 to the estrogen receptor [433]. Besides this, Notch signaling is influenced by the interaction of Smad1 with the Notch intracellular domain (NICD) and the recruitment of other co-activators as CBP/p300 [434, 435]. Finally, an intermediate of the *Drosophila* Toll pathway, Ecsit, complexes with Smad1/4 and binds to BMP target genes to positively modulate signaling [436].

Transcriptional co-activators increase transcription by bringing the sequence-specific transcription factors into proximity to the RNA polymerase II. The CREB-binding protein (CBP) and p300 are two closely related transcriptional co-activators which often form a complex. Both possess an acetyl transferase (HAT) domain which

modifies chromatin structure; hyperacetylated chromatin is transcriptional active. CBP/p300 strongly interacts with C-terminally activated R-Smads. Binding to Smad4 is also necessary for efficient CBP/p300-mediated co-activation [437] [438, 439]. The co-activators MSG-1 and GCN-5 associate with CBP/p300 and further enhances its co-activating function [440, 441]. Like CBP/p300, ZEB-1 is also implicated in the regulation of both BMP and TGFβ signaling. After binding to R-Smads, ZEB-1 enhances ligand responses by recruiting CBP/p300 to the transcriptional complex. Interestingly, the related ZEB-2 downregulates signaling by recruiting the transcriptional co-repressor C-terminal binding protein (CtBP) [442-444]. The early hematopoietic zinc finger (EHZF), highly homologous to OAZ, binds to Smad1/4 and promotes BMP signaling [445]. Other co-activators interacting with the BMP Smad complex are SMIF and the Smad-interacting zinc finger protein (Sizn-1) [446, 447].

Unlike these proteins, co-repressors of the Smad complex inhibit Smad-dependent transcription. The co-repressor has a general affinity for Smad proteins. Tob interacts with BMP R-Smads and inhibits BMP signaling in osteoblasts [448]. Also TGFβ R-Smad complexes undergo a Tob-mediated transcriptional suppression [449]. Furthermore, Tob interacts with I-Smad6. The co-repressor supports the binding of Smad6 and BMP type I receptors and thereby further downregulates BMP signaling [450]. The Zn finger protein Znf-8 and SNIP-1 act negatively on BMP signaling through interaction with the Smads [451, 452]. Notably, several proto-oncogenes are among the co-repressors linking the inhibition of Smad signaling to malignant transformation. The Zn finger protein Evi-1, for example, binds to R-Smads and suppresses the ligand response due to recruitment of the co-repressor CtBP, which was shown for the TGFβ pathway [453, 454]. The proto-oncogene c-Ski also affects both BMP and TGFβ pathways. Inside the BMP path, c-Ski interacts with Smad1/4 and disrupts the functional complex which results in signaling repression [455-457]. Furthermore, c-Ski engages other co-repressors as well as histone deacetylases (HDACs) to silence transcription [458]. There is first evidence that the related SnoN protein interferes besides TGFβ signaling also with BMP signaling [459]. Finally, the c-Ski/SnoN-related protein Fussel-15 was recently described to associate with Smad1 and 4 leading to the suppression of signaling [460].

1.5 Non-Smad signaling

Besides BMP signaling via Smads, several other signaling pathways, including mitogen-activated protein kinase (MAPK) pathways, can be activated by BMP which mediate specific BMP-induced processes as osteogenic differentiation and apoptosis. Despite their diverse characters, MAPKs share some characteristic features. MAPKs are activated by a protein kinase cascade containing at least two upstream kinases, named MAPK kinase (MAPKK), MAPK kinase kinase (MAPKKK), etc. MAPKs require both tyrosine and threonine phosphorylation to become highly active [461].

The p38 MAPK pathway is probably the best studied non-Smad signaling path. As opposed to Smads, p38 can not directly be phosphorylated by the type I receptor. The BRI-associated protein BRAM-1 links the TAK binding protein 1 (TAB-1) to the receptor complex [253]. TAB-1 is the activator for the TGFβ-activated kinase 1 (TAK-1) [254]. XIAP also binds the receptor complex and TAB-1 and thereby supports TAB-1/TAK-1 function in non-Smad BMP signaling [254, 255]. Moreover, the protein NRAGE is able to associate to and function with the TAK-1/TAB-1/XIAP complex facilitating p38 activation [462]. TAK-1 can not only be activated by TGFβ [463], but also by stress leading on the one hand to the induction of the MAPKK MKK3/6 and p38 and on the other hand to the activation of the MAPKK MKK4 and JNK [464]. Consistent with this, in *Xenopus* BMP signaling TAB-1 and TAK-1 cooperate via MKK3/6 [254]. Interestingly, TAB-1 can also directly induce autophosphorylation of p38 which identified a MKK-independent route of p38 activation [465, 466]. Furthermore, TAK-1 binds the I-Smads 6 and 7 which blocks the BMP-induced TAK-1 activation and hence p38 phosphorylation. This inhibits not only BMP-induced apoptosis but also BMP-mediated neurite outgrowth [467, 468].

The Erk MAPK pathway is also involved in non-Smad BMP signaling. First indication for that was given by Xu et al. who added Ras/Raf signaling, which can activate Erk, to the BMP-induced mesoderm induction of *Xenopus* embryos [469]. Confirming this, MEK-1/Erk signaling participates in BMP-induced target gene transcription [470]. In addition, signaling via JNK and c-jun contributes to BMP signaling [469].

Intriguingly, cell type-dependent BMP stimulation differentially affects these pathways. In the mesenchymal progenitor cell line C3H10T1/2 BMP-2 strongly induces Erk-1/-2 phosphorylation [471]. In C2C12 cells (myoblastic cells) BMP

activates Erk and p38, but not JNK [472]. The BMP-related factor GDF-5 has exactly the same effect in the prechondrocytic cell line ATDC5 [473]. On the contrary, Vinals and co-worker did not observe Erk phosphorylation, but activation of p38 in C2C12 cells [474]. The preosteoblastic cell line MC3T3 also shows less Erk phosphorylation in response to BMP, but p38 activation leading to ALP induction and JNK activation resulting in the expression of *osteopontin* [475]. It is demonstrated that in human osteoblastic cells BMP triggers p38 phosphorylation and the expression of *type I collagen*, *fibronectin*, *osteopontin*, *osteocalcin* and *ALP*. On the other hand BMP can also mediate Erk phosphorylation leading to the induction of *fibronectin* and *osteopontin* mRNA [476]. Due to studies on *Xenopus* ectoderm, Goswami et al argued that the neural fate-repressing action of BMP is caused by inhibition of Erk via the TAK-1/p38 path [477]. Besides these pathways, other signaling molecules participate in non-Smad BMP signaling. During chondrogenesis, PKA can be activated by the BMP ligand leading to CREB phosphorylation [478]. The proapoptotic effect of BMP in primary human osteoblasts was shown to be mediated by PKC without activation of other known BMP target molecules [479]. Lemmonier et al. suggested that PKD might be involved in p38 and JNK activation in reponse to BMP [480]. Furthermore, in osteoblasts and bone marrow stromal cells BMP requires phosphoinositide-3 kinase (PI3K) and PKB/Akt signaling for induction of *ALP* and *osteopontin* [481, 482]. Analog to these findings, in C2C12 cells PI3K signaling via the p70S6 kinase and expression of *ALP* and *osteocalcin* are induced by BMP [474]. p70S6 kinase might also contribute to p38 phosphorylation in osteoblasts [483]. Moreover, Langenfeld and co-workers proclaimed that the phosphorylation of the mammalian target of rapamycin (mTOR) and the activation of its downstream target p70S6 kinase can be observed in lung cancer cells [484]. The BMP-induced non-Smad pathways are summarized in **Figure 1.10**.

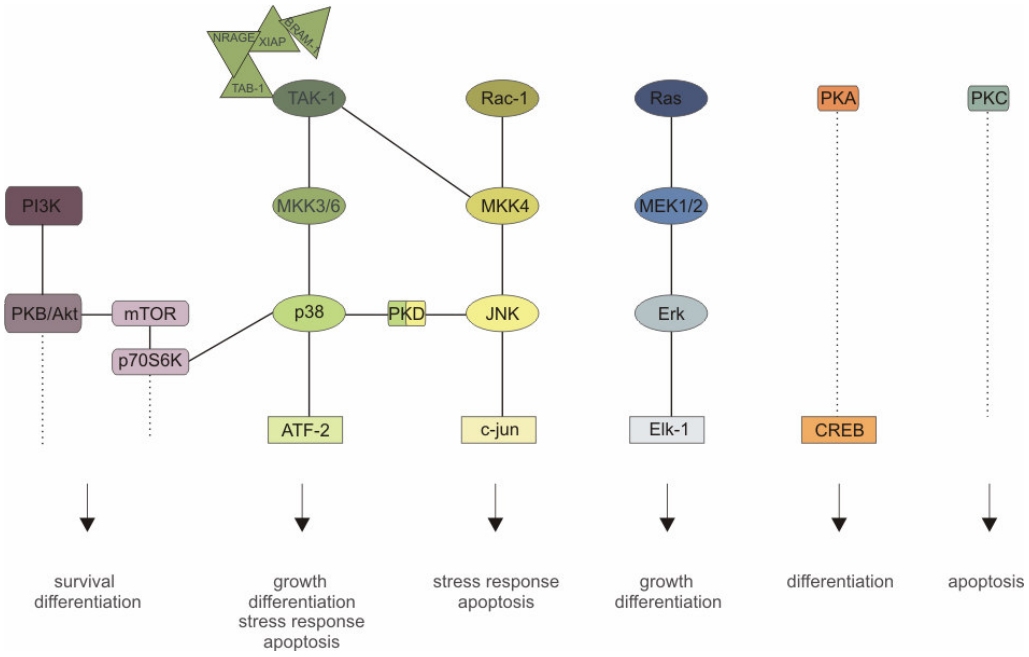

Figure 1.10 Non-Smad signaling activated by BMP. The induced signaling pathways, their components and the cellular responses to BMP stimulation are illustrated.

The BMP-induced Smad and non-Smad pathways can cooperate with each other as shown for instance for the induction of the BMP target gene *pparγ* [408], or work side by side. Actually, they can influence each other as already described in chapter 1.4.1. BMP-7-stimulated renal epithelial cell morphogenesis goes via p38 which in turn is negatively regulated by the Smad pathway [485]. Furthermore, PKB/Akt seems to modulate Smad signaling [481]. Moreover, Ras/Erk signals arising from integrin signaling are described to support Smad-mediated transcription [486, 487].

1.6 BMP signaling in cell- and tissue-specific context

Since the BMP pathway regulates a plethora of physiological events, BMP signaling in cell- and tissue-specific context should be addressed in the following chapter with focus on its skeletal function, its role in vascular smooth muscle cells and its function in stem cells.

In skeletal tissue BMPs are very important for the osteoblastic and chondrogenetic differentiation. Bone tissue that derives from the mesenchymal stem cell lineage consists of osteoblasts (immature bone cells), osteocytes (mature osteoblasts that are responsible for bone formation, matrix maintencance and

calcium homeastasis) and osteoclasts (bone resorbing cells to allow bone remodeling). Bones are built by mesenchymal ossfication or by chondral ossification. Mesenchymal ossification forms bone tissue that originates directly from the mesenchyme. During chondral ossification, the bone tissue is formed via a cartilage intermediate stage, also originating from the mesenchym. The subform endochondral ossification describes ossification from the inside of the “cartilage skeleton” which is responsible for the bone growth in length. Perichondral ossification specifies the bone growth in thickness due to ossification from the outside.

BMPs were originally identified as bone-inducing factors [5] indicating a key role in osteoblastogenesis. Moreover, several knockout studies in mice further support its function (see chapter 1.2.1). In osteoblasts an autoregulatory loop BMP-2 and BMP-4 can be found [488-490]. In accordance to other physiological studies, TGFβ stimulation opposes the positive effect of BMP on osteoblast differentiation [491]. On the other hand, TGFβ-1, fibroblast growth factor 2 (FGF-2) or platelet-derived growth factor AB (PDGF-AB) can upregulate BRIb expression and hence the BMP-induced osteogenic differentiation [492]. However, hepatocyte growth factor (HGF) inhibits BMP Smad signaling leading to diminished expression of osteogenic markers [493]. Over the years, several intracellular osteoblastic and chondrogenic regulators of BMP signaling were identified. The probably most important one is the DNA-binding transcription factor Runx-2 since *runx-2*$^{-/-}$ mice show a severe skeletal phenotype; they lack bone [494, 495]. *Runx-2* mRNA is upregulated after BMP stimulation in the mesenchymal stem cell line C2C12 to induce osteoblastic differentiation, as well as in osteoblasts and chondrocytes [496-498] suggesting a key role in both differentiation events and in the differentiated, mature cells. The Runx-2 isofoms I and II are expressed in osteoblasts. Runx-2 is a positive transcriptional regulator of diverse osteoblastic marker proteins as osteocalcin, osteopontin and collagen I [7, 478]. As demonstrated, BMP antagonists as Noggin or Gremlin suppress *runx-2* expression and thus downstream events like *osteocalcin* induction [122, 499]. Another transcription factor, Osterix, is also very important for bone formation since ablation of *osterix* in mice lead to normal cartilage development, but to lack of bone [500]. BMP stimulation results in increased Osterix expression in osteoblasts and chondrocytes via Runx-2 and via additional activation of MAPK pathway [500-504]. Mammalian homologs of *Drosophila* Dlx proteins are also essential for skeletal development which in osteoblasts is concomitantly expressed

with Osteocalcin [7, 505]. BMP upregulates *dlx5* expression [506] which participates in the induction of Runx-2, osterix and ALP [503, 507-510]. *Msx-1* and *msx-2* are expressed in skeletal cells and modulate osteogenesis. Knockout studies demonstrate the function of *msx* proteins since the mice exhibit defects in bone growth and limb development [511, 512]. The expression of Msx-2 is induced by BMP-2 and thus the BMP-triggered differentiation of C2C12 cells into the osteoblastic lineage is mediated by Msx-2 [7, 513]. Moreover, Osteoactivin stimulates osteoblastic differentiation markers as a downstream mediator of BMP-2 without affecting cell proliferation or viability [514, 515]. Both, vitamin D and the parathyroid hormone (PTH) also stimulate the expression of osteoblastic marker proteins in bone marrow-derived mesenchymal stem cells [516]. Moreover, integrin signaling through the focal adhesion kinase (FAK) positively contributes to osteogenic BMP signaling [517]. Finally, several other proteins influence the osteoblastic function of BMP, as the mesenchymal forkhead-1 (MFH-1) [518], Bapx-1/Nkx3.2 [519, 520], the C/EBP family [7, 521], Pitx-2 [522] and cas-interacting zinc finger protein (CIZ) [523, 524]. Via crosstalk mechanisms, BMPs positively influence the expression of proosteoblastic factors as insulin-like growth factors (IGFs) [525], LDL receptor-related protein 5 (LRP5, a Wnt receptor) [526] or N- and E-cadherins [527]. All regulatory mechanisms on BMP ligands, receptors, Smads and associated proteins, described in the chapters before, may also contribute to the activity of BMP signaling in bone and cartilage development. Regarding bone tissue homeostasis, the role of BMP signaling can be expanded to the regulation of osteoclastogenesis. On the one hand, BMP induces the expression of Osteoprotegerin, a cytokine inhibiting osteoclasts [413], and inhibits the expression of Collagenase 3 that cleaves type I and type II collagens [528]. On the other hand, osteoblasts produce besides self-maintaining factors also factors important for osteoclast differentiation. A key protein is the receptor activator of NF-κB ligand (RANK-L). BMPs enhance the susceptibility of osteoclasts for the RANK-L effect [7].

Vascular smooth muscle cells (VSMCs), originating from mesenchymal stem cells, coat blood vessels and thus regulate the vascular tone. VSMCs express in their contractile, differentiated state smooth muscle cell-specific proteins as α-actin and smooth muscle myosin. Proliferation of VSMCs comes along with phenotypic modulation forming cells in a synthetic, dedifferentiated state; these cells express ECM proteins as collagen, fibronectin and osteopontin. Proliferation and migration is

always associated with the loss of the SM phenotype and enhanced ECM synthesis. *In vitro* proliferation of VSMCs is normally induced by PDGF or serum stimulation [529]. BMP inhibits *in vitro* and *in vivo* proliferation of rat and human VSMCs [530, 531]. Consistently, the BMP antagonist Gremlin induces proliferation of rat VSMCs [532] as well as a dominant-negative Smad1 [533]. The anti-proliferative effect of BMP on VSMCs seems to involve the induction of apoptosis through downregulation of Bcl-2 or activation of caspases and cytochrom c release [534, 535]. Moreover, a BMP-mediated inhibition of the cyclin-dependent kinase 2 (cdk-2) which is activated after PDGF can be observed [530]. Upregulation of voltage-gated K+-channels and heme oxygenase 1 (HO-1) through BMP ligands contribute to the anti-proliferative effect of the cytokine [536, 537]. Additionally, smooth muscle cell-specific gene expression is regulated by BMP signaling [538-540]. A recent study revealed that the induction of the contractile phenotype of human VSMCs, i.e. the operation of anti-proliferative signals, by BMP and TGFβ is mediated by miRNA-21 (miR-21). miR-21 downregulates programmed cell death 4 (PDCD-4) that is a negative modulator of smooth muscle gene expression. Interestingly, miR-21 biogenesis via DROSHA is controlled by Smads [541]. All these findings suggest that BMP signaling is essential for the homeostasis of vascular tissue. Indeed, a severe vascular disorder, pulmonary arterial hypertension (see chapter 1.7), which is characterized by hyperproliferation of VSMCs and vascular endothelial cells, is associated with heterozygous germline mutations in BRII [213-215, 542]. The BRIa/BRII receptor complex is responsible for BMP signal transduction [218, 543] and BRII is required for the BMP-mediated growth arrest in human PASMCs since cells harboring BRII PAH mutants are insensitive for the BMP-induced anti-proliferative effect [251, 544]. This is supported by the finding that suppression or inactivation of BRII results in increased thickness of pulmonary arteries and increased muscularization of small pulmonary arteries and altered vascular tone [539, 540]. Mutations in BRII causing PAH disrupt Smad signal transduction specifically at the transcriptional level; but also non-Smad signaling via MAPK p38 or Erk-1/-2 seems to be affected by these mutations [216, 231, 545]. Despite these strong indications, some publications claim that a second genetic hit is necessary for the development of PAH. Candidates are the serotonin and the IL-6 pathway. Aberrant serotonin signaling causes hyperplasia of the pulmonary artery [546]. Long et al. described a croostalk to the BMP pathway since serotonin inhibits Smad signaling and enhances the susceptibility to PAH in

BRII-deficient mice [547]. IL-6 signal transduction is also implicated in PAH since IL-6 stimulates Smad signaling and IL-6 expression is dysregulated in BRII-defective PASMCs [548]. Deletion of BRII in VSMCs furthermore lead to increased levels of Tenascin-C, a protein that promotes VSMC proliferation [545] and osteoprotegerin [549]. Crosstalk to other signaling pathways, e.g. via BRII-associated proteins, increases the complexity of the BMP signaling system and is assumed to influence pulmonary hypertension diseases [191, 261, 264, 268].

Stem cells play an important role in cellular specification and pattern formation. As a special feature they exhibit the potential for self-renewal which requires maintenance of their proliferation potential, inhibition of apoptosis and blocking of differentiation [550]. The molecular mechanism of self-renewal, however, is poorly understood. Three types of stem cells exist: somatic stem cells that specify to the mesenchymal and hematopoietic lineage, germinal stem cells which are derived from the embryonic precursors of the adult gametes, and embryonal stem (ES) cells that come from the inner cell mass of the blastocyst and are able to produce all three germ layers. The neural crest stem cells (NCSCs) are derivates of ES cells [9]. Mouse ES (mES) cells can be cultured on fibroblastic feeder cells which produce a set of factors necessary for mES cell self-renewal. Wnt signaling is associated with self-renewal of embryonic stem cells as well as TGFβ signaling [551-553]. The leukemia inhibitory factor (LIF) is another factor that supports mES cell growth [554, 555]. But LIF cannot maintain the pluripotency of mES cells and instead induces neural differentiation in the absence of serum [550]. Cooperation of LIF with BMP enables cultivation of mES cells in an undifferentiated state since BMP inhibits neural differentiation [556, 557]. This maintaining action probably functions via Id protein upregulation because overexpression of Ids in the presence of LIF (in the absence of serum and feeder cells) is sufficient for self-renewal of mES cells [557]. Also a contribution of the MAPK pathways is suggested [558].

In human ES (hES) cells the situation is different. Whereas mES cells require LIF to maintain self-renewal, hES cells need basic fibroblast growth factor (bFGF) to support their pluripotency [553, 559, 560]. bFGF in combination with the BMP antagonist noggin for BMP activity reduction supports long-term cultivation of hES cells in an undifferentiated state [561]; a similar effect is achieved by Activin A that suppresses BMP expression in hES cells [562]. Inhibition of BMP via Noggin in mES cells, however, resulted in cardiomyocyte differentiation [563]. BMP, FGF and Activin

A mediate hepatic specification of mES cells [564]. BMP and TGFβ co-treatment in hES cells results in chondrogenically differentiated cells [565].

Importantly, also the microenvironment in which stem cells are found are regulated by BMPs. This microenvironment is named stem cell niche [566], which is composed of specific other cell types interacting with the stem cells to regulate stem cell fate. Stem cell niches are found in vertebrates in the bone marrow (hematopoietic stem cell niche), at the hair follicle or in the intestinal system. However, the stem cell niche for ES cells is the trophoblast. Zhang et al. could show that BMP signaling is important for the control of hematopoietic stem cell niches and thus for hematopoietic stem cell numbers [567].

1.7 Diseases related to BMP signaling and its components

Since BMP signaling and related pathways are strictly regulated within the body, mutations in genes involved in this complex network of signaling are linked to several diseases.

Pulmonary arterial hypertension (PAH, OMIM178600; formerly known as primary pulmonary hypertension), mapped to chromosome 2q33, is an autosomal dominant vascular disease which is characterized by narrowing of the pulmonary artery and formation of plexiform lesions caused by vascular remodeling of the small pulmonary arteries through abnormal proliferation of VSMCs and endothelial cells (**Figure 1.11**).

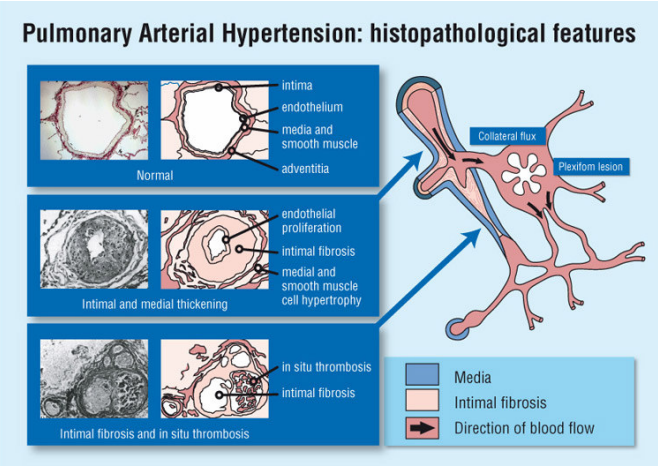

Figure 1.11 PAH exhibits characteristic histological features including medial hypertrophy, intimal thickening, plexiform lesions and *in-situ* thrombosis. PAH is defined as elevation of the mean pulmonary arterial pressure by more than 25 mmHg at rest or by more than 30 mmHg while exercising. Image from http://www.pah-info.com.

Accompanied with vasoconstriction, PAH patients suffer from elevated pressure in the pulmonary artery and right ventricular failure leading in severe cases to death [568]. PAH can occur idiopathically (idiopathic or sporadic PAH (IPAH)) or sometimes is inherited (familial PAH (FPAH)). The majority of cases of familial PAH (>50%) but also some cases of idiopathic PAH (10-25%) has been shown to be associated with heterozygous germline mutations in BRII [13, 213-215, 542]. Most of these mutations represent missense, nonsense or frame-shift mutations in BRII and are supposed to lead to the loss of BRII function. Studies in endothelial cells or SMCs of the pulmonary artery, isolated from PAH patients, revealed altered growth response to TGFβ and BMP stimulation [544], reduced expression of BRII [569] and insusceptibility to BMP-induced apoptosis [534, 535]. Smooth muscle-specific expression of mutant BRII in transgenic mice suggests that loss of BRII function in smooth muscle cells is sufficient to cause a PAH phenotype. Conditional ablation of *br2* results in increased thickness of pulmonary arteries, increased muscularization of small pulmonary arteries and altered gene expression affecting cytoskeletal rearrangements, inflammation and vascular tone [539, 540]. Furthermore, Takeda et al. found significant increased expression of BRIb (ALK6) in PASMCs from patients without genetic BRII mutations that might contribute to altered mitosis function in these cells [570]. Taken together, dysregulated BMP signaling strongly affects the pathogenesis of PAH but the detailled mechanism behind this genotype-to-phenotype axis is still unclear. Treatments of PAH range from decreasing the pulmonary vasculare resistance (vasodilators (nitric oxide, sildenafil, calcium channel blockers) and anticoaglutants) to increasing cardiac output (digoxin). Moreover, BRII gene therapy in rats can attenuate hypoxic pulmonary hypertension [571].

Fibrodysplasia ossificans progressiva (FOP, OMIM135100) is a rare and severe disease of extraskeletal, heterotropic ossification of connective tissue and muscle [145], mapped to chromosome 2q23-24. The disease begins in childhood and is induced by trauma or occurs sporadic. The progressive ossification also affects all major joints which lead to stiffness of the limbs making movement nearly impossible. **Figure 1.12** shows the extensive extraskeletal bone formation of a FOP patient:

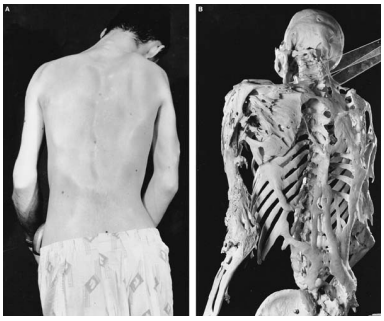

Figure 1.12 Extensive heterotropic bone formation of the back of a FOP patient. (left) photography, (right) 3D computer tomography scan (Kaplan: The molecules of immobility: searching for the skeleton key, Vol 11, 1998, UPOJ)

FOP seldom is inherited since the severe disability is responsible for a low reproductive fitness. Therefore, it is difficult to identify gene mutations. Nevertheless, mutations in the BMP receptor ActRIa (ALK2) were found, among others near the GS Box of the receptor [572]. Furthermore, some cases of FOP can also be attributed to mutations in the BMP antagonist Noggin [146-149]. Interestingly, BMP-induced heterotopic ossification can be influenced *in vivo* by local delivery of Noggin variants [573]. Moreover, BMP signaling is thought to be dysregulated in FOP patients [574]. BMP-2/-4 expression is upregulated in some sick persons [575, 576], which is supported by Kan et al. who established a FOP-like phenotype in mice overexpressing BMP-4 [577]. Isolated lymphocytes from FOP patients show not only altered extracellular modulation of the BMP ligand [578], but also exhibit a dysregulation of BMP type I receptor trafficking [579] and MAPK-p38 signaling which is the major BMP pathway in these cells [580].

Another disease associated with TGFβ and BMP signaling is hereditary hemorrhagic telangiectasia (HHT, also known as Osler-Weber-Rendu syndrome). This inherited autosomal dominant disorder is characterized by multi-vascular malformations, the telangiectasias occurring on digits, skin mucosal linings, in brain, lung and the gastrointestinal tract. The blood vessel dysplasia lead to bleeding from nose and the gastrointestinal tract causing chronic anemia and can be accompanied with stroke [13]. Several types of HHT exist. Genetic analysis of HHT1 (OMIM187300) patients revealed chromosome 9q33-34 as mutated site, the gene locus of endoglin [581]. The protein is a known co-receptor for TGFβ and BMP (see chapter 1.3.3) and the more than 150 known mutations mainly occur in the extracellular part [13, 582]. HHT2 (OMIM600376) is mapped to chromosome 12q11-14 and is caused by mutation of ALK1 [583, 584], a receptor for BMP-10 [239]. Most

of the more than 120 known mutations probably cause truncation or misfolding of the receptor [13, 582]. Another TGFβ superfamily signaling molecule is implicated in a HHT/juvenile polyposis syndrome (OMIM175050) overlap disease, the co-Smad4 [585]. Also an overlapping syndrome of HHT and PAH was identified [586] [587].

The juvenile polyposis syndrome (JPS, OMIM174900) is a hereditary autosomal dominant disease. JPS patients show gastrointestinal mamartomatous polyps and are predisposed for gastrointestinal cancer, mainly colorectal cancer; sometimes this disorder is accompanied with cardiac failure and microcephaly [13]. Two BMP signaling players are known mutated molecules within this disease, BRIa and co-Smad4. More than 20% of the JPS patients show genetic affection of the *br1a* gene. The mutations mainly influence ligand binding and kinase activity of the receptor [13, 588-590]. Co-Smad4 mutations causing JPS are more prominent in the C-terminus of the protein affecting oligomerization with Smads and binding to DNA, but are less frequently compared to BRIa [13, 588, 591]. Interestingly, studies in mice revealed that inhibition of BMP-4 by overexpression of Noggin lead to a phenotype that copies that one of JPS patients [592]; moreover, conditional inactivation of *br1a* in mice causes tumors resembling the human JPS [593].

Several lines of evidence besides the JPS suggest that BMP signaling may contribute to the carcinogenesis of several tissues and organs. In the following, the main cancer types associated with impaired BMP signaling are briefly introduced. BMP signaling participates in apoptosis and is thus as a negative regulator of proliferation and potential modulator of tumor growth [594]; metastasis, however, seems to correlate with overexpression of components of BMP signaling [595]. Pancreatic cancer is often associated with mutations in the *smad4* gene, which since then is a well known tumor suppressor gene [282, 353]. Furthermore, mutations of the *smad4* locus or near by the locus were found in other tumor tissues, as breast cancer and malignant skin tumors [596]. During skin carcinogenesis, loss of BMP and TGFβ Smads and concomitant overexpression of I-Smad7 contribute to the loss of growth inhibition mediated by BMP and TGFβ signaling resulting in tumor progression [597]. Furthermore, analysis of stromal cells of skin carcinomas revealed that reduced BMP signaling might contribute to the establishment of a favorable microenvironment for tumors [598]. Inactivation of epidermal BRIa signaling lead to hair follicle tumor formation [599]. In renal cancer SOSTDC-1, an inhibitor of cell proliferation as well as a BMP antagonist (see chapter 1.2.3), is downregulated [132].

Furthermore, inhibited BMP-2 expression may be related to gastric carcinogenesis [600]. Several studies revealed moreover, that BMP signaling affects the development of colorectal cancer [601-604]. Yamada et al. suggest the presence of BMP receptors and hence a functional role for BMPs in malignant glioma [605]. Additionally, BMPs inhibit the tumorigenic potential of tumour-initiating cells in brain [606]. In medulloblastomas BMP-2 mediates cell apoptosis in a retinoid-dependent manner [607]. Osteo- and chondrosarcomas express several BMP variants and BRII; furthermore, overexpression of BRII correlates with poor prognosis in malignant and metastatic bone tumors [608]. Studies in malignant prostate tumors suggest that BMP signals inhibit growth of prostate tumor cells [609]. Finally, overexpression of BMPs and BRIa are associated with the malignancy of oral epithelium [610].

Besides other influences, some cases of osteoporosis could be linked to mutations in the *bmp-2* gene [611]. Furthermore, some BMP antagonists are also involved in the pathogenesis of diseases as sclerosteosis affecting bone and joints (see chapter 1.2.3).

1.8 Nitric oxide (NO)/ cyclic guanosine 3',5'- monophosphate (cGMP) signal transduction via cGMP-dependent protein kinases

Exogenous and endogenous factors as hormones, neurotransmitters and toxins transduce their signal through the second messenger cyclic guanosine 3',5'-monophosphate (cGMP). Synthesis of cGMP via nitric oxide (NO)-sensitive guanylyl cyclases, targeting of cGMP-dependent protein kinases (cGKs) and cyclic nucleotide-gated (CNG) cation channels, and degradation via phosphodiesterases (PDEs) is highly regulated and dysfunction of these processes affects mainly vascular physiology. Signaling via cGMP plays a key role in vascular homeostasis, cellular permeability, cell survival and proliferation. NO can also influence other cellular processes independent of cGMP [612], which will be not discussed here.

1.9 NO synthases and NO

NO is a gaseous free radical and a cellular second messenger involved in vascular regulation, immunity, defense and neurotransmission. Impaired NO levels result in

vascular dysfunctions, and are also implicated in the development of diabetes mellitus, neurodegenerative disorders, cerebral infarction and septic shock. In the 19th century, the first evidence for the benefical effects of NO on cardiovascular tissue was shown by treatment of angina and heart failure with organic nitrates. For the discovery of NO as a cell signaling molecule in the cardiovascular system, the 1998 Nobel Prize in Medicine has been awarded to Robert F. Furchgott, Louis J. Ignarro and Ferid Murad.

NO is generated from L-arginine, molecular oxyene and NADPH by NO synthases (NOS). L-arginine is enzymatically synthesized from the organic compound citrulline, molecular oxygen and NADPH. L-arginine is not only a precursor molecule for the synthesis of NO, but also for the production of urea, polyamines and proline. The reaction is catalyzed by NO synthases (NOS) which exist in three isoforms: neuronal NOS (nNOS), inducible NOS (iNOS) and endothelial NOS (eNOS) [613, 614]. nNOS (NOS1, 160 kDa) is constitutively expressed in neural tissue and skeletal muscle. It is a Ca^{2+}/calmodulin (CaM)-dependent enzyme. eNOS (NOS2, 133 kDa) activity is also Ca^{2+}/CaM-dependent and its expression can be observed in the endothelium. However, iNOS (NOS3, 131 kDa) can ubiquitiously be induced in all tissues which are subjected to cytokines, endotoxins or other proinflammatory stimuli. NOS is a bidomain protein with an N-terminal oxygenase domain, which binds heme, and a C-terminal reductase domain with FMN, FAD and NADPH binding sites. In between sits a central CaM binding motif. Heme, FMN, FAD, CaM as well as tetrahydrobiopterin (BH_4) are essential co-factors for the activity of all NOS isoforms. Furthermore, homodimerization is required for NOS function [613]. All NOS proteins interact with the protein inhibitor of NOS (PIN) which inhibits NOS activity by dissociating the active homodimers. Moreover, inactive NOS proteins associate with caveolin isoforms suggesting a localization at the membrane, whereas upon activation NOS probably drifts away from caveolin [613]. nNOS furthermore contains an N-terminal PDZ domain indicating a localization to cell-cell contacts [613]. iNOS associates with the Rho-like GTPases Rac1 and Rac2 (Ras-related C3 botulinum toxin substrate 1 and 2) that regulate the cellular distribution of iNOS [615]. Finally, NOS function is modulated by phosphorylation through kinases as CaMK, PKC, PKA and cGK. The latter will be addressed in chapter 1.11. Several chemical compounds as N^G-nitro-l-arginine methyl ester (L-NAME) were shown to inhibit NOS [616].

1.10 cGMP and its effectors

Extracellular cGMP was first described in 1963 as a molecule detected in rat urine [617] soon after the discovery of adenosine 3', 5'- monophosphate (cAMP). cGMP is synthesized by guanylyl cyclases (GCs) and degraded by specific phosphodiesterases (PDEs).

1.10.1 Generation and degradation of cGMP and target molecules of cGMP

1.10.1.1 cGMP generation via guanylyl cyclases

While adenylyl cyclases are membrane-bound enzymes, GCs exist in a membrane-bound and in a cytosolic variant. The cytosolic GCs are named soluble GCs (sGCs) and the membrane-bound ones particulate GCs (pGCs). sGCs are the receptors for NO and pGCs bind natriuretic peptides which generally induce natriuresis and diuresis. However, both enzymes groups catalyze the conversion of guanosine 5´-triphosphate (GTP) to guanosine 3´, 5´-monophosphate (cGMP) (**Figure 1.13**).

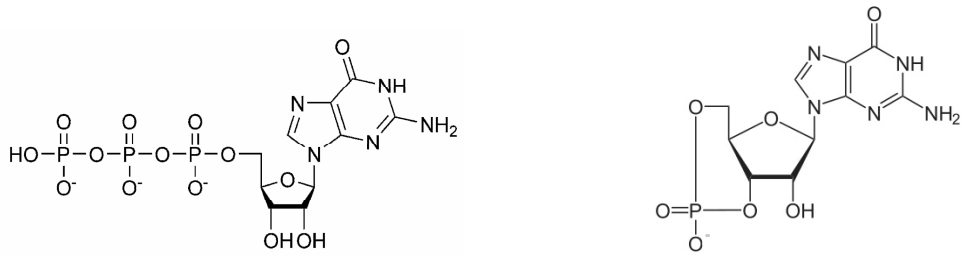

Figure 1.13 The conversion from GTP (left) to cGMP (right) is catalyzed by guanylyl cyclases under the generation of pyrophosphate.

sGCs are expressed in almost all mammalian tissues and participate in inhibition of platelet aggregation and vasodilation as well as neural signal transduction [618]. They exist as a heterdimer with a large α subunit (about 80 kDa) and a small β subunit (about 70 kDa). Each subunit has several isoforms. The most abundant heterodimer is the $\alpha 1/\beta 1$ heterodimer that exhibits a high and specific activity [618,

619]; but also α2/β1 and α1/β2 heterodimers can be found whereas the β2 isoform is associated with tumorigenesis [620]. Furthermore, about 10% of the sGCs exist as homodimers [621]. An atypical sCG expressing only a single β isoform was also isolated [622].

Each isoform can be structurally divided into three domains: an N-terminal regulatory domain, a central dimerization domain and a substrate recognition/catalytic domain at the C-terminus. The N-terminal domain binds heme at a prosthetic group. Heme is a five-membered nitrogen-containing ring with four nitrogens around the central iron plus an additional nitrogen from the imidazol group of His105 [618, 623]. The heme moiety, sandwiched between the two subunits, keeps the cyclase in a restricted conformation. Binding of NO to Fe^{2+} induces the formation of ferrous-nitrosyl heme and a conformational change leading to increased activity of the cyclase. Heme ablation results in enhanced cGMP-generating ability [618, 624]. The central domain is necessary for dimerization. Heterodimerization is a prerequisite for the catalytic activity of the enzyme [625]. The C-terminal catalytic domain is structurally similar to the catalytic domain of adenylyl cyclases but specifically differ in residues needed for substrate recognition and catalysis. The catalytical core is formed by the two subunits making both subunits indisensible for the enzymatic reaction [618]. For the expression of maximal catalytic activity, sGCs require further substrate co-factors and allosteric modulators as divalent cations (Mg^{2+}, Mn^{2+}). Furthermore, several chemical compounds are known to influence the catalytic activity of sGCs. Compounds of the BAY series such as BAY 58-2667 [626] and YC-1 [627] are potent activators, whereas 1H-[1,2,4]oxadiazolo[4,3-a]quinoxalin-1-one inhibits sGC function [628]. Interestingly, potential CaMK, PKC, PKA and cGK sites within the sGC proteins were identified, but the results are discussed controversially. On the one hand cGK phosphorylates sGC *in vitro* leading to decreased sGC activity [629], and on the other hand cGK stimulation resulted in reduced sGC phosphorylation [630]. In addition, other interactions or post-translational modification are suggested to regulate the subcellular localization of sGCs. Although sGCs imply to be soluble, about 20% of α1/β1 heterodimers are found in the heart in the membrane fraction [631]. Moreover, in endothelial cells the majority of sGCs is tethered to the membrane likely through eNOS, whereas in VSMCs - lacking eNOS - most of sGCs is found in the cytosol [632].

The membrane-bound pGCs are expressed in almost all tissues and seven mammalian variants, pGC-A to pGC-G, are known. They are classified in natriuretic peptide (NP) receptors, intestinal peptide-binding receptors and orphan receptors. pGC-A and pGC-B, both with a molecular weight of about 118 kDa, bind NPs. Atrial NP (ANP) maintains cardiovascular homeostasis and binds strongly to pGC-A. The circulating, mature form of the hormone has 28 aa [618, 633]. A 17 aa loop is stabilized by an intrachain disulfide bridge and N- and C-terminal extensions. Brain NP (BNP) has 26 aa in total and exhibits the conserved loop structure as well as the C-terminus [634, 635]. C-type NP (CNP) is 22 aa long. It displays the loop, but no N- and C-terminal extensions. CNP generally fulfills the same tasks as ANP and BNP, but is less potent [636]. Interestingly, mice lacking CNP develop dwarfism and inversely, overexpression of CNP or BNP resulted in bone overgrowth [637-639].

pGCs are structurally organized in extracellular domain, single transmembrane domain, cytoplasmic juxtamembrane domain, regulatory domain, hinge domain and the C-terminal catalytic domain [618]. Some isoforms exhibit a further C-terminal extension. The extracellular domain is homolog among the isoforms, but shows specific variations. It contains N-linked glycosylation sites which might be involved in ligand binding. Two conserved cysteine residues control ligand-independent complex formation, since pGCs exist as preformed homodimers in the basal state [640]. The juxtamembrane domain is probably involved in regulating alternate signaling processes. The regulatory domain is a kinase homology domain with several phosphorylation sites for the modulation of enzymatic activity. The hinge region connects the regulatory with the catalytic domain and mediates dimerization of the catalytic domain. The catalytic core is closely related to the corresponding domain in adenylyl cyclases. But three invariant residues are responsible for the nucleotide specificity [641]. A striking difference to sGCs is that homodimeric pGCs offer two substrate sites in one single cleft which can bind two substrate molecules per dimer, whereas in sGCs a single active site is formed by two catalytical subunits which binds one substrate per dimer. The C-terminal tail, if present, is involved in protein internalization and modulation of the enzymatic activity [618].

1.10.1.2 cGMP degradation via phosphodiesterases

Inside the cell, a balance exist between cGMP production via GCs and degradation by 3´,5´-cyclic nucleotide phosphodiesterases (PDEs). In mammals, eleven families of PDEs were identified. Each PDE subfamily harbors several isoforms. PDE5, 6 and 9 are highly selective for cGMP. PDE1, 2 and 11 show dual substrate affinity, whereas PDE3 and 10 are cGMP-sensitive, but cAMP-selective. The primary cGMP hydrolyzing PDEs in the cardiovascular system are PDE1, 2 and 5 [642] which are in the focus of this section.

PDE5 (100 kDa) is a cytosolic protein that is highly expressed in lung, heart, platelets and vascular smooth muscle and is selective for cGMP hydrolysis. cGMP binds two N-terminal GAF domains within the PDE5 molecule. GAF domain is an abbreviation for mammalian cGMP binding PDEs, *Anabaena* adenylate cyclase and *E.coli* Fh1A, since all proteins harbor a homolog cGMP binding domain. This domain has a high affinity for cGMP and after binding, a conformation of the catalytic domain is induced which is more potent for cGMP binding and thus degradation [642, 643]. This auto-feedback loop is furthermore affected by specific phosphorylation. Corbin and co-workers elucidated a PKA- and cGK-dependent phosphorylation at Ser102 which is involved in activation of the human enzyme. Phosphorylation at Ser102 enhances the enzymatic activity and binding of cGMP to its allosteric cGMP binding sites [644]. Moreover, cGMP or sildenafil binding to the catalytical site enhances cGMP binding at the allosteric sites [645, 646]. Interestingly, cAMP and cGMP can also induce *pde5A* mRNA transcription [642, 643]. PDE5 is specifically inhibited by sildenafil and the related compounds tadalafil and vardenafil [647]. Interestingly, the effectiveness of PDE5 can also be blocked by the NOS inhibitor L-NAME; mice lacking eNOS display no sildenafil-mediated PDE5 inhibition. Both indicate a selective interaction of PDE5 and NO-stimulated cGMP [643, 648].

PDE1 is expressed in heart, brain, lung and smooth muscle. PDE1A, 1B and 1C isoforms (61-72 kDa) are Ca^{2+}/CaM-dependent and have a low activity for cGMP and cAMP hydrolysis in the absence of Ca^{2+}. Furthermore, the binding affinity for cGMP is markly reduced after PKA- and CaMKII-mediated phosphorylation. cGMP binding itself is not suitable to regulate PDE1 since the enzyme lacks the GAF domain. Specific inhibitors such as KS-505a or IC 86340 downregulate the activity of PDE1. Expression of PDE1A is upregulated upon nitrate treatment. Interestingly,

pde1C mRNA is transcribed in proliferating human arterial SMCs but not in quiescent SMCs. The status of VSMCs also influences the subcellular localization. In synthetic VSMCs PDE1A is found in the nucleus, but it is predominatly cytosolic in contractile cells suggesting that nuclear PDE1A plays a role in the regulation of VSMC proliferation and apoptosis [642, 643]. Besides this, *pde1B*$^{-/-}$ mice display increased locomotor activity and dysfunctions in spatial learning [649].

As PDE1, also PDE2 hydrolyzes cAMP and cGMP, when it is the primary substrate. PDE2 is expressed in heart, lung, liver and platelets and is localized to the membrane since the protein contains a hydrophobic sequence at the N-terminus. Moreover, in neurons PDE2A is associated to lipid raft and co-localizes there with other NO/cGMP signaling components such as NOS. The phosphodiesterase is allosterically stimulated by cGMP binding to its GAF domain. Among other stimuli, PDE2A expression is increased in human umbilical vein endothelial cells (HUVECs) via TNFα and p38 MAPK action. PDE2 can be blocked by EHNA or BAY 60-7550 [642, 643].

1.10.1.3 Target molecules of cGMP

Target molecules of cGMP are cyclic nucleotide-dependent kinases, mainly cGK and, with less sensitivity also PKA, and cyclic nucleotide-sensitive phosphodiesterases. cGKI, one of the cGMP-dependent kinases, is discussed in detail in the following chapter (chapter 1.11). Also PDEs are controlled by cGMP through cGMP binding to GAF domains (see chapter 1.10.1) [642, 643]. Besides cGKs and PDEs, cyclic nucleotide-gated (CNG) cation channels are also regulated by the ligand cGMP. In 1985, it was discovered that cGMP can directly activate the light-dependent channel of rods [650]. cGMP-sensitive CNGs are gated open by cGMP. A specific feature of these channels is their Ca^{2+} permeability. Ca^{2+} current is crucial for excitation and adaption of photoreceptors and chemosensory cells since Ca^{2+} regulates several enzymes involved in signal transduction events. In addition, similar cGMP-sensitive channels with Ca^{2+} flow were identified in the brain and in nonneuronal tissue [651].

In humans, a family of six genes encodes for four α subunits (CNGA1-4) and two β subunits (CNGB1 and 3). The α subunits can form a functional homomeric channel on their own. However, the β subunits are unable to homodimerize and are thus seen as the modulatory subunits. The channels are structurally dissected in the

N-terminal CaM binding motif, the transmembrane region with a voltage-sensitive segment and the pore region, and C-terminal the binding site for cyclic nucleotides and a glutatmic acid-rich peptide. The cyclic nucleotide is bound through polar and nonpolar interactions and induces conformational changes within the CNG cation channel [651]. Surprisingly, in *cnga2*- and *3*-deficient mice no phenotypic alterations were reported other than loss of smell and vision, respectively, although they are widely expressed [651].

1.11 cGMP-dependent protein kinases

cAMP-dependent- and cGMP-dependent protein kinases show striking similarities in the amino acid sequence. Cyclic nucleotides bind and activate the protein kinases. However, the kinases specifically bind different cyclic nucleotides. Structural analysis of the cGMP binding domains of the cGMP-dependent protein kinases (cGKs) revealed that an alanine/threonine difference has the potential for discriminating between cAMP and cGMP and thus may be important in the evolutionary divergence of cyclic nucleotide binding sites [652, 653]. Another difference is, that PKA consists of several subunits; the regulatory, i.e. the autoinhibitory domain, and the catalytical domain do not lie on one polypeptide strand. These subunits dissociate upon cAMP binding for protein kinase activation. However, the activity of cGKs is regulated by radical conformational changes within one single polypeptide strand.

The cGKs are serine/threonine kinases and are found in a variety of eukaryotes ranging from the unicellular organism *Paramecium* to *Homo sapiens*. cGK type I (cGKI) was first desribed at the beginning of the 1970s [654]. In 1981, De Jonge et al. identified the membrane-bound type II cGK (cGKII) in the intestinal epithelium [655, 656].

1.11.1 cGMP-dependent protein kinase I (cGKI): Structure, activation and regulation

cGKI is a soluble serine/threonine kinase which exists in two alternative splice variants, cGKIα (671 aa) and cGKIβ (686 aa). cGKI is expressed at high concentrations in all smooth muscle cells and platelets, in cerebellum, hippocampus,

dorsal root ganglia, neuromuscular junction end plate and kidney. Low expression levels are found in cardiac muscle, vascular endothelium, granulocytes, osteoclasts, chondrocytes and diverse brain nuclei [657]. In lung, heart, dorsal root ganglia and cerebellum, the cGKIα is the major isoform. However, platelets, hippocampal neurons and olfactory bulb neurons mainly contain cGKIβ.

The cGKI enzyme has a rodlike structure which is divided in three regions: The N-terminus, the regulatory domain and the C-terminal kinase region. **Figure 1.14** illustrates the protein structure of cGKI which exist as a homodimer:

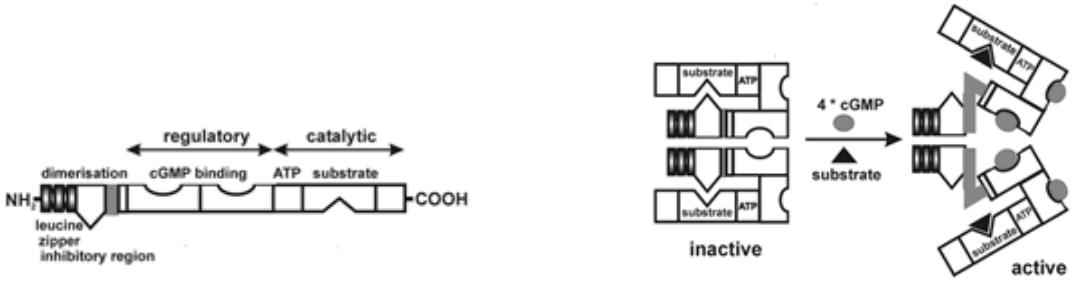

Figure 1.14 Structural and functional characteristics of homodimeric cGKI [658]. (Left) The functional domains inside each subunit are illustrated, the N-terminal dimerization and autoinhibitory domain, the regulatory region and the catalytic domain at the C-terminus. **(Right)** Binding of four cGMP molecules to dimeric cGKI are necessary to induce a conformational change from the inactive to the active state.

The N-terminal domain comprises the first aa 1-89 in Iα and the first aa 1-104 in Iβ. This region is responsible for the autoinhibition of the kinase domain due to the pseudo-substrate sequence. Furthermore, some single residues (Glu63 in Iα and Ile78 in Iβ) are essential for maintaining the inactive state of the cGKI protein [659]. The second function of the N-terminal is accomplished by a leucine zipper motif which allows homodimerization of two cGKI molecules as well as specific association with proteins. The cGKIβ isozyme includes eight leucine/isoleucine heptad repeats. Studying the impact of these residues revealed that homodimerization of the protein increases the sensitivity of the enzyme for cGMP activation [660]. Additionally, it is suggested that the N-terminal cGKIβ-specific region may interact with other proteins through the leucine zipper motif and has a transcriptional activation function [661]. As a third function, the N-terminaly domain determines the distribution of cGKI since it targets the kinase to subcellular localizations [657]. Interestingly, the isoforms show a 15fold different activation upon cGMP stimulation and specific amino acid sequences

in the N-terminal region of cGKIα are thought to be responsible for this high affinity activation of the Iα isoform [662].

The regulatory region contains two tandem cGMP binding sites for allosteric cGMP interaction. A high affinity interaction exists between the C2 amino group of cGMP and the hydroxyl side chain of a threonine residue conserved in most cGMP binding sites. The first cGMP binding motif is the slow cGMP site, i.e. cGMP slowly dissociates from this site due to high affinity binding, whereas the second motif is the fast dissociating but low affinity cGMP binding site [663]. The occupation of both cGMP binding sites induces a large conformational change resulting in a more elongated protein [664]. Interestingly, occupation of both cGMP binding sites is required for maximal stimulation of heterophosphorylation, whereas occupation of the slow site alone is sufficient for stimulation of autophosphorylation [665]. Besides the natural compound cGMP, there are a lot of cGMP analogous available, but also several inhibitors are known. **Table 1.5** gives an overview.

cGMP analog or other compounds	cGKIα	cGKIβ	cGKII	relative lipophilicity
activators				
cGMP	x	x	x	1
8-Br-cGMP	x	x	x	2.5
8-pCPT-cGMP	x	x	x	56
PET-cGMP	x	x	x	50
8-Br-PET-cGMP	x	x	(x)	115
Sp-8-Br-PET-cGMPS	x	x		182
Sp-5,6-DCl-cBIMPS	x	x		79
inhibitors				
Rp-cGMPS	x			1.3
Rp-8-Br-cGMPS	x	x		3.3
Rp-8-pCPT-cGMPS	x	x	x	6.8
Rp-8-Br-PET-cGMPS	x	x		115
H89	x			
KT5823	x			
PKI	x			
DT-2	x			
DT-3	x			

Table 1.5 The activating and inhibiting compounds for cGKs. According to [666] and all references therein. 8-Br-cGMP, 8-Bromoguanosine-3',5'-cyclic monophosphate; 8-pCPT-cGMP, 8-(4-Chlorophenylthio)guanosine-3',5'-cyclic monophosphate; 8-Br-PET-cGMP, 8-Bromo-β-phenyl-1,N²-ethenoguanosine-3',5'-cyclic monophosphate; Sp-8-Br-PET-cGMPS, 8-Bromo-β-phenyl-1,N²-ethenoguanosine-3',5'-cyclic monophosphorothioate, Sp- isomer; Sp-5,6-DCl-cBIMPS, 5,6-Dichlorobenzimidazole riboside-3',5'-cyclic monophosphorothioate, Sp- isomer; Rp-cGMPS, ; Rp-8-Br-cGMPS, 8-Bromoguanosine-3',5'-cyclic monophosphorothioate, Rp- isomer; Rp-8-pCPT-cGMPS, 8-(4-Chlorophenylthio)guanosine-3',5'-cyclic monophosphorothioate, Rp- isomer; Rp-8-Br-PET-cGMPS, 8-Bromo-β-phenyl-1,N²-ethenoguanosine-3',5'-cyclic monophosphorothioate, Rp- isomer; PKI, protein kinase inhibitor; DT-2 and -3, cKI inhibitor peptides.

The cGMP analogous differ from the natural compound mainly in selectivity, membrane-permeating property (lipophilicity) as well as susceptibility for PDE hydrolysis. These compounds can be modified at several positions of the purinbase. Hydrogen replacement at position eight by bromine (Br) makes the molecule more stable. The PET compounds show a phenyl-substituted 5-membered ring system fused to the purin structure. The CPT modification comprises the replacement of the hydrogen at position eight of the purinbase by the lipophilic 4-chlorophenylthio moiety. S stands for a modification where an exocyclic oxygen atom of the cyclic phosphate moiety is exchanged by sulfur (according to technical information of the Biolog company, http://www.biolog.de). *In vitro* studies revealed the following sensitiveness for activators:

cGKIα: 8-Br-cGMP > 8-Br-PET-cGMP / PET-cGMP > 8-CPT-cGMP

cGKIβ: 8-Br-PET-cGMP > PET-cGMP > 8-Br-cGMP / 8-CPT-cGMP

Similarily, also inhibitory cGMP analogous show different sensitivities:

cGKIα: Rp-8-Br-PET-cGMP > Rp-8-CPT-cGMP

cGKIβ: Rp-8-Br-PET-cGMP > Rp-8-CPT-cGMP

In vivo two parameters can alter the susceptibility of the cGMP analogous: the lipophilicity and PDE hydrolysis [666].

The third region following the regulatory region is the catalytic domain. This domain harbors the ATP binding site and the peptide binding pocket. The consensus sequence for cGKI is -R/K_{2-3}-X-S/T- [667]. Upon cGMP binding and changes in the secondary structure, the N-terminal autoinhibitory/pseudo-substrate site is released from the kinase domain and allows the phosphorylation of target molecules [668, 669]. Recently, it was described that upon cGMP binding the catalytic domain gets more disclosed [670]. VASP and PDE5 are good targets to monitor cGKI kinase activity in cells (see chapter 1.11.2). Studying VASP phosphorylation is suitable in vascular tissue, platelets, T-lymphocytes, endothelial cells, fibroblasts and myocytes. However, phosphorylation kinetics of PDE5 can nicely be analyzed in smooth muscle cells, platelets and cerebellum [666]. Furthermore, inside the kinase domain an NLS was identified which is required for cGMP-induced nuclear translocation of the cGKI protein [671]. cGMP-mediated nuclear translocation of endogenous cGKI has been

demonstrated in neuronal cells, neutrophils, macrophages and some embryonal smooth muscle cells. On the contrary, in other cell systems (primary VSMCs, HEK293 and CV-1 cells) no cGKI nuclear translocation was observed or nuclear cGKI was only found in a minority of the cell [672]. Casteel et al. suggested that cGKI´s nuclear translocation might be regulated by cell type-specific anchoring of the kinase in non-nuclear sites [673].

Constitutively active kinase variants can be generated via different ways. First, the N-terminal region, which harbors the pseudo-substrate region for autoinhibition of the kinase domain, can be truncated. Second, the whole regulatory domain can be cut off resulting in a non-regulated and thus constitutively activated kinase domain. However, N-terminal truncation increases the degradation of the cGKI protein [666, 674-677]. Third, steric hindrance can be another tool. For example, mutations can be introduced interfering with the interaction of the positively charged pseudo-substrate and the negatively charged catalytic domain. Or mimicking of autophosphorylation can be done (cGKIα-S64Q or cGKIα-T58E; cGKIβ-S79Q). cGKIβ-S79Q mutation induces a conformational change that is different from that caused by cGMP binding [666, 678-680]. Inversely, catalytically inactive cGKI is generated by mutating the critical lysine, inside the kinase domain which binds ATP. The mutants are cGKIα-K390A and cGKIβ-K405A [666, 681, 682]. Aspartic acid to alanine substitution at position 516 inside the catalytic domain of cGKIβ also results in a catalytically inactive enzyme (cGKIβ-D516A). The Asp516 corresponds to Asp184 inside the catalytic subunit of PKA, which coordinates with the Mg^{2+} that is complexed with ATP in the active center of the enzyme [671]. Additionally, the mutation T516A within cGKIα creates a kinase-inactive enzyme [666]. Interestingly, the catalytically inactive cGKI mutants compete with the wildtype kinase for cGMP and thus represent a cGMP sink [666].

Studies in knockout mice revealed interesting insights into the physiological importance of cGKI. Global knockout of *cgk1* resulted in impaired NO/cGMP-dependent vasodilation [683-685]. Another study showed enhanced platelet aggregation upon genetic ablation of *cgk1* [686]. Furthermore, defective axon guidance and nociception defects were observed. Inflammation-associated sensitivity for pain is also reduced in mice lacking *cgk1* [687, 688]. Finally, Yamahara and co-workers identified that the ischemia-induced angiogenesis is impaired in *cgk1*$^{-/-}$ mice [689]. Smooth muscle cell-specific *cgk1* knockout revealed reduced development of

smooth muscle cell-derived plaques indicating a proatherogenic role of NO/cGKI [690]. *cgk1* knockout in cardiac myocytes resulted in cells with an attenuated cardiac negative inotropic response to cGMP supposing that cGKI contributes to the weakening of cardiac muscle contraction upon cGMP [691]. cGKIβ-negative hippocampal neurons have an age-dependent long-term potentiation (LTP) [692]. LTP is the permanent improvement in communication between two neurons which results from simultaneous stimulation. Neurons communicate via chemical synapses and the memories are supposed to be stored within these synapses. Thus, LTP and its opposing process, long-term depression (LTD), are through to be the major cellular mechanisms that underlie learning and memory. Interestingly, genetic ablation of *cgk1α* in Purkinje cells resulted in a strong reduction of LTD [693].

1.11.2 Target proteins regulated by NO/cGMP/cGKI and the phyiological role

The cGMP/cGKI pathway influences various cellular responses by direct regulation of proteins, by indirect control through upstream pathways and by influencing gene transcription. Vasorelaxation is probably the most important process involving NO/cGMP/cGKI. VSMC contractility is highly dynamic and regulated by hormonal and neuronal inputs. Contraction of VSMCs is initiated by the rise and the relaxation is mediated by the fall of cytosolic Ca^{2+} concentration. Ca^{2+} ions are either released from intracellular stores via IP_3 or flow from the extracellular room into the cell via voltage-dependent and -independent Ca^{2+} channels. This activates the Ca^{2+}-/CaM-dependent myosin light chain kinase (MLCK) which phosphorylates the myosin light chain (MLC) resulting in myosin ATPase stimulation, actomyosin cross-bridging and increase in tension. Upon Ca^{2+} decrease, the MLCs are dephosphorylated by the myosin light chain phosphatase (MLCP). Additionally, the Rho/Rho kinase pathway inhibits this phosphatase leading to a higher level of phosphorylated MLCs and Ca^{2+} sensitization of contraction. This pathway and its downstream targets are major regulators of the actin cytoskeleton and are deeply involved in VSMC contractility and motility as well as differentiation. Basically, the balance between unphosphorylated and phosphorylated MLCs determines the contractile state of VSMCs [657, 672].

Smooth muscle cell contraction is mainly initiated by phosphorylation of the MLC through MLCK. The leucine zipper region of cGKIα mediates the interaction with

the myosin binding subunit of the MLCP which targets cGKIα to the contractile apparatus. Uncoupling of cGKIα/MLCP interaction inhibits cGMP-dependent dephosphorylation of the MLC which demonstrates that this interaction is essential to the regulation of vascular smooth muscle cell tone [694-696]. The myosin targeting subunit (MYPT1) of the myosin phosphatase is regulated by phosphorylation of Ser695 in response to cGMP/cGKI. Subsequently, the RhoA-mediated phosphorylation of Thr696 inside MYPT1 is excluded. Thus, the phosphatase stays active [697]. Moreover, RhoA is a target for cGKI-mediated phosphorylation. The GTPase RhoA is activated by G-protein-coupled receptors and increases actin polymerization. Moreover, RhoA transferes an inhibitory phosphorylation to the myosin light chain phosphatase (MLCP) supporting smooth muscle contraction. The addition of the charged group to Ser188 of RhoA by cGKI negatively regulates RhoA activity resulting in reduced MLC phosphorylation [672, 698, 699]. cGKI is deeply involved in RhoA signaling. cGKI acts upstream of RhoA inhibiting its activation as well as downstream by inhibiting RhoA target effects [672, 673, 699]. Furthermore, the protein telokin, which is indentical to the C-terminus of MLCK, is also a substrate of cGKI. MLCK gets phosphorylated and thereby inhibited by cGKI leading to muscle relaxation [700]. Also Troponin T is modulated by cGKI. It belongs to a well characterized muscle-specific protein family, the troponins. They are localized in the myofibrillar apparatus and are involved in the Ca^{2+}-dependent regulation of muscle contraction. In the cardiac muscle, the interaction with Troponin T brings cGKI into proximity to Troponin I. Thereby induced phosphorylation of Troponin I regulates muscle contraction [701].

Phospholamban controls the Ca^{2+} pump in cardiac muscle and skeletal muscle cells. Dephosphorylated phospholamban interacts with the sarco/endoplasmic reticulum Ca^{2+} ATPase (SERCA) leading to inactivation of the pump and decrease of the Ca^{2+} uptake into the sarcoplasmic reticulum. cGKI phosphorylates phospholamban and thus enhances the Ca^{2+} uptake by SERCA [702, 703]. The inositol 1,4,5-trisphosphate receptor (IP_3R)-associated cGMP kinase substrate (IRAG) specifically interacts with cGKIβ via the N-terminal leucine zipper [704, 705]. cGKIβ affects the IP_3R-dependent release of intracellular Ca^{2+} by phosphorylation of IRAG. cGKIβ can phosphorylate four serines within the IRAG protein. cGKIβ-dependent phosphorylation of Ser696 is necessary to decrease Ca^{2+} release from inositol 1,4,5-trisphophate (IP_3)-sensitive stores. This indicates that the cGMP-

induced reduction of cytosolic Ca^{2+} concentrations requires the regulation of IRAG via cGKIβ [704, 706]. Furthermore, cGKIα attenuates IP_3 generation through direct activation of the regulator of G-protein signaling-2 (RGS-2) [707].

Vasodilator-associated phosphoprotein (VASP) is as mentioned before, a cytoskeleton-associated protein which is involved in actin polymerization and aggregation of platelets. VASP is a RhoA downstream target. VASP shows three phosphorylation sites in humans, whereby Ser157 and Ser239 can be phosphorylated by both PKA and cGKI [666, 708]. Phosphorylation blocks the effect of VASP on actin dynamics. In platelets, Ser157 is more rapidely phosphorylated by PKA, whereas Ser239 is the main site for cGKI-mediated phosphorylation [709]. But also cross-reactivity, i.e. Ser157 phosphorylation via cGKI and Ser239 phosphorylation via PKA, occurs. Generally, cGMP-mediated cGKI activation inhibits platelet aggregation. Also, cGKI-independent activation of platelets through cGMP is reported. However, also an activating function of cGMP in platelet aggregation is published (based on controversially discussed results) [666]. Additionally, an isoform-specific association is described between vimentin and cGKIα. Vimentin is an intermediate filament belonging to the desmin family [710].

The cGMP-degrading PDE5 is also phosphorylated by cGKI (see chapter 1.10.1) as well as by PKA. Ser102 is exposed for phosphorylation after allosteric binding of cGMP [711-713]. Therefore, a negative feedback mechanism regulates cell contraction/relaxation of smooth muscle cells.

cGKIβ also interacts with the cystein-rich protein 2 (CRP2) and phosphorylates the protein at Ser104. Co-localization as well as the functional impact suggest that CRP2 is a novel substrate of cGKI in neurons and smooth muscle of the small intestine [714]. Furthermore, CRP2 is supposed to play an important role in cGKI-mediated nociception [715]. Phosphorylation of septin-3, a protein associated with exocytotic events on Ser91 by cGKI in nerve terminals is involved in vesicular trafficking [716].

Interestingly, several phosphatase inhibitors are modified and thus regulated by cGKI. DARPP-32, a dopamine- and cAMP-regulated phosphoprotein, can be phosphorylated on Thr34 by cGMP-activated cGKI. Phosphorylation at this residue converts DARPP-32 into a potent inhibitor of protein phosphatase 1 (PP1). cAMP and cGMP, likely via activation of cGKI, induce phosphorylation of phosphatase inhibitor 1

(I1). G-substrate is phosphorylated by cGKI at two threonines which makes G-substrate to a more potent PP2A inhibitor than PP1 inhibitor [717-719].

Furthermore, BK_{Ca}, a Ca channel, is phosphorylated by cGKI. This interaction is thought to induce membrane hyperpolerization [720]. A male germ cell-specific function suggests the interaction of cGKIα isoform with the 42-kDa cGMP-dependent protein kinase anchoring protein (GKAP42). cGKIα phosphorylates GKAP42 [721]. Other proteins such as the heatshock protein Hsp27, Pak1 and TRIM39R are throught to be potential cGKI substrates [657, 722, 723].

Interestingly, also MAPK pathways are affected by the cGMP/cGKI cascade. In several cell types as endothelial cells, cardiac myocytes, T-lymphocytes and certain cancer cells, the MAPK Erk1/2 is activated in response to cGMP stimulation and subsequent cGKI activation [672, 724-726]. In primary VSMCs, cGMP/cGKI can stimulate the basal Erk1/2 activity in a MEK1/2-ddependent manner, but in early passage VSMCs, the growth factor-induced MAPK activation is inhibited by treatment with NO or NPs. Similarily, a cGKI-mediated phosphorylation of Raf-1 and the induction of the MAPK inhibitor 1 (MPK-1) block Erk1/2 activation in mesengial cells and fibroblast-like cells [672, 727-729]. Furthermore, NO stimulates the MAPK p38 in cardiac myocytes, VSMCs, hemotopoietic cells and others, but not for example in neonatal cardiomyocytes. It is suggested that this cell type-specific activation involves cGKI-mediated stimulation of MEK3/6 [672, 730, 731]. Other studies in cardiomyocytes revealed that cGKIα interacts with p38 and inhibits the phosphorylation and activation of the MAPK. Thus, the TAB1-p38-MAPK-induced apoptosis is blocked [732]. The MAPK JNK is upregulated by cGMP in dependence of cGKI in VSMCs, fibroblasts and colon cancer cells [672, 727, 733].

Remarkably, posttranscriptional regulation of gene expression, i.e. pre-mRNA splicing, mRNA stability and translation, is influenced by cGMP/cGKI signaling. cGKI specifically phosphorylates the splicing factor 1 (SF-1) at Ser20 resulting in an inhibition of spliceosome assembly [734]. As described for the asialo-glycoprotein receptor (ASGR), a surface lectine, cGMP/cGKI modulates transcription by shifting *asgr* mRNA to transcriptional active pools. This occurs likely via a cGKI-mediated phosphorylation and therefore inhibition of the negative translational factor COPI [735, 736].

Interestingly, also a diverse set of transcription factors is directly regulated by cGMP/cGKI action. The cAMP response element (CRE) binding protein (CREB) is a

basic leucine zipper-containing transcription factor. This factor controls proliferation, differentiation and survival of cells. CREB is activated by different stimuli via phosphorylation at Ser133. Furthermore, it functionally recruits the CREB binding protein (CBP) [672]. C*reb* knockout mice suffer from dwarfism and cardiac myopathy [737]. Independent from PKA and MAPK kinases, cGMP stimulation enhances CREB Ser133 phosphorylation in VSMCs, neuronal cells and cGKI-transfected baby hamster kidney (BHK) cells. cGKI directly phosphorylates Ser133 which leads to activation of CRE-dependent transcription. This activation depends not only on CREB phosphorylation, but also requires nuclear translocation of cGKI; an NLS mutant of cGKI can not induce the CRE response [671, 738].

The transcription factor ATF-1 is phosphorylated on Ser188 in response to cGKI activation by cGMP. This results in *rhoA* promoter transactivation due to enhanced DNA binding ability of ATF-1 [699, 738].

The serum response factor (SRF) is a widely expressed transcription factor binding to sites within promoters of mitogen-inducible immediate early genes and of muscle-specific genes. The latter are activated by SRF in response to RhoA which increases actin polymerization. The transcription factor MAL, which is a co-factor of SRF, senses these changes in actin dynamics and transduces the signal to SRF. NO/cGMP, partly via cGKI, inhibits SRE/SRF-dependent transcription through blocking of RhoA function effects [672, 699, 739].

The general transcription factor TFII-I (see chapter 5.3) is ubiquitiously expressed and regulates many genes such as *c-fos*. It regulates transcription of *Inr* element-containing promoters through interaction with the basal transcriptional machinery. Several transcription factors, for example serum response factor (SRF), TCF and c-MYC, as well as HDACs interact with TFII-I [672, 740]. TFII-I specifically interacts with the cGKIβ isoform which phosphorylates the factor at Ser371 and Ser743. This leads to enhancement of *c-fos* promoter transactivation [673, 705].

The transcription factor nuclear factor-κB (NF-κB), involved in inflammatory responses, is inactive when bound to its cytoplasmic inhibitor I-κB. Multiple stimuli including cytokines mediate I-κB degradation and the activation and nuclear translocation of NF-κB [672]. I-κB is *in vitro* phosphorylated by cGMP-activated cGKI. *In vivo*, this lead to degradation of I-κB and to nuclear translocation and increased DNA binding capability of NF-κB [741]. Furthermore, NF-κB can be activated via cGMP/cGKI in a non-canonical process. cGKI phosphorylates the NF-κB subunits

p65, p50 and p52 and thus enhances their DNA binding ability [742, 743]. However, cytokine-induced NF-κB can be inhibited in a NO- and NP-dependent manner [672].

Other transcription factors as the nuclear factor of activated T-cells (NF/TA) and myocyte enhancer factor-2 (MEF-2) also underlie a cGKI-mediated control [672]. **Figure 1.15** shows schematically the cGKI interaction partners and substrates.

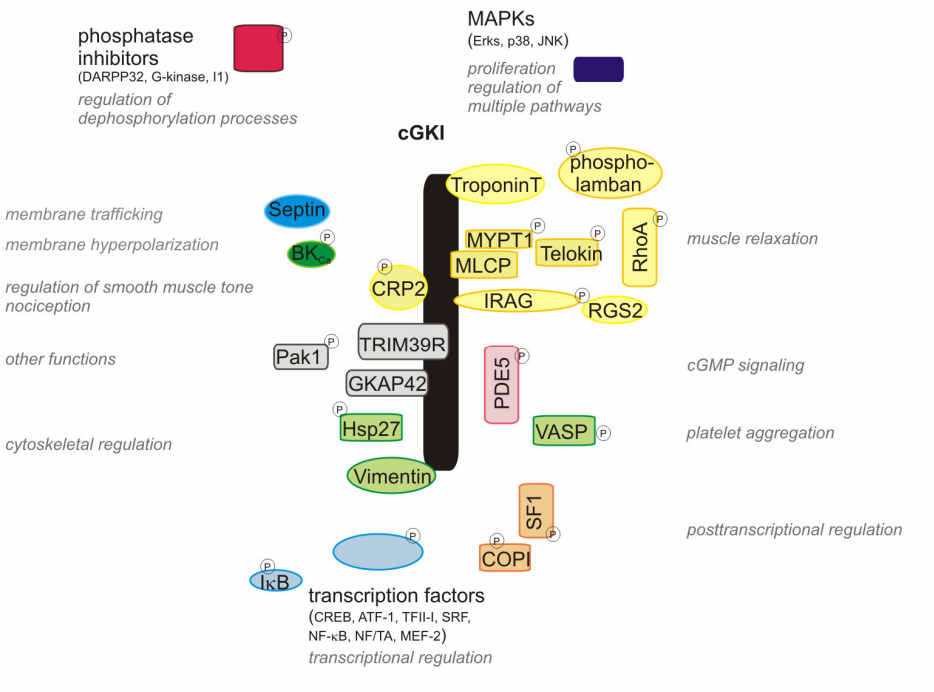

Figure 1.15 Associated proteins and substrates of cGKI. cGKI is depicted in black. Associated physiological functions of the interacting protein are depicted.

1.11.3 Genes regulated by NO/cGMP/cGKI signaling and their physiological role

A multiplicity of genes is controlled by the NO/cGMP/cGKI cascade.

Interestingly, components of the cGMP cascade are regulated via the own signals in form of a negative feedback loop. In early passage VSMCs and cardiomyocytes, stimulation with cGMP (as well as with cAMP) lead to decreased expression of *cgk1* mRNA. During inflammation, cGKI is also downregulated in response cytokine-induced iNOS expression [672, 744, 745]. Site-specific binding of the transcription factor Sp-1 to the *cgk1* promoter seems to be involved in this suppression, mediated by NO and cyclic nucleotides [746]. Similarily, the genes for several guanylyl cyclases (*sgc α1* and *β1* as well as *pgc-A*) undergo a cGMP-

induced downregulation, mainly studied in VSMCs [672, 747, 748]. As already mentioned, inflammatory cytokines as TNFα, Il-1 and interferonγ (IFγ) induce iNOS expression. In cardiomyocytes and VSMCs, the cytokine-induced *inos* mRNA level can be increased by NO and cGMP stimulation, whereas in the absence of cytokines, no effect is detectable. In the same cell systems, *tnfα* mRNA can be upregulated by NO, ANP and cGMP analogous [672, 741, 749].

The cGMP/cGKI cascade also regulates numerous processes associated with cell proliferation. Among these processes, there is the gene transcriptional control of specific proteins. Depending on the cell type, cGMP acts pro- or antiproliferative. For VSMCs, mesengial cells, fibroblasts, neuronal cells, epithelial cells and breast cancer cells, an antiproliferative role is described. The mRNA of *mkp-1* is induced by NO donors, ANP and cGMP and subsequent cGKI activation. MKP-1 is an ubiquitiously expressed threonine/tyrosine-directed MAPK phosphatase that dephosphorylates Erks, p38 and JNK [672, 729, 750-752]. Furthermore, cGMP-mediated attenuated cell proliferation comes along with G1 cell cycle arrest or delay in G1/S phase transition. cGMP treatment decreases the expression of *cyclin A*, *cyclin D1* and *cyclin E* mRNA. Additionally, cGMP upregulates the gene transcription of cell cycle inhibitors ($p21^{Waf1/Cip1}$ and $p16^{Inka}$) [672, 753-755]. Growth factor synthesis is also affected by activation of the cGMP pathway. This is mainly observed in VSMCs and cardiac fibroblasts. *Endothelin* mRNA level is diminished in response to cGMP, as well as the mRNA amount of *connective tissue growth factor (ctgf)* [672]. On the contrary, in VSMCs and in endothelial cells also a proproliferative action of cGMP on growth factor-induced proliferation, which mostly involves cGKI and Erk acctivation, is described [676, 690, 756-759].

cGMP/cGKI plays a major role in regulation of differentiation and function of VSMCs. During vascular injury or *in vitro* culture, VSMCs alter their state from the differentiated and contractile phenotype to a dedifferentiated, synthetic phenotype. In the dedifferentiated state, the cells can proliferate, migrate and produce ECM proteins as Osteopontin. This phenotype comes along with the loss of *cgk1* expression and, as a consequence, the transcriptional downregulation of contractile proteins (*smooth muscle myosin heavy chain 2, smooth muscle α-actin* and *smooth muscle calponin*). Transfecting cGKI into cGKI-deficient VSMCs, for example, can restore the more contractile phenotype [529, 672, 675, 760, 761].

Also on apoptosis, cGMP stimulation acts either proapoptotic or antiapoptotic. In VSMCs, endothelial cells, epithelial cells and cardiac myocytes, NO and cGMP induce apoptosis. It is suggested that the cGMP-reduced expression of antiapoptotic proteins as *Mcl-1* contribute to this. Hereby, cGKI action involves JNK [733, 762, 763]. cGMP/cGKI acts also proapoptotic through attenuating antiapoptotic gene expression for example via β-catenin [672]. However, antiapoptotic effects of cGMP/cGKI via Bcl-2 and associated proteins are described in neuronal cells, hepatocytes and lymphocytes. In addition, cGMP mediates the inhibition of caspase 3 activation, as well as stimulation of the antiapoptotic PI3K/Akt pathway [672, 764-770].

Angiogenesis and ECM synthesis are positively controlled by cGMP/cGKI. VEGF synthesis is upregulated by cGMP which likely involved Erk as well as PI3K/Akt signaling [672, 724, 725, 771]. Moreover, the expression of the secreted angiogenesis inhibitor thrombospondin is blocked by cGMP and subsequent cGKI activation. In addition, ECM proteins such as *collagens*, *fibronectin* and *osteopontin* are also downregulated in response to cGMP [672, 675, 677, 768, 772]. Also, the expression of matrix metalloproteinases (MMPs), which are important for angiogenesis due to their capability to degrade matrix proteins, and their inhibitors (TIMPs) is modulated by cGMP/cGKI signaling [672].

The differentiation of the neural plate is mainly regulated by Sonic hedgehoc (Shh) signaling which can be upregulated by cGMP. This indicates that the cGMP/cGKI pathway is involved in neuronal differentiation and function. Indeed, also specific forms of synaptic plasticity are associated with this pathway. Synaptic plasticity describes the capability to form synaptic connections which includes learning and memory. As already mentioned *cgk1* knockout studies revealed that the cGMP/cGKI pathway is involved in LTP and LTD (see chapter 1.11.1) [692, 693]. Moreover, hormone synthesis in the hypothalamus is also affected by cGMP [672].

Intriguingly, gene expression of several transciption factors is regulated through this pathway. The *c-fos* gene encodes for the immediate early-induces transcription factor c-fos which regulates growth factor-induced cell cycle progression, differentiation, apoptosis and control of synaptic plasticity [672]. *c-fos* is induced by NO donors, NPs and cGMP analogous. Three specific sites within the *c-fos* promoter are of special interest in this aspect: the *CRE* site, the AP-1 site and the serum response element (*SRE*). cGMP/cGKI can transactivate the promoter through

regulation of the CREB protein, as already described. Moreover, the transcription factor AP-1 showed an increased DNA binding affinity upon NO and cGMP stimulation resulting in enhanced transactivational activity. Finally, the *SRE* is bound by several transcription factors such as TFII-I or TCF which in turn are regulated by cGMP/cGKI [672, 753, 773-776]. In PC12 cells and neuroblastoma cells the *egr-1* gene is induced by NO donors and NPs [776, 777]. The Zn finger transcription factor early growth response gene 1 (Egr-1) plays an important role in cell cycle control, differentiation, apoptosis and control of synaptic plasticity. Furthermore, the Egr-1 DNA binding affinity is increased upon cGMP stimulation which can further be enhanced by cGKI expression [778]. In VSMCs the *pparγ* gene transcription is activated by cGMP analogous which could not be found in *cgk1*$^{-/-}$ VSMCs [690]. NO triggers mitochondrial biogenesis in adipose brown tissue as well as in cardiac and skeletal. The peroxysome proliferator-activated receptor y (PPARγ) is a transcription factor that regulates mitochondrial biogenesis, adipogenic differentiation and glucose homeostasis. Its co-activator PGC-1 is also induced by NO stimulation. eNOS-deficient mice have low levels of PPARγ and PGC-1 and show abberant mitochondrial biogenesis [672, 779]. Other genes of transcription factors such as *growth arrest-specific homeobox gene (gax)* and the proto-oncogene *junB*, which will not be discussed here, are also controlled by cGMP/cGKI pathway [672].

Other cGMP-regulated genes can not be classified in one of the described sections. Erythropoietin, important for growth and differentiation of erythroid cells, can be induced by cGMP. Genes encoding for globin proteins are also activated by cGMP. The *plasminogen activator inhibitor 1 (PAI-1)* gene reacts on NO, NPs or cGMP stimulation with reduction of *PAI-1* mRNA level which does not occur in *cgk1*-deficient mice [672]. Interestingly, NO also inhibits TGFβ/Smad-dependent transcription of genes [780]. **Figure 1.16** summarizes the gene regulatory mechanisms mediated by NO/cGMP/cGKI signaling:

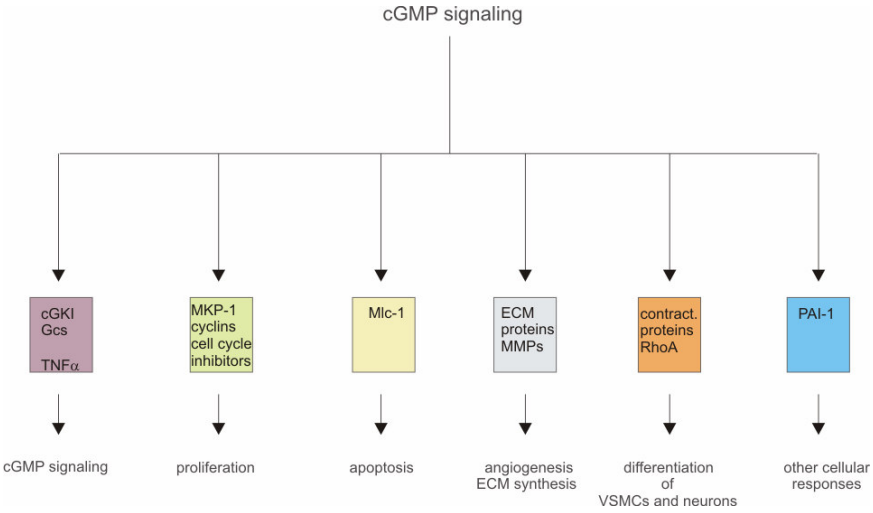

Figure 1.16 Genes controlled by cGMP signaling and the cellular outcome. The main target genes as well as the most frequent cellular responses are displayed.

1.11.4 cGMP-dependent protein kinase II (cGKII):Structure, activation and regulation

cGKII is a major regulator of electrolyte and water secretion by epithelial tissues in response to the hormones guanylin and uroguanylin as well as to enterotoxins. It further controls renal and adrenal secretion processes and the adjustment of the biological clock. Furthermore, cGKII regulates endochondral ossification. The kinase is expressed in the intestine, the brain and the kidney. Also, cGKII is found in chondrocytes and in the growth plate of bones [656].

cGKII is structurally similar to cGKI. It has 762 aa and a MW of about 87 kDa. The N-terminal autoinhibitory and dimerization domain shows low homology to cGKI isozymes. As cGKI, this region comprises a leucine zipper motif that mediates homodimerization. The two tandem-binding sites for cGMP are 50% identical to that of cGKI, regarding the amino acid sequence. Moreover, the positions of the binding sites are reversed. The first cGMP binding motif is the fast, i.e. rapidely dissociating site with a low affinity, whereas the second motif is the slow dissociating but high affinity cGMP binding site. Another difference exists since binding of cGMP alone to the high affinity cGMP site has no effect on cGKII activity, while in the case of cGKI this at least leads to a partial activation. Highest homology (about 70%) between cGKs is found in the C-terminal kinase domain [656, 781, 782]. Interestingly, cGKII is myristoylated at the N-terminus to bind to the membrane [782]. Although the absence

of the myristoyl moiety does not influence enzyme activity itself, it affects cGKII-mediated regulation of membrane-associated proteins such as the cystic fibrosis transmembrane conductance receptor (CFTR) caused by a cytosolic redistribution. CFTR is a key regulator of intestinal chloride and water secretion [656, 783]. Between the regulatory and and the catalytical domain as well as at the very C-terminus lie short sequences with unknown function. The latter also occurs in cGKI.

For its activation, cGKII requires cGMP which is generated by both NO-sensitive soluble GCs and particulate GCs. Its specificity to cGMP compared to low affine cAMP comes from two residues, Thr243 and Ser366 [784]. In the absence of cGMP, the autoinhibitory region, i.e. the residues of the pseudo-substrate, interacts with the catalytical domain. Upon cGMP binding to both cGMP binding sites, the kinase is released and can phosphorylate its substrates [669]. The different affinities for cGMP analogous further distinguish type I and type II kinases. While the PET-containing analogous stronger bind to cGKI isoforms, the CPT variants of cGMP-related activators (8-CPT-cGMP>8-Br-cGMP>PET-cGMP) and inhibitors (Rp-8-CPT-cGMP>Rp-8-Br-PET-cGMP) have a higher affinity for cGKII [656, 666].

A catalytically inactive cGKII molecule is generated by mutating the critical lysine (cGKII-K482A) [785]. Upon cGMP activation, cGKII undergoes autophosphorylation at several residues within the autoinhibitory N-terminal region (Ser110, Ser114, Ser117/Thr109 and Ser126). Also Ser445 is autophosphorylated. Furthermore, the N-terminal mutant cGKII-S126E is a constitutive active kinase [656]. The consensus sequence phosphoryalated by cGKII is -R-R-X-S/T- which is similar to cGKI or PKA. Substrates of cGKII are in part shared with cGKI, for example DARPP-32, G-substrate and the phosphatase inhibitor 1. But also specific target proteins as the chlorid channel CTFR are known substrates [656]. Furthermore, myosin is besides others a GKAP for cGKII to keep the kinase in a specific subcellular microenvironment [786]. Genes that are regulated by NO/cGMP/cGKII signaling also include c-fos [672].

Knockout studies of *cgk2* in mice revealed that the kinase is involved in endochondral ossification of long bones. *cgk2*$^{-/-}$ mice suffer from dwarfism and show intestinal secretory effects due to enterotoxin resistance. Moreover, during grewing, short limbs and cranial abnormalities become apparent. Endochondral ossification is initiated by the growth plate of long bones where resting mesenchymal cells proliferate and differentiate to hypertrophic chondrocytes (which deposit cartilage)

and finally to chondrocytes which deposite calcium for ossification. cGKII is expressed in late proliferative and early hypertrophic chondrocytes. *cgk2* null mice exhibit in the growth plate an irregular and broadened hypertrophic zone with patches of non-hypertrophic chondrocytes. cGK type I, also expressed in hypertrophic chondrocytes, was not affected by the knockout [787]. It is suggested that cGKII is involved in the maturation of chondrocytes, via inhibition of the transcription factor Sox9, or via inhibition of MAPK pathway [787, 788].

1.12 cGMP signaling in health and disease

As shown in detail, cGMP signaling plays an important role in cardiovascular health and disease. Thus, malfunction or deficiency of components of the cGMP signaling cascade is often associated with the development of cardiovascular diseases. Inversely, drugs which physiologically affect cGMP signaling, have successfully passed through clinical trials and are nowadays routinely used to treat cardiovascular failures.

NO and ANP are medically used to relax small arteries and arterioles leading to decreased blood pressure. Acute vasoconstriction as well as thrombosis can be prevented by NO treatment. NO can raise platelet cGMP level and thus inhibits platelet aggregation in a cGKI-dependent manner [789]. Furthermore, it was found that platelets from certain patients with chronic myelocytic leukemia show a decreased expression of cGKI [790]. The pathogenesis of vasculoproliferative disorders as atherosclerosis and restenosis can be affected by NO and NP signaling [657]. Atherosclerosis, a form of artheriosclerosis, is caused by the formation of multiple plaques within the arteries. These plaques are accumulation and swelling in the artery walls resulting from cell deposit which additionally contains lipids, calcium and/or fibrous connective tissue. Restenosis describe the reoccurance of this artherial blockage. Also, the pathogenesis of chronic disorders associated with cardiac remodeling can be affected by NO and NP signaling. The development of congestive heart failure or cardiac hypertrophy is associated with increased expression of NPs. Moreover, the NO donorglyceryl trinitrate successfully treats angina pectoris [657, 791]. Besides the vascular system, NO also acts as a neurotransmitter when produced by neurons of Alzheimer patients. It is suggested that the induced nitroxidative stress participates in the degenerative processes

observed in Alzheimer's disease [792]. In addition, excessive NO production has also been identified as a major reason for the pathogenesis of other neurodegenerative diseases such as Parkinson disease.

The nNOS in skeletal muscle participates in the development of Duchenne muscular dystrophy (OMIM310200), a recessive X-chromosome-linked disease that is characterized by progressive muscle degeneration. nNOS complexes with dystrophin, the protein mutated in this disease [793]. Interestingly, mutations within some components of cGMP signaling affect the eye. Retinal dystrophies (Leber's congenital amaurosis, dominant cone-rod dystrophy, cone dystrophy, and central areolar choroidal dystrophy) could be mapped to the human gene for the guanylyl cyclase pGC-E [618]. Moreover, nNOS and downstream cGMP/cGKI prevents or negatively regulates the pathogenesis of cardiac hypertrophy, a disease which is characterized by the thickening of the heart muscle due to myocyte enlargement [672].

Mutations within several CNGs cause retinitis pigmentosa (RP) that is characterized by a progressive degeneration of the rod and cone photoreceptors ultimately leading to blindness, as well as achromatopsia, a rare autosomal recessive disorder characterized by the total loss of color discrimination and severely reduced visual acuity [651].

As already mentioned, the PDE5-specific inhibitor Sildenafil, which increases the cGMP level inside VSMCs, is used against erectile dysfunction and pulmonary hypertension [794]. The compound Sildenafil is the main component of Viagra (Pfizer) which is a treatment for penile erection dysfunction. The cGMP level in the VSMCs of the corpus cavernosum is determined by both the rate of synthesis and the rate of hydrolyzation. An increase of cGMP - through Sildenafil - and subsequent binding to cGK resulted in reduced intracellular Ca^{2+} levels by phosphorylation of specific target proteins. As a consequence, VSMCs relaxe and the blood flow increases which lead to tumescence of the penis and concomitant blocking of the venous outflow. The result is penile erection [643]. Furthermore, studies from several independent laboratories propose cGKI as a new therapeutic target in cancer. Anti-tumor effects of PKG in colon cancer cells including inhibition of tumor growth and angiogenesis were identified [795]. Manipulating the NO/cGMP signaling system will be an important tool for regenerative therapies since a functional NO/cGMP cascade is active early during the differentiation of embryonic stem cells [796].

1.13 Aim of the project

The initial consideration for this study was to find novel regulators of the BMP type II receptor (BRII) which regulate BMP signaling. According to the literature, this receptor is thought to have interesting functions both in and beyond BMP signaling. Two BRII isoforms arise from alternative splicing. The long splice variant, BRII long form (BRII-LF), has a long cytoplasmic extension (BRII-tail), which is unique among mammalian TGFβ receptors [75]. The short splice variant, BRII short form (BRII-SF) lacks this tail region. Several studies showed equal signaling outputs for both splice variants [72, 195]. However, specific cellular functions could be attributed to the C-terminal tail of BRII [261, 266, 268]. It has been shown that a key regulator for actin dynamics, LIM kinase I (LIMKI), interacts with BRII-tail and thereby is inhibited, which leads to dysregulation of actin depolymerization [191]. Moreover, Ser757 within BRII-tail is a regulatory site. Upon overexpression and activation of the receptor tyrosine kinase c-Kit, Ser757 is phosphorylated and thereby BMP signaling is promoted [266]. Furthermore, mutations in BRII, occurring also in the tail domain, cause the rare autosomal disease pulmonary arterial hypertension [13]. Still, little is known about the importance of BRII-tail for cellular responses.

To follow up this issue, the impact of a newly identified BRII-associated kinase, the cGMP-dependent kinase I, on BMP receptors, on Smad proteins, and on the final cellular output of BMP signaling should be investigated.

2 Material and solutions

2.1 Chemicals and materials

chemicals/material	manufacturer
antibodies	BD Biosciences (Franklin Lakes, NJ, USA)
	Cell Signaling Technologies Incorporation (Danvers, MA, USA)
	Dianova GmbH (Hamburg, Germany)
	Millipore Corporate (Billerica, MA, USA)
	Roche Diagnostics GmbH (Mannheim, Germany)
	Promega Corporation (Madison, WI, USA)
	Santa Cruz Biotechnology Incorporation (Santa Cruz; CA, USA)
	Sigma-Aldrich GmbH (Hannover, Germany)
	Stressgen Biotechnologies Corporation (San Diego, CA, USA)
bacterial strains	Stratagene Corporation (San Diego, CA, USA)
	Invitrogen Corporation (Carlsbad, CA, USA)
bacterial growth media	Carl Roth GmbH & Co. KG (Karlsruhe, Germany)
cells	LGC Promochem GmbH (Wesel, Germany)
	PromoCell GmbH (Heidelberg, Germany)
cell culture media and reagents	Biochrom AG (Berlin, Germany)
	Invitrogen Corporation (Carlsbad, CA, USA)
	PAA Laboratories GmbH (Pasching, Austria)
	Polyplus-transfection Incorporation (New York, NY, USA)
	Roche Diagnostics GmbH (Mannheim, Germany)
consumables, sterile, for cell culture	Greiner Bio one GmbH (Frickenhausen, Germany)
	Hartenstein Laborbedarf (Wuerzburg, Germany)
	Nunc GmbH & Co. KG (Wiesbaden, Germany)
consumables, sterile	Bio-Rad Laboratories (Hercules, CA, USA)
chemicals, highest purity	Carl Roth GmbH & Co. KG (Karlsruhe, Germany)
	Merck KGaA (Darmstadt, Germany)
	Pierce Biotechnology Incorporation (Rockland, IL, USA)
	Serva Electrophoresis GmbH (Heidelberg, Germany)
	Sigma-Aldrich GmbH (Hannover, Germany)
consumables, non-sterile	Carl Roth GmbH & Co. KG (Karlsruhe, Germany)
	Eppendorf AG (Hamburg, Germany)
	Greiner Bio one GmbH (Frickenhausen, Germany)
enzymes/substrates	Fermentas GmbH (St- Leon-Rot, Germany)
	New England Biolabs (Ipswich, MA, USA)
	Qbiogene Incorporation (Morgan Irvine, CA, USA)
	Roche Diagnostics GmbH (Mannheim, Germany)
	Sigma-Aldrich GmbH (Hannover, Germany)
growth factors/ligands	Biolog GmbH (Bremen, Germany)
	Biopharm GmbH (Heidelberg, Germany)
	Tebu-Bio GmbH (Offenbach, Germany)

chemicals/material	manufacturer
kits	Ambion Incorporation (Foster City, CA, USA)
	Peqlab Biotechnologie GmbH (Erlangen, Germany)
	Promega Corporation (Madison, WI, USA)
nitrogen, liquid/carbon dioxide	Linde AG (Munich, Germany)
oligonucleotides	Invitrogen Corporation (Carlsbad, CA, USA)
	Thermo Fisher Scientific GmbH (Schwerte, Germany)
others	Minerva Biolabs GmbH (Berlin, Germany)
	Southern Biotech Incorporation (Birmingham, AL, USA)
	Whatman (Dassel, Germany)
plasmid preparation	Qiagen GmbH (Hilden, Germany)
radiochemicals	Hartmann Analytic GmbH (Braunschweig, Germany)
standards	Bio-Rad Laboratories (Hercules, CA, USA)
	Fermentas GmbH (St. Leon-Rot, Germany)
	New England Biolabs (Ipswich, MA, USA)
	Sigma-Aldrich GmbH (Hannover, Germany)
vectors/sequencing	Clontech Laboratories Incorporation (Mountain View, CA, USA)
	GE Healthcare Biosciences corporation (Piscataway, NJ, USA)
	Invitrogen Corporation (Carlsbad, CA, USA)
	LGC Promochem GmbH (Wesel, Germany)
	Promega Corporation (Madison, WI, USA)
	GATC Biotech AG (Konstanz, Germany)

Table 2.1 Manufacturer information about used chemicals and material.

All solutions and media were prepared using deionized water (dH_2O) of Millipore quality.

2.2 Technical devices

device	type	manufacturer
agarose gelelectrophoresis	Sub Cell GT	Bio-Rad Laboratories (Hercules, CA, USA)
	Mini Sub Cell GT	Bio-Rad Laboratories (Hercules, CA, USA)
autoclave	5075 ELV	Systec GmbH, Labor-Systemtechnik (Wettenberg, Germany)
balance	XB4200C Precisa	PESA Waagen GmbH (Bisingen, Germany)
	SBA33	Scaltec Instruments GmbH (Goettingen, Germany)
centrifuge, table	5417C	Eppendorf AG (Hamburg, Germany)
	5804	Eppendorf AG (Hamburg, Germany)
centrifuge, table, refrigerated	5417R	Eppendorf AG (Hamburg, Germany)
centrifuge, refrigerated	Sorvall RC 6	Thermo Fisher Scientific GmbH (Schwerte, Germany)
centriguge, speed vac	speed vac concentrator	Bachofer GmbH (Reutlingen, Germany)
clean bench	HeraSafe	Heraeus GmbH (Hanau, Germany)
confocal microscope	Leica DMR	Leica Microsystems GmbH, Wetzlar, Germany
deionization system	Milli-Q	Millipore Corporate (Billerica, MA, USA)
developing machine, X-ray film	Optimax Typ TR	MS Laborgeräte GmbH (Wieloch, Germany)
electrophoresis power supply	Consort E831	Consort nv (Turnhout, Belgium)
	PowerPac HC	Bio-Rad Laboratories (Hercules, CA, USA)

device	type	manufacturer
electroporator	Micro pulser	Bio-Rad Laboratories (Hercules, CA, USA)
fluorescence microscope	Axiovert 200M	Carl Zeiss AG, Jena, Germany
incubator	HeraCell 240	Heraeus GmbH (Hanau, Germany)
inbubator for shaking	Duomax 1030	Heidolph Instruments GmbH & Co. KG (Schwabach, Germany)
light microscope	IMT-2	Olympus GmbH (Hamburg, Germany)
	Axiovert 40CFL	Carl Zeiss AG (Jena, Germany)
luminometer	FB12	Berthold Detection Systems (Pforzheim, Germany)
luminometer, plate	Mithras LB 940	Berthold Detection Systems (Pforzheim, Germany)
microplate reader	Sunrise reader	Tecan AG (Zuerich, Switzerland)
PCR cycler	PTC-200	MJ Research Incorporation (Waltham, MA, USA)
	Cyclone 25	Peqlab Biotechnologie GmbH (Erlangen, Germany)
pH meter	761 calimatic	Knick Elektronische Messgeräte GmbH & Co. KG (Berlin, Germany)
pipets, microlitre	research	Eppendorf AG (Hamburg, Germany)
phosphor-imager	FLA-5000	Fujifilm Corporation (Stamford, CT, USA)
protein blotting	Mini-V 8.10	Bio-Rad Laboratories (Hercules, CA, USA)
protein gel elecrophoresis	Mini-Protean III system	Bio-Rad Laboratories (Hercules, CA, USA)
rocking table	Polymax 1040	Heidolph Instruments GmbH & Co. KG (Schwabach, Germany)
scanner	Perfection 2480 photo	Epson Deutschland GmbH (Meerbusch, Germany)
	ScanJet 2100C	Hewlett-Packard GmbH (Boeblingen, Germany)
shaker with heating	Thermomixer 5437	Eppendorf AG (Hamburg, Germany)
shaker	Schüttelmaschine LS20	C. Gerhardt GmbH & Co. KG, Laboratory Systems (Koenigswinter, Germany)
sonicator	UW 70	Bandelin electronic GmbH & Co.KG (Berlin, Germany)
spectrophotometer	Nanodrop ND-1000	Peqlab Biotechnologie GmbH (Erlangen, Germany)
	UV 1202	Shimadzu Europa GmbH (Duisburg, Germany)
UV-transilluminator	-	Herolab GmbH (Wiesloch, Germany)
	printer UP-860CE	Sony GmbH (Berlin, Germany)
vortexer	-	Heidolph Instruments GmbH & Co. KG (Schwabach, Germany)
water bath	-	Memmert GmbH & Co. KG (Schwabach, Germany)

Table 2.2 Information about used technical devices.

2.3 Kits

Luciferase reporter activity	Dual-Luciferase™ Reporter Assay (Promega)
Plasmid DNA preparation	Qiagen Plasmid Kits (Qiagen)
Polymerase chain reaction	*Taq* core Kit (Qbiogene)

Generation of siRNA	Silencer™ siRNA construction kit (Ambion)

2.4 Enzymes and substrates

2.4.1 Kinases

Bovine cGMP-dependent protein kinase Iα was purchased from Promega.

2.4.2 Restriction endonucleases

All restriction enzymes were supplied by Fermentas or New England Biolabs.

2.4.3 DNA- and RNA-modifying enzymes

DNA amplification	*Taq* polymerase (New England Biolabs) *Pwo* SuperYield DNA Polymerase (Roche Diagnostics)
DNA ligation	T4-DNA ligase (Promega)
RNA degradation	RNase (Roth)
RNA degradation	RNasin™ (Promega)
RNA transcription	*MMLV* reverse transcriptase (Promega)

2.4.4 Substrates

Alkaline phosphatase substrate para-nitrophenylphosphate (pNPP) (Sigma-Aldrich)

2.5 Oligonucleotides

Oligonucleotides were synthesized by and obtained from Thermo Fisher Scientific (HPLC quality) or by Invitrogen. Primers used for PCR reactions are listed in the appendix (see 0, oligonucleotides).

2.6 Standards

2.6.1 DNA standards

100 bp DNA ladder (New England Biolabs)	100 bp - 200 bp - 300 bp - 400 bp - 500/517 bp - 600 bp - 700 bp - 800 bp - 900 bp - 1000 bp - 1200 bp - 1517 bp
1 kb DNA ladder (New England Biolabs)	500/517 bp -1000 bp -1500 bp - 2000 bp - 3001 bp - 4001 bp - 5001 bp - 6001 bp - 8001 bp - 10002 bp

2.6.2 Protein standards

SDS7B Molecular Weight Standard Mixture, prestained (Sigma-Aldrich)	26.6 kD - 36.5 kD - 48.5 kD - 58 kD - 84 kD - 116 kD - 180 kD (with small lot dependent variations)
Precision Plus Protein all blue Standard (Bio-Rad)	10 kD - 15 kD - 20 kD - 25 kD - 37 kD - 50 kD -75 kD -100 kD - 150 kD - 250 kD (with 25 kD, 50kD and 75 kD as more intense reference bands)

PAGERuler^{TM} Prestained Protein Ladder Plus (Fermentas)

10 kD - 15 kD - 27 kD - 35 kD - 55 kD - 70 kD - 100 kD - 130 kD - 250 kD (with 27 kD and 70 kD as red reference bands; with small lot-dependent variations)

2.7 Bacterial strains

E. coli DH5α

*deo*R, *end*A1, *gyr*A96, *hsd*R17(r_k^-, m_k^+), *rec*A1, *rel*A1, *sup*E44,*thi*-1, Δ(*lac*ZYA-argF)U169, ϕ80d*lac*ZDM15, F^- [797]

E. coli C600

*lac*Y1, *leu*B6, *mcr*B^+, *sup*E44, *thi*-1, *thr*-1, *ton*A21, F^- [798]

E. coli MC1061/P3

*ara*D139, *gal*K, *gal*U, *hsd*R2(r_k^-,m_k^+), *rps*L, *thi*-1, (*ara-leu*)7696, *lac*X74, F-(P3*Kan*^{r} amber *Amp*^{r}amber *Tet*^{r}) (Invitrogen)

E. coli XL1 blue

*rec*A1, *end*A1, *gyr*A96, *thi*-1, *hsd*R17 (r_k^-, m_k^+), *sup*E44, *rel*A1, *lac* [F, *pro*AB, *lac*1^qZDM15, *Tn*10(*Tet*^{r})] (Stratagene)

E. coli BL21(DE)

F^-, *omp*T, *hsd*$S_β$, ($r_β^-$, $m_β^-$), *dcm*, *gal*, λ(DE3), *ton*A [799]

2.8 Expression vectors

2.8.1 Prokaryotic expression vectors

pGEX-4T-1 (GE Healthcare Biosciences)
vector for expression of recombinant protein in bacteria; expression is controlled by the isopropyl-β-D-thiogalactopyranoside (IPTG)-inducible *tac* promoter (for high level expression); the vector encodes for ampicillin resistance for bacterial selection; the protein of interest is generated as a N-terminal glutathion S transferase (GST)-fusion protein which can be removed by a thrombin cleavage site. This vector originates from pGEX-2T.

pGEX-KG (LGC Promochem)
vector for expression of recombinant protein in bacteria; expression is controlled by the IPTG-inducible *tac* promoter (for high level expression); the plasmid harbors a *β-lactamase* gene which provides ampicillin resistance; the respective protein is generated as a N-terminal GST-fusion protein; the tag can be removed by a thrombin cleavage site. pGEX-KG originates from pGEX-2T.

pGEX-KGl (R. Pilz, UCSD, San Diego, CA, USA)
vector for recombinant protein expression in bacteria; expression is controlled by the IPTG-inducible *tac* promoter (for high level expression); the plasmid encodes an ampicillin resistance gene; the respective protein is generated as a N-terminal GST-fusion protein; GST can be removed by a thrombin protease cleavage [705].

pMAL-p2C (New England Biolabs)
vector for expression of recombinant protein in bacteria; expression is controlled by the IPTG-inducible *P lac* promoter (for high level expression); the plasmid harbors a *β-lactamase* gene which provides ampicillin resistance; the respective protein is generated as a N-terminal maltose-binding protein (MBP) fusion protein; the tag can be removed by factor Xa protease cleavage.

2.8.2 Eukaryotic expression vectors

pCB6 (LGC Promochem)
mammalian expression vector driven by the promoter of the *Cytomegali virus* (CMV) which facilitates constitutive high level expression; the vector encodes for ampicillin and neomycin resistance and originates from pCB3 and pBR322.

pcDEF3
mammalian expression vector driven by the elongation factor 1a (EF1a) promoter (constitutive high expression); the vector encodes for ampicillin as well as neomycin resistance [800].

pcDNA1 (Invitrogen)
mammalian expression vector for CMV promoter driven transcription (constitutive high level expression); the plasmid encodes for the tRNA supressor F gene (supF) which demands transformation in bacteria strains that carry the P3 episome (i.e. *E. coli* MC1061/P3); sensitivity to tetracycline and ampicillin is generated by supression of the amber mutations.

pcDNA3 (Invitrogen)
mammalian expression vector driven by the CMV promoter (constitutive high level expression); the vector encodes for ampicillin resistance as well as for neomycin resistance.

pCMV2 (D. Russell, UTSW, Dallas, TX, USA)
mammalian expression vector driven by the CMV promoter (constitutive high level expression); the vector encodes for ampicillin resistance [801].

pCMV5 (D. Russell, UTSW, Dallas, TX, USA)
mammalian expression vector driven by the CMV promoter (for constitutive high level expression); the vector encodes for ampicillin resistance [801].

pCMV-GST

mammalian expression vector driven by the CMV promoter (constitutive high level expression); the respective protein is generated as a N-terminal GST fusion protein; the tag can be removed by thrombin cleavage; the vector encodes for ampicillin resistance [802].

pCMV-GST-D (R. Pilz, UCSD, San Diego, CA, USA)

mammalian expression vector which was constructed by inserting a linker into the multiple cloning site of the vector pCMV-GST [673].

pDH105

mammalian expression vector which is driven by the simian CMV IE94 promoter (constitutive high level expression); the vector encodes for ampicillin resistance. The vector originates from pCS2+ [803].

pENTR/U6 (Invitrogen)

mammalian expression vector driven by the human U6 promoter which allows RNA polymerase III-dependent expression of short hairpin RNA (shRNAs); the plasmid carries a kanamycin resistance.

peGFP (Clontech Laboratories)

mammalian expression vector driven by the *lac* promoter; the plasmid encodes for kanamycin resistance; the vector encodes for the a green fluorescence protein (GFP) variant optimized for maximal fluorescence when excited by UV light (360–400 nm).

pGL3basic (Promega)

vector harbors the *luciferase* gene from the firefly *Photinus pyralis* as backbone; in front, a gene regulatory element can be cloned that originates from respective promoters and/or enhancer elements to enable quantitative analysis of the factor of interest.

pMM9

mammalian expression vector which is CMV promoter driven (constitutive high level expression); the vector harborsn the *β-lactamase* gene for ampicillin resistance,

furthermore the plasmid encodes for neomycin resistance [804].

RL-TK (Promega)
mammalian expression vector driven by the thymidine kinase promoter for constitutive but low expression; the plasmid encodes for ampicillin resistance and carries the sequence for a *luciferase* from the sea pansy *Renilla reniformis* and is used as reference plasmid in dual luciferase reporter gene assays.

2.9 Constructs

2.9.1 Prokaryotic expression constructs

construct	insert	vector	tag	donor/reference
pGST-cGKIα aa1-93	human cGKIα aa1-9	pGEX-KGI	GST, N-term.	R. Pilz, San Diego, CA, USA [705]
pGST-cGKIβ aa3-110	human cGKIβ aa3-110	pGEX-KGI	GST, N-term.	R. Pilz, San Diego, CA, USA [705]
pGST-BRII-SF	human BRII-SF aa175-530	pGEX-KG	GST, FLAG, N-term.	[265]
pGST-BRII-tail	human BRII-tail aa530-1038	pGEX-KG	GST, FLAG, N-term.	[265]
pMBP-Smad1	human Smad1	pMAL-p2C	MBP, N-term.	O. Huber, Charite, Germany

Table 2.3 Information about used prokaryotic expression constructs to generate recombinant proteins.

2.9.2 Eukaryotic expression constructs

construct	insert	vector	tag	donor/reference
pcGKIα	human cGKIα	pCB6	-	R. Pilz, UCSD, CA, USA
pGST-cGKIα	human cGKIα	pCMV-GST-D	GST, N-term.	R. Pilz, UCSD, CA, USA
pGST-cGKIα aa1-93	human cGKIα aa1-93	pCMV-GST-D	GST, N-term.	R. Pilz, UCSD, CA, USA [673]
pcGKIβ	human cGKIβ	pCB6	-	R. Pilz, UCSD, CA, USA
pcGKIβ	human cGKIβ	pMM9	-	[804]
pcGKIβ D516A	human cGKIβ D516A	pCB6	-	[671]
pGST-cGKIβ	human cGKIβ, lacks aa1-4	pCMV-GST-D	GST, N-term.	R. Pilz, UCSD, CA, USA [673]
pGST-cGKIβ aa3-110	human cGKIβ aa3-110	pCMV-GST-D	GST, N-term.	R. Pilz, UCSD, CA, USA [673]
pGST-cGKIβ Δaa350	human cGKIβ Δaa350	pCMV-GST-D	GST, N-term.	R. Pilz, UCSD, CA, USA [673]
pGST-cGKIβ aa3-351	human cGKIβ aa3-351	pCMV-GST-D	GST, N-term.	R. Pilz, UCSD, CA, USA [673]
pGST-cGKIβ Δaa92	human cGKIβ Δaa92	pCMV-GST-D	GST, N-term.	R. Pilz, UCSD, CA, USA [673]
p-HA-BRIa	human BRIa	pcDNA3	HA, N-term.	[227]
pHA-BRIb	mouse BRIb	pcDNA3	HA, N-term.	[227]

construct	insert	vector	tag	donor/reference
pHA-BRII-LF	human BRII-LF	pcDNA1	HA, N-term.	[195]
pHA-BRII-LF K230R	human BRII-LF K230R	pcDNA1	HA, N-term.	[266]
pHA-BRII-TC8	human BRII-TC8 aa1-1021	pcDNA3	HA, N-term.	[195]
pHA-BRII-TC7	human BRII-TC7 aa1-982	pcDNA3	HA, N-term.	[195]
pHA-BRII-TC6	human BRII-TC6 aa1-746	pcDNA3	HA, N-term.	[195]
pHA-BRII-TC5	human BRII-TC5 aa1-711	pcDNA3	HA, N-term.	[195]
pHA-BRII-TC4	human BRII-TC4 aa1-637	pcDNA3	HA, N-term.	[195]
pHA-BRII-SF	human BRII-SF	pcDNA3	HA, N-term.	[195]
pHA-BRII-SF K230R	human BRII-SF K230R	pCMV5	His, C-term.	J. Massague, MSKCC, NY, USA
pHA-BRII-TC3	human BRII-TC3 aa1-500	pcDNA3	HA, N-term.	[195]
construct	insert	vector	tag	donor/reference
pHA-BRII-TC1	human BRII-TC3 aa1-207	pcDNA3	HA, N-term.	[195]
pHA-BRIa	human BRIa	pcDNA3	HA, N-term.	[195]
pSmad1	human Smad1	pDH105	-	J. Massague, MSKCC, NY, USA [805]
pFLAG-Smad5	mouse Smad5	pcDEF3	FLAG, N-term.	A. Moustakas, LICR, Sweden [356]
pTFII-I-MYC	human TFII-I, Δ isoform	pCB6	MYC, C-term.	R. Pilz, UCSD, CA, USA [673]
pTFII-I-S371A/S734A-MYC	human TFII-I, Δ isoform S371A/S734A	pCB6	MYC, C-term.	R. Pilz, UCSD, CA, USA [673]
pTRI-HA	human TRI	pcDNA3	HA, C-term.	S. Souchelnytskyi, Karolinska Institute Stockholm, Sweden
pMYC-TRII	human TRII	pcDNA1	MYC, N-term.	Y. Henis, Tel Aviv University, Israel
p*BRE*$_2$-luc	firefly luciferase from *Renilla reniformis* controlled by *BRE* from *Id1* promoter	pGL3basic	-	ten Dijke, University of Leiden, The Netherlands [806]
p*SBE*-luc	firefly luciferase from *Renilla reniformis* controlled by *SBE* from *JunB* promoter	pGL3basic	-	A. Moustakas, LICR, Sweden [807]
p*CAGA*$_{12}$-luc	luciferase from *Photinus pyralis* controlled by *CAGA* element from *Col1A2* promoter	pGL3basic	-	ten Dijke, University of Leiden, The Netherlands [808]
RL-TK	luciferase from *Renilla reniformis* controlled by the constitutive active thymidine kinase pormoter	RL-TK	-	Promega
psh-hcGKI	shRNA specific for human cGKI	pENTR/U6	-	H. Volkmer, NMI Reutlingen, Germany
psh-cGKI	shRNA specific for mouse cGKI	pENTR/U6	-	H. Volkmer, NMI Reutlingen, Germany
psh-non targeting	unspecific shRNA (*Arabidopsis thaliana)*	pENTR/U6	-	H. Volkmer, NMI Reutlingen, Germany
pβ-Gal	β-Galactosidase	pcDNA1	-	S. Souchelnytski, Karolinska Institute Stockholm, Sweden
peGFP	eGFP from *Aequorea victoria*	peGFP	-	Clontech

Table 2.4 Information about eukaryotic expression constructs for overexpression studies in mammalian cells.

2.10 Cell lines

C2C12 (LGC Promochem, CRL-1772)
murine muscle myoblast cell line; the cells differentiate under low serum conditions to myotubes and under BMP treatment to osteoblasts; adherent; fibroblasts

C2C12, stable expressing BRII [809]
stable transfected C2C12 cells using the retroviral system; different cell pools express BRII truncations as well as the naturally occuring splice variants of BRII; the pools were selected with G418.

Cos7 (LGC Promochem, CRL-1651)
african green monkey kidney cell line containing the large T-antigen from simian virus 40 (SV40); adherent; fibroblasts

HAoSMC (PromoCell)
human aortic smooth muscle cell line; adherent

MC3T3 (LGC Promochem, CRL-2593-96)
murine embryonic/fetal bone/calvaria preosteoblast cell line; the cells were established from the mouse strain C57BL/6 and the cell clones (CLR-2593-96) show different stages of osteoblast differentiation; the cells produce high amounts of collagen; adherent; fibroblasts

HEK293T (LGC Promochem CRL-11268)
human embryonic kidney cell line containes adenovirus 5 DNA and is transformed with the large T-antigen from SV40; semi-adherent; epithelial cells

2.11 Growth media and reagents for cell culture

Dulbecco`s modified eagle medium (DMEM) (Invitrogen, Biochrom)
prepared according to manufacturer´s instructions,
sterile filtered

Fetal bovine serum (FBS) (Invitrogen, Biochrom)	heat-inactivated at 56°C for 30 min before use
G418 (PAA Laboratories)	stock solution 50 mg/ml aminoglycoside antibiotic to select for neomycin resistance; added to media for C2C12 stably expressing BRII to a final concentration of 0.6 mg/ml
L-glutamine (Biochrom)	stock solution 200 mM added to media to a final concentration of 2 mM
Penicillin G (Biochrom)	prepared according to manufacturer´s instructions, sterile filtered; added to media to a final concentration of 100 U/ml
Streptomycinsulfate (Biochrom)	prepared according to manufacturer´s instructions, sterile filtered; added to media to a final concentration of 100 U/ml
Trypan blue (Biochrom)	staining solution to determine living cells

Trypsin (Biochrom)	prepared by dissolving trypsin and EDTA in PBS; sterile filtered; used concentration depends on the treated cell line

2.12 Growth factors

BMP-2 recombinant BMP-2 was a kind gift from W. Sebald**,** University of Wuerzburg, Wuerzburg, Germany.
GDF-5 and GDF-5 mutants were given by Biopharm GmbH.
PDGF-BB and TGFβ-1 were obtained from Tebu-Bio GmbH.

2.13 Antibodies

2.13.1 Primary antibodies

1st antibody	type/origin	epitope	IP	IF	WB	WB blocking
α-β-Actin (Sigma-Aldrich)	monoclonal IgG_1 mouse	slightly modified N-terminal peptide Ac-DDDIAA LVIDNGSGL, conjugated to KLH, of cytoplasmic β-actin; clone AC-15	-	-	1:10.000 0.1% TBS-T	3% skim milk 0.1% TBS-T
α-BRII G-17 (Santa Cruz Biotechnology)	polyclonal goat	peptide within the extracellular domain of human BRII	1 µg	-	1.200-1:500 0.1% TBS-T	3% skim milk 0.1% TBS-T
α-BRII T-18 (Santa Cruz Biotechnology)	polyclonal goat	peptide within the intracellular domain of human BRII	1 µg	-	-	-
α-BRII (FB-60) (P. Knaus, Berlin, Germany) [195]	polyclonal rabbit	peptide SMNMMEAAAS-EPSLDLDN, conjugated to KLH-Glu, in the juxtamembrane region of human BRII	50 µl*	-	-	-
α-BRIa (FB-14) (P. Knaus, Berlin, Germany)	polyclonal rabbit	peptide LEQDEAFIPVG ESLKDLC in the juxtamembrane region of human BRIa	50 µl*	-	-	-

1st antibody	type/origin	epitope	IP	IF	WB	WB blocking
α-β-Tubulin (Sigma-Aldrich)	monoclonal mouse		-	-	1:1.000 0.1% TBS-T	3% skim milk 0.1% TBS-T
α-cGKIβ L-16 (Santa Cruz Biotechnology)	polyclonal goat	peptide near the N-terminus of human cGKIβ	0.5-1 µg	1:100-1:200	-	-
α-cGKIβ E-20 (Santa Cruz Biotechnology)	polyclonal goat	peptide within human human cGKIβ, reacts also with cGKIα	-	-	1:1.000 0.1% TBS-T	3% skim milk 0.1% TBS-T
α-cGKI (Stressgen)	polyclonal rabbit	peptide (DEPPPDDNSG-WDIDF) respresenting aa657-671 of human cGKIα, reacts also with cGKIβ	1:1.000	1:300	1:1.000 0.1% TBS-T	3% skim milk 0.1% TBS-T
α-GST B-14 (Santa Cruz Biotechnology)	monoclonal IgG_1 mouse	peptide representing full length glutathion S transferease (GST)	1 µg	-	1.1.000 0.1% TBS-T	3% skim milk 0.1% TBS-T
α-HA (Roche Diagnostics)	monoclonal $IgG_{2bκ}$ mouse	peptide (YPYDVPDYA) within the haemagglutinin (HA) protein of *influenza virus*; 12CA5	0.5-1 µg	1:300	1.1.000 0.1% TBS-T	3% skim milk 0.1% TBS-T
α-HA (P. Knaus, Berlin, Germany)	monoclonal IgG_1 mouse	peptide (YPYDVPDYA) within the haemagglutinin (HA) protein of *influenza virus*; 12CA5 [810]	1 µg	-	1:200-1:1.000 0.1% TBS-T	3% skim milk 0.1% TBS-T
α-HA Y-11 (Santa Cruz Biotechnology)	polyclonal rabbit	internal peptide within the haemagglutinin (HA) protein of *influenza virus*	-	1:50	-	-
α-His H-15 (Santa Cruz Biotechnology)	polyclonal rabbit	peptide representing polyhistidine domains	-	-	1:1000 0.1% TBS-T	3% skim milk 0.1% TBS-T
α-LaminA/C (BD Biosciences)	monoclonal IgG_1 mouse	peptide aa398-490 within the human LaminA/C	-	-	1:1000 0.1% TBS-T	3% skim milk 0.1% TBS-T
α-LaminA/C (L. Bengtsson, Berlin, Germany) [811]	monoclonal mouse	peptide within human Lamin A/C	-	-	1:1.000 0.1% TBS-T	3% skim milk 0.1% TBS-T
α-MYC (P. Knaus, Berlin, Germany)	monoclonal IgG_1 mouse	peptide (EQKLISEEDL) within the C-terminus of human c-myc, 9E10	1 µg	-	1:1000	3% skim milk 0.1% TBS-T
α-pp38 (Promega)	polyclonal rabbit	peptide pTGpY, corresponding to pThr182 and pTyr184, of mammalian pp38	-	-	1:1.000 0.1% TBS-T + 0.1% BSA	1% BSA 0.1% TBS-T
α-pSmad1/5/8 (Cell Signaling Technology)	polyclonal rabbit	peptide within the C-terminus of human pSmad5, conjugated to KLH, reacts also with pSmad1 and 8	1:1.000	1:300	1:500-1:1.000 0.1% TBS-T+ 5% BSA	3% BSA 0.1% TBS-T

1st antibody	type/origin	epitope	IP	IF	WB	WB blocking
α-pSmad1/5/8 (P. ten Dijke, University of Leiden, The Netherlands) [812]	polyclonal rabbit	peptide (KKKNPISSVS) within the C-terminus of human pSmad1/5; cross-reacts with pSmad3	1:100	-	1:1.000 0.5% TBS-T	5% BSA 0.5% TBS-T
α-pVASP Ser239 (Santa Cruz Biotechnology)	polyclonal rabbit	peptide representing aa around pSer239 of human pVASP	-	-	1.1.000 0.1% TBS-T	3% BSA 0.1% TBS-T
α-Smad1 A-4 (Santa Cruz Biotechnology)	monoclonal IgG_1 mouse	peptide representing full length human Smad1	1 µg	1:200	1:500-1:1.000 0.1% TBS-T	3% skim milk 0.1% TBS-T
α-Smad1/5 (Millipore)	polyclonal rabbit	peptide representing aa147-258 of human Smad1 (recognizes also Smad5)	-	1:200	1:400-1:500 0.1% TBS-T	3% skim milk 0.1% TBS-T
α-Smad1	polyclonal rabbit	peptide representing aa around Ser 190 of human Smad1	-	-	1:1000 0.1% TBS-T + 5% BSA	3% skim milk 0.1% TBS-T
α-Smad4 B-8 (Santa Cruz Biotechnology)	monoclonal IgG_1 mouse	peptide representing full length human Smad4	1 µg	1:200	1:500-1:1.000 0.1% TBS-T	3% skim milk 0.1% TBS-T
α-TFII-I (BD Biosciences)	monoclonal IgG_1 mouse	peptide within murine TFII-I	-	-	1:1000 0.1% TBS-T	3% skim milk 0.2% TBS-T
α-TβRII (FB-260) (P. Knaus, Berlin, Germany) [813]	polyclonal rabbit	peptide CSEEKIPEDGS-LNTTK in the C-terminal region of human TRII	50 µl*	-	-	-
α-TβRI (VPN44A) (P. Knaus, Berlin, Germany) [814]	polyclonal rabbit	peptide VPNEEDPSLD-RPFISEGTTLKD in the juxtamembrane region of human TRI	50 µl*	-	-	-

Table 2.5 Information about used primary antibodies. * means 50 µl of protein A-sepharose slurry, as these antibodies were covalently linked to sepharose beads (see 3.4.6). All antibody solutions for immunoblotting were additionally supplemented with 0.1% sodium azide.

2.13.2 Secondary antibodies

2nd antibody	type/origin	epitope	conjugate	IF	WB
goat α-mouse-HRP (Dianova)	goat	heavy and light chains of mouse IgGs	HRP	-	1:5.000-1:10.000 0.1% TBS-T
goat α-rabbit-HRP (Dianova)	goat	heavy and light chains of rabbit IgGs	HRP	-	1:10.000 0.1% TBS-T
donkey α-goat-HRP (Santa Cruz Biotechnology)	donkey	heavy and light chains of goat IgGs	HRP	-	1:2.000-1:5.000 0.1% TBS-T
mouse α-goat-Cy3 (GE Healthcare)	mouse	heavy and light chains of goat IgGs	Cy3	1:200	-
goat α-rabbit-Cy2 (Dianova)	goat	heavy and light chains of rabbit IgGs	Cy2	1:200	-

2nd antibody	type/origin	epitope	conjugate	IF	WB
goat α-mouse-Alexa Fluor 488 (Invitrogen)	goat	heavy and light chains of mouse IgGs	Alexa Fluor 488	1:300	-
goat α-mouse-Alexa Fluor 594 (Invitrogen)	goat	heavy and light chains of mouse IgGs	Alexa Fluor 594	1:300	-
goat α-rabbit-Alexa Fluor 594 (Invitrogen)	goat	heavy and light chains of rabbit IgGs	Alexa Fluor 594	1:300	-

Table 2.6 Information about used secondary antibodies.

3 Methods

3.1 Microbiological methods

3.1.1 Sterilization and disinfection

The premise of microbiological and cell biological work is the absence of unwanted microorganisms. Microorganisms can be removed or their number can be reduced by a variety of methods:

Heat sterilization
Heat-stable and non-volatile solutions, media and materials are sterilized by autoclaving for 20 min at 1.1 bar and a resulting increase of the boiling temperature of water (121°C).
Glassware can be sterilized using dry heat (180°C) for 3 hrs.

Sterile filtration
Non-heat-stable and volatile solutions and media are sterilized via sterile filtration using sterile filters with a pore size of 0.2 - 0.4 µm (Schleicher & Schuell).

Sterilization using irradation
Media and materials can be sterilized through irradiation using UV light or γ-irradiance.

Disinfection
The number of microorganisms can be reduced through disinfection using physical (wiping) or chemical methods (i.e. alcohol, halogen disinfection or specific chemicals as Mycoplasma-Off (Minerva Biolabs)).

3.1.2 Bacterial growth media

Luria Bertani (LB) medium	10 g/l Trypton 5 g/l Yeast extract 10 g/l NaCl dissolved in dH_20 autoclave
LB agar plates	LB medium 15 g/l agar autoclave cool down to 40°C supplement with antibiotic(s) pour liquid LB agar in plates
SOB medium	20 g/l Trypton 5 g/l Yeast extract 0.5 g/l NaCl 0.83 g/l KCl dissolved in dH_20 adjust pH 7.0 with NaOH autoclave
SOC medium	sterile SOB medium 10 mM $MgCl_2$ 10 mM $MgSO_4$ 40% v/v glucose
2xYT medium	16 g/l Trypton 10 g/l Yeast extract 5 g/l NaCl dissolved in dH_20 autoclave

3.1.3 Cultivation and conservation of *E. coli* strains

For cultivating bacteria, LB medium or LB agar plates with the appropriate antibiotics were used. Generally, cultures were grown at 37°C under permanent shaking. For long-term conservation 500 µl freshly prepared bacterial culture (optical density at 550 nm ($OD_{550\ nm}$) > 0.6) was mixed with 200 µl sterile 86% glycerol in a sterile cryo-vial and was stored at -80°C.

Antibiotics

Ampicillin	stock solution 100 mg/ml dissolved in dH_20 stored in aliquots at -20°C stable for 4 weeks at 4°C
Kanamycin	stock solution 100 mg/ml dissolved in dH_20 stored in aliquots at -20°C stable for 4 weeks at 4°C
Tetracycline	stock solution 7.5 mg/ml dissolved in dH_20 stored in aliquots at -20°C stable for 4 weeks at 4°C protect from light

3.1.4 Preparation of competent *E. coli* strains

3.1.4.1 Preparation of heat-competent *E. coli* strains

For the transformation of *E. coli* using heat shock, the bacteria have to be treated like the following to be able to accept plasmid DNA.

The *E. coli* strain was plated on an agar plate and cultivated at 37°C over night. Several fresh clones were inoculated to 250 ml SOC medium and cultivated again at 37°C for 6 hrs to an $OD_{550\ nm}$ of 0.6. Then, the cells were transferred to ice, incubated for 10 min and centrifuged (4.000 rpm, 10 min, 4°C). The pellets were resuspended in 10 ml ice cold sterile TB buffer each, pooled in two reaction tubes and filled up to 40 ml each with ice cold TB buffer. The cells were incubated on ice again for 10 min and centrifuged (3.500 rpm, 4°C). The two pellets were resuspended in each 5 ml ice cold TB buffer, pooled and 8.5 ml of ice cold TB buffer were added. Then, on ice, 1.5 ml dimethylsulfoxide (DMSO) was added dropwise and under careful pivoting to the cell suspension. Cells were incubated on ice for 10 min, portioned (200 µl) into sterile cryo vials and immediately frozen in liquid nitrogen, and stored at -80°C.

TB buffer	10 mM Pipes
	15 mM $CaCl_2$
	250 mM KCl
	dissolved in dH_20
	adjust pH 6.7 with KOH
	55 mM $MnCl_2$
	autoclave

3.1.4.2 Preparation of electro-competent *E. coli* strains

For the transformation of *E. coli* using electroporation, the bacteria have to be treated like the following to be able to accept plasmid DNA.

The *E. coli* strain was cultivated in 20 ml 2xYT over night culture without antibiotics. The culture was transferred to 250 ml 2xYT-over day cultures and grew to $OD_{550\ nm}$ of 0.6. The cultures were incubated on ice for 40 min and centrifuged (3.500 rpm, 10 min, 4°C). The bacterial pellets were thoroughly resuspended in 250 ml ice cold dH_2O and centrifuged again (3.500 rpm, 10 min, 4°C). 125 ml of ice cold dH_20 were added and after resuspension 2 solutions were pooled. Following a third centrifugation step (3.500 rpm, 15 min, 4°C), the bacteria were resuspended in 1 ml 1

mM Hepes/10% v/v 86% v/v glycerol, pooled and filled up to 30 ml with 1 mM Hepes/10% v/v 86% glycerol. The bacterial cells were pelleted by centrifugation (10.000 rpm, 15 min, 4°C) and thoroughly resupended in 1.6 ml 1 mM Hepes/10% v/v 86% v/v glycerol. After aliquotation (100 µl) in sterile cryo-vials, bacteria were immediately frozen in liquid nitrogen and stored at -80°C.

For determination of the transformation rate of competent bacteria, 1 ng of plasmid DNA was added to 100 µl of competent bacteria solution. A good transformation rate for electroporated *E. coli* is at least 10^9 colonies per µg of transformed plasmid DNA.

3.1.5 Transformation of competent *E. coli* strains

Transformation describes a method of introducing plasmid DNA into bacteria.

3.1.5.1 Transformation of competent *E. coli* strains via heat shock

Transformation of *E. coli* strains using heat shock demands heat-competent bacteria (3.1.4.1).

After thawing heat-competent bacteria on ice, 1-500 ng of plasmid DNA were added to the suspension, carefully mixing, and incubated on ice for 30 min. Subsequently, the bacteria were incubated for 90 sec at 42°C and immediately resuspended in 1 ml pre-warmed SOC medium. Following DNA uptake, the bacterial cells were cultivated for 30 min at the appropriate temperature (30°C or 37°C). Afterwards, 100 µl of the bacterial suspension (or more after centrifugation (5.000 rpm, 5 min)) were plated on agar with antibiotics and incubated over night at the respective temperature (30°C or 37°C) to get single bacterial clones.

3.1.5.2 Transformation of competent *E. coli* strains via electroporation

Transformation of *E. coli* strains using electroporation demands electro-competent bacteria (see 3.1.4.2).

Electro-competent bacteria were thawn on ice and 1-500 ng of plasmid DNA were added to 45 µl bacterial solution. The suspension was transferred to an ice cold electroporation cuvette (BioRad) and cells were treated with an electro shock (6 ms, 1.8 kV) in the electroporator to allow DNA uptake. Immediately, 1 ml of pre-warmed SOC medium was added and the bacteria were incubated for 30 min at the appropriate temperature (30°C or 37°C) under permanent rotation. 100 µl of the suspension (or more after centrifugation (5.000 rpm, 5 min)) were plated on selective agar plates and incubated over night at the respective temperature (30°C or 37°C) to get single colonies.

3.2 Molecular biological methods

3.2.1 Amplification and isolation of plasmid DNA from transformed bacteria

For amplification of transformed bacteria, a 2 ml LB-over day culture was used directly or inoculated to 100-250 ml LB-over night culture with the appropriate antibiotics. Plasmid DNA isolation was carried out according to manufacturer´s instructions (Mini, Midi and Maxi Plasmid Kits, Qiagen). The principle of these kits is based on alkaline lysis and binding of plasmid DNA to an anion exchange resin under low-salt conditions, pH 7.0. RNA, protein and other impurities are removed by washing under medium-salt conditions. Plasmid DNA is eluted with a high-salt buffer followed by DNA concentration, desalting and precipitation with 2-propanol. Plasmid DNA was redissolved in an appropriate volume of dH_2O or TE and stored at -20°C.

3.2.2 Determination of nucleic acid concentrations

The concentration of an aqueous nucleic acid solution can be determined by absorption measurement at a wavelength of 260 nm using a spectrophotometer (Nanodrop ND-1000, Thermo Fisher Scientific). 2 µl of the solution were pipetted onto the sensor and the measurement was carried out in an absorption spectrum in the range of 240-320 nm. The photometer was calibrated with pure dH_2O. The output value is determined including the extinction coefficient of the respective nucleic acid (33 for cDNA; 50 for DNA; 40 for RNA) and has the unit µg/µl.

3.2.3 Sequencing of DNA

Plasmid DNA was sent to GATC Biotech for sequencing.

3.2.4 Digestion of DNA via restriction endonucleases

Specific endonucleases from bacteria, generated to fend off foreign DNA, can be used to cut DNA for cloning purpose.

DNA was dissolved in dH_2O and an enzyme-specific buffer was added. After adding 1-5 U of restriction enzyme to the sample, DNA digestion was carried out for 1 hr at the enzyme-specific temperature. Digestion efficiency was checked using agarose gelelectrophoresis (see 3.2.6).

3.2.5 Isolation of RNA and semi-quantitative polymerase chain reaction

3.2.5.1 Extraction of RNA

RNA isolation from eukaryotic cells was accomplished using the principle of phenole/chloroform extraction.

Cells were washed once with PBS and RNA was extracted using Tri-fast (Peqlab Biotechnologie) according to the protocol. The method is based on the onestep-liquid-phase-extraction. Tri-fast contains phenol and guanidinisothio-cyanate and after adding chloroform and subsequent centrifugation, the solution forms 3 phases. RNA was found in the upper aqueous phase whereas DNA is in the organic and the interphase. Proteins are located in the organic phase. By adding 2-propanol to the isolated aqueous phase RNA was concentrated, desalted and precipitated. RNA was redissolved in 20 µl RNase-free dH_2O. Yield and quality of RNA was determined using spectrophotometry (see 3.2.2). RNA solutions were directly used for reverse transcription or stored at -20°C.

PBS	10 g/l NaCl 0.25 g/l KCl 1.45 g/l Na_2HPO_4 0.25 g/l KH_2PO_4 dissolved in dH_20 adjust pH 7.4
RNase-free dH_2O	0.1% v/v diethylpyrocarbonate (DEPC) dissolved in dH_20 for 1 hr at RT autoclave

3.2.5.2 Reverse transcription of RNA

To transcribe RNA into DNA, specific viral polymerases, e.g. *Moloney murine leukemia virus (MMLV)* reverse transcriptase, are suitable to generate single-stranded (ss) cDNA.

2 µg RNA were subjected to cDNA synthesis using 120 fm oligo-dT primers and RNase-free dH_2O. Denaturation was carried out for 5 min at 70°C. On ice, 0.4 mM dNTPs, 1x *MMLV* buffer, 1.6 U RNase inhibitor and 8 U *MMLV* reverse transcriptase were added and the reaction mix was filled up with RNase-free dH_2O to a final volume of 25 µl. Polymerase reaction takes place for 50 min at 42°C and the enzyme was inactivated by a final incubation for 15 min at 70°C. The synthesized cDNA was used directly for PCR or stored at -20°C.

3.2.5.3 Polymerase chain reaction

To amplify small amounts (in the range of fg) of cDNA or DNA fragments, polymerase chain reaction (PCR) can be performed.

The method´s principle can be described as follows: double-stranded (ds) DNA is denaturated in a first step followed by a second step where specific oligonucleotides are allowed to anneal to their target sequence. The third step is characterized by elongation of the fragments using a heat-stable DNA polymerase (i.e. *Taq* polymerase from *Thermus aquaticus*).

A standardized PCR was carried out using the following protocol:

Standard PCR reaction mix		2 µl cDNA 1 pM forward primer 1 pM reverse primer 200 pM dNTPs 1x DNA polymerase buffer 1.5 U DNA polymerase add dH_20 to final volume 50 µl
Standard PCR cycler program		5 min, 95°C
	25-30 cycles	30 sec, 95°C (denaturation) 30 sec, specific temperature for primer annealing 1 min, 72°C (elongation)
		10 min, 72°C

A critical step in PCR reaction is the primer annealing, for which the most efficient temperature has to be established. In this work it was sometimes necessary to use a biphasic PCR cycling program where the proper annealing temperature is converged gradually with ascending temperature during the 30 cycles. The annealing temperature depends on the DNA base composition of the primers. The melting temperatue (T_D) of an oligonucleotide can be calculated using the following formula:

$$T_D=[(C_n + G_n) \times 4 + (A_n + T_n) \times 2]°C$$

3.2.6 Agarose gelelectrophoresis

DNA and DNA fragments can be seperated due to their molecular weight using agarose gelelectrophoresis.

Therefore a 1-2% agarose gel in TAE buffer was prepared containing 0.5 µg/ml ethidium bromide (EtBr). DNA solutions were mixed with 6x DNA sample buffer and loaded onto the gel. Electrophoresis was performed at 100 V. The separated DNA was analyzed using an UV-transilluminator since EtBr intercalates into the double helix of DNA and can be fluorescently stimulated at a wavelength of 254 nm.

TAE buffer	400 mM Tris/acetate pH 8.2 10 mM EDTA dissolved in dH_20 adjust pH 8.5 with acidic acid
6x DNA sample buffer	0.25% w/v xylene cyanole (0.25% w/v bromphenole blue) 30% v/v glycerole dissolved in dH_20

3.2.7 Knockdown of gene expression via shRNA

The technology of silencing specific genes reaches its hitherto climax with the nobel award for medicine or physiology 2006 for A. Fire and C. Mello. They were awarded for the discovery of gene silencing using small RNAs in *C. elegans* [815]. The process was called RNA interference (RNAi). RNAi was first described in plants [816], but in 2001 the group around T. Tuschl discovered that RNAi also works in mammalian cell culture [817]. These findings opened new perrspectives for one of the most successful tools in cell biological studies. The mechanism of generation of small interfering RNAs (siRNAs) and their effect is the following: Upon introduction, the long double-stranded RNAs (dsRNAs) get processed into 20-25 nucleotide (nt) siRNAs by an RNase III-like enzyme called Dicer (initiation step). Then, the siRNAs assemble into endoribonuclease-containing complexes known as RNA-induced silencing complexes (RISCs). In the effector step the siRNA strands subsequently guide the RISCs to complementary RNA molecules, where they cleave and thereby destroy the cognate RNA [818].

The system used in this work is based on stable expression of shRNAs, which were introduced via a mammalian expression vector driven by the human U6 promoter, which allows RNA polymerase III-dependent expression of shRNAs.
Depending on the assay, C2C12 cells ($1*10^5$ per 6-well for subsequent RNA extraction (see 3.2.5.1) or $2*10^4$ per 24-well for subsequent *BRE-luc* reporter gene assay (see 3.3.6.2) or R-Smad phosphorylation assay (see 3.3.6.1)), were seeded and transiently transfected with sh-cGKI or sh-scrambled vectors using Lipofectamine™ (see 3.3.3.2). We also used siRNA molecules, generated using a siRNA constructer kit (Ambion) which are specific for cGKI and compared the results to a control siRNA (siGFP). Cells were incubated over night at 37°C. As mentioned before the transfected cells were used in different cellular assays to analyze the effect of endogenous cGKI downregulation.

3.2.8 Chromatin immunoprecipitation

The target of this method is to determine the binding of proteins (i.e. transcription factors) to specific domains of endogenous chromatin of living cells or tissues and is therefore an *in vivo* technique. The method is based on the following essential steps: (1) cross-linking of DNA and proteins, (2) fixation, (3) cell lysis and sonication to break DNA in 0.2-1 kb fragments, (4) immunoprecipitation of DNA/protein complexes with a specific antibody, (5) complex purification, and (6) PCR with specific oliginucleotides.

Chromatin immunoprecipitation (ChIP) was performed as described by Weiske and Huber [819] with minor modifications. Briefly, C2C12 cells were grown on 10 cm plates to a confluence of 80-90%. Cells were serum starved for 24 hrs and following the addition of 10 nM BMP-2 and 1 µM 8-Br-cGMP for 4 hr, cells were washed twice with PBS, fixed with 2 mM disuccinimidyl-glutarate for 30-45 min at room temperature (RT) and cross-linked for 10 min at RT using 1% v/v formaldehyde. Nuclei were disrupted by sonication with three pulses each for 20 sec in a UP 50H sonicator (Hielscher Ultraschall Technologie) at a setting of cycle 0.5 and amplitude 30%. This yielded genomic DNA fragments with a bulk size of 0.2-1 kb. For immunoprecipitation, 50 µg of DNA and 2.5-5.0 µg of α-cGKI, α-Smad1 (Santa Cruz Biotechnology) or 2.5 µg α-TFII-I antibodies were used.

For two-step-ChIP, the immunocomplexes were eluted by adding 100 µl 10mM dithiothreitol (DTT) at 37°C for 30 min and diluted 1:40 in ChIP dilution buffer followed by incubation with the second antibodies. First and second ChIP of the two-step ChIP were performed in the same way as the first immunoprecipitation.

For subsequent PCR analysis, 2 µl of the extracted DNA (50 µl) were used as a template amplification. The used oligonucleotides are specific for the murine *Id1* promoter (see 0, oligonucleotides). PCR was performed using the following parameters: An initial incubation of 2 min at 94°C to activate the *Taq* polymerase (New England Biolabs) was followed by 35 cycles of denaturation for 15 sec, annealing for 30 sec at 55°C, elongation for 45 sec at 72°C and a final extension for 3 min at 72°C. PCR products were separated on an 8% polyacrylamide gel, stained with EtBr and were observed by use of UV light.

ChIP dilution buffer	16.7 mM Tris/HCl pH 8.1
	167 mM NaCl
	1.2 mM EDTA
	1.1% v/v Triton X-100
	0.01% w/v SDS

3.3 Cell biological methods

3.3.1 Cultivation and cryo-conservation of cells

Line-dependent, cells were cultivated in DMEM (low glucose) supplemented with 10% FBS v/v, 1% penicillin/streptomycine and 2 mM L-glutamine. To select for stable C2C12 cell pools, 0.6 mg/ml G418 were added to the medium. Cells were incubated at 95% atmospheric moisture at 37°C and 5% CO_2 (HEK293T) or 10% CO_2 (C2C12, Cos7, MC3T3-E1).

Ongoing adherent cell culture was done by detaching cells with 2x trypsin for 2-5 min at 37°C; the enzymatic activity was stopped by the addition of FBS-containing medium. Generally cells were passaged every 2-4 d and splitted 1:10-1:15.

Cryo-conservation of cell was carried out by harvesting cells (1.200 rpm, 3 min), resuspending thoroughly in DMEM/10% DMSO v/v and immediately freezing at -80°C in cryo-vials (over night). Long-term conservation took place in liquid nitrogen at -196°C.

3.3.2 Determination of cell number

The number of living cells can be determined using the trypan blue dye which can only enter dead cells.

Therefore, a cell suspension was diluted 1:1 with trypan blue and 10 µl of the dilution was applied to a Neubauer chamber for cell counting (Hartenstein Laborbedarf). Vital cells were counted in 2 of 4 quadrants and the number of cells per ml was calculated from the mean including the dilution factor by multiplying with the chamber factor 10^4.

3.3.3 Transfection of eukaryotic cells

Transfection is a method of introducing foreign nucleic acids (plasmid DNA, ssDNA, siRNA, shRNA, antisense RNA) into eukaryotic cells in culture. Two types of transfection can be distinguished, on the one hand the transient transfection where the introduced nucleic acids get lost during a few passages (with the exception of selecting for an encoded antibiotic resistance), on the other hand the stable transfection where the imported nucleic acid is stably integrated into the host´s genome.

3.3.3.1 Transient transfection of HEK293T using calcium-phosphate co-precipitation

The principle of this transient transfection method is based on the formation of calcium-phosphate complexes which can co-precipitate with the applied DNA on the cells. The distinct uptake mechanism is still unknown.

This transfection method was used for HEK293T cells. For this purpose the cells were seeded and cultivated over night. Prior to transfection the medium was replaced by fresh growth medium and for equilibration of pH cells were incubated

under CO_2 gassing again. Plasmid DNA was mixed with sterile dH_2O and sterile $CaCl_2$ was added. The solution was mixed rigorously and 2x HBS buffer, pH 7.0 (must be adjusted very precisely) was pipetted to the samples by "bubbling". The solution was distributed dropwise with caution onto the cells and the cells were cultivated for 7-10 hrs in the incubator. The transfection medium was replaced by fresh growth medium and cells were incubated further for 24-48 hrs. The transfected cells were analyzed for transfection efficiency using eGFP or β-galactosidase (see 3.3.4) and afterwards used for different cellular assays.

---------	6 cm dish	6-well
HEK293T cells	$1*10^6$	$3\text{-}4*10^5$
total DNA	5 µg	2 µg
dH_20	438 µl	219 µl
$CaCl_2$	62 µl	31 µl
2x HBS	500 µl	250 µl

Table 3.1 The table depicts cell numbers, used transfection solution volumes, and DNA amounts for calcium-phosphate transfection of HEK293T cells in 6 cm dishes and 6-well plates.

$CaCl_2$

stock solution 2 M $CaCl_2$
dissolved in dH_20
autoclave
stored in aliquots at -20°C

2x HBS buffer

50 mM Hepes pH 7.0
10 mM KCl
280 mM NaCl
1.5 mM Na_2HPO_4
12 mM dextrose
dissolved in dH_20
adjust pH 7.0 with NaOH
autoclave
stored in aliquots at -20°C
(up to 6 months)

3.3.3.2 Transient transfection of C2C12 cells using Lipofectamine™/2000

This transfection method is based on the principle of lipofection using a kationic lipid which forms complexes with DNA. The complex can fuse with the plasma membrane and internalize via endosomes. The double-layered micelle maturates and gets acidic due to a pH shift. The DNA is released but the occuring nuclear entry is still not clarified in detail.

For transfection, C2C12 cells were seeded into cell culture dishes and cultivated over night under growth conditions. Lipofection was carried out using Lipofectamine™/2000 (Invitrogen) according to manufacturer´s instructions. For reporter gene assays (see 3.3.6.2), *BRE*-luc or *SBE*-luc reporter and renilla luciferase reporters were transfected additionally to total DNA. Post transfection, cells were cultured at 37°C/10% CO_2 for 24 hrs and transfection efficiency was determined using eGFP or β-galactosidase (β-gal) (see 3.3.4). Subsequently, cells were used for different cellular assays.

-------	6-well	12-well	24-well	48-well	96-well
C2C12 cells	$1*10^5$	$5*10^4$	$2*10^4$	$1*10^4$	$1*10^3$
total DNA	2 µg	1 µg	0.5 µg	0.2 µg	50 ng
Lipofectamine™	10 µl	5 µl	2 µl	1 µl	0.2 µl
™ premix + DMEM	200 µl + 800 µl	100 µl + 400 µl	40 µl + 160 µl	20 µl + 80 µl	10 µl + 40 µl
Lipofectamine2000	10 µl	5 µl	2 µl	1 µl	0.2 µl
2000 premix	500 µl	200 µl	100 µl	50 µl	20 µl

Table 3.2 The table depicts cell numbers, used transfection solution volumes, and DNA amounts for Lipofectamine™/2000 transfection of C2C12 cells in different cell culture plates.

3.3.3.3 Transient transfection using polyethylenimine

Cell transfection using polyethylenimine (PEI) can also be classed into the lipofection method.

PEI is an organic polymer with very high cationic-charge-density potential which can be used as vector for gene delivery into mammalian nuclei [820]. Its efficiency lies in the ability to buffer the acidic pH in the lysosome which protects the transfected DNA against nuclease digestion. Furthermore, the cytotoxicity of PEI is low [820].

HEK293T, Cos7 and C2C12 cells were used for protein overexpression studies and transfected using PEI (Sigma-Aldrich). In short, HEK293T cells were seeded into cell culture dishes and cultivated in DMEM/10% v/v FBS over night. Transfection mixture was prepared using DMEM without supplements, DNA and PEI. After incubation at RT for 30 min, pre-warmed DMEM without supplements was added to each transfection mixture. After removing growth medium from the cells, the transfection medium was added and incubated on the cells at 37°C/10% CO_2 for 5 hrs. Transfection medium was replaced by growth medium (DMEM/10% v/v FBS) and cells were cultured at 37°C/10% CO_2 for 24-48 hrs. Transfection efficiency was determined using eGFP or β-gal (see 3.3.4) and afterwards cells were used for different cellular assays.

-------	15 cm dish	10 cm-dish	6 cm dish	6-well	24-well	chamber slide (16)
HEK293T cells	-	-	$1*10^6$	$3\text{-}4*10^5$	$2*10^4$	$1*10^4$
total DNA	-	-	5 µg	2.5 µg	1 µg	0.2 µg
C2C12 cells	$5*10^6$	$1*10^6$	-	-	-	-
total DNA	20 µg	10 µg	-	-	-	-
PEI	40 µg	20 µg	10 µg	5 µg	2 µg	0.4 µg
premix	2 ml	1 ml	200 µl	200 µl	40 µl	10 µl
+ DMEM	+ 6 ml	+ 3 ml	+ 1.3 ml	+ 800 µl	+ 160 µl	+ 40 µl

Table 3.3 The table depicts cell numbers, used transfection solution volumes, and DNA amounts for PEI transfection of HEK293T cells and C2C12 cells in different cell culture dishes and plates.

PEI (Roth)

stock solution 2 µg/µl PEI
dissolved in dH_2O
sterile filtrated
stored in the dark at 4°C

3.3.3.4 Transient transfection of VSMCs using Fugene

Fugene HD (Roche Diagnostics) is a reagent to transfect cells; it´s principle is based on lipofection of cells.

VSMCs were transfected with Fugene since transfection of these cells with Lipofectamine 2000 or PEI lead to cell death or viable, but untransfected cells, respectively. Transfection with jetPEI (Polyplus-transfection) showed transfected

cells, but less than with Fugene HD. In short, VSMCs were seeded into cell culture dishes and cultivated in 231 medium/5% v/v SMGS over night. Transfection mixture was prepared using Opti-MEM, DNA and Fugene HD. After incubation at RT for 30 min, pre-warmed 231 medium/5% v/v SMGS without antibiotics was added to the cells; the transfection medium was added and incubated on the cells at 37°C/5% CO_2 over night. Transfection efficiency was determined using eGFP or β-gal (see 3.3.4) and afterwards cells were used for different cellular assays. Despite several test series, the transfection efficiency of these cells with Fugene HD was less than 10% and needs to be optimized.

-------	6-well	24-well	48-well	96-well
VSMCs	$2*10^5$	$5*10^4$	$2*10^4$	$1*10^4$
total DNA	2 µg	0.5 µg	0.2 µg	80 ng
Fugene HD	6 µl	2 µl	1 µl	0.4 µl
premix	200 µl	100 µl	50 µl	20 µl

Table 3.4 The table depicts cell numbers, used transfection solution volumes, and DNA amounts for Fugene HD of VSMCs in different cell culture plates.

3.3.3.5 Stable integration of DNA into C2C12 cells using retroviral infection

Retroviral infection is based on the following principle: A packaging cell line (i.e. HEK293T cells) is transfected with *gag*-, *env*- and *pol*-encoding vectors as well as with a retroviral vector containing the gene of interest. Infectious but replication-deficient virus particles are generated and target cells were infected. After transduction, viral sequences including the gene of interest integrated into the genome of the host cells as a so called *provirus*. Gene flanking *internal ribosomal entry sites* (*IRES)* sequences directed the translation and genes is stably expressed in the transduced cell.

In this work, C2C12 cells were stably transfected with BRII or BRII mutants according to the method described by us [809]. Cells were selected using G418 (see 2.11).

3.3.4 Determination of transfection efficiency

Determination of transfection efficiency was done by transfecting cells with a control gene. The plasmid used encoded either for enhanced green fluorescence protein (eGFP) or for the enzyme β-gal. Both methods define the ratio of transfected and untransfected cells.

eGFP was found in the jellyfish *Aequorea victoria* and emittes light at a wavelength of 509 nm after excitation (488 nm). Transfection efficency was analyzed using a fluorescence microscope.

The β-gal assay is based on the β-gal-mediated catalysis of X-gal, a colorless lactose analog, to a blue reaction product. In short, 24-48 hrs post transfection the control cells were fixed with x-gal fixation solution containing glutaraldehyde for 15 min at 37°C. After removing the fixation solution X-gal staining buffer containing the substrate for the β-gal, was added to the cells for 20-60 min until blue colored cells were visible. Analysis of transfection efficiency was done at a light microscope.

X-gal fixation solution	PBS 3.6% v/v glutaraldehyde
X-gal staining buffer	10 mM PBS 1 mM $MgCl_2$ 3.3 mM $K_4Fe(CN)_6$*$3H_20$ 3.3 mM $K_3Fe(CN)_6$ adjust pH 7.0 add freshly 0.2% v/v X-gal
X-gal	2% v/v stock solution of 5-bromo-4-chloro-3-indolyl-b-D-galactoside dissolved in DMSO

3.3.5 Treatment of cells with growth factors and protein activators/inhibitors

In this work, cells were treated with starvation medium (DMEM/0.2-2% v/v FBS) for different times (2-24 hrs) before application of the ligand or the chemical compound. Through starvation cells get synchronized in cell cycle and get susceptible for the folling treatment.

------	IP	IF	pSmad	luc	ChIP	*Id1* mRNA	p38	*ALP* mRNA	ALP
starvation time	3 hrs	2-3 hrs	24 hrs	5 hrs	24 hrs	24 hrs	different, mostly 5hrs	24 hrs	5 hrs
BMP-2 concentration	10 nM	10 nM	10 nM	1 nM	10 nM	10-20 nM	10 nM	20 nM	20 nM
8-Br-cGMP concentration	1 µM	1 mM	1 µM - 100 µM	1 µM - 100 µM	1 µM	1 µM	1 µM - 100 µM	1 µM	1 µM - 100 µM
stimulation time	30 min	30 min	30 min	24 hrs	4 hrs	4 hrs	1 hr	24 hrs	72 hrs
stimulation time -kinetics	5 min - 60 min	5 min - 60 min	-	-	-	-	-	-	-

Table 3.5 Pre-treatment and ligand stimulation necessary for the performed cellular assays.

3.3.6 Cellular assays for BMP-2 functionality

3.3.6.1 Determination of phosphorylation of R-Smads

The phosphorylation of R-Smads is an early event in BMP-2 signaling which is detectable within 5 min of BMP-2 application.

HEK293T or C2C12 cells were transfected using PEI or Lipofectamine™/2000 as described above (see 3.3.3.2). For some experiments parental C2C12 cells were used as control. The experiments were done in 6-well or 24-well plates. 24 hrs after transfection or after seeding, cells were starved in DMEM/0.5% FBS v/v for 24 hrs and stimulated with 10 nM BMP-2 and/or 1 µM 8-Br-cGMP (Biolog) in starvation medium (DMEM/0.5% v/v FBS) for 30 min (see 3.3.5). Whole cell lysates were prepared using Triton lysis buffer containing protease and phosphatase inhibitors and cells were lysed by freezing at -20°C, thawing and overhead rotation for 10 min. Lysates for SDS-PAGE were prepared as described in 3.4.3 and protein content was

determined using BCA assay (see 3.4.4). 30 µg of protein each were separated on SDS-PAGE (see 3.4.10) followed by western blotting (see 3.4.12). The membrane was incubated consecutively with α-pSmad1/5/8 (Cell Signaling Technologies) and α-β-actin or α-β-tubulin antibodies. Overexpression was checked by α-cGKI antibody, and in some experiments by α-pVASP antibodies for phosphorylation of the vasodilator-stimulated phosphoprotein (VASP) [708] (see chapter 1.11.2). Smad phosphorylation was quantified relative to protein amount using ImageJ (Wayne Rasband (National Institutes of Health, NIH); http://rsb.info.nih.gov/ij).

Triton lysis buffer	1% v/v Triton X-100 20 mM Tris/HCl pH 7.5 150 mM NaCl (1 mM EDTA) Protease inhibitors (PI) 1 mM PMSF Phosphatase inhibitors (PPI): 2 mM NaF 5 mM NaP_2O_7 dissolved in dH_20
Protease inhibitor mix	Complete® EDTA free (Roche Diagnostics) dissolved in dH_2O stored in aliquots at 4°C
Phenymethysulfonylfluoride (PMSF)	100 mM stock solution dissolved in 2-propanol at 4°C stored in aliquots at -20°C
NaP_2O_7	200 mM stock solution

3.3.6.2 Determination of transcriptional activity using reporter gene assays

Reporter gene assays are based on the activity measurement of a certain reporter gene, e.g. a luciferase, which is expressed under the control of an inducible promoter. The promoter sequence is cloned from a target gene of the analyzed signaling pathway to examine the effect of a specific protein or chemical compound of interest.

For this study three different responsive reporter gene constructs were used, which were cloned in front of the *luciferase* gene (*luc*) from firefly *Photinus pyralis.*

p*BRE*-luc is characterized by a *BMP response element* (*BRE*). Korchynskyi and ten Dijke identified two BMP-responsive regions in the murine promoter of the *Id1* gene, an early target gene of the BMP signaling cascade [806]. One region contains two Smad binding elements, the other the palindromic sequence GGCGCC, which is flanked by two CAGC and two CGCC motifs. Both sequences are necessary for an efficient BMP reponse; the reporter gene is BMP-specific.

p*SBE*-luc consists of four *Smad binding elements* (*SBEs*) with the sequence CAGACA which were cloned from the promoter of murine *JunB*, an immediate early gene of TGF-β, Activin, and BMP-2 [807]. Thus, the pSBE-luc reporter can be induced by BMP-2 as well as TGFβ.

p$CAGA_{12}$-luc is a construct where 12 repeats of the *Smad3 binding element CAGAC* were cloned in front of the *luciferase* gene. Thus, the reporter is specific for the TGFβ pathway. The CAGAC sequences were found in the human *Col1A2* promoter [808]

The assay was done as follows: C2C12 cells were plated on a cell culture plate and transfected with the respective constructs using Lipofectamine™/2000 as described in 3.3.3.2. Additionally, the appropriate reporter construct and the constitutive luciferase reporter (from the sea pansy *Renilla reniformis*) were transfected per well. The *Renilla* luciferase reporter serves as a control for transfection efficiency to normalize the inducible reporter activity (dual reporter gene assay).

-------	6-well	12-well	24-well	48-well
total DNA	2 µg	1 µg	0.5 µg	0.2 µg
reporter	1 µg	0.5 µg	0.2 µg	0.1 µg
control reporter	0.3 µg	0.15 µg	60 ng	30 ng

Table 3.6 The table depicts the DNA amounts of the reporter constructs used for reporter gene analysis in C2C12 cells.

24 hrs after transfection, cells were treated for 5 hrs with starvation medium (DMEM/0.5% FBS v/v) and stimulated with 1 nM BMP-2 and/or 1 µM 8-Br-cGMP in DMEM/0.5% FBS v/v for 24 hrs. In the case of TGFβ stimulation, cells were starved in DMEM/0.2% FBS v/v and stimulated with 100 pM TGFβ-1. Luciferase activity was measured according to manufacturer´s instructions using the Dual-Luciferase® Reporter Assay System (Promega) and a FB12 or Mithras LB 940 luminometer (Berthold Detection Systems). If possible, expression control was examined by immunoblot (see 3.4.12) with α-cGKI, α-HA and/or TFII-I antibodies.

3.3.6.3 Determination of *Id1* mRNA

Inhibitor of differentiation (Id) proteins are helix-loop-helix transcription factors described to be upregulated by BMP stimulation within 1hr (BMP-immediate early target gene) [821]. 10^5 parental C2C12 cells per well were seeded in a 6-well plate and cultivated over night. Cells were starved in DMEM/0.5% FBS v/v for 24 hrs and treated with 10 or 20 nM BMP-2 and/or 1 µM 8-Br-cGMP in starvation medium (DMEM/0.5% FBS v/v) for 4 hrs. Cells were washed once with PBS and RNA was extracted using Tri-fast (see 3.2.5.1) according to the protocol. RNA yield was determined using a spectrophotometer (see 3.2.2) and purified mRNA was reversed transcribed into cDNA using *MMLV* reverse transcriptase (see 3.2.5.2). Analysis of *Id1* mRNA amount was performed via PCR (see 3.2.5.3) using *Id1*-specific oligodeoxynucleotides (see 0, oligonucleotides). Subsequently, agarose gelelectrophoresis and sample analysis under UV light was done.

3.3.6.4 Determination of phosphorylation of MAPK p38

Besides the Smad pathway, BMP signaling can also activate the MAPK p38 (see chapter 1.5) within 1 hr.

C2C12 cells were transfected using PEI or Lipofectamine^{TM}/2000 as described above (see 3.3.3.2). For some experiments, parental C2C12 cells were used. The experiments were done in 6-well or 24-well plates. The starvation time for this assay needs to be established for every new cells batch to get a sufficient ligand-dependent phosphorylation of p38. 24 hrs after transfection or after seeding, cells were starved in DMEM/0.5% FBS v/v (mostly for 5 hrs) and stimulated with 10 nM BMP-2 and/or 1 µM 8-Br-cGMP in DMEM/0.5% FBS v/v for 1 hr (see 3.3.5). Whole cell lysates were prepared using Triton lysis buffer containing protease and phosphatase inhibitors. After harvesting, cells were lyzed by freezing at -20°C, thawing and overhead rotation for 10 min. Lysates for SDS-PAGE were prepared as described in 3.4.3 and protein content of the samples was determined using BCA assay (see 3.4.4). 30 µg of protein each were separated on SDS-PAGE (see 3.4.10) followed by transfer on nitrocellulose membrane (see 3.4.12). The membrane was analyzed consecutive using α-pp38 and α-β-actin or α-β- tubulin antibodies. Overexpression of cGKI was checked by α-cGKI antibody.

3.3.6.5 Determination of *ALP* mRNA

Alkaline phosphatase (ALP) is an osteoblast marker protein; its expression can be stimulated through BMP treatment mainly via the p38-MAPK pathway [195, 472] (see chapter 1.5).

For this assay, 1* 10^5 parental C2C12 cells were seeded on a 6-well plate and cultivated over night. Cells were starved in DMEM/0.5% FBS v/v for 24 hrs and treated with 10 or 20 nM BMP-2 and/or 1 µM 8-Br-cGMP in starvation medium (DMEM/0.5% FBS v/v) for 24 hrs. Cells were lyzed and cDNA was generated as described in 3.2.5.1 and 3.2.5.2. Analysis of *ALP* mRNA amount was performed via PCR (see 3.2.5.3) using *ALP*-specific oligodeoxynucleotides (see appendix, sequences, oligonucleotids). Subsequently, agarose gelelectrophoresis and sample analysis under UV-light was done.

3.3.6.6 Determination of ALP activity

Cells were transfected with Lipofectamine™ as described above (see 3.3.3.2). For some experiments non-transfected C2C12 cells ($1*10^4$) were used. The assay was done in a 96-well plate. 24 hrs after transfection or seeding, cells were starved in DMEM/2% FBS v/v for 5 hrs and stimulated with 20-50 nM BMP-2 and/or 1 µM 8-Br-cGMP in ALP-starvation medium (DMEM/2% v/v FBS) for 72 hrs. Prior lysis, cells were washed once with PBS and lyzed in 100 µl ALP buffer 1 (1 hr, rocking plate, RT). 100 µl ALP buffer 2, containing an ALP substrate, was added to the lysates and enzymatic reaction was observed under shaking at RT. ALP enzymatic activity was measured using an microplate reader (Tecan) with a testfilter of 405 nm (absorbance 405 nm).

ALP buffer 1	0.1 M glycine pH 9.6 1 mM $MgCl_2$ 1 mM $ZnCl_2$ 1% v/v NONIDET P-40 dissolved in dH_20
ALP buffer 2	0.1 M glycine pH 9.6 1 mM $MgCl_2$ 1 mM $ZnCl_2$ dissolved in dH_20 2 mg/ml pNPP
para-nitrophenylphosphate (pNPP) (Roth)	20 mg/ml stock solution dissolved in dH_20

3.3.7 Immunofluorescence microscopy

Immunofluorescence microscopy allows to study expression and subcellular distribution of proteins in cells *in vivo.* Living cells can be monitored by use of an antibody against an extracellular protein epitope (i.e. in the case of transmembrane receptors). Furthermore, transmembrane receptors by can be enriched in “patches”

due to cross-linking via the primary antibody. Staining intracellular proteins can be facilitated by fixing and permeabilizing of the cells.

3.3.7.1 Co-localization studies after receptor co-patching

For co-localization studies, C2C12 cells stably expressing N-terminally HA-tagged BRII-SF or BRII-LF were seeded into a Lab-Tek™ II chamber slide (4-well) and cultured in growth medium overnight. Staining was done as described by [219]. Living cells were incubated in 200 µl Hanks buffer (Biochrom) at 4°C for 1 hr. Receptors were visualized using α-HA antibody (Roche Diagnostics) (1 hr, RT) followed by Cy2-conjugated goat α-mouse IgG (1 hr, RT, in darkness). Cells were fixed with 200 µl ice cold methanol (5 min) and afterwards 200 µl acetone (2 min) both at -20°C and endogenous cGKIβ was stained with α-cGKIβ antibody (L-16, Santa Cruz Biotechnology) (1 hr, RT) and Cy3-conjugated mouse α-goat IgG (1 hr, RT, in darkness). After embedding cells in Kaisers Glyzeringelatine (Merck), cells were analyzed using a Leica DMR confocal microscope (Leica Microsystems) with a 63-fold magnification.

Hanks buffer	Hanks solution (Biochrom) 20 mM Hepes 1% w/v BSA

3.3.7.2 Co-localization studies

To examine co-localization of cGKI with Smad proteins or co-localization of Smad1 with TFII-I, parental C2C12 cells were seeded into a Lab-Tek™ II chamber slide (16-well), were starved for 3 hrs in 100 µl DMEM/0.5% FBS v/v and either stimulated with 20 nM BMP-2 and/or 1 mM 8-Br-cGMP for 30 min. In other experiments a time course was examined with 10 nM BMP-2. Staining of cell was done as described [822]. Cells were fixed with 100 µl PBS/3.7% v/v para-formaldehyde (PFA) for 15 min and permeabilized with 100 µl PBS/0.5% v/v Triton X-100 for 10 min. Unspecific binding was blocked with 100 µl PBS/3% w/v BSA for 30 min and endogenous proteins were stained using α-cGKI, α-Smad1, α-Smad4 and/or TFII-I antibodies for 1 hr at RT. Bound primary antibodies were visualized with goat α-rabbit IgGs

conjugated to Alexa Fluor 594 or Alexa Fluor 488 (incubation for 1 hr, RT, in darkness). The incubation with the secondary antibodies was done simultaniously or subsequently. Nuclear staining was carried out using Hoechst dye (1:1000, 2 min, RT). Cells, embedded in FluoromountG (Southern Biotech), were analyzed with 63-fold magnification using an Axiovert 200 M fluorescence microscope (Zeiss). All microscope slides were stored at 4°C in darkness.

Hoechst dye (33342)	1 mg/ml stock solution dissolved in dH_2O

3.3.8 Analysis of subcellular protein localization

3.3.8.1 Immunofluorescence-based analysis of protein localization

To examine the expression pattern of cGKI and associated proteins, parental C2C12 cells seeded into a Lab-Tek™ II chamber slide (16-well) or 293T cells, transfected or not, were starved for 3 hrs in 100 µl DMEM/0.5% FBS v/v and either stimulated with 10-20 nM BMP-2 and/or 1 mM 8-Br-cGMP 5 min to 4 hr, in starvation medium. In some cases, 3-isobutyl-1-methylxanthine (IBMX), a PDE inhibitor [823] was added. Cells were fixed, permeabilized and blocked as described in 3.3.7.2. Endogenous cGKI was stained using α-cGKI antibody (Stressgene) and α-HA (Roche Diagnostics) for 1 hr at RT. Bound primary antibodies were visualized with goat α-rabbit IgGs conjugated to Alexa Fluor 594 and goat α-mouse IgGs conjugated to Alexa Fluor 488 for 1 hr at RT in darkness. Nuclear staining was carried out using Hoechst dye for 2 min at RT. Cells, embedded in FluoromountG, were analyzed using fluorescence microscopy (63-fold magnification). All microscope slides were stored at 4°C in darkness.

IBMX (Merck)	1 M stock solution dissolved in DMSO stored in aliquots at -20°C

3.3.8.2 Analysis of protein localization via nuclear-cytoplasmic fractionation

Another method to examine the subcellular localization of cGKI is nuclear-cytoplasmic fractionation. Two different protocols were used.
Transfected HEK293T cells were collected in ice cold PBS and transferred to safe lock reaction tubes. Cells were centrifuged (3.000 rpm, 4°C, 5 min), the pellet was resuspended in 300 µl hypotonic lysis buffer and incubated (for swallowing) on ice for 15 min. Afterwards, cells were lyzed by addition of NONIDET P-40 detergent to a final concentration of 0.5% v/v. Cells were vortexed 20x using a shearer and nuclei were collected by centrifugation (3.300 rpm, 4°C, 10 min). The supernatant, the cytoplasmic fraction, was transferred to a new reaction tube. The remaining sample was centrifuged (12.000 rpm, 4°C, 1 min) and the supernatant was discarded. Pelleted nuclei were resuspended in 100 µl high salt buffer, incubated on ice for 30 min and centrifuged (12.000 rpm, 4°C) for 20 min. The supernatant, the nuclear fraction, was then transferred to a new reaction tube. Both lysates were stored at -20°C or directly subjected to SDS-PAGE (see 3.4.10) and Western blot analysis (see 3.4.12).

Hypotonic lysis buffer	10mM Hepes pH 8.0 10mM KCl 0.1mM EDTA 1mM DTT PI 1 mM PMSF dissolved in dH_20
High salt buffer	20mM HEPES pH 8.0 25% v/v glycerol 0.4M NaCl 1mM EDTA 1mM DTT PI 1 mM PMSF dissolved in dH_20

C2C12 cells, transfected or not, were fractionated using another protocol. Cells were starved in DMEM/0.5% v/v FBS for 3 hr, stimulated with 10 nM BMP-2 for 30 min and collected in ice cold PBS. After centrifugation (1.200 rpm, 4°C, 3 min), cells were resuspended in cytosolic lysis buffer and incubated on ice for 10 min. After addition of NONIDET P-40 at a final concentration of 0.5% v/v, cells were incubated on ice for 5 min. Nuclei were collected by vortexing for 10 sec twice and centrifugation at 12.000 rpm for 30 sec. The isolated nuclei were resuspended and lyzed in nuclear lysis buffer plus phosphatase inhibitors. Cytoplasmic and nuclear lysates were cleared by high-speed centrifugation at 12.000 rpm for 10 min and subjected to immunoprecipitation or directly to SDS-PAGE and western blot.

Cytosolic lysis buffer	10 mM Hepes pH 7.4
	2 mM $MgCl_2$
	10 mM KCl
	1 mM EDTA
	PI
	1 mM DTT
	PPI:
	10 mM NaF
	0.1 mM Na_3VO_4
	dissolved in dH_20
Nuclear lysis buffer	1% v/v Triton X-100
	20 mM Tris/HCl pH 7.5
	150 mM NaCl
	PI
	1 mM PMSF
	PPI:
	20 mM $Na_2H_2P_2O_7$
	5 mM NaF
	2 mM $NaVO_4$
	dissolved in dH_20

3.3.9 *in vivo* kinase assay

To analyze the effect of cGKI on BRII protein, an α-phosphopetide-specific antibody was used which recognizing phosphorylation of arginine-dependent kinases like cGKI (PKGI) or PKA (α-pPKA/PKG substrate antibody) (see 2.13.1).

C2C12 cells were transfected with cGKI constructs or empty vector. After 24 hr, cells were starved for 3 hrs and stimulated with 1 µM 8-Br-cGMP for 30 min. Cells were lyzed in Triton-X 100 lysis buffer containing phosphatase inhibitors and lysates were cleared by centrifugation (12.000 rpm, 4°C, 10 min) (see 3.4.3). Afterwards, lysates were subjected to immunoprecipitation (see 3.4.9) for protein enrichment and separation by SDS-PAGE (see 3.4.10) and immunoblotting (see 3.4.12) the samples were probed with an α-pPKA/PKG substrate antibody. Additionally, membranes were incubated with α-BRII (G17, Santa Cruz Biotechnology) and α-cGKI antibodies to control expression and protein loading. BRII phosphorylation was quantified relative to the BRII protein amount using ImageJ (Wayne Rasband, NIH).

Lysis buffer	1% v/v Triton X-100
	20 mM Tris/HCl pH 7.5
	150 mM NaCl
	PI
	1 mM PMSF
	PPI:
	5 mM NaF
	2 mM $NaVO_4$
	20 mM $Na_2H_2P_2O_7$
	dissolved in dH_20

3.3.10 Proliferation assay

Cell proliferation defines the increase of cell number as a result of cell division and cell growth. Proliferation can be measured by determining the DNA content, metabolic activity, or analyzing specific proliferation markers or PCNA (essential for DNA replication).

To analyze cell proliferation in vascular diseases as pulmonary arterial hypertension, VSMCs were used. Fugene-transfected cells were were starved in medium 231/0.5% (v/v) smooth muscle growth supplement (SMGS) for 18 hrs and stimulated either with 20 nM PDGF or serum (medium 231/5% (v/v) SMGS) for 24 hrs. Proliferation was measured with the CellTiter 96® AQ_{ueous} One Solution Cell Proliferation Assay (Promega) according to manufacturer´s instructions. This assay measures metabolic activity of the cells. The quantity of the formazan product as measured by the amount of 450 nm absorbance (maximum according to the manufacturer at 490 nm) is directly proportional to the number of living cells in the culture.

3.4 Protein chemical methods

3.4.1 Amplification and purification of recombinant proteins

To yield a high quality as well as a high amount of recombinant proteins, freshly transformed bacteria (*E. coli* BL21(DE)) were used. 300 ml of LB medium were inoculated with one bacterial clone and cultivated over night. Bacteria were grown to an optical density of OD_{600} = 0.5-0.6. Protein expression was induced by addition of isopropyl β-D-1-thiogalactopyranoside (IPTG) at a final concentration of 1 mM. Protein expression was carried out at the appropriate temperatures (GST, 30°C; GST-BRII-SF, 30°C; GST-BRII-tail, 20°C; MBP-Smad1, 30°C) for 1 hr; temperature and induction time are parameters which influence the solubility of the recombinant protein and thus have to be optimized for each protein individually. Afterwards, bacterial cells were incubated on ice for 10 min and collected by centrifugation (6.000 rpm, 4°C, 15 min). Each pellet was resuspended in 10 ml STE buffer and the membrane of the cells was distroyed by sonification (40% power, 4°C, 3x 30 sec). Lysates were cleared by centrifigation (4°C, 15.000 rpm, 30 min). The supernantant was incubated with 600 µl of glutathion-sepharose slurry (GE Healthcare Biosciences) for 3 hrs under rotation to precipitate the glutathion-S-transferase (GST)-fused proteins. The pellets were washed three times with ice cold STE buffer and 2x with ice cold 20 mM Tris/HCl pH 7.4 and resuspended in 1 ml 20 mM Tris/HCl pH 7.4. An aliquot was subjected to SDS-PAGE (see 3.4.10) for Coomassie-G

staining (see 3.4.11) to determine the amount of purified protein. The protein solution was stored at -80°C. For subsequent assays 1 µg of recombinant protein was used.

IPTG	1 M stock solution dissolved in dH_20 stored in aliquots at -20°C
STE buffer	10 mM Tris pH 8.0 150 mM NaCl 1 mM EDTA 1 mM DTT 9 µg/µl aprotinin (Roche Diagnostics) dissolved in dH_20

3.4.2 *in vitro* kinase assay

1 µg of recombinant protein (see 3.4.1) or immunopurified protein (see 3.4.9) were washed 1x with washing buffer and in the respective combination the proteins were subjected to *in vitro* kinase assay. Proteins coupled to sepharose beads were supplemented with 25 µl kinase buffer containing 25 µM 8-Br-cGMP or not. Then, phosphorylation was initiated by the addition of 1 µCi (γ-^{32}P)ATP (Hartmann Analytics) and the protein precipitates were incubated at 30°C for 30 min. The proteins were eluted with 6x protein sample buffer, separated on SDS-PAGE (see 3.4.10) and transferred to nitrocellulose membrane (see 3.4.12). The phosphorylated proteins were detected using a phospho-imager (FLA-5000, Fujifilm) or X-ray films (Konica-Minolta). Subsequent immunoblotting with the respective antibodies monitored the protein amounts.

Washing buffer	150 mM NaCl 20 mM Hepes pH 7.4 1 mM DTT dissolved in dH_20

Kinase buffer	150 mM NaCl 20 mM Hepes pH 7.4 75 mM $MgCl_2$ 500 µM ATP 1 mM DTT dissolved in dH_2O

3.4.3 Preparation of cell lysates

For cell lysis, adherent cells were first washed with PBS, while non-adherent cells were directly harvested in the respective lysis buffer (see particular cell method). The specific volume of lysis buffer to adjust the amount of detergent depends on the number of cells which should be lyzed. **Table 3.7** depicts the volumes that were used for preparing (co-) immunoprecipitation lysates (see 3.4.9) and direct lysates for SDS-PAGE (see 3.4.10). Cells were removed from the plate either by shaking on a rocking plate (4°C) or by using a cell scraper (Hartenstein Laborbedarf). Subsequently, cells were lyzed under rotation at 4°C for 30 min. To clear the lysates, resulting samples were centrifuged (12.000 rpm, 4°C, 10 min). The supernatants were separated from the pelleted insoluble cell components and transferred to new reaction tubes. The lysates were supplemented with 6x protein sample buffer, boiled at 95°C for 3 min, and stored at -20°C, or used for subsequent protein chemical assays.

sown cell number			cultivation format	volume lysis buffer
C2C12	**293T**	**VSMC**		
$2*10^6$	$5*10^6$	-	15 cm dish	3-5 ml
$1*10^6$	-	-	10 cm dish	2-3 ml
$3*10^5$	$1*10^6$		6 cm dish	1-1.5 ml
$1*10^5$	$5*10^5$	$2*10^5$	6-well	300-700 µl
$5*10^4$	-	-	12-well	200 µl
$2*10^4$	$1*10^5$	$5*10^4$	24-well	100-200 µl
$1*10^4$	-	$2*10^4$	48-well	50 µl

Table 3.7 The table shows the volume of lysis buffer used against the sown cell number after 48 hrs of cultivation/treatment.

6x protein sample buffer	0.125 M Tris/HCl pH 6.8 30% v/v glycerol 10% w/v SDS 0.6 M DTT 0.012% w/v bromphenole blue dissolved in dH_20

3.4.4 Determination of protein content using BCA assay (according to Redinbaugh)

Determination of protein amounts in cell lysates was done using the bichinonic acid (BCA) method [824] to apply a defined amount of protein of each sample to SDS-PAGE. The method is based on the measurement of the absorption spectrum of the reaction product. The purple product emerges from the chelate formation between two molecules of BCA and one Cu^{2+} ion.

The cell lysates were diluted in dH_2O (1:10), and 20 µl of each dilution as well as a BSA standard series was transferred in duplicates to a 96-well plate. BCA solution A and B were mixed (49:1) and 200 µl of the mixture was added to each lysate dilution. After an incubation step for 30-45 min at 60°C, the lysates changed color to purple. The samples were measured with a testfilter at 550 nm using a microplate reader. The protein concentrations were calculated referring to the calibration curve of the BSA standards.

BSA standard	25 µg/ml - 50 µg/ml - 75 µg/ml - 100 µg/ml - 150 µg/ml - 200µg/ml - 250 µl/ml dissolved in dH_20
BCA solution A	1.35% w/v $NaHCO_3$ 0.58% w/v NaOH 1% w/v bichinonic acid 0.57% w/v $KNaC_4H_4O_6*4\ H_2O$ dissolved in dH_20 stored in aliquots at -20°C

BCA solution B	2.3% w/v $CuSO_4$ dissolved in dH_20

3.4.5 Precipitation of proteins using TCA/acetone

To precipitate the protein, the 8-fold volume of ice cold acetone/10% v/v trichloracid (TCA) v/v according to the sample was given to the protein sample. Protein was precipitated over night at -20°C. Following this, the samples were centrifuged (13.000 rpm, 30 min, 4°C) and washed with ice cold acetone. After a second centrifugation step (13.000 rpm, 15 min, 4°C), the pellets were denaturated in 6x protein sample buffer at 95°C and diluted in dH_2O to reach 1x sample buffer concentration. Subsequently, the samples were subjected to SDS-PAGE (see 3.4.10) and western blotting (see 3.4.12).

3.4.6 Covalent antibody linking to sepharose

To covalently link polyclonal antibodies to protein A-sepharose beads, 9 ml linking buffer A and 0.5 ml of protein A-sepharose slurry, equilibrated with linking buffer A, were added to 2 ml antibody serum and incubated under rotation at 4°C over night. The direct supernatant after over night incubation was saved for a second round of antibody linking. The antibody-bound beads were washed 5x with linking buffer A and then, 2x with linking buffer B. All centrifugation steps were at 1.200 rpm for 3 min at 4°C. The sepharose beads were resuspended in linking buffer C containing dimethylsuberimidate (DMS) (Pierce Biotechnology) and incubated at RT for 1 hr under rotation. Afterwards, the supernatant was replaced by 50 mM Tris, pH 8.0 and the suspension was again rotated for 2 hrs at RT. The antibody-linked beads were washed 4x with TBS buffer and diluted 1:2 in PBS/0.1% w/v sodium azide.

The efficiency of covalent linking was checked via SDS-PAGE and denaturation with 6x protein sample buffer using 10 µl each beads, taken before DMS, and beads, taken after DMS.

Linking buffer A	10 mM Hepes pH 7.4 150 mM NaCl 1 mM EDTA dissolved in dH_20
Linking buffer B	0.2 M sodium borate pH 9.0 dissolved in dH_20
Linking buffer C	0.2 M sodium borate pH 9.0 10 mg/ml DMS dissolved in dH_20
TBS buffer	20 mM Tris/HCl pH 7.5 150 mM NaCl dissolved in dH_20

3.4.7 Protein pulldown via GST-fused bait proteins

To study protein-protein interaction, pulldown experiments with glutathion-S-transferase (GST)-fused proteins can be performed. Therefore, recombinant GST-fused bait proteins have to be generated and are used to fish for prey proteins, i.e. interaction partners, in protein lysates.

Lysates of C2C12 cells (see 3.4.3), transfected or not, were incubated with GST-fused proteins, immobilized to glutathione sepharose, at 4°C on an overhead-rotator over night. Subsequently, protein complexes were precipitated using glutathione sepharose and precipitates were washed three times with the respective lysis buffer. Finally, the pellets were eluted in 2x protein sample buffer and boiled at 95°C for 3 min. Denaturated proteins were subjected to SDS-PAGE (see 3.4.10) and immunoblotting (see 3.4.12) to detect associated proteins of the tested fusion proteins.

2x protein sample buffer	0.125 M Tris/HCl pH 6.8 4% w/v SDS 10% v/v β-mercaptoethanol 0.005% w/v bromphenol blue dissolved in dH_20 or diluted with dH_20 from 6x protein sample buffer

3.4.8 *in vitro* binding

To examine direct interaction of proteins, *in vitro* binding using GST-BRII cytoplasmic domains for pulldown was performed.

For that, 1 µg of GST, GST-BRII-SF or GST-BRII-tail bound to glutathione sepharose were incubated for 1 hr at 4 °C with 1 µg of MBP or MBP-cGKIβ in 50 µl of binding buffer. Post intense washing (3x with binding buffer), BRII-bound protein was isolated on glutathione sepharose beads. Finally, the pellets were eluted in 2x protein sample buffer and boiled at 95°C for 3 min. The denaturated proteins were subjected to SDS-PAGE (see 3.4.10) and immunoblotting (see 3.4.12) to detect associated proteins of the tested fusion proteins.

MBP-cGKIβ was generated by J. Weiske, Charité, Germany. Briefly, MBP-tagged cGKIβ was generated by amplification of the cGKIβ cDNA in pMM9 with specific oligodeoxynucleotide pairs (see chapter 9, oligonucleotide sequences). The PCR product was ligated into pMAL (New England Biolabs) treated with BamHI and calf intestinal phosphatase. Sequence of the construct was confirmed by cycle sequencing and subsequent analysis on an ABIPrism 310 genetic analyzer. To obtain recombinant MBP-cGKIβ proteins, *E. coli* strain BL21RE4 was transformed with the plasmid pMal-cGKIβ, and expression was induced with 1 mM IPTG. After 1 hr at 37°C, bacteria were harvested by centrifugation, and the pellets were resuspended in lysis equilibration wash buffer. Cells were lysed by sonication, and insoluble material was removed by centrifugation at 24.000 x *g* for 30 min at 4 °C. The MBP fusion protein was purified by affinity chromatography on amylose resin (New England Biolabs).

Binding buffer	0.1% (v/v) NONIDET P-40 150 mM NaCl 20 mM Tris/HCl pH 7.5 1 mM EDTA 0.5 mM DTT 0.1% BSA 10% (v/v) glycerol PI 1 mM PMSF dissolved in dH_20
Lysis equilibration wash buffer	40 mM Tris, pH 8.0 150 mM NaCl PI: Complete™ protease inhibitor mixture (Roche Diagnostics)

3.4.9 Co-immunoprecipitation

Co-immunoprecipitation allows to analyze protein-protein interactions occuring in the living cell. Immunoprecipitation is based on the specific interaction of an antibody with its antigen, i.e. protein-of-interest. The immune complex is then precipitated using protein A-sepharose since protein A (from *Staphylococcus aureus*) specifically binds to the antibody´s F_c part. Therefore, the resulting precipitates consist of the protein-of-interest, the antibody, the protein A-sepharose-coupled beads and, additionally, associated proteins.

Lysates of transfected or untransfected HEK293T cells or C2C12 cells (see 3.4.3) were incubated at 4°C over night under rotation with 0.5-1 µg of antibody against the protein which should be immunoprecipitated. Afterwards, 50 µl of protein A-sepharose slurry (Sigma-Aldrich) were added and the samples were again incubated at 4°C on an overhead incubator for 1 hr. Then, the pellets were washed

3x in the respective lysis buffer and immune complexes were eluted in 50 µl of 2x protein sample buffer upon boiling. The supernatants were used for SDS-PAGE (see 3.4.10) and subsequent western blot analysis (see 3.4.12).

Protein A-sepharose	protein A-sepharose (Sigma-Aldrich) swallowed in sterile PBS diluted 1:1 in sterile PBS

3.4.10 SDS polyacrylamide gelelectrophoresis

SDS (sodiumdodecylsulfate) polyacrylamide gelelectrophoresis (SDS-PAGE) was performed as described [825] by loading protein samples on a discontinous gel (7.5 - 12.5%) to electrophoretically separate proteins according to their molecular weight. Stacking and resolving gels were prepared as follows:

----------	10% resolving gel	stacking gel
Acrylamide/Bis-acrylamide	3 ml	0.25 ml
Lower Tris	2.25 ml	-
Upper Tris	-	0.5 ml
dH_20	3.75 ml	1.25 ml
APS	15 µl	4 µl
TEMED	15 µl	4 µl

Table 3.8 Pipetting scheme for one mini gel for the Mini Protean gelelectrophoresis systems (Bio-Rad)

Acrylamide/bis-acrylamide	30% w/v acrylamide 1% w/v bis-acrylamide dissolved in dH_20 30% w/v stock solution (Roth)

Lower Tris	4x stock solution 1.5 M Tris 0.4% w/v SDS dissolved in dH_20 adjust pH 8.8
Upper Tris	4x stock solution 0.5 M Tris 0.4% w/v SDS dissolved in dH_20 adjust pH 6.8
Ammoniumpersulfate (APS) (Carl Roth)	40% w/v APS dissolved in dH_20 stored in aliquots at -20°C stable at 4°C
TEMED (N,N,N',N'-tetramethylethylenediamine)	
SDS running buffer	25 mM Tris 190 mM glycine 0.1% w/v SDS dissolved in dH_20

3.4.11 Coomassie-G stain of proteins

Staining of proteins with Coomassie-G is based on the unspecific adsorption of this triphenylmethane dye to basic or aromatic residues of proteins. Coomassie-G stain is normally performed after SDS-PAGE (see 3.4.10) and recognizes as little as 0.5 µg total protein. Coomassie-R, which is more sensitive (0.1 µg protein), can be used in place of Coomassie-G.

Briefly, after SDS-PAGE the gel was washed with dH_2O and proteins were prefixed in gel fixation/desataining solution for 15 min. Afterwards, the gel was stained in Coomassie-G staining solution from 2 to 24 hrs until the gel is uniformly blue colored. Destaining was accomplished by the addition of 25% v/v 2-propanol/10% v/v acidic acid or dH_20 until the background is clear.

Gel fixation/destaining solution	25% v/v 2-propanol 10% v/v acidic acid dissolved in dH_20
Coomassie-G staining solution	0.006% v/v Coomassie-G-250 (Roth) 10% v/v acidic acid dissolved in dH_20

3.4.12 Western blot and detection of proteins via enhanced chemiluminescence

Beside Coomassie-G staining (see 3.4.11), proteins can be specifically vizualized by western blot (WB) analysis. For this, electrophoretically separated proteins were transferred to and fixed on a nitrocellulose or a polyvinylidenfluoride (PVDF) membrane to detect specific proteins by subsequent immunoblotting (IB) and enhanced chemiluminescence (ECL). This method was introduced for the first time by W.N. Burnette [826].

For the protein transfer, the “wetblot” method (Mini-V 8.10 system, Bio-Rad) was used. The transfer was carried out at 100 V for 60 to 75 min in cooled WB transfer buffer. To control protein transfer as well as equal loading in certain cases, the membrane was stained with the reversible dye Ponceau S and backround-destained with dH_2O or 0.1% TBS-T. To avoid unspecific binding of the primary antibody, the membrane was saturated with skim milk or bovine serum albumine (BSA) (1-5%) in 0.1% TBS-T at RT under shaking for 1 hr. Subsequently, the primary antibody was incubated according to manufacturer´s instructions at RT for 1 hr or at 4°C over night on a shaker. After intense washing with 0.1% TBS-T, a species-specific secondary antibody conjugated to horseradish peroxidase (HRP) was given

to the membrane for 1 hr at RT under shaking. In some cases the secondary antibody solution was supplemented with skim milk or BSA. Intense washing with 0.1% TBS-T was followed by vizualizing the respective proteins using ECL reaction. For this, 1 ml of ECL solution A and 1 ml ECL solution B solution per membrane were mixed on the blot and incubated for 30-60 sec. The HRP catalyzes the reaction of luminol to its oxidized form and thereby emitted light was detected by X-ray films.

In some cases, the primary antibodies had to be removed for a second round of immunoblotting. This was done by denaturating the antibodies through incubation of the membrane in WB stripping buffer containing β-mercaptoethanol and SDS for 30-45 min at 60°C. Before starting a new IB, the membrane was intensively washed with PBS until foaming completely stopped.

WB transfer buffer	25 mM Tris 190 mM glycine 20% v/v methanol dissolved in dH_20
Ponceau-S staining solution	0.5% w/v Ponceau-S 3% v/v TCA dissolved in dH_20
WB washing buffer	50 mM Tris/HCl pH 8.0 150 mM NaCl 0.1% v/v or 0.5% v/v Tween-20 dissolved in dH_20
ECL solution A	volumes per 1 membrane 1 ml luminol solution 4.4 µl para-coumaric acid

Luminol solution	2.5 mM 3-aminophtal-hydrazide (Merck) dissolved in DMSO 0.1 M Tris/HCl pH 8.5 dissolved in dH_20
Para-coumaric acid	90 mM para-coumaric acid dissolved in DMSO stored in aliquots at -20°C stable at 4°C
ECL solution B	volumes per 1 membrane 1 ml 0.1 M Tris/HCl pH 8.5 1 µl H_20_2
H_20_2	30% v/v stock solution
WB stripping buffer	62.5 mM Tris/HCl pH 6.5 10% w/v SDS 0.7% v/v β-mercaptoethanol dissolved in dH_20

4 Results

4.1 Characterization of cGKI/BRII interaction

The BMP type II receptor (BRII) is an exceptional receptor inside TGFβ superfamily receptors. The receptor exists as two alternative spliced variants. BRII long form (BRII-LF) in contrast to the short form (BRII-SF) exhibits a long cytoplasmic extension the BRII-tail, which is unique among mammalian TGFβ receptors [75]. The *Drosophila* BMP type II receptor wishful thinking (wit) has also long cytoplasmic tail [827]. Although several studies showed equal signaling behaviour of BRII-LF and BRII-SF [72, 195], some functions were assigned to the long C-terminal tail of BRII [191, 261, 264, 266, 268]. But the importance of BRII-tail for BMP signaling is not clear yet, particularly with regard to findings that mutations in BRII underlie hypertension diseases [13].

4.1.1 Identification of cGKI as BRII-associated protein

To identify novel interaction partners of BRII and thus potential regulators of BMP signaling, a proteomics-based screen for BRII interactors was performed [265]. Therefore, different BRII cytoplasmic regions fused to GST were used as bait for associated proteins in C2C12 cell lysates. Among these identified proteins was the cGMP-dependent kinase I (cGKI) (**Figure 4.1**).

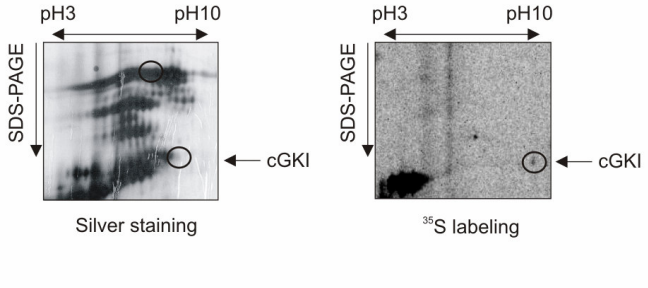

protein		cGMP dependent protein kinase I
accession no.		AF084547
probability		9.8e-001
z-value		0.66
sequ. coverage		20%
exp. value	pI	5.3
	MW	78.34 kD
theor. value	pI	5.08 (Iβ); 5.87 (Iα)
	MW	77.79 kD (Iβ); 76.35 kD (Iα)

Figure 4.1 Identification of cGKI as a BRII-tail-associated protein. cGKI/BRII-tail complexes in C2C12 cells were isolated using GST-BRII-tail for pulldown. Identification of the proteins was done by subsequent two dimensional gelelectrophoresis (silver stain and ^{35}S labeling) and MALDI-TOF mass spectrometry analysis. The table (right) depicts the proteomics data. pI isoelectric point, MW molecular weight.

Figure 4.1 shows that cGKI was identified as a BRII-tail-associated protein (left panels, silver stain and ^{35}S labeling). The proteomics data listed in the table (right) indicate that the experimental values of both the isoelectric point (pI) and the molecular weight (MW) correspond very well with the theoretical values known for cGKI. Due to alternative splicing two cGKI isoforms, cGKIα and cGKIβ , exist which differ in their N-terminal amino acid sequence [657] (**Figure 4.2**).

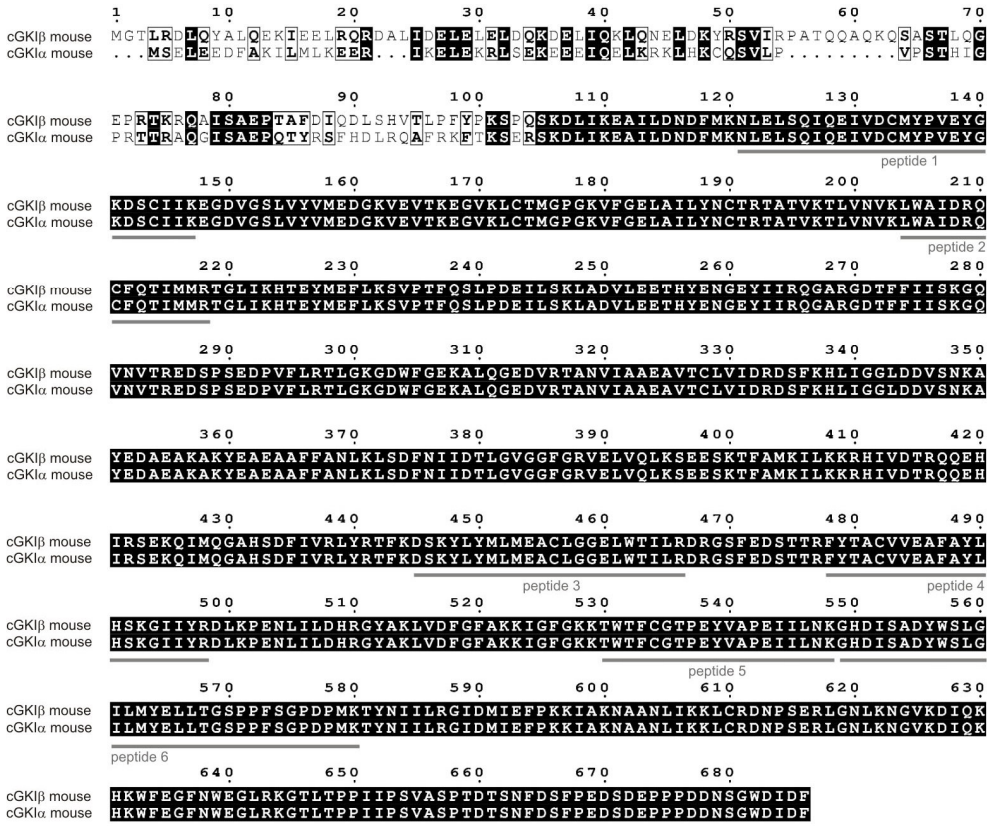

Figure 4.2 Protein sequence analysis of murine cGKI isoforms. The alignment using ClustalW shows that murine cGKIα and β exclusively differ in the N-terminus. Peptides identified via MALDI-TOF mass spectrometry are designated (in grey). The numbers above refer to murine cGKIβ.

Figure 4.2 reveals that the isoforms are identical up to aa105 in Iβ and aa89 in Iα respectively. Both isoforms are expressed in C2C12 cells [673]. Since the peptides identified by mass spectrometry (n=6) did not allow a differentiation between α or β isoform, both isoforms were used for further experiments.

To confirm the identified interaction between cGKI and BRII, co-immunoprecipitation (co-IP) assays were done. For that, cGKIα or β and HA-tagged

BRII-LF were transiently transfected into HEK293T cells and BRII-LF binding to cGKI was assayed via co-immunoprecipitation (co-IP).

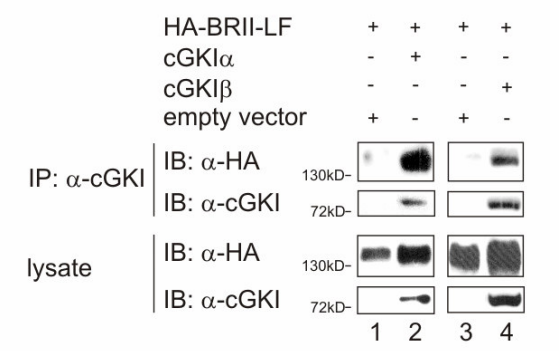

Figure 4.3 Interaction of cGKI isoforms with BRII-LF. cGKI was immunoprecipitated from HEK293T cells transfected with vectors expressing cGKIα or β and HA-BRII-LF. BRII-LF and cGKI variants in α-cGKI immunoprecipitates were detected with α-HA and a-cGKI antibodies (upper panels). Lysates were controlled for BRII-LF and cGKI expression (lower panels). This result is a representative one (n>3). IP, immunoprecipitation; IB, immunoblot.

As **Figure 4.3** shows, BRII-LF interacted with both cGKIβ (upper panel, lane 4) and α (upper panel, lane 2) upon overexpression. To rule out that the observed cGKI/BRII interaction was driven by overexpression of the proteins, endogenous co-IP analysis in C2C12 cells was done (**Figure 4.4**).

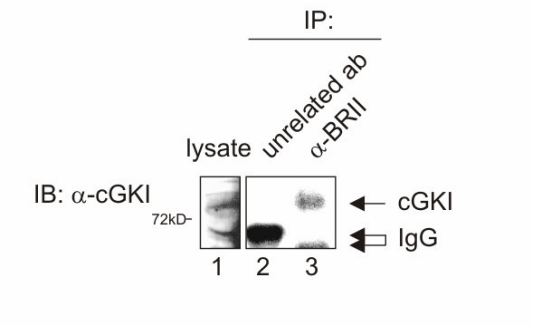

Figure 4.4 Endogenous binding of cGKI and BRII. Endogenous interaction studies were done in C2C12 cells using α-BRII antibody for IP (lane 3). Binding of cGKI was verified by immunoblotting with α-cGKI antibody. An unrelated antibody (ab) was used as control (lane 2). A representative assay out of at least three independent experiments is shown. IP, immunoprecipitation; IB, immunoblot.

Figure 4.4 shows that endogenous cGKI was found in the α-BRII precipitate (lane 3). The α-BRII antibody, a polyclonal rabbit antibody which was covalently linked to protein A-sepharose (see 3.4.6), recognizes both BRII splice variants since it is directed against a juxtamembrane peptide in BRII [195].

cGKI is a soluble cytoplasmic kinase [672]. To investigate the localization of cGKI relative to BRII, confocal immunofluorescence microscopy in C2C12 cells stably expressing BRII after receptor co-patching was performed.

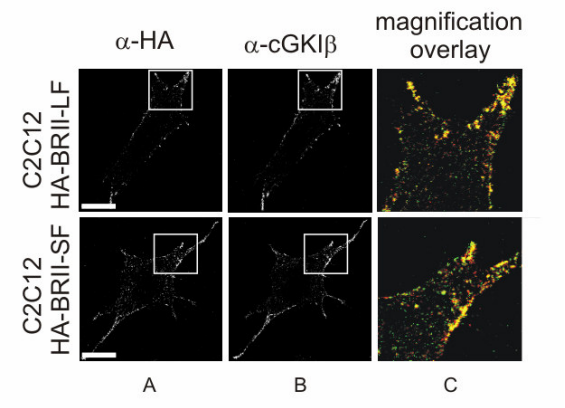

Figure 4.5 Co-localization of cGKIβ and BRII. Co-localization of cGKIβ and BRII (panels C) was studied after receptor co-patching (panels A) and α-cGKIβ staining (panels B) by confocal immunofluorescence microscopy (63-fold magnification) in C2C12 cells stably expressing N-terminally HA-tagged BRII. This result is representative for three independent experiments. Bar 20 µm.

The living C2C12 cells stably expressing HA-tagged BRII-LF or BRII-SF were labeled leading to receptor clustering at the cell surface (**Figure 4.5**, panels A). Following cell fixation, intracellular cGKIβ was stained (panels B). The merged images demonstrated the co-localization of endogenous cGKIβ with overexpressed HA-BRII-LF and interestingly also with HA-BRII-SF predominantly at the cell surface (panels C). From these observations it was concluded that the cGKIβ co-localizes with BRII-LF, and that the kinase has also an affinity for BRII-SF, which does not have the C-terminal extension, the tail.

4.1.2 Mapping of BRII and cGKI interaction sites

To further analyze the interaction of cGKI with BRII, mapping experiments were performed. For that, different N-terminally HA-tagged BRII truncation mutants (TCs) were used [195] (**Figure 4.6**).

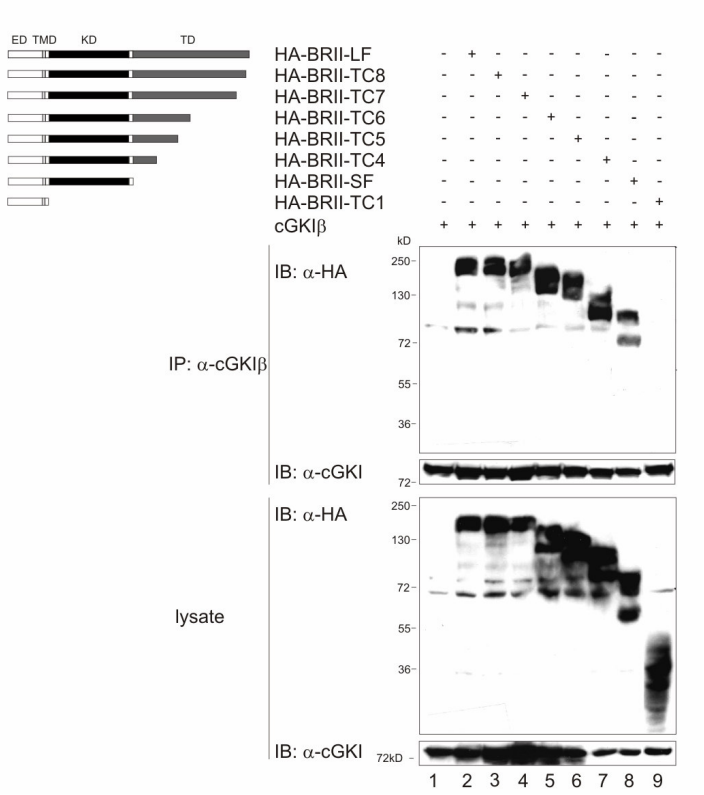

Figure 4.6 Mapping of cGKIβ binding site on BRII. (Left) Scheme of the truncation mutants (TCs) of BRII. ED extracellular domain (white), TMD transmembrane domain (light grey), KD kinase domain (black), TD tail domain (grey). The truncations were shortened beginning at the C-terminus by introducing stop codons at specific sites [195]. All truncations as well as the naturally occurring splice variants of BRII carry an N-terminal HA-tag. **(Right)** HEK293T cells were transfected with cGKIβ and N-terminally HA-tagged truncation mutants of BRII (lanes 3-7, 9), BRII-LF (lane 2) or BRII-SF (lane 8). α-cGKIβ immunoprecipitates (upper panels) and lysates (lower panels) were analyzed by immunoblotting using α-HA and α-cGKI antibodies. This result was reproduced in three independent experiments. IP, immunoprecipitation; IB, immunoblot.

The scheme in **Figure 4.6** depicts the mapping of the cGKIβ interaction site on BRII using BRII truncation mutants. For that purpose, cGKIβ and the N-terminally HA-tagged BRII variants were transiently expressed in HEK293T cells. As shown, cGKIβ was immunoprecipitated and the precipitates were examined for association of the BRII mutants. All BRII truncations (TC4-8) as well as both splice variants BRII-LF and BRII-SF associated with cGKIβ (upper panel, lanes 2-8). Only BRII-TC1, the shortest deletion mutant lacking the receptor kinase and tail domain, did not bind cGKIβ (upper panel, lane 9). Consistent with this result, C2C12 cells stably expressing HA-BRII-TC1 showed significantly reduced co-localization of endogenous cGKIβ and the TC1 at the cell surface when compared to wildtype BRII (data not shown). Furthermore, a stronger interaction of cGKIβ with BRII-LF was observed

when compared to BRII-SF (upper panel, lanes 2 and 8), as detected in several experiments (n>5). It was therefore assumed that BRII-LF has a stronger binding affinity for cGKI than BRII-SF which lacks the C-terminal tail. Moreover, the kinase domain somehow seems to be important for cGKI/BRII binding since BRII-SF binds cGKI and TC1 does not.

The next step was to verify these interactions by pulldown experiments. For that purpose, the recombinant BRII cytoplasmic domains, fused to GST, GST-BRII-SF (leucine 175 to arginine 530) or GST-BRII-tail (methionine 501 to leucine 1038), were used as bait [265]. GST alone was used as control. Prey proteins were provided either by C2C12 whole cell lysates expressing cGKI isoforms or *in vitro* as recombinant proteins (MBP or MBP-cGKIβ). First, after expression and purification of the fusion proteins in *E. coli* BL21 (see 3.4.1), the amount and purity of the proteins were checked by Coomassie-G stain after SDS-PAGE (**Figure 4.7**) (see 3.4.11).

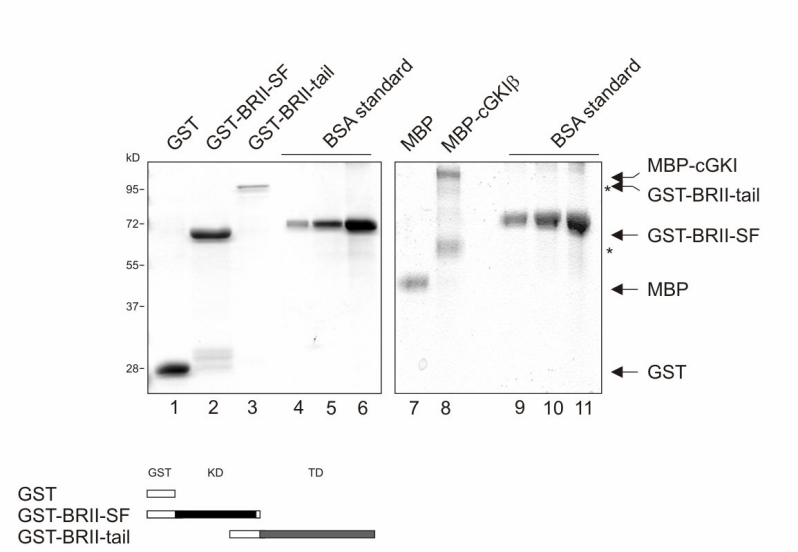

Figure 4.7 Analysis of the protein amount and purity of recombinant BRII GST fusion proteins and MBP-cGKIβ. Purified proteins immobilized to glutathion-sepharose (GST (lane 1), GST-BRII-SF (lane 2), or GST-BRII-tail (lane 3)) or already separated from beads (MBP (lane 7) or MBP-cGKIβ (lane 8)) were analyzed via Coomassie-G staining and BSA standards (1 µg, lanes 4 and 9; 2 µg, lanes 5 and 10; 5 µg, lanes 6 and 11). The asterisks mark degradation bands. The scheme below depicts the BRII GST fusion proteins; KD, kinase domain, TD, tail domain.

As **Figure 4.7** detected, the protein purity was high, but the GST-BRII-tail expression (lane 3; 250 µg protein per 500 ml culture) was less compared to GST (lane 1; 3 mg protein per 500 ml culture) or GST-BRII-SF (lane 2; 3 mg protein per 500 ml culture). This was observed several times, as the tail alone, i.e. structural isolated, seems to be either hard to purify from bacteria or easily degrades in solution. Cloning,

expression and purification of MBP and MBP-cGKIβ was done by J. Weiske, Charité, Germany. MBP-fused cGKIβ showed two additional bands, which were most likely caused by protein degradation (lane 8).

1 µg of each BRII fusion protein was used to fish for binding partners in C2C12 cells transiently overexpressing cGKIα or β isoform (**Figure 4.8**).

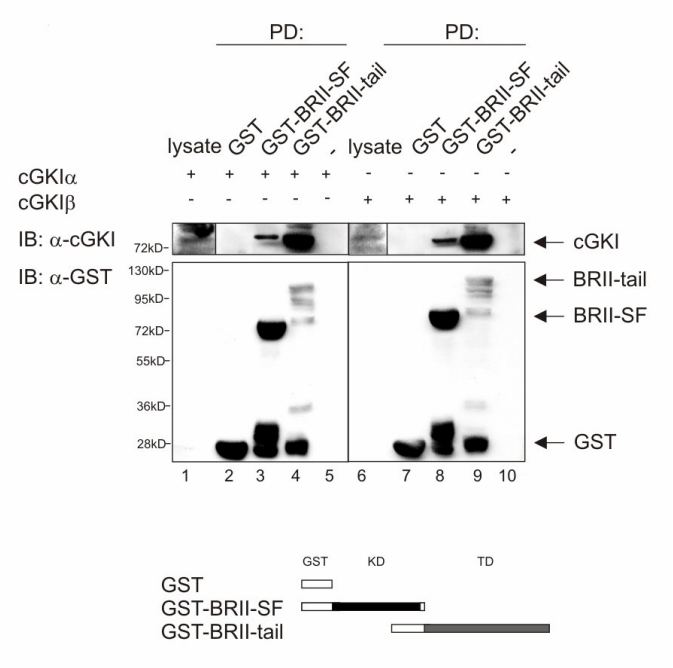

Figure 4.8 Interaction of cGKI isoforms and BRII in a pulldown analysis. GST-BRII-SF (leucine 175 to arginine 530; lanes 3 and 8) and GST-BRII-tail (methionine 501 to leucine 1038; lanes 4 and 9) immobilized to glutathion-sepharose beads were incubated with C2C12 cell lysates expressing cGKI isoforms. Purified protein complexes (upper panel) and cGKIα/β expression (upper panel, lanes 1 and 6) were examined by immunoblotting with α-cGKI, BRII fusion proteins with α-GST antibody (lower panel). "- construct" indicates sepharose control. These data are representative for two independent experiments. PD, pulldown; IB, immunoblot. The scheme below depicts the BRII GST fusion proteins; KD, kinase domain, TD, tail domain.

The pulldown assay in **Figure 4.8** confirmed the results from the studies presented above. Both isoforms of cGKI were pulled down with BRII cytoplasmic domains (upper panel, lanes 3, 4 and 8, 9). BRII-tail formed a strong complex with cGKIα and β (lanes 4 and 9), but also BRII-SF interacted with both isoforms (lanes 3 and 8). Analogous to **Figure 4.6** where BRII-LF exhibiting the tail binds stronger to cGKI than BRII-SF, here the tail alone shows a 10-fold stronger affinity to cGKI than BRII-SF.

Since BRII-tail and BRII-SF are mutually exclusive, the *in vivo* interaction of both BRII cytoplasmic domains with cGKI is puzzling. To clarify this more in detail, *in vitro* binding assays were done. For that GST, GST-BRII-SF or GST-BRII-tail were

used as bait in a pulldown analysis where MBP or MBP-cGKIβ were offered as prey proteins (**Figure 4.9**).

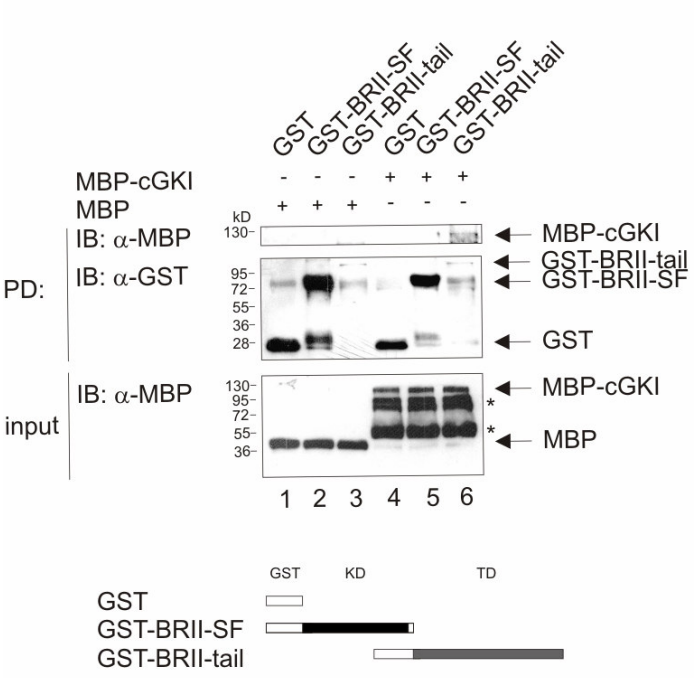

Figure 4.9 *In vitro* binding of cGKIβ and BRII-tail in a pulldown analysis. GST (lanes 1 and 4), GST-BRII-SF (lanes 2 and 5), or GST-BRII-tail (lanes 3 and 6) immobilized to glutathion-sepharose beads were incubated with MBP (lanes 1-3) or MBP-cGKIβ (lanes 4-6). Purified protein complexes were examined by immunoblotting with α-MBP (upper panel) and α-GST antibodies (middle panel). Lower panel monitors the input of MBP or MBP-cGKIβ. The result of a representative assay is shown (n=2). PD, pulldown; IB, immunoblot. The asterisks mark degradation bands. The scheme below depicts the BRII GST fusion proteins; KD, kinase domain, TD, tail domain.

With this experiment it could be shown that cGKIβ directly binds to BRII-tail (**Figure 4.9**, upper panel, lane 6), while there was no direct binding to BRII-SF (lane 5). Latter suggests that the observed *in vivo* interaction of cGKI with BRII-SF (**Figure 4.6** and **Figure 4.8**) is indirect.

To map the interaction site of BRII on cGKI, GST-fused cGKIα and β truncation mutants were used in pulldown and co-IP experiments. The different cGKI mutants [657, 673] represent succinct regions of the protein which have distinct known functions, for instance the N-terminal leucine-rich domain regulates autoinhibition, dimerization and protein targeting (see chapter 1.11.1). **Figure 4.10** schematically draws the used cGKI mutants.

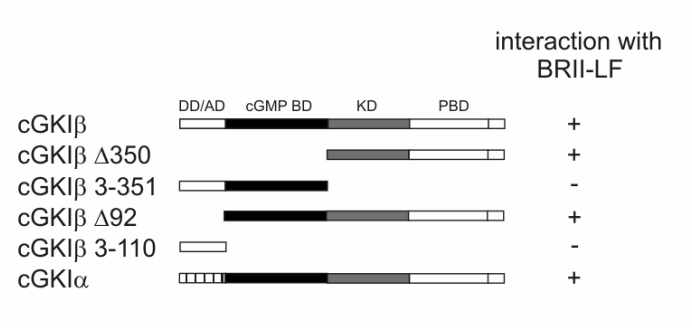

Figure 4.10 Mapping of BRII-LF binding site on cGKI. HEK293T cells were transfected with different GST-fused cGKI truncation mutants and HA-tagged BRII-LF, and the lysates were either analyzed via pulldown using glutathion-sepharose or IP with α-HA or α-GST antibody. Pellets and lysates were subsequently analyzed via SDS-PAGE and immunoblotting. The result after analyzing all assays (n>6) is depicted. The N-terminally GST-fused cGKI mutants are shown in the scheme, DD/AD dimerization domain/autoinhibitory domain (cGKIβ white, cGKIα stripped), cGMP BD cGMP binding domain (black), KD kinase domain (grey), PBD peptide binding domain (white).

Co-IP and pulldown assays in HEK293T cells overexpressing the cGKI mutants and HA-tagged BRII-LF verified again that the receptor binds to cGKI full length (**Figure 4.10**). Furthermore, these experiments confirmed that BRII does not interact with cGKIβ N-terminal region, although the same approach with cGKIα N-terminal region repeatedly showed an interaction. Like cGKIβ, cGKIα N-terminal region exhibits a leucine zipper motif and this domain is assumed to be very sticky (personal communication with R. Pilz, UCSD, CA, USA). Thus, most probably unspecific binding occurs, so that the Iα N-terminus was left out in all of the following mapping experiments due to falsification of the results. However, the data suggest BRII binding to the kinase domain of cGKI, since BRII did not associate to the truncation mutant comprising Iβ´s N-terminal domain plus the cGMP binding domain.

Taken together, both cGKIα and β interact with BRII via cGKI´s C-terminal part including the kinase domain. *Vice versa*, the association is mediated via the C-terminal tail domain of BRII as shown by direct binding studies.

4.1.3 Impact of cGKI association on BRII

Since both cGKI and BRII proteins have serine/threonine kinase activity and interact with each other, it was investigated whether the kinase activity is needed for the

association. This was primarily tested by complex formation of either wildtype cGKIβ or kinase-inactive mutant cGKIβ-D516A [671] with BRII-LF. Wildtype or kinase-inactive cGKIβ and BRII-LF were expressed in HEK293T cells and cGKIβ was immunoprecipitated (**Figure 4.11**).

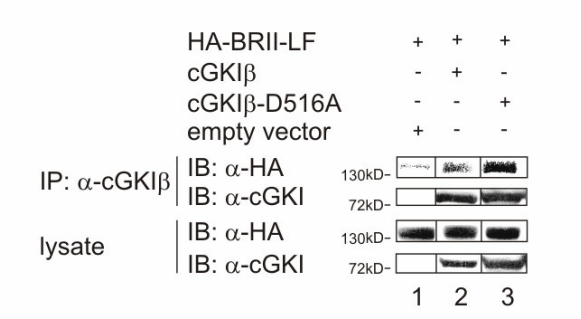

Figure 4.11 Interaction of cGKIβ-D516A, a kinase-dead mutant, with BRII-LF. cGKIβ immunoprecipitates (upper panels) and lysates (lower panels) from HEK293T cells expressing BRII-LF and cGKIβ variants were analyzed using α-HA and α-cGKI antibodies. These data are representative for at least three independent experiments. IP, immunoprecipitation; IB, immunoblot.

Like wildtype cGKIβ, the kinase-inactive mutant of cGKIβ interacted with BRII-LF (**Figure 4.11**, upper panel, lane 3). Interestingly, the association of cGKIβ-D516A with BRII-LF was stronger or more stable than wildtype cGKIβ/BRII-LF complexes (upper panel, lanes 2 and 3), as found in several experiments (n>3). *Vice versa*, kinase-dead BRII-LF (BRII-LF-K230R [266]) bound to cGKI (data not shown).

It was previously shown for BRII complexes with the receptor tyrosine kinase c-Kit as well for BRII/Tctex-1 complexes that phosphorylation events occur within these complexes [261, 266]. Therefore, the consideration was examined whether cis- or trans-phosphorylation of cGKI or BRII is affected by the association of both proteins. For this study, recombinant GST-BRII-tail and GST-BRII-SF (**Figure 4.7**) and recombinant cGKIα enzyme (Promega) were subjected to *in vitro* phosphorylation using γ-^{32}P-ATP (**Figure 4.12**). To activate cGKIα, 8-Br-cGMP was added [828].

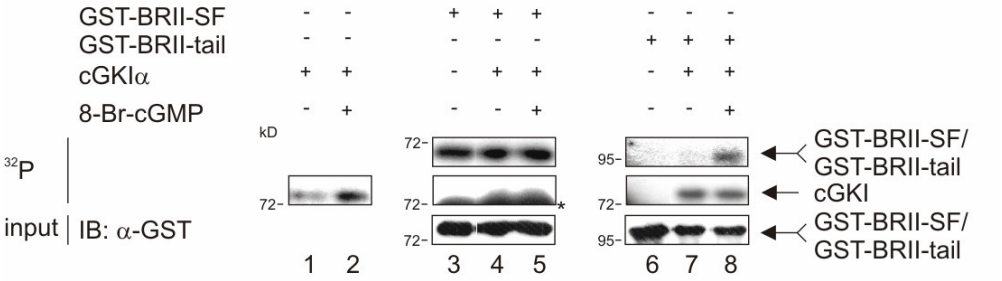

Figure 4.12 Phosphorylation study of cGKI and BRII-SF or BRII-tail *in vitro*. GST-BRII-SF (lanes 3-5) and GST-BRII-tail (lanes 6-8) immobilized to glutathion-sepharose beads were subjected to *in vitro* phosphorylation assay with cGKIα. cGKIα was activated with 8-Br-cGMP or not (lanes 2, 5, 8). Incorporated ^{32}P was detected by autoradiography (upper panel). Middle panel shows autophosphorylation of cGKIα in a longer exposure of the upper panel, the asterisk marks concomitant detected autophosphorylation of BRII-SF. The input of fusion proteins was visualized by immunoblotting using α-GST antibody (lower panel). The results shown here were reproduced two times in independent experiments. IB, immunoblot; ^{32}P, autoradiography

Figure 4.12 demonstrates that BRII-tail was phosphorylated by activated cGKIα (upper panel, lane 8). However, BRII-SF showed autophosphorylation, which was unaffected by the absence or presence of cGKIα (upper panel, lanes 4 and 5). In turn, cGKIα was not phosphorylated by the kinase of BRII-SF, but cGKIα showed autophosphorylation, already without 8-Br-cGMP activation (middle panel, lanes 1, 4 and 7). In a separate experiment, cGKIβ enhanced BRII-LF phosphorylation as detected in immunoprecipitates of BRII-LF upon co-expression of cGKIβ and subsequent *in vitro* phosphorylation.

Additionally, *in vitro* kinase assays with immunopurified BRII-SF and cGKIβ variants with or without 8-Br-cGMP were carried out (**Figure 4.13**).

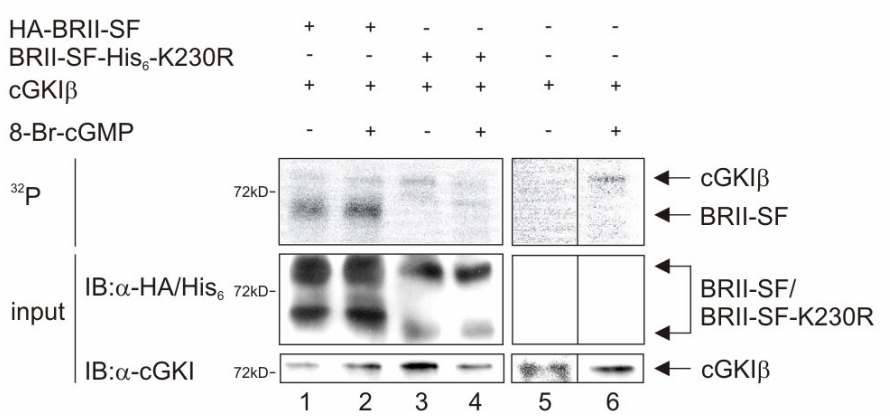

Figure 4.13 Phosphorylation study of cGKI and BRII-SF or BRII-SF-K230R *in vitro*. cGKIβ, BRII-SF or kinase-deficient BRII-SF-K230R proteins, overexpressed in HEK293T cells, were immunoprecipitated using specific antibodies (α-cGKIβ, α-HA or α-His_6). Immunopurified proteins were subjected to *in vitro* kinase assay in the presence or absence of 8-Br-cGMP (lanes 2, 4, and 6). After SDS-PAGE and protein blotting to a nitrocellulose membrane, incorporated ^{32}P was detected by autoradiography (upper panel). BRII-SF and cGKIβ input was controlled by α-HA, α-His_6 and α-cGKIβ immunoblotting (middle and lower panels). The cGKIβ control samples without BRII-SF or BRII-SF-K230R were run on a separate gel (lanes 5 and 6). IB, immunoblot; ^{32}P, autoradiography

Consistent with the data from **Figure 4.12**, here BRII-SF autophosphorylation was not altered upon cGKIβ activation (**Figure 4.13**, upper panel, lanes 1 and 2) and *vice versa*. Furthermore, kinase-dead BRII-SF (BRII-SF-K230R [195], see chapter 1.3.1), which showed no autophosphorylation, was not phosphorylated by cGKIβ (upper panel, lanes 3 and 4).

Having these indications, it was investigated whether cGKI phosphorylates BRII *in vivo* (**Figure 4.14**). In this work, HEK293T cells were mainly used for protein overexpression with a subsequent interaction study, whereas the pluripotent mesenchymal precursor cell line C2C12 was used for the functional assays. Therefore, C2C12 cells were transiently transfected either with wildtype cGKIβ, kinase-inactive mutant cGKIβ-D516A or empty vector, and were stimulated with 8-Br-cGMP. Endogenous BRII was immunoprecipitated with an antibody directed against BRII extracellular domain. The precipitates were immunoblotted with an antibody specific for substrates which were phosphorylated by arginine-dependent kinases like cGKs (PKGs) and the cAMP-dependent kinase (PKA) (**Figure 4.14)**.

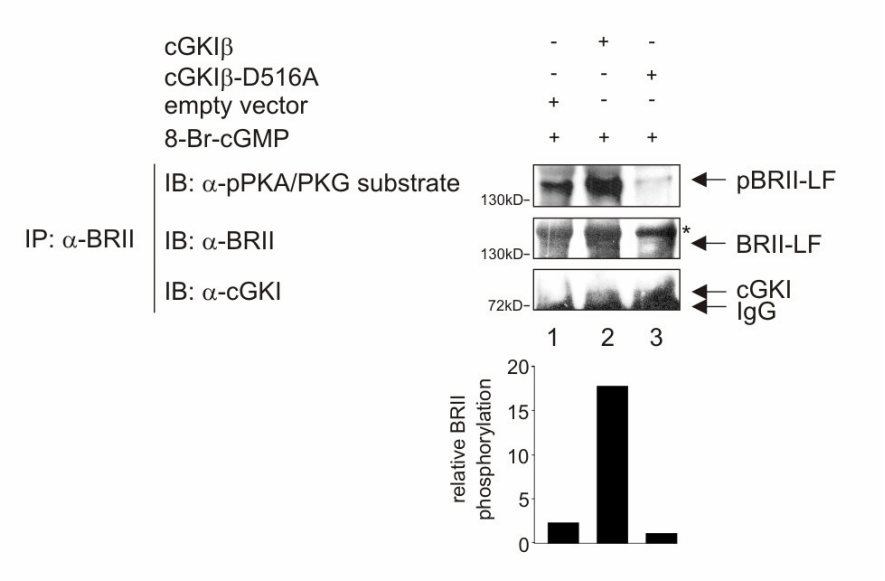

Figure 4.14 Phosphorylation study of cGKIβ and BRII *in vivo*. Phosphorylation of endogenous BRII-LF (enriched by IP) through cGKIβ or cGKIβ-D516A in C2C12 cells was analyzed using a pPKA/PKG substrate-specific antibody (upper panel). Protein amount in the precipitates was monitored with α-BRII (asterisk marks unspecific band, middle panel) and α-cGKI antibodies (lower panel). Intensities of pBRII-LF and BRII-LF bands were measured with ImageJ, and the ratio of the intensities (pBRII-LF/BRII-LF) is depicted as relative BRII phosphorylation (graph below). The results are representative for two independent experiments. IP, immunoprecipitation; IB, immunoblot.

It was found in **Figure 4.14**, compared to empty vector-transfected cells, that BRII-LF is strongly phosphorylated upon overexpression of wildtype cGKIβ (upper panel, lanes 1 and 2). On the other hand, the full length receptor was weakly phosphorylated when kinase-inactive cGKIβ was expressed (upper panel, lanes 1 and 3). Since immunoblotting with α-BRII antibody revealed unequal BRII protein loading, the results were quantified using ImageJ, i.e. BRII phosphorylation was measured relative to BRII protein load. The quantification seen in the graph below confirmed the result seen by eye. Thus, it is assumed that wildtype cGKIβ modifies BRII-LF by phosphorylation, whereas kinase-inactive cGKIβ does not. During these *in vivo* experiments it was hard to detect BRII-SF in the pellet, although the BRII antibody recognizes both isoforms and C2C12 cells do express both BRII splice variants [195]. Therefore, it was difficult to draw a conclusion on BRII-SF *in vivo* phosphorylation, but anyhow, the *in vitro* assays (**Figure 4.12** and **Figure 4.13**) clearly ruled out a cGKI-mediated BRII-SF phosphorylation.

In sum, these results show that the serine/threonine kinase activities of cGKI and BRII are not necessary for their interaction, but the kinase function of cGKI

seems to regulate the strength or stability of the interaction with BRII. And, cGKI does phosphorylate BRII-tail *in vitro* and BRII-LF *in vivo.*

4.1.4 Influence of BMP-2 on BRII/cGKI interaction

To investigate the fate of cGKIβ in response to activation of the BMP pathway, i.e. what happens to cGKIβ/BRII complexes upon BMP-2 ligand binding, interaction studies using co-IP were accomplished. Chan et al. could show that the dynein light chain Tctex-1 dissociates from BRII upon BMP treatment [268]. For that purpose, HEK293T cells were transiently transfected with HA-BRII-LF and cGKIβ constructs. After starvation for 3 hr, the cells were stimulated with BMP-2 for 5 to 60 min and cGKIβ was immunoprecipitated (**Figure 4.15**).

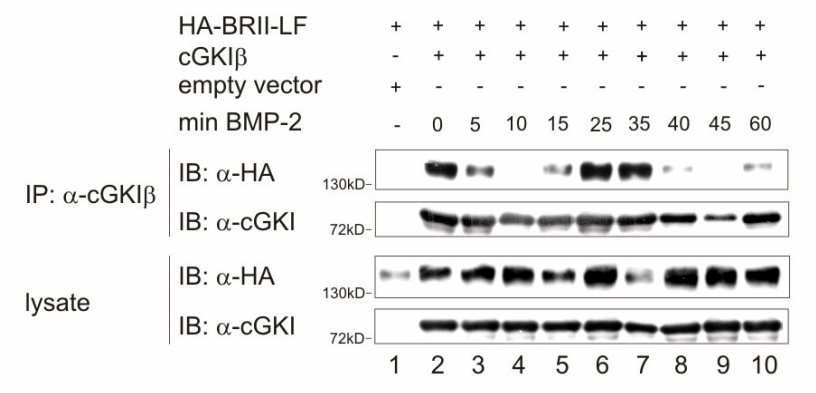

Figure 4.15 Interaction of cGKIβ and BRII-LF upon BMP-2 stimulation. HEK293T cells were co-transfected with cGKIβ and HA-tagged BRII-LF. Starved cells (3 hrs) were stimulated with 10 nM BMP-2 for 5 to 60 min and cGKIβ was immunoprecipitated from the lysates. The precipitated complexes (upper panels) and the lysates (lower panels) were examined by immunoblotting with α-HA and α-cGKI antibodies. This result is representative for at least three independent experiments. IP, immunoprecipitation; IB, immunoblot.

Figure 4.15 shows that upon serum starvation, cGKIβ and BRII-LF do interact (upper panel, lane 2). Interestingly, stimulation for 10 min entirely disrupted the interaction of cGKIβ with BRII-LF (upper panel, lane 4). Stimulation with BMP-2 for more than 15 min, however, resulted in recovery of BRII-LF/cGKIβ complexes (upper panel, lane 10); after 40-45 min of BMP-2 stimulation, the association is again disrupted (upper panel, lanes 8 and 9) to recover (60 min; lane 10). This experiment points out that

BRII/cGKI interaction depends on a specific dynamic after binding of BMP-2 to the receptors, which is characterized through break and recovery phases. Similar approaches were done to examine the BMP-2-dependent interaction dynamics of complexes between kinase-dead mutants of cGKI and/or BRII. However, the respective results differ from experiment to experiment (data not shown). Thus, a conclusion of how cGKI and BRII kinase mutants and their binding mode behave upon BMP-2 treatment could not be drawn. But repeatedly observed was that starvation of the cells is very critical in this aspect. For IP studies with prior BMP-2 stimulation, the cells were always starved for 3 hrs in medium with 0.5% v/v FBS. Inside the studies of BRII/cGKIβ mutant interaction, variations in strength and stability of the association were observed (data not shown). However, analyzing the influence of the starvation time on wildtype BRII/cGKI interaction revealed that within a first period (5-45 min) the association was still there, than it disappeared (60-120 min), to regenerate again (>180 min) (data not shown). Thus, further approaches should be done, to elucidate these interesting, but complex dynamics in interaction.

4.1.5 Subcellular distribution of cGKI upon stimulation with BMP-2 and 8-Br-cGMP

The next question was what happens to cGKI after it is released from the BMP type II receptor. Therefore, immunofluorescence (IF) assays in C2C12 cells were performed and cGKI was stained (**Figure 4.16**).

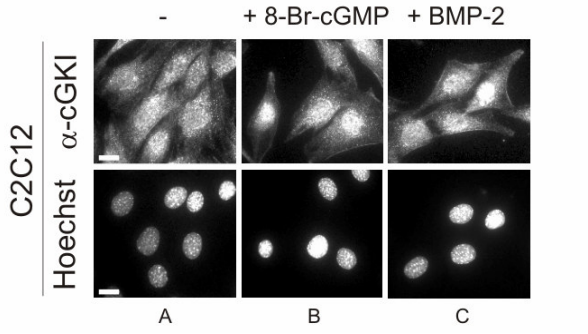

Figure 4.16 Localization of cGKI in C2C12 cells after treatment with 8-Br-cGMP or BMP-2. Immunofluorescence staining of cGKI in C2C12 cells was carried out after cell starvation (3 hrs) and cell stimulation with 1 mM 8-Br-cGMP (upper panel B) or 20 nM BMP-2 (upper panel C) for 30 min. Nuclei were labeled using Hoechst dye (lower panels). This result is representative for three independent experiments. Pictures were taken at 63-fold magnification. Bar 20 µm.

Figure 4.16 illustrates the analysis of endogenous cGKI in starved and stimulated C2C12 cells using immunofluorescence staining. Without ligand, cGKI was pancellularly distributed (upper panel A). Upon activation with 8-Br-cGMP, cGKI redistributed to the nucleus (upper panel B), as published for other cell lines [672]. Consistent with the co-IP data shown above that BMP-2-triggered cGKI dissociates from BRII (**Figure 4.15**), stimulation with BMP-2 induced translocation of endogenous cGKI into the nucleus (upper panel C). During the establishment of this assay, C2C12 cells were also stimulated or co-stimulated with 500 µM 3-isobutyl-1-methylxanthine (IBMX). This compound is a PDE inhibitor to increase intracellular cGMP levels, which then promotes cGKI activation and, in a sensitive cell system, induces nuclear translocation of cGKI [671]. But in our cells system -/+ IMBX had no effect on the nuclear translocation of cGKI (data not shown).

It is known from several studies, that some cell lines including untransformed HEK293 cells do not exhibit nuclear translocation of cGKI upon cGMP treatment [672, 674]. However, to confirm our conclusion from **Figure 4.15** and **Figure 4.16**, cytoplasmic-nuclear fractionation of HEK293T cells was done after transfection with cGKIβ and stimulation with BMP-2 (**Figure 4.17**).

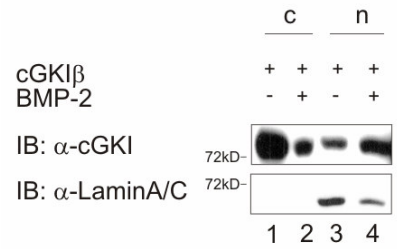

Figure 4.17 Analysis of the subcellular distribution of cGKIβ in HEK293T cells. cGKIβ-/Smad1-transfected HEK293T cells were starved for 2 hrs and stimulated with 20 nM BMP-2 for 30 min. The subcellular localization of cGKIβ was analyzed after cell fractionation and subsequent SDS-PAGE and immunoblotting with α-cGKIβ antibody (upper panel). Fractionation was controlled with α-LaminA/C antibody (lower panel). This result is representative for two independent experiments. IB, immunoblot; c, cytosol; n, nucleus.

Figure 4.17 demonstrates that BMP-2 stimulation induced redistribution of cGKIβ from the cytoplasm (lanes 1 and 2) to the nucleus (lanes 3 and 4) upon BMP-2 stimulation (lanes 2 and 4). Similarily, upon BMP stimulation of HEK239T cells, cGKIβ translocated into the nucleus when BRII was co-expressed (data not shown).

Thus, it is assumed that cGKI undergoes nuclear translocation upon activation of the BMP signaling pathway.

Taken together, the data from **4.1** proved that (a) cGKI interacts directly with BRII-tail, (b) the kinase function of cGKI and BRII are not necessary for the interaction itself, (c) cGKI exclusively phosphorylates BRII-tail *in vitro* and BRII-LF *in vivo*, and (d) BMP-2 triggers both detachment of cGKI from BRII, i.e. from the receptor complex, and nuclear translocation of cGKI.

4.2 Interaction of cGKI with BRI

Since the TGFβ superfamily of serine/threonine kinase receptors comprises five type II receptors and seven type I receptors [3], it was interesting to test, whether cGKI also binds to the BMP type I receptor. For that, endogenous co-IP studies in C2C12 cells were undertaken. The BMP type I receptor (BRIa) and BRII were immunoprecipitated using polyclonal rabbit antibodies which were covalently linked to protein A-sepharose (see 3.4.6) (**Figure 4.18**).

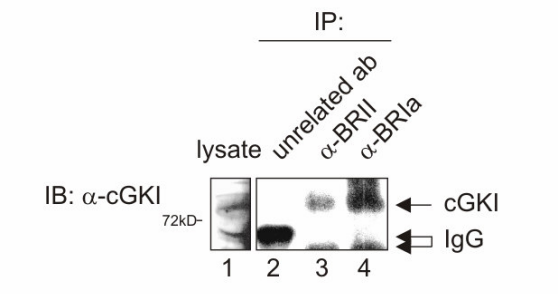

Figure 4.18 Interaction of endogenous cGKI with BRII and BRIa in C2C12 cells. Endogenous complexes of cGKI with BMP receptors in C2C12 cells were analyzed via α-cGKI immunoblot after receptor IP using antibodies covalently linked to protein A-sepharose. An unrelated antibody (ab) was used as control. The lysate (lane 1) was controlled for endogenous cGKI expression. IP, immunoprecipitation; IB, immunoblot.

As **Figure 4.18** shows, cGKI bound besides BRII (**Figure 4.4**) also to BRIa endogenously (lane 4). A similar result was also seen endogenously in the preosteoblastic cell line MC3T3.

Verification of this result was done by co-IP in HEK293T cells upon overexpression. Unfortunately, cGKI/BRIa binding under overexpression conditions was mainly unspecific, since also binding of the respective co-immunoprecipitated

protein to protein A-sepharose has been observed. Thus, another BMP type I receptor, BRIb was used (**Figure 4.19**). Please note that in general BRIa and BRIb are not interchangeable, especially in functional assays. Even so the receptors have similar cytoplasmic domains, they interact with different proteins and have different binding affinities for BMP and GDF ligands [829].

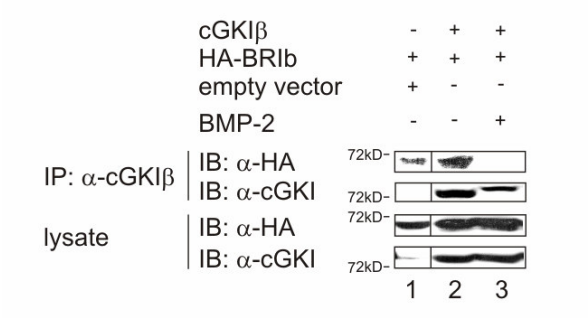

Figure 4.19 Interaction of cGKIβ and BRIb after stimulation with BMP-2. HEK293T cells co-expressing cGKIβ and BRIb were starved for 3 hrs and stimulated with 10 nM BMP-2 for 30 min. cGKIβ was immunoprecipitated from the lysates. Precipitates (upper panels) and lysates (lower panels) were analyzed with α-HA and α-cGKI antibodies. IP, immunoprecipitation; IB, immunoblot.

Despite unspecific binding of BRIb to sepharose (upper panel, lane 1), **Figure 4.19** illustrates that cGKIβ associates to BRIb without ligand (upper panel, lane 2). BMP-2 stimulation for 30 min seemed to disrupt the interaction, which correlates well with the interaction dynamic studies done for cGKI and BRII (**Figure 4.15**). This result sheds more light on the interaction mechanism of cGKI with the BMP receptors, supposing that cGKI binds to preformed complexes of the BMP receptors which already exist without ligand. But one should be cautious since BMP-2 is not the high-affinity ligand for BRIb.

In sum, these data presented in **4.2** suggest that cGKI generally interacts with BMP receptor complexes; this interaction is ligand sensitive since stimulation with BMP-2 abrogates association between cGKI and BRII/BRI complexes.

4.3 Characterization of cGKI/Smad interaction

Signaling of the TGFβ/BMP superfamily is characterized by ligand binding to a specific set of heteromeric receptors, which then transduce the signal after intra- and

intermolecular processes to R-Smad proteins. TGFβ R-Smads are bound in cooperation with SARA to the TGFβ receptor complex and are phosphorylated by TRI upon ligand stimulation. Signaling is then continued during receptor endocytosis via clathrin-coated pits (CCPs), before the R-Smads together with co-Smad4 translocate into the nucleus [3] (see chapter 1.4.1). In BMP signaling these processes are different. Until now it is not clear whether R-Smads bind the receptors before and/or upon BMP ligand stimulation. But it is known that BMP R-Smads are C-terminally phosphorylated by BRI at the plasma membrane, and that internalization via CCPs is needed for the continuation of BMP signaling. Like TGFβ-activated Smad2 and 3, also Smad1, 5 and 8 undergo nuclear translocation upon BMP stimulation [227].

4.3.1 Interaction of cGKI with R-Smad1 and 5

The dissociation of cGKI from the BMP receptors and its subsequent nuclear translocation presented in the chapters 4.1.4 and 4.1.5 closely mirrors the behavior of the BMP signal transducers Smads. As mentioned, R-Smads get phosphorylated at the SSXS motif and migrate to the nucleus [3]. Therefore, it was tested whether cGKI also associates with Smad1 and 5 and/or co-Smad4. First, cGKIα or β, fused to GST, and Smad1 were overexpressed in HEK293T cells and complex formation was analyzed via IP of cGKI (**Figure 4.20**).

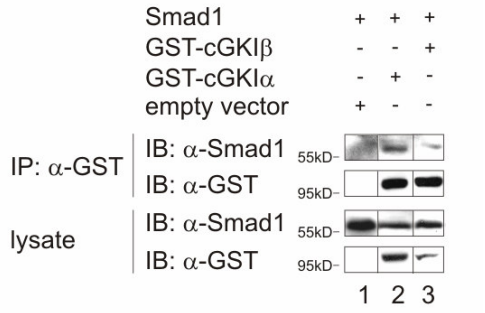

Figure 4.20 Interaction of cGKI isoforms with Smad1. HEK293T cells were co-transfected with GST-fused cGKIα or β and Smad1, and IP was performed using α-GST antibodies. Binding analysis was done using α-Smad1 and α-GST immunoblotting (upper panels) and lysates were controlled for protein expression using α-Smad1 and α-GST antibodies (lower panels). This result is representative one for n>3. IP, immunoprecipitation; IB, immunoblot.

Both isoforms interacted with Smad1 (**Figure 4.20**, upper panel, lanes 2 and 3). This observation indicates that the isoform-specific N-terminus of cGKI is not necessary for R-Smad interaction, as shown already for BRII interaction (**Figure 4.3**, **Figure 4.8**, and **Figure 4.10**). Consistent with this, endogenous Smad1 was not pulled down with recombinant cGKIα and β N-termini from C2C12 cells (data not shown; diploma thesis V. Ezerski, 2006, FU Berlin, Germany). Besides this, also kinase-inactive cGKI could bind Smad1 suggesting that kinase activity is not a prerequisite for the interaction (data not shown).

To investigate the ligand dependency and the dynamics of cGKI/R-Smad interaction, cGKI-/R-Smad-transfected HEK293T cells or C2C12 cells were stimulated with BMP-2, and subsequently analyzed by co-IP (**Figure 4.21**).

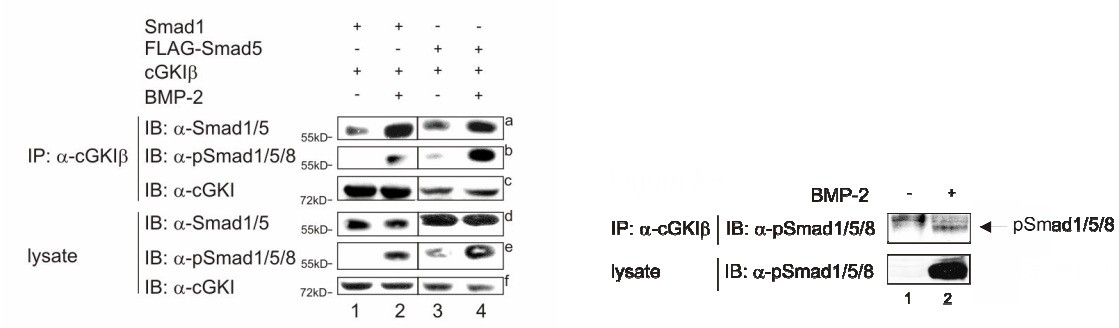

Figure 4.21 Interaction of cGKIβ and BMP R-Smads upon BMP-2 stimulation. (Left) HEK293T cells were co-transfected with cGKIβ and Smad1 or FLAG-Smad5 and starved and stimulated with BMP-2 or left untreated. cGKIβ immunoprecipitates were subjected to immunoblotting using α-Smad1/5, α-pSmad1/5/8, and α-cGKI antibodies (panels a-c). Levels of Smad1/5, pSmad1/5, and cGKIβ were detected using the lysates (panel d-f). These data were reproduced in three independent experiments. **(Right)** C2C12 cells were starved for 3 hrs and stimulated with 10 nM BMP-2 for 30 min. Endogenous complex formation of cGKIβ and phosphorylated Smad1/5/8 was studied by co-IP using α-cGKIβ antibody. Binding of activated Smad1/5/8 to cGKIβ was analyzed with α-pSmad1/5/8 antibody (upper panel), also the lysate control was done with this antibody (lower panel). This is a representative result (n=2). IP, immunoprecipitation; IB, immunoblot.

These experiments revealed that Smad1 (**Figure 4.21**, left, panel a, lanes 1 and 2) and Smad5 (left, panel a, lanes 3 and 4) form complexes with cGKIβ already in the absence of ligand. However, stimulation with BMP-2 strongly enhanced complex formation in both cases (left, panel a, lanes 2 and 4). cGKIβ also associated with phosphorylated Smad1 and Smad5 (left, panel b, lanes 2 and 4). Furthermore, in C2C12 cells endogenous cGKIβ formed a complex with BMP-2-activated, i.e. phosphorylated Smad1/5/8 (right, lane 2). These data deliver evidence that cGKI´s

binding to Smad1 and Smad5 is regulated by BMP-2 and that cGKI preferentially binds phosphorylated R-Smads.

4.3.2 Mapping of cGKI and Smad1 interaction sites

To map the interaction site of Smad1 on cGKI, GST-fused cGKIα and β truncation mutants were used in co-IP assays and pulldown experiments. Therefore, cGKI mutants were used [673] (**Figure 4.10**). The drawing in **Figure 4.22** schematically presents the data.

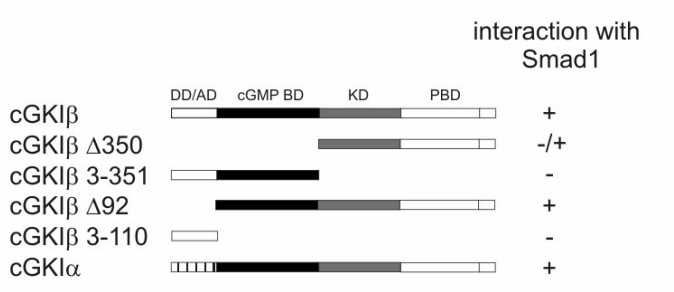

Figure 4.22 Mapping of the Smad1 binding site on cGKI. Lysates of HEK293T cells transfected with different GST-fused cGKI truncation mutants and Smad1, were either analyzed via pulldown using glutathion-sepharose or IP using α-Smad1 or α-GST antibody. Pellets and lysates were subsequently analyzed via SDS-PAGE and immunoblotting. The data from all experiments (n>3) are summarized. cGKI mutants, N-terminally fused to GST, are shown in the scheme, DD/AD dimerization domain/autoinhibitory domain (cGKIβ white, cGKIα stripped), cGMP BD cGMP binding domain (black), KD kinase domain (grey), PBD peptide binding domain (white).

These binding studies in HEK293T cells overexpressing the cGKI mutants and Smad1 (**Figure 4.22**) confirmed that Smad1 on the one hand binds both cGKI isoforms (as already shown in **Figure 4.20**), and on the other hand does not associate to cGKIβ´s N-terminal region. Furthermore, Smad1 did not associate with the truncation mutant comprising Iβ´s N-terminal domain plus the common cGMP binding domain. This indicates Smad1 interaction with the kinase domain, the same domain that also binds BRII (**Figure 4.10**).

In summary, both isoforms of cGKI bind to Smad1 most likely via cGKI´s kinase domain, whereas upon ligand activation of the BMP pathway the interaction increased. Thus, the interaction is enhanced after phosphorylation and therefore modification of the R-Smad molecule.

4.3.3 Association with co-Smad4

Since it is known that activated Smad1/5/8 form a complex with co-Smad4 before translocating into the nucleus [272, 283, 305], the putative interaction of cGKI with Smad4 was tested. Both proteins were transiently overexpressed in HEK293T cells (**Figure 4.23**, left). To confirm this under endogenous conditions, C2C12 cells were used (**Figure 4.23**, right). Afterwards, the cells were stimulated with BMP-2 and cGKIβ was immunoprecipitated.

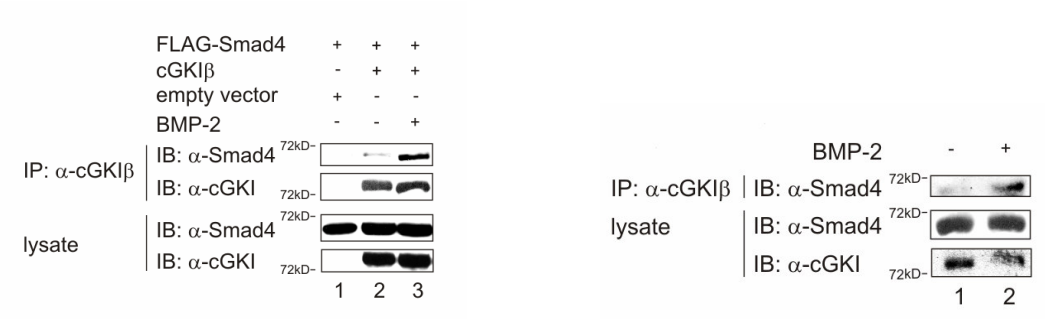

Figure 4.23 Interaction of cGKIβ with co-Smad4. (Left) HEK293T cells were co-transfected with cGKIβ and FLAG-Smad4 and after starvation (3 hrs) the cells were treated with 10 nM BMP-2 for 30 min or left untreated. cGKIβ was immunoprecipitated and precipitates (upper panels) and lysates (lower panels) were analyzed via α-Smad4 and α-cGKIβ immunoblotting. The result shown is representative for at least three independent experiments. **(Right)** C2C12 cells were stimulated with 10 nM BMP-2 for 30 min after starving the cells for 3 hrs. Endogenous BMP-2-induced complex formation of cGKIβ and Smad4 was examined via IP using α-cGKIβ antibody. Precipitates (upper panel) and lysates (lower panels) were immunoblotted using α-Smad4 and α-cGKIβ antibodies. IP, immunoprecipitation; IB, immunoblot.

Figure 4.23 shows that indeed also Smad4 associated with cGKIβ (left, upper panel, lanes 2 and 3), and stimulation with BMP-2 enhanced this interaction 8-fold (left, upper panel, lanes 2 and 3). This result was reproduced endogenously in BMP-2-treated C2C12 cells (right, lane 2) suggesting that cGKI preferentially binds to BMP-2-induced complexes of R-Smads and co-Smad. In addition, kinase-deficient cGKI still interacts with Smad4, shown already for Smad1 (data not shown); this underscores that an active kinase of cGKI is not required for an interaction with the Smad complex.

4.3.4 Mapping of cGKI and Smad4 interaction sites

For mapping the interaction site of Smad4 on cGKI, the cGKI truncation mutants described in **Figure 4.10** [673], were transfected together with Smad4 into HEK293T. Subsequently, co-IP or pulldown analysis was done (**Figure 4.24**).

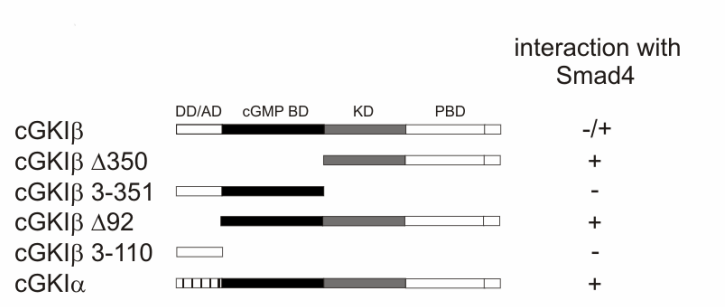

Figure 4.24 Mapping of the Smad4 binding site on cGKI. HEK293T cells were transfected with different GST-fused cGKI truncation mutants and Smad4, and the lysates were either analyzed via pulldown using glutathion-sepharose or IP using α-Smad4 or α-GST antibody. Pellets and lysates were subsequently analyzed via SDS-PAGE and immunoblotting. The result from all assays (n>3) is summarized. The N-terminally GST-fused cGKI mutants are shown in the scheme, DD/AD dimerization domain/ autoinhibitory domain (cGKIβ white, cGKIα stripped), cGMP BD cGMP binding domain (black), KD kinase domain (grey), PBD peptide binding domain (white).

The overall result is summarized in **Figure 4.24**. As shown for BRII (**Figure 4.10**) and Smad1 (**Figure 4.22**), Smad4 interacted with both cGKI isoforms, indicating that the N-terminus of cGKI is not responsible for cGKI binding to Smad4. This was underlined by the finding that endogenous Smad4 was not pulled down from C2C12 cells with recombinant cGKIα and β N-termini (diploma thesis V. Ezerski, 2006, FU Berlin, Germany). Furthermore, cGKI´s C-terminus including the serine/threonine kinase domain associated with Smad4, but the N-terminal part comprising the leucine zipper region from Iβ and the common cGMP binding site did not.

Unfortunately, mapping experiments to determine the cGKI interaction site within Smad4 (MH1 domain, linker or MH2 domain) did not reveal a definite result. After expression and purification of the Smad4 GST fusion proteins (Smad4-MH1-GST, Smad4-MH2-GST, Smad4-ΔMH2-GST), the truncations were used as prey proteins in binding studies. The entire data of this were inconsistent and thus, the interaction domain of cGKIβ on Smad4 is not clearly identified yet. It can be considered that intra- and intermolecular rearrangements take place during cGKI complex formation with R- and co-Smad.

In summary, both cGKIα and β interact with Smad4 presumably via cGKI´s kinase domain. Upon BMP-2 stimulation the BMP pathway is activated and the cGKI/Smad4 association is enhanced.

4.3.5 Interaction of cGKI on Smads in different cellular compartments

Ligand-activated Smad proteins are known to accumulate in the nucleus within a short period of time (<30 min). As shown before, cGKI undergoes nuclear translocation as well when stimulated with BMP-2 (**Figure 4.16** and **Figure 4.17**). To further examine these findings, endogenous cGKI/Smad complexes in different cellular compartments were analyzed. For that purpose, C2C12 cells were stimulated with BMP-2 or left untreated, and IP of cGKIβ was performed (**Figure 4.25**).

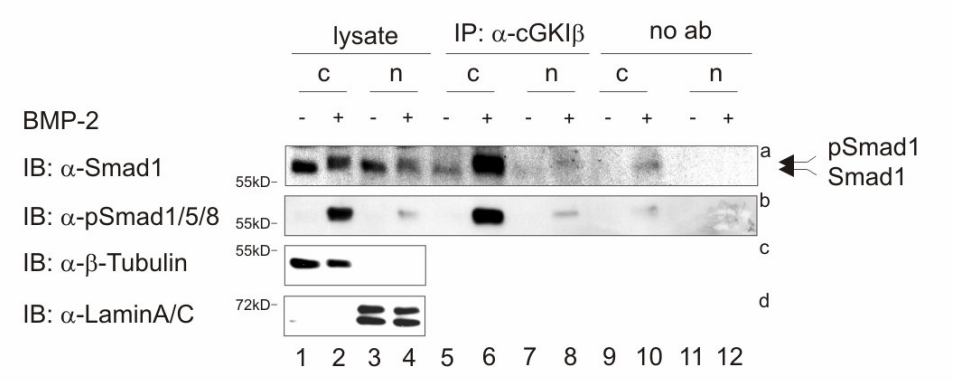

Figure 4.25 Interaction of endogenous cGKI and BMP R-Smads in C2C12 cells in different cellular compartments. C2C12 cells starved and BMP-2-stimulated were subjected to cytoplasmic-nuclear fractionation, and cGKIβ was immunoprecipitated from both cytoplasmic (lanes 5, 6 and 9, 10) and nuclear fractions (lanes 7, 8 and 11, 12). IP antibody (ab) was ommited as a control for the sepharose. Pellets (lanes 5-12) and lysates (lanes 1-4) were analyzed by immunoblotting using α-Smad1 (panel a) and α-pSmad1/5/8 (panel b) antibodies. To control fractionation, lysates were probed with α-β-Tubulin (panel c) and α-LaminA/C antibodies (panel d). A representative result of at least three independent experiments is shown. IP, immunoprecipitation; IB, immunoblot; c, cytosol; n, nucleus.

Consistent with previous data, cGKI associated with Smad1 in the cytoplasm already in the absence of ligand (**Figure 4.25**, panel a, lane 5). Stimulation with BMP-2 lead to phosphorylation of Smad1 (panels a and b, lanes 2, 4, 6 and 8), and to enhanced binding of phosphorylated Smad1 and cGKI in the cytoplasm (panels a and b, lane 6). Complex of cGKI and phosphorylated Smad1 were also detected in the nuclear

fraction (panels a and b, lane 8), albeit weaker than in the cytoplasm (panels a and b, lane 6). These experiments were performed in the absence of phosphatase inhibitors. Since Smads get dephosphorylated in the nucleus [1], the relative lower amount of phospho-Smads in the nucleus compared to the cytoplasm can be explained (panels a and b, lanes 6 and 8). The sepharose control where antibody was left out (lanes 9-12) showed significantly less up to no binding compared to the IP samples (lanes 5-8). Thus, it is assumed that cGKI migrates together with Smad1 to the nucleus upon stimulation with BMP-2. While this compartment-specific interaction between cGKI and Smad1 could be reproduced several times (n>3), the study of cGKI/Smad4 interaction in different cell compartments revealed divergent results (data not shown). Again, it is possible that inter- and/or intramolecular rearrangements within this cGKI/R-Smad/co-Smad complex take place in the nucleus, likely in a specific time frame which might be missed in the study shown here (stimulation with BMP-2 for 30 min).

To further study the subcellular distribution of cGKI and Smad1 or Smad4, immunofluorescence microscopy using C2C12 cells stimulated with BMP-2 for different time periods (5 to 60 min) was performed (**Figure 4.26**; diploma thesis V. Ezerski, 2006, FU Berlin, Germany).

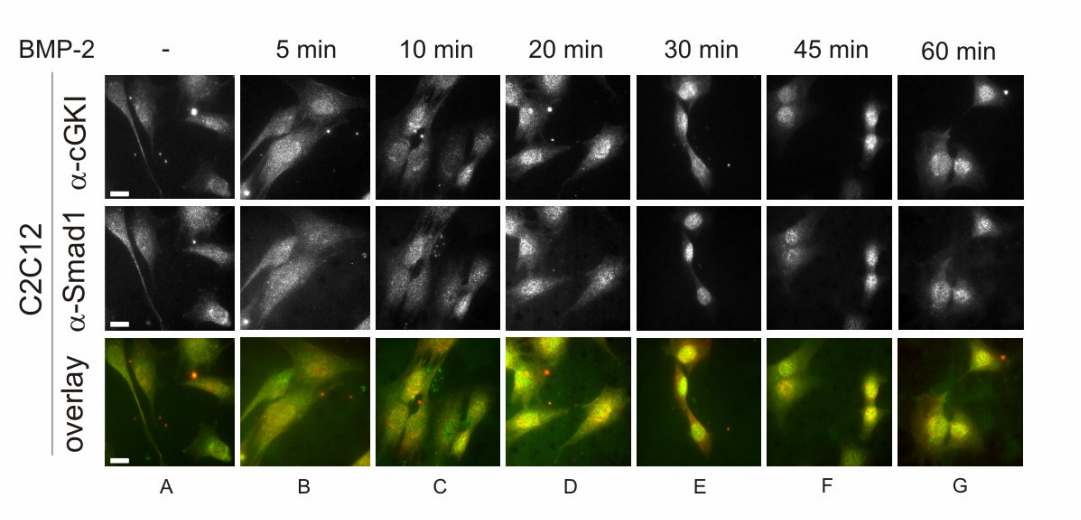

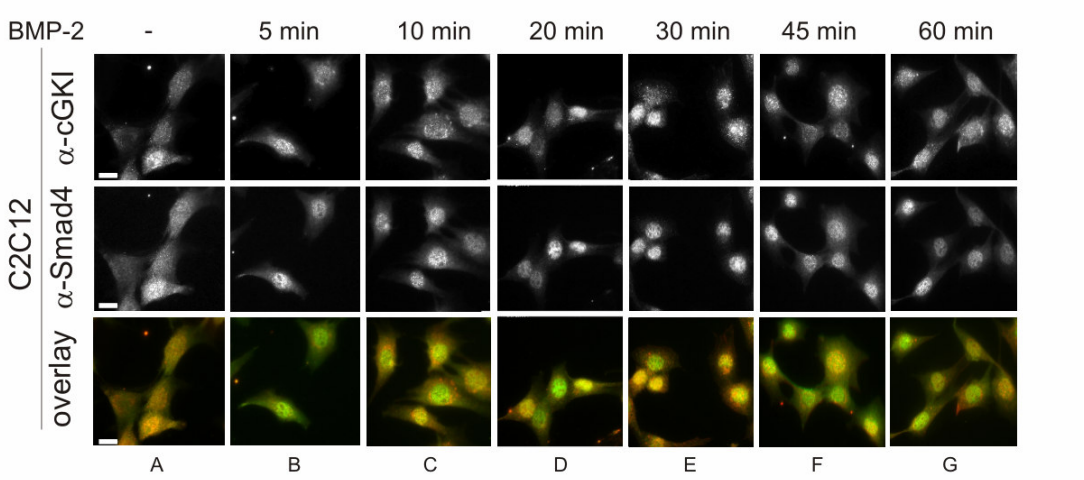

Figure 4.26 Co-localization of endogenous cGKI and Smad1 or co-Smad4 in C2C12 cells after BMP-2 stimulation. C2C12 cells starved and stimulated with BMP-2 (5 to 60 min, panels B-G) or left untreated (-, panels A), were co-labeled for intracellular cGKI and Smad1 (upper panels) or Smad4 (lower panels) using specific antibodies. The colored pictures monitor the co-localization by merging the upper two panels, respectively. These data are representative for three independent experiments. 63-fold magnification. Bar 20 µm. Diploma thesis V. Ezerski, 2006, FU Berlin, Germany.

Figure 4.26 show that in the absence of ligand, the examined proteins were pancellularly distributed (panels A). Following BMP-2 stimulation, cGKI accumulated with both Smad1 and Smad4 in the nucleus with identical time kinetics (5 to 30 min, panels B-E). Moreover, cGKI and Smad1 or cGKI and Smad4 partly co-localized in the cytoplasm as well as in the nucleus of BMP-2-treated cells (5 to 30 min, panels B-E). Most of cGKI and R-Smad/Smad4 co-localization was found in the nucleus 20 to 45 min after stimulation with BMP-2 (panels D-F). After 45 min, cGKI, Smad1 and Smad4 were starting to redistribute into the cytoplasm (panels G).

Next, the question was asked what happens to the cGKI/Smad complexes in the nucleus. The function of Smad complexes in the nucleus is to regulate transcription of BMP target genes [2]. Therefore, the binding of cGKI and Smad1 to promoter sites of BMP-2 target genes such as *Id1* [821] was examined. A tool to test this is chromatin immunoprecipitation (ChIP) (see 3.2.8). ChIP assays were performed in collaboration with J. Weiske and O. Huber (Charité, Germany) with either untreated or BMP-2- and/or 8-Br-cGMP-stimulated C2C12 cells to pull down *Id1*-specific promoter sequences with certain antibodies (**Figure 4.27**).

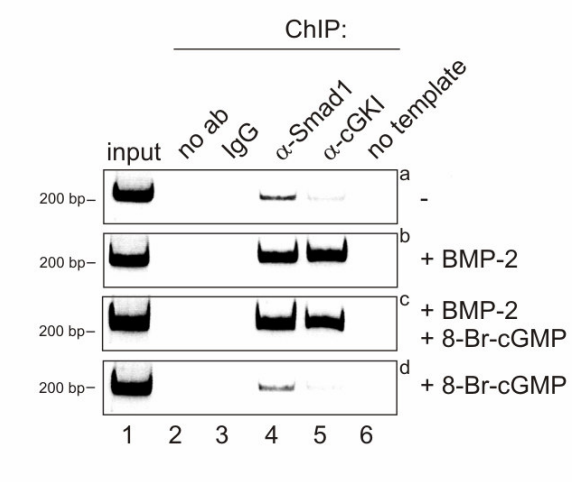

Figure 4.27 Binding of endogenous cGKI and Smad1 to the *Id1* promoter in BMP-2-treated C2C12 cells. C2C12 cells were starved for 24 hrs and stimulated for 4 hrs with 10 nM BMP-2 (panel b) and/or 1 µM 8-Br-cGMP (panels c and d) or left unstimulated (panel a). Chromatin immunoprecipitation (ChIP) was performed with α-Smad1 or α-cGKI antibody. Subsequent PCR analysis with *Id1* promoter-specific primers revealed the protein binding, respective. Either unspecific antibodies (IgG, lane 3) or no antibody (ab, lane 2) served as control. Lane 1 shows the DNA input for each ChIP. A representative result of two independent experiments is shown. In collaboration with J. Weiske and O. Huber, Charité, Germany.

In unstimulated cells a small fraction of Smad1 was detectable at the *Id1* promoter (**Figure 4.27**, panel a, lane 4), whereas after BMP-2 stimulation the association of Smad1 with the *Id1* promoter increased [403] (panel b, lane 4). Interestingly, cGKI was recruited to this *Id1* promoter site upon stimulation with BMP-2 (panel b, lane 5). Co-stimulation with 8-Br-cGMP or stimulation with 8-Br-cGMP alone did not affect the binding implying that activation of cGKI by cGMP is not required (c and d, lane 5). The same result was observed in HEK293T cells (data not shown).

To investigate whether cGKI and Smad1 bind to the *Id1* promoter in a complex, two-step ChIP was carried out in collaboration with J. Weiske and O. Huber (Charité, Germany) (**Figure 4.28**). The α-Smad1 antibody was used for the first ChIP, and the α-cGKI antibody for the second one or *vice versa*.

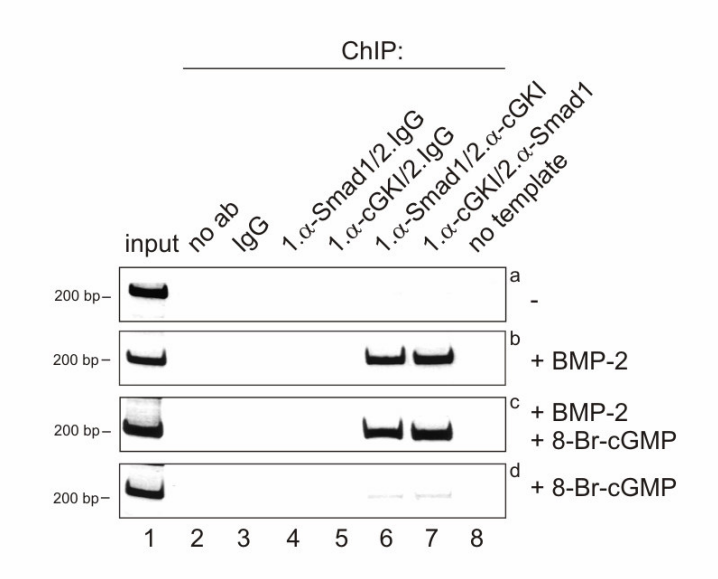

Figure 4.28 BMP-2-induced co-localization of endogenous cGKI and Smad1 at the *Id1* promoter in C2C12 cells. C2C12 cells were starved and stimulated with BMP-2 (panel b) and/or 8-Br-cGMP (panels c and d) or left unstimulated (panels a). Complex formation was analyzed by two-step ChIP using α-Smad1 followed by α-cGKI antibody or *vice versa*. Subsequent PCR analysis with *Id1* promoter-specific primers revealed the protein binding, respective. As control for unspecific binding, antibody (ab) was omitted (lane 2) in the ChIP experiment, or IgG antibody was included (lanes 3 and 9). To control unspecific amplification, the template was left out in the PCR (lane 8). Lane 1 shows the DNA input for each ChIP. Representative data of two independent experiments is shown. In collaboration with J. Weiske and O. Huber, Charité, Germany.

This experiment demonstrates that Smad1 and cGKI indeed bound to the *Id1* promoter in a complex, both in BMP-2- and BMP-2/8-Br-cGMP-treated C2C12 cells (**Figure 4.28**, panels b and c, lanes 6 and 7). When IgG was used as a control, no complex formation was observed (lanes 4 and 5). The data from **Figure 4.27** and **Figure 4.28** indicate that cGKI does bind to the *Id1* promoter, even in complex with Smad1, and that it is the BMP-2 signal that directs cGKI binding to the *Id1* promoter, not the cGMP signal.

Thus, the data from chapter **4.3** show that (a) cGKI associates with R-Smads already in the absence of ligand whereas their interaction is strongly enhanced after BMP-2 stimulation. It is concluded that within the activated Smad complexes (b) cGKI also interacts with Smad4 and (c) translocates with these complexes into the nucleus. Moreover, (d) cGKI and Smad1 form a complex at the *Id1* promoter which is specifically induced by BMP-2.

4.4 Functional relevance of cGKI for BMP-2-induced Smad pathway

An essential step in the signaling cascade of cytokines of the TGFβ superfamily, is the C-terminal R-Smad phosphorylation via the respective type I receptor [3, 306]. This process controls Smad activity and availability, and is therefore highly regulated. As described in chapter 1.4.1 and 1.4.2, several cytoplasmic proteins like Endofin [340], diverse MAPK as Erk2 [330], or the phosphatase PP2A (see chapter 7.2) affect R-Smad phosphorylation, nucleocytoplasmic shuttling, and continuation of the BMP pathway. Also some nuclear proteins like nuclear membrane proteins as importin 7/8 [396] or MAN1 [346], nuclear phosphatases as SCPs [332, 337, 339], and finally transcription factors [2] regulate Smad shuttling, status, and activity.

4.4.1 Effect of cGKI knockdown on R-Smad phosphorylation

Having estalished that cGKI phosphorylates BRII-LF (**Figure 4.12** and **Figure 4.14**), the consequences induced by the interaction of cGKI with Smads in respect to C-terminal Smad phosphorylation were studied. Analysis was done using RNA interference (RNAi). For that, a shRNA-based cGKI knockdown in C2C12 cells was established (**Figure 4.29**).

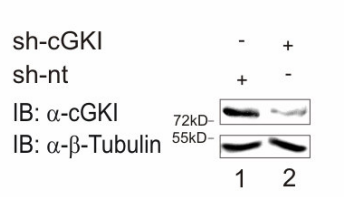

Figure 4.29 Analysis of the protein knockdown of endogenous cGKI in C2C12 cells using a cGKI-specific shRNA. C2C12 cells were transfected with a shRNA specific for cGKI (sh-cGKI) or a non-targeting shRNA (sh-nt). 48 hrs after transfection, the cGKI knockdown was examined using α-cGKI immunoblotting (upper panel) and β-Tubulin (lower panel) was used as a control for protein loading. IB, immunoblot.

Figure 4.29 exemplifies that transfection of C2C12 cells with a mouse-specific cGKI-shRNA efficiently downregulated the expression of endogenous cGKI (>50%) (upper panel, lanes 1 and 2). A non-targeting shRNA (sh-nt) specific for an mRNA from

Arabidopsis thaliana was applied as control (upper panel, lane 1). The targeting sequences of both shRNAs are listed in chapter 9.

The same cGKI-specific shRNA was used in BMP R-Smad phosphorylation experiments in C2C12 cells to further examine the role of cGKI in BMP signaling (**Figure 4.30**).

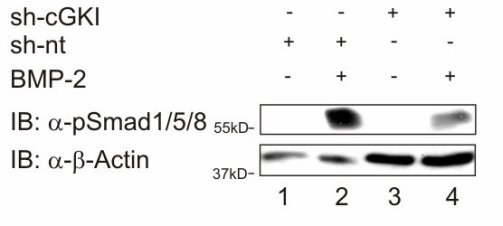

Figure 4.30 Phosphorylation study of BMP R-Smads in C2C12 cells after cGKI knockdown. shRNA-transfected C2C12 cells were starved for 24 hrs and stimulated with 10 nM BMP-2 for 30 min. Whole cellular extracts were analyzed by immunoblotting using α-pSmad1/5/8 (upper panels) and α-β-Actin antibodies (lower panel). The result is representative for three independent experiments. IB, immunoblot.

Downregulation of endogenous cGKI by sh-cGKI resulted in a reduced Smad1/5/8 phosphorylation (**Figure 4.30**, upper panel, lanes 2 and 4).

R-Smads get phosphorylated at the C-terminal SSXS motif by the respective type I receptor; the type I receptor activation occurs via serine phosphorylation of a distinct motif upstream the kinase domain, the GS-box, through ligand-activated type II receptor [3]. To examine the observed attenuation of Smad phosphorylation upon cGKI knockdown more in detail, BRIa activation, i.e. BRIa serine phosphorylation, was studied in cGKI knockdown cells (**Figure 4.31**).

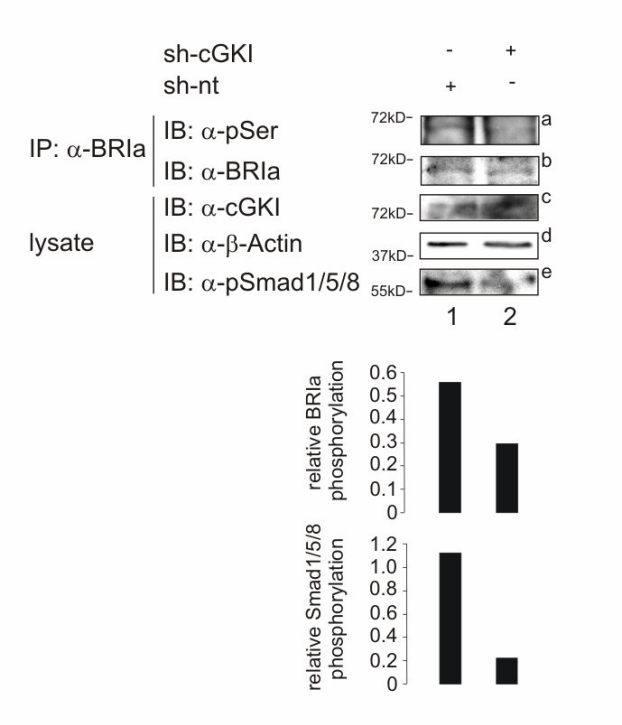

Figure 4.31 Phosphorylation study of BRIa and R-Smads in C2C12 cells after cGKI knockdown. shRNA-transfected C2C12 cells were lysed and whole cellular extracts were subjected to IP using α-BRIa antibody. Analysis of the precipitates was done by immunoblotting using α-pSer (panel a), α-BRIa (panel b), α-cGKI (panel c), α-β-Actin (panel d), and α-pSmad1/5/8 (panel e). Quantification of the result was performed using ImageJ. Intensities of pBRIa and BRIa bands as well as pSmad1/5/8 and β-Actin bands were measured. The ratios of the intensities (pBRIa/BRIa) and (pSmad/β-Actin) are depicted as relative BRIa phosphorylation (upper graph) and relative Smad1/5/8 phosphorylation (lower graph). The data shown are representative for two independent experiments. IP, immunoprecipitation; IB, immunoblot.

This experiment yielded in a 2-fold reduced serine phosphorylation of BRIa in cGKI knockdown cells (**Figure 4.31**, panel a; upper graph). Moreover, downregulation of endogenous cGKI (panel c) lead to an attenuation of C-terminal Smad phosphorylation by a factor of 5 (panel e; lower graph). Inversely, other studies revealed that cGKI overexpression enhances the BMP-2-induced serine phosphorylation of BRIa (data not shown).

Including the results shown before, cGKI seems to be involved not only in BRII modulation, but consequently also in the regulation of serine phosphorylation, i.e. activation of BRIa and thus of Smad phosphorylation.

4.4.2 Effect of cGKI expression and activation on R-Smad phosphorylation

The next step was to examine the effect of cGKI protein expression on the phosphorylation of BMP R-Smads. C2C12 cells were transfected with the indicated constructs and stimulated with BMP-2 and 8-Br-cGMP before lysis (**Figure 4.32**).

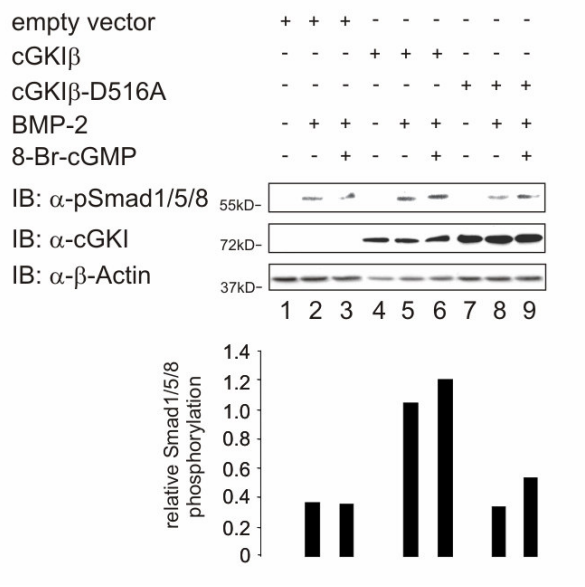

Figure 4.32 Phosphorylation study of Smad1 *in vivo* under the influence of cGKIβ variants. C2C12 cells were transfected with cGKIβ, cGKIβ-D516A mutant, or empty vector. After starvation (24 hrs) the cells were stimulated for 30 min with 10 nM BMP-2, 10 nM BMP-2/1 µM 8-Br-cGMP or left untreated. Whole cellular extracts were subjected to SDS-PAGE and immunoblotting using α-pSmad1/5/8 and α-cGKI antibodies. β-Actin was used as a loading control. Quantification of the result was performed using ImageJ. Intensities of pSmad1/5/8 and β-Actin bands were measured. The ratios of the intensities (pSmad/β-Actin) are depicted as relative Smad1/5/8 phosphorylation (graph below). This result is representative for at least three independent experiments. IB, immunoblot.

Figure 4.32 shows that co-expression of cGKIβ increased the level of phospho-Smad1 upon BMP-2 stimulation (upper panel, lanes 2 and 5). In contrast, kinase-inactive cGKIβ-D516A did not affect the ligand-induced Smad1/5/8 phosphorylation (upper panel, lanes 2 and 8), suggesting that the kinase activity of cGKIβ is necessary to enhance C-terminal phosphorylation of Smad1. Co-stimulation with 8-Br-cGMP did not influence R-Smad phosphorylation compared to samples stimulated only with BMP-2 (upper panel, lanes 2, 3, 5, 6, and 8, 9). From these observations it was concluded that cGKI promotes C-terminal phosphorylation of R-Smads.

Since 1 µM of 8-Br-cGMP is a relative low concentration to activate cGKI *in vivo*, experiments were done with higher concentrations of the compound.

Subsequently, either Smad C-terminal or VASP phosphorylation was examined (**Figure 4.33**).

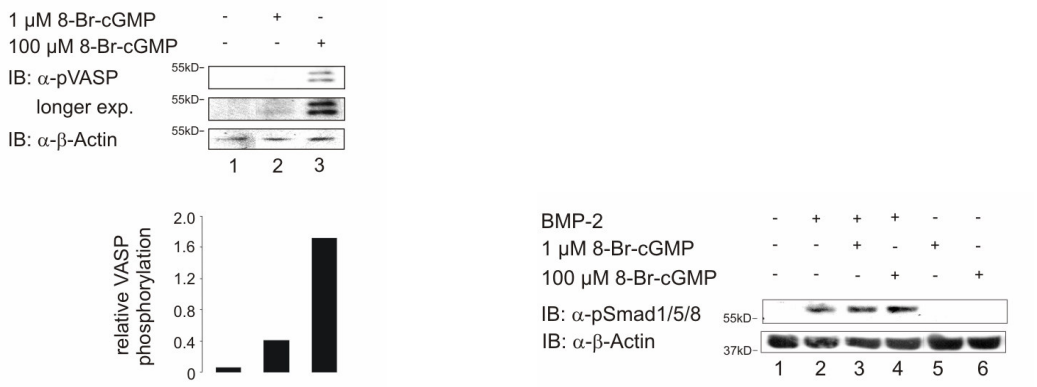

Figure 4.33 Phosphorylation study of Smad1/5/8 and VASP in C2C12 cells upon stimulation with 8-Br-cGMP. (Left) Endogenous VASP phosphorylation in C2C12 cells was monitored in response to stimulation with 1 µM or 100 µM 8-Br-cGMP for 30 min after cell starvation for 24 hrs. Whole lysates were analyzed by immunoblotting with α-pVASP (upper panels) and α-β-Actin antibodies (lower panel). Phosphorylation of VASP on Ser239 was used to monitor cGKI activity. The upper band is caused by concomitant phosphorylation on Ser157, a PKA site [709]. Quantification of the result was performed using ImageJ. Intensities of pVASP and β-Actin bands were measured. The ratios of the intensities (pVASP/β-Actin) are depicted as relative VASP phosphorylation (graph below).This result is representative for two independent experiments. **(Right)** Endogenous Smad1/5/8 phosphorylation was examined after starvation (24 hrs) and stimulation (30 min) of C2C12 cells with 10 nM BMP-2 and/or 1 µM or 100 µM of 8-Br-cGMP. Lysed cells were immunoblotted with α-pSmad1/5/8 (upper panel) and, as control, with α-β-Actin antibodies (lower panel). A representative result of at least three independent experiments is shown. IB, immunoblot.

VASP is a well known substrate of cGKI [708]. Therefore, phosphorylation of VASP can be used as an indicator for cGMP/cGKI activity. **Figure 4.33** shows that 100 µM 8-Br-cGMP strongly induced phosphorylation of VASP (16-fold; left, upper panel, lanes 1 and 3). But already 1 µM 8-Br-cGMP was enough to phosphorylate VASP, albeit much weaker (4-fold; left, middle panel, lanes 1 and 2). A similar result was observed in HEK293T cells (data not shown). Furthermore, **Figure 4.33** again demonstrates that endogenous Smad1/5/8 phosphorylation was not affected by stimulation or co-stimulation with different concentrations of 8-Br-cGMP (right, upper panel, lanes 3-6). Studying the BMP and 8-Br-cGMP effect over time (0-180 min) also showed no significant changes in Smad C-terminal phosphorylation when 8-Br-cGMP was present (data not shown). These results demonstrate that there are cGMP-sensitive cGKI molecules in C2C12 cells and HEK293T cells although 8-Br-cGMP seems not to be necessary for the induction of Smad phosphorylation.

Taken together, these data suggest that cGKI enhances Smad phosphorylation depending on its kinase activity. Additional activation of the kinase through its ligand cGMP seems not to influence Smad phosphorylation suggesting that the receptor-bound cGKI is already active.

4.4.3 Effect of cGKI on Smad1 *in vitro*

To analyze this cGKI-mediated Smad phosphorylation more in detail, *in vitro* kinase assays with recombinant Smad1 and cGKIα were performed. Smad1, N-terminally fused to the maltose binding protein (MBP), was expressed in and purified from *E. coli* BL21 (see 3.4.1), and examined by Coomassie-G stain (**Figure 4.34**) (see 3.4.11).

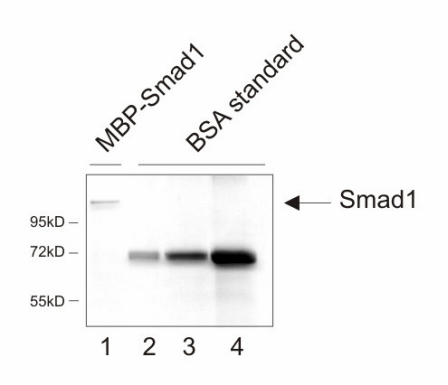

Figure 4.34 Analysis of protein amount and purity of recombinant Smad1 MBP fusion protein. Purified MBP-Smad1 protein (lane 1) immobilized to amylose resin was analyzed via Coomassie-G staining and BSA standards (1 µg, lane 2; 2 µg, lane 3; 5 µg, lane 4).

As **Figure 4.34** shows that the obtained MBP-Smad1 protein had a high purity. However, the rate of yield was relative low (250 µg protein from a 500 ml culture) and needs to be optimized.

For *in vitro* phosphorylation 1 µg of MBP-Smad1 was applied, and supplemented with cGKIα or not (**Figure 4.35**). To activate cGKI, 8-Br-cGMP was added.

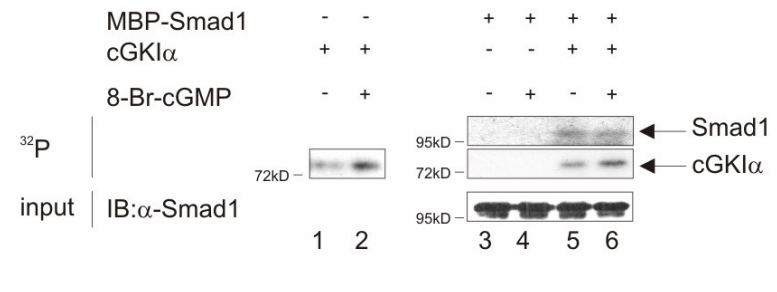

Figure 4.35 Phosphorylation study of cGKI and Smad1 *in vitro*. MBP-Smad1 (lanes 3-6) immobilized to amylose resin was subjected to an *in vitro* phosphorylation assay with cGKIα, activated with 8-Br-cGMP or not. Incorporated ^{32}P was detected by autoradiography (upper panel). The middle panel shows autophosphorylation of cGKIα. Input of MBP fusion protein was visualized by immunoblotting using a Smad1-directed antibody (lower panel). IB, immunoblot; ^{32}P, autoradiography.

Figure 4.35 indicates that MBP-Smad1 is phosphorylated *in vitro* in the presence of cGKIα, independent of 8-Br-cGMP activation (upper panel, lanes 3 and 4). Since the MBP control is missing in this experiment, the detected phosphorylation could be an unspecific one due to phosphorylation of the fused MBP via cGKIα. If there is a specific phosphorylation by cGKI, it is not clear yet which site in the Smad1 protein is phosphorylated.

4.4.4 Effect of cGKI knockdown on BMP-2-induced nuclear translocation of R-Smads

As demonstrated, Smad C-terminal phosphorylation is attenuated in cGKI knockdown cells (**Figure 4.30**). R-Smad phosphorylation at the SSXS motif is known to induce nuclear accumulation of R-Smads [306]. To follow this effect, nuclear translocation of Smad1 in cGKI knockdown cells were examined (**Figure 4.36**).

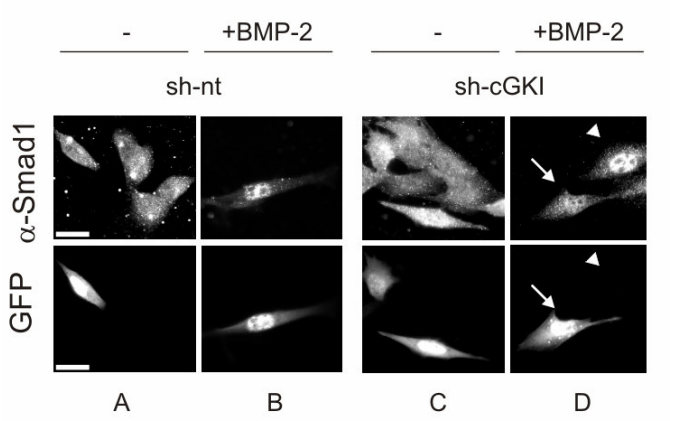

Figure 4.36 Nuclear translocation study of Smad1 in cGKI knockdown C2C12 cells. C2C12 cells were transfected with sh-nt and a vector encoding GFP or sh-cGKI and GFP. After 48 hr, cells were starved for 2 hrs and stimulated with 10 nM BMP-2 for 30 min. Endogenous Smad1 was immunostained and GFP-positive, i.e. transfected cells were analyzed via immunofluorescence microscopy. Quantification was done by determining the respective number of cells with BMP-2-induced nuclear Smad1 from all GFP-positive cells of two independent experiments. Error bars represent standard error of the mean. 63-fold magnification. Bar 20 µm.

Figure 4.36 demonstrates that the BMP-2-induced Smad1 nuclear translocation was inhibited in cells when cGKI was downregulated via a mouse-specific shRNA (panels D, arrow with solid line). Compared to this, cells transfected with sh-nt/GFP showed a strong nuclear accumulation of Smad1 upon ligand treatment (panels B, arrowhead). This suggests that cGKI, since it is important for Smad phosphorylation, does also regulate nuclear migration of R-Smads.

Since C-terminal phosphorylated R-Smads bind to co-Smad4 to undergo nuclear translocation, endogenous complex formation of Smad1/co-Smad4 under the influence of cGKI was examined. For that, C2C12 cells were transfected with non-specific sh-nt or sh-cGKI. To trigger Smad1/Smad4 complex formation, BMP-2 was added to the cells (**Figure 4.37**).

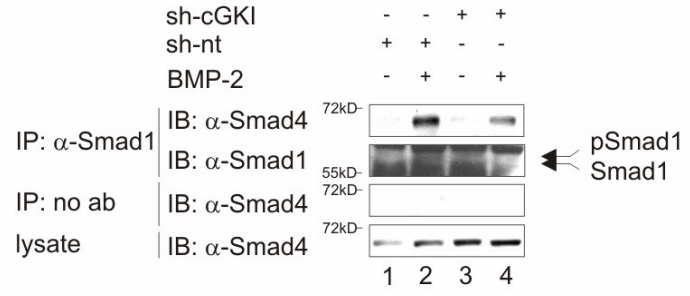

Figure 4.37 Endogenous complex formation of Smad1/co-Smad4 upon BMP-2 stimulation in cGKI knockdown C2C12 cells. 48 hrs after transfection, sh-nt-or sh-cGKI-transfected C2C12 cells were starved for 3 hrs and stimulated with 10 nM BMP-2 for 30 min. Cells were lyzed and subjected to IP using α-Smad1 antibody. The α-Smad1 immunoprecipitates were analyzed for Smad4 and Smad1 (upper panels) and lysates were checked for Smad4 (lower panel). This result is representative for two independent experiments. IP, immunprecipitation; IB, immunoblot.

As shown in **Figure 4.37**, C-terminally phosphorylated Smad1 formed a strong complex with Smad4 in the control cells (upper panel, lane 2), whereas complex formation of Smad1 and Smad4 was diminished in cGKI knockdown cells (lane 4). This indicates that the presence of cGKI is important for R-Smad/co-Smad complex formation.

In sum, these results suggest that not only R-Smad C-terminal phosphorylation is affected by cGKI, but also the heteromeric R-Smad/co-Smad4 complex formation and nuclear translocation of R-Smads are regulated. Thus, cGKI is important for the continuation of Smad signaling from the cytoplasm to the nucleus.

4.4.5 Effect of cGKI knockdown on the activity of a BMP-2-responsive reporter gene

To investigate the functional role of cGKI in the BMP-2-triggered downstream BMP signaling, the expression of Smad-dependent BMP-2 target genes was analyzed. For that purpose, the *BMP response element* (*BRE* from *Id1* promoter) luciferase reporter gene assay was used [806] (see 3.3.6.2). For cGKI knockdown, C2C12 cells were transiently transfected with the *BRE* reporter and the indicated mouse-specific shRNAs or siRNAs. Afterwards, the cells were stimulated with BMP-2 (**Figure 4.38**).

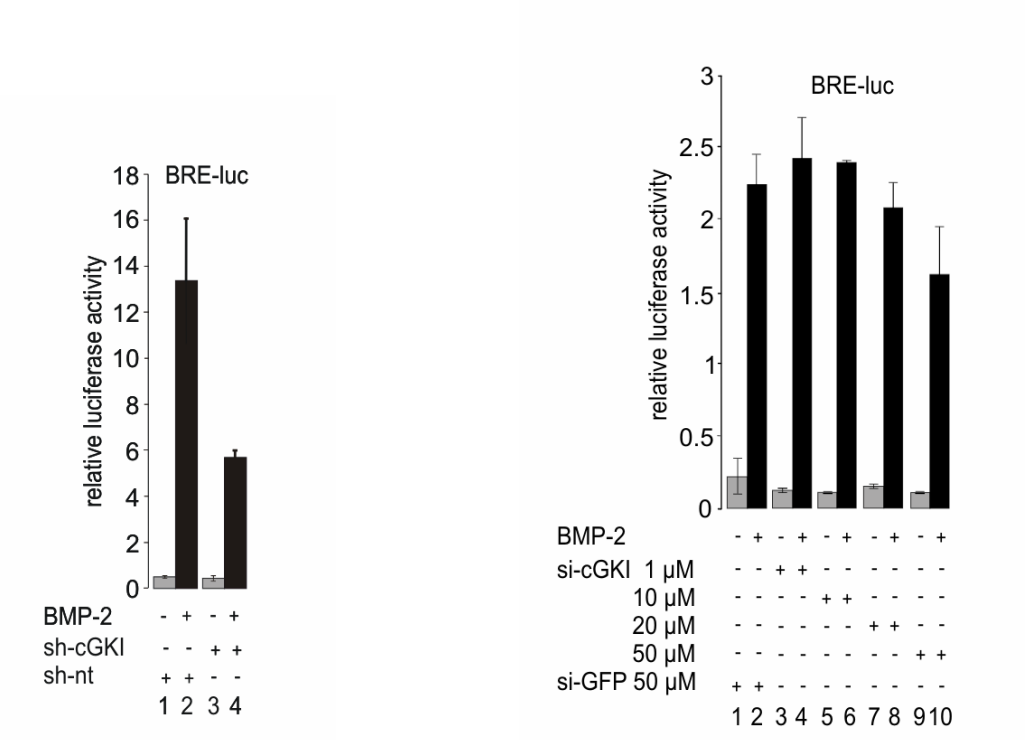

Figure 4.38 Effect of cGKI knockdown on the BMP-2-induced transcriptional activity in C2C12 cells using the *BRE*-luciferase reporter gene. (Left) C2C12 cells were co-transfected with *BRE*-luc, RL-TK, and sh-nt or sh-cGKI. After starvation for 5 hr, the cells were treated with 1 nM BMP-2 for 24 hrs (black column) or left untreated (grey column). The *BRE*-driven luciferase activity was measured according to manufacturer´s instructions using the Dual-Luciferase® Reporter Assay System. Error bars represent standard error or the mean. The result is representative for three independent experiments. **(Right)** C2C12 cells were co-transfected with *BRE*-luc, RL-TK, and different amounts of a siRNA specific for cGKI (si-cGKI). Transfection of cells with a siRNA directed against *GFP* mRNA (si-GFP) was used as a control. After starvation, the cells were treated with BMP-2 for 24 hrs (black column) or left untreated (grey column) and *BRE*-luc activity was measured. Error bars represent standard error of the mean. This result is representative for two independent experiments.

Knockdown of endogenous cGKI using mouse-specific sh-cGKI attenuated *BR*E reporter gene response upon ligand stimulation 2.4-fold when compared to control cells transfected with sh-nt (**Figure 4.38**, left, compare black columns 2 and 4). Additionally, a murine siRNA targeting cGKI was used (see 2.3), and increasing amounts of this siRNA were transfected into C2C12 cells to analyze *BRE* reporter gene response upon BMP-2 stimulation. *BRE* reporter gene response was attenuated upon cGKI siRNA-based knockdown in a dose-dependent manner (right). Compared to cells transfected with 50 µM of a control siRNA (si-GFP, columns 1 and 2), *BRE* activity was decreased in cells transfected with 20 to 50 µM si-cGKI (right, columns 7-10).

As expected, regarding the data from analyzing the effect of cGKI on R-Smad phosphorylation and downstream, downregulation of endogenous cGKI resulted in attenuation of Smad-dependent target gene transcription.

4.4.6 Effect of cGKI expression on the activity of a BMP-2-responsive reporter gene

To further investigate the effect of cGKI on the expression of Smad-dependent BMP-2 target genes, overexpression studies of cGKI in C2C12 cells were done using *BRE* reporter gene assay. Cells were transfected with cGKI variants and the reporter plasmids, and were stimulated with BMP-2 (**Figure 4.39**).

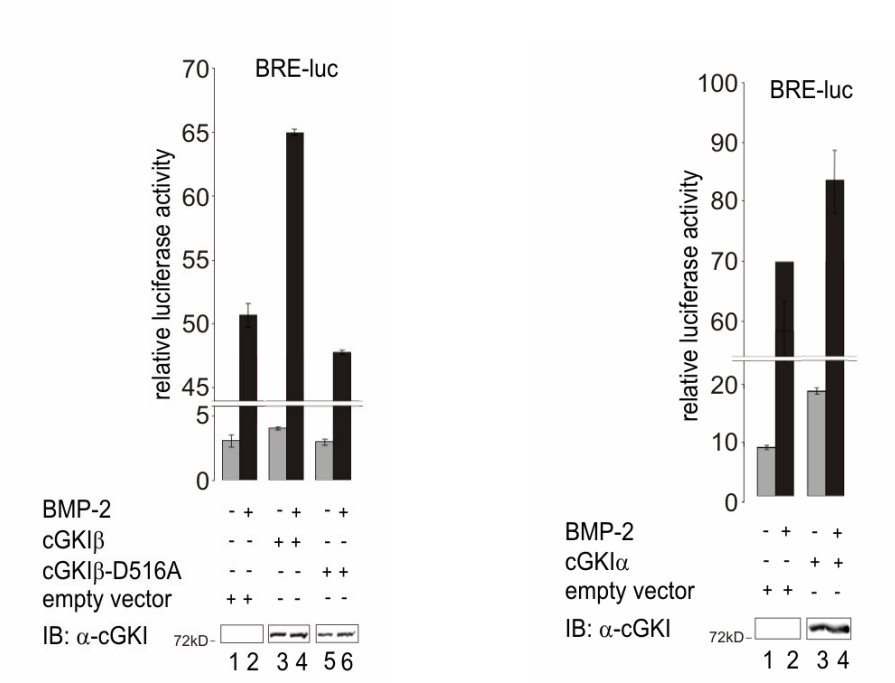

Figure 4.39 Effect of cGKI variants on the BMP-2-induced transcriptional activity in C2C12 cells using the *BRE* luciferase reporter gene. C2C12 cells were co-transfected with *BRE*-luc, RL-TK, and cGKIβ or cGKIβ-D516A (left) or α (right). After starvation, the cells were treated with BMP-2 for 24 hrs (black columns) or left untreated (grey columns) and luciferase activity was measured. Error bars represent standard error of the mean. Data are representative for at least three independent experiments. To control cGKIα/β expression, samples were subjected to SDS-PAGE and immunoblotting with α-cGKI antibody. IB, immunoblot.

It was found that both cGKIα and β stimulated the *BRE* reporter in C2C12 cells (**Figure 4.39**). Wildtype cGKI increased *BRE* reporter activity (left, black columns 2 and 4; right graph, compare black columns 2 and 4), whereas the kinase-inactive

mutant cGKIβ-D516A failed to do so (left, compare black columns 2 and 6). Additionally, both isoforms increased the reporter gene activity even in the absence of BMP-2 (slightly in the left graph, grey columns 1 and 3; strongly in the right graph, grey columns 1 and 3). The same result was achieved upon overexpression of cGKIβ by using the *SBE* reporter, a reporter gene responsive for both BMP and TGFβ Smads ([807]; see 3.3.6.2) (data not shown). It is suggested that the stimulatory effect of cGKI observed for Smad activation is continued down to the expression of a BMP-responsive reporter gene, i.e. to the expression of BMP target genes. Furthermore, it is assumed that cGKI´s function in BMP signaling depends on its kinase activity.

4.4.7 Effect of overexpression of cGKI on *Id1* expression

Chapter 4.4.5 and 4.4.6 describe the impact of cGKI knockdown or overexpression on the activation of a BMP-2-specific reporter gene. This reporter was cloned from the murine promoter of the BMP-2 target gene *Id1* [806]. In the following, the endogenous *Id1* expression in C2C12 cells was examined under the influence of cGKI. *Id1* mRNA is upregulated within 1 hr of BMP-2 stimulation [403]. cGKIβ was transiently transfected into these cells. Afterwards, cells were stimulated with BMP-2 and the relative *Id1* mRNA amount was measured in comparison to empty vector-transfected cells (**Figure 4.40**).

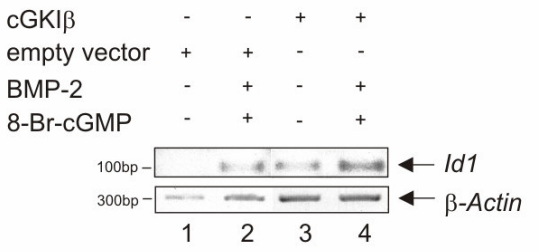

Figure 4.40 Effect of cGKIβ on the expression of *Id1*. Mock- or cGKIβ-transfected C2C12 cells were starved for 24 hrs and treated with 20 nM BMP-2/1 µM 8-Br-cGMP for 4 hrs or left untreated. Cells were analyzed for expression of endogenous *Id1* by RT-PCR and subsequent PCR using *Id1*-specific primers. *β-Actin* was used as a control.

Figure 4.40 indicates that overexpression of cGKI upregulated the expression of *Id1* (lanes 2 and 4), as it was found in the *BRE*-luc assay (**Figure 4.39**).

4.4.8 Effect of cGKI activation on the activity on the BMP target gene expression

In accordance to the analysis of Smad phosphorylation upon stimulation with 8-Br-cGMP and thus activation of cGKI, *Id1* target gene expression as well as *BRE*-dependent reporter gene activity in C2C12 cells upon cGMP stimulation were examined (**Figure 4.41**).

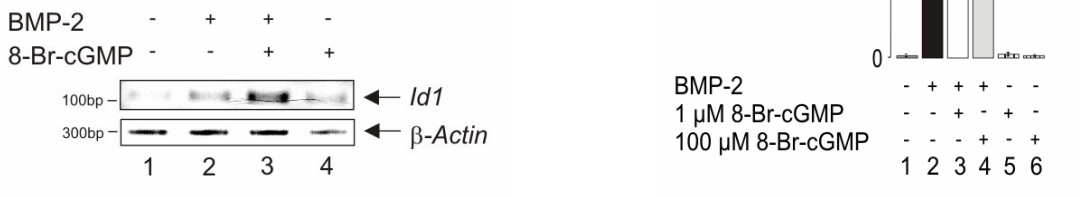

Figure 4.41 Effect of 8-Br-cGMP on the BMP target gene activity in C2C12 cells using an Id1 expression assay and the *BRE* luciferase reporter gene. (Left) Starved (for 24 hrs) C2C12 cells were stimulated with 20 nM BMP-2 and/or 1 µM 8-Br-cGMP for 4 hrs or left untreated. Total mRNA was examined for endogenous *Id1* expression by RT-PCR and subsequent PCR using *Id1*-specific primers. *β-actin* was used as a control. This result is representative for three independent experiments. **(Right)** C2C12 cells transfected with *BRE*-luc and RL-TK were, after starvation, stimulated with BMP-2 (black column), BMP-2/1 µM 8-Br-cGMP (white column), BMP-2/100 µM 8-Br-cGMP (light grey column), 1 µM 8-Br-cGMP (striped column), 100 µM 8-Br-cGMP (narrow striped column), or left unstimulated (grey column). Luciferase activities are presented as mean values and error bars represents standard error of the mean. This result is representative for at least three indepdendent experiments.

Analysis of the endogenous *Id1* transcription by RT-PCR revealed an 8-Br-cGMP-dependent increase of the BMP-2-induced transcription (**Figure 4.41**, left, upper panel). While BMP-2 induced a more than 2-fold activation of *Id1* transcription (left, upper panel, lanes 1 and 2), BMP-2 together with 8-Br-cGMP resulted in 5-fold

induction (left, upper panel, lane 2 and 3). However, it was found that neither co-stimulation nor stimulation with 1 µM or 100 µM 8-Br-cGMP alone did affect *BRE* reporter gene activity, while it was strongly induced by BMP-2 alone (right, **Figure 4.41**). The same negative result was revealed by using the *SBE* reporter, which responds to BMP and TGFβ Smads (data not shown). This result is puzzling since both cGKI downregulation and overexpression of cGKI affects Smad target gene transcription (**Figure 4.38** and **Figure 4.39**). Furthermore, the enhancing effect seems to depend on cGKI´s kinase activity (**Figure 4.39**). On the other hand it was repeatedly observed *in vitro* and *in vivo* that cGKI exhibits a high basal kinase activity without cGMP stimulation, which was sufficient to phosphorylate and/or regulate cGKI targets (**Figure 4.12**, **Figure 4.39** and data not shown). Thus, it is assumend that the cGMP/cGKI pathway influences the artificial BMP reporter, controlled by a minimal promoter cloned from the *Id1* gene, and the endogenous *Id1* promoter differently.

4.4.9 Effect of a cGKI NLS mutant on R-Smad phosphorylation and on the activity of a BMP-responsive reporter gene

As demonstrated, cGKI undergoes nuclear translocation upon BMP-2 stimulation (**Figure 4.16** and **Figure 4.26**) and regulates ligand-induced R-Smad phosphorylation (**Figure 4.30** and **Figure 4.32**). To further examine the role of cGKI in BMP signaling, a cGKI mutant deficient in cGMP-mediated nuclear translocation, the NLS mutant cGKI-K407A/R409A [671], was investigated. First, C-terminal phosphorylation of R-Smads upon the expression of the cGKI NLS mutant was analyzed (**Figure 4.42**).

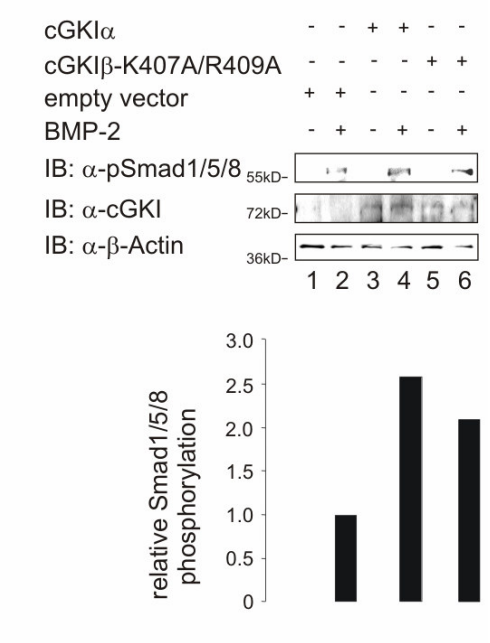

Figure 4.42 Phosphorylation study of Smad1 *in vivo* under the influence of cGKI variants. C2C12 cells were transfected with cGKIα, cGKIβ-K407A/R409A mutant, or empty vector. After starvation (24 hrs) the cells were stimulated with 10 nM BMP-2 for 30 min or left untreated. Whole cellular extracts were subjected to SDS-PAGE and immunoblotting using α-pSmad1/5/8 and α-cGKI antibodies. β-Actin was used as a loading control. Quantification of the result was performed using ImageJ. Intensities of pSmad1/5/8 and β-Actin bands were measured and the ratio of the intensities (pSmad/β-Actin) is depicted as relative Smad1/5/8 phosphorylation (graph below). This experiment is a representative one (n=2). IB, immunoblot.

Figure 4.42 shows again that co-expression of cGKIβ increased the level of phosphorylated Smad1/5/8 upon BMP-2 stimulation (2.6-fold; upper panel, lanes 2 and 4). Also the NLS mutant cGKIβ-K407A/R409A enhanced the ligand-induced Smad1/5/8 phosphorylation (2.1-fold; upper panel, lanes 2 and 6). Furthermore, co-IP assays revealed that the NLS mutant still can bind BRII-LF (data not shown). These results suppose that the NLS mutant can fulfill the same function in the cytoplasm as wildtype cGKI does.

Next, the effect of cGKIβ-K407A/R409A on BMP target gene expression was tested. For that, a *BRE* reporter gene assay was performed with C2C12 cells transfected with cGKIβ variants and the reporter plasmids (**Figure 4.43**).

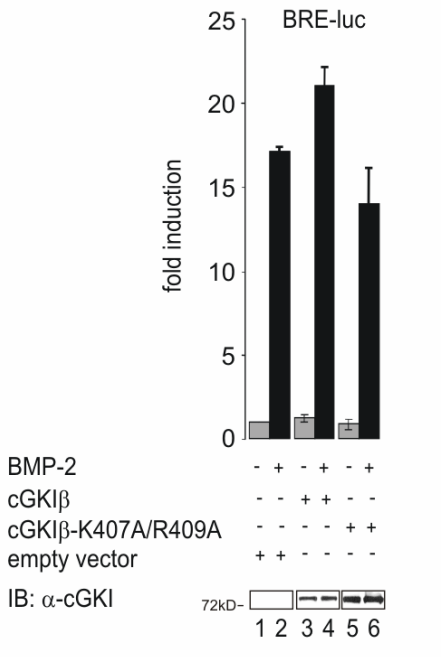

Figure 4.43 Effect of cGKI variants on the BMP-2-induced transcriptional activity in C2C12 cells using the *BRE* luciferase reporter gene. C2C12 cells were co-transfected with *BRE*-luc, RL-TK, and cGKIβ, cGKIβ-K407A/R409A, or empty vector. After starvation for 5 hr, the cells were treated with 1 nM BMP-2 for 24 hrs (black columns) or left untreated (grey columns) and luciferase activity was measured. *BRE* activity is presented as fold induction relative to the activity measured in empty vector, - BMP-2 from two out of three independent experiments. Error bars represent standard error of the mean. To control cGKIβ expression, samples were subjected to SDS-PAGE and immunoblotting with α-cGKI antibody. IB, immunoblot.

As already shown, expression of cGKIβ upregulated the reporter gene activity (**Figure 4.43,** 1.3-fold; black columns 2 and 4), albeit moderately in this experiment. On the contrary, the NLS-deficient cGKIβ did not increase BRE activity (black columns 2, 4 and 6) indicating that nuclear localization of cGKI is important for BMP signaling.

In sum, these results from chapter 4.4 show that (a) cGKI enhances Smad phosphorylation and Smad-dependent downstream signaling, (b) cGKI´s kinase activity is important to fulfill this function whereas cGMP-mediated activation seems not to be required, (c) a NLS cGKI mutant exhibits the same cytoplasmic function as the wildtype cGKI but (d) this mutant affects BMP target gene transcription which indicates that the proper localization of the cGKI to the nucleus is also important for performing its task in BMP signaling.

4.5 Functional relevance of cGKI for BMP-2-induced non-Smad pathway

BMP signaling is known to induce several genes which are involved in osteogenic differentiation, but also in other processes [12]. To analyze whether cGKI plays a role in the regulation of other BMP-2 target genes than *Id1*, the induction of the osteogenic marker alkaline phosphatase (ALP) and the activation of the upstream p38-MAPK [195] was examined in C2C12 cells.

4.5.1 Effect of cGKI on p38-MAPK phosphorylation

It is known from studies in cardiomyocytes that cGKIα inhibits the TAB1-p38-MAPK-induced apoptosis by inhibiting the phosphorylation and activation of p38 [732]. Here, the BMP-2-dependent induction of the MAPK p38 was examined [195], but also a lot of crosstalk mechanisms influence p38 activation. In this respect, it has to be mentioned that studying p38-MAPK and associated processes is very difficult, since it is a stress-responsive kinase [461]. The BMP-2-induced activation of MAPK p38, a key component in non-Smad BMP signaling, in C2C12 cells was checked under the influence of cGKIβ and cGKI activation. For that, C2C12 cells were transfected with the indicated constructs or left untransfected, and stimulated with BMP-2 and/or 8-Br-cGMP (**Figure 4.44**).

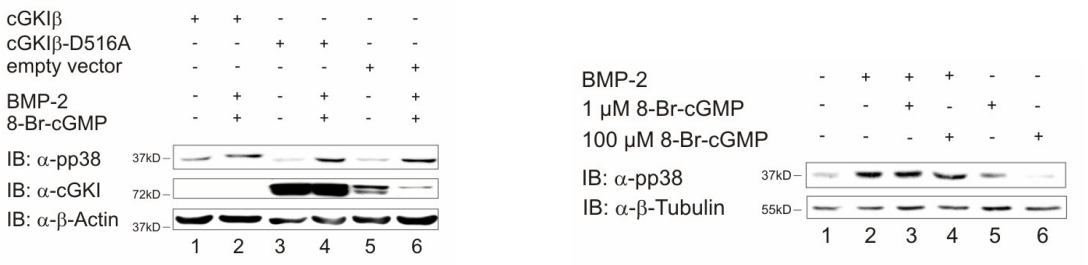

Figure 4.44 Phosphorylation study of p38-MAPK *in vivo* under the influence of cGKI. (Left) C2C12 cells were transfected with cGKIβ, cGKIβ-D516A or empty vector. After starvation for 5 hr, cells were treated with 10 nM BMP-2/ 1 µM 8-Br-cGMP for 1 hr or left untreated. Whole cellular extracts were subjected to SDS-PAGE and α-pp38 immunoblotting (upper panel). Expression of cGKIβ variants and protein loading was checked with α-cGKI (middle panel) and α-β-Actin antibodies (lower panel). This result is representatibe for two independent experiments. **(Right)** Starved (5 hrs) C2C12 cells were stimulated with 10 nM BMP-2 and different concentrations of 8-Br-cGMP for 1 hr. Whole cellular extracts were separated by SDS-PAGE and analyzed by α-pp38 immunoblotting (upper panel). β-Tubulin was used as loading control (lower panel). This result is representative for at least three independent experiments. IB, immunoblot.

It was observed that neither cGKIβ nor cGKIβ-D516A had any effect on the BMP-2-induced phosphorylation of p38-MAPK (**Figure 4.44**, left, upper panel, lanes 2, 4, and 6). Furthermore, stimulation or co-stimualtion with 8-Br-cGMP, neither with 1 µM nor 100 µM, showed any effect on BMP-2-mediated phosphorylation of p38 (right) indicating that this component of the non-Smad BMP signaling is not BMP-dependently regulated by cGKI.

4.5.2 Effect of cGKI expression on alkaline phosphatase expression/activation

To explore whether the expression and thus activity of one of the downstream targets of p38, ALP, is influenced by cGKI, studies on transfected or untransfected C2C12 cells were performed. Cells were additionally treated with BMP-2 and/or different concentrations of 8-Br-cGMP (**Figure 4.45**).

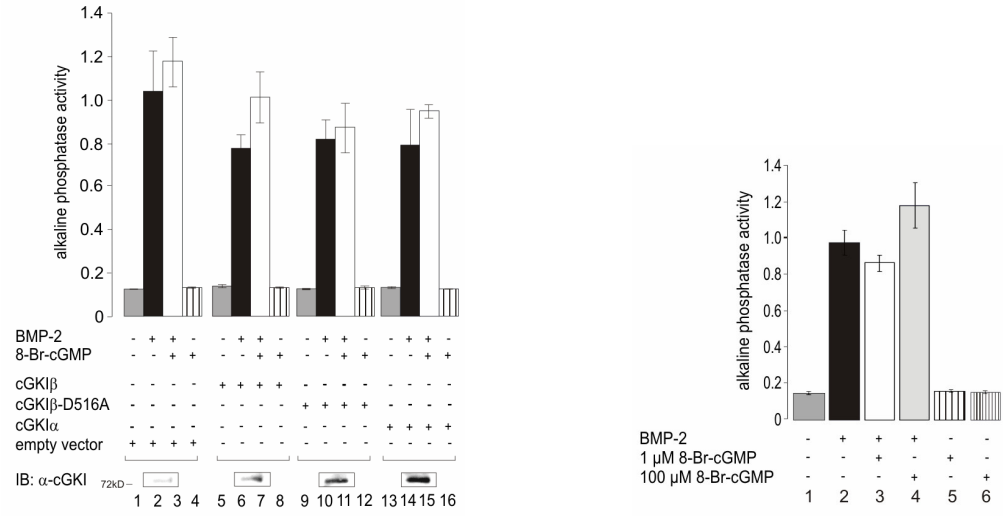

Figure 4.45 Analysis of ALP expression and activation in C2C12 cells under the influence of cGKI. (Left) C2C12 cells transfected with the indicated construct were stimulated for 72 hrs with 20 nM BMP-2 (black columns), 20 nM BMP-2/1 µM 8-Br-cGMP (white columns), 1 µM 8-Br-cGMP (striped columns), or left untreated (grey columns). ALP activity of the mean of triplicate transfection is presented. Error bars are the standard error of the mean. For cGKI expression control, the samples were pooled, protein was TCA/acetone-precipitated and subjected to α-cGKI immunoblotting. This l s a representative assay (n=2). IB, immunoblot. **(Right)** C2C12 cells were stimulated for 72 hrs with 20 nM BMP-2 (black column), 20 nM BMP-2/1 µM 8-Br-cGMP (white column), 20 nM BMP-2/100 µM 8-Br-cGMP (light grey column), 1 µM 8-Br-cGMP (striped column), 100 µM 8-Br-cGMP (narrow striped column), or left untreated (grey column). ALP activity was measured and error bars represent standard error of the mean. This result was reproduced three times.

Figure 4.45 shows that the overexpression and the concomitant activation of cGKI variants had no significant effect on the induction of ALP (left). While cGKIα (left, columns 13-16), cGKIβ (left, columns 5-8) or cGKIβ-D516A (left, columns 9-12) expression seemed to slighly lower the induction of ALP in this experiment compared to empty vector-transfected cells (left, colums 1-4), overexpression of cGKI in several other assays did not influence ALP activity (data not shown). Stimulation or co-stimulation with 8-Br-cGMP had no significant effect (left). Next, the impact of higher concentrations of 8-Br-cGMP on ALP activity was investigated, since several studies described a higher concentration of 100 µM to be necessary for *in vivo* studies [666]. Again, neither stimulation with 1 µM nor with 100 µM 8-Br-cGMP nor co-stimulation with BMP-2 changed the activity of ALP (right). Following up the impact of cGKI on ALP, RT-PCR analysis of *ALP* expression under 8-Br-cGMP stimulation was performed. It could be demonstrated that *ALP* mRNA expression was not affected by 8-Br-cGMP in a BMP-dependent manner after 24 hrs (data not shown).

From these results presented in chapter 4.5 it is concluded that specifically the Smad pathway of BMP signaling, and not the non-Smad pathway via MAPK-p38 is regulated by cGKI.

4.6 Relevance of cGKI/TFII-I association for BMP-2-induced Smad pathway

Specific transcription factors such as Runx-2 (see chapter 1.4.3) which interact and cooperate with BMP Smads regulate BMP target gene expression [2]. Interestingly, cGKIβ also physically binds to and phosphorylates the basal transcription factor TFII-I, which leads to an increased transactivation potential of TFII-I [673]. An involvement of TFII-I in BMP signaling was not described yet. In the following, the effect of TFII-I for BMP signaling is investigated.

4.6.1 Characterization of TFII-I/Smad interaction

Previous results demonstrated that cGKI binds to the BMP R-Smads 1 and 5 (**Figure 4.20**, **Figure 4.21** and **Figure 4.25**) and to the co-Smad4 (**Figure 4.23**). Interestingly, it

is published that the cGKIβ-associated protein TFII-I can bind Smad2 [830] as well as Smad3 [831]. To investigate whether TFII-I is also associated with cGKIβ/Smad complexes, co-immunoprecipitation experiments in C2C12 cells with the endogenous proteins were carried out (**Figure 4.46**).

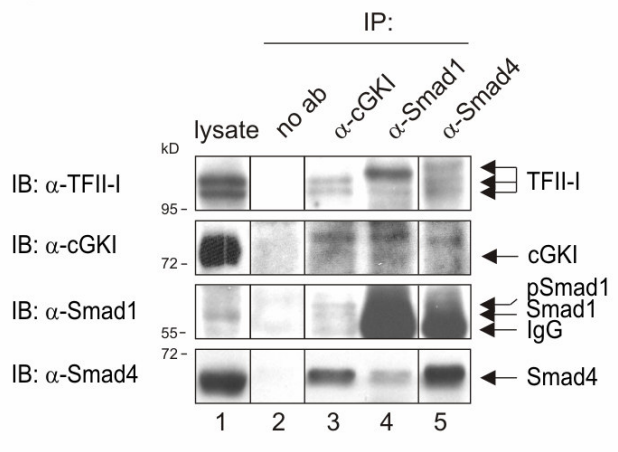

Figure 4.46 Interaction of endogenous TFII-I with cGKIβ and Smads in C2C12 cells. Endogenous protein complexes from C2C12 cells containing TFII-I and cGKIβ, Smad1 or Smad4 were examined by co-IP using α-cGKIβ (lane 3), α-Smad1 (lane 4), and α-Smad4 (lane 5) antibodies. Precipitates (lanes 3-5) and the lysate (lane 1) were analyzed by immunoblotting with the indicated antibodies. Antibody (ab) was ommited to control the sepharose (lane 2). This result is representative for two independent experiments. IP, immunoprecipitation; IB, immunoblot.

This co-IP experiment revealed complex formation of endogenous TFII-I with cGKI, Smad1 and Smad4 in C2C12 cells (**Figure 4.46**, upper panel, lanes 3, 4 and 5). The double band seen for TFII-I represents the two splice forms, β and Δ [832] (upper panel, lane 1). Interestingly, a slower migrating form of TFII-I also co-precipitated with Smad1 and co-Smad4 (upper panel, lanes 4 and 5). It is suggested that TFII-I indeed binds to Smad proteins; however, it is not clear whether Smad complexes prefer to interact with this modified TFII-I or whether the modification occurs as a consequence of the interaction with Smad/cGKIβ complexes and subsequent phosphorylation by cGKIβ. Also other protein modifications must be considered.

For studying the effect of BMP-2 stimulation on the interaction of TFII-I with Smad proteins, HEK293T cells were transiently transfected with Smad1 and TFII-I, stimulated with BMP-2, and Smad1 was immunoprecipitated (**Figure 4.47**).

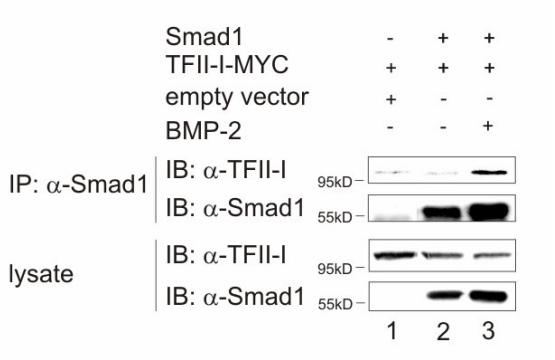

Figure 4.47 Interaction of TFII-I and Smad1 upon BMP-2 stimulation. HEK293T cells were transfected with TFII-I and Smad1. After starvation for 3 hrs and stimulation with 10 nM BMP-2 for 30 min, association of TFII-I and Smad1 was analyzed by IP using a Smad1-directed antibody. Precipitates (upper panels) and lysates (lower panels) were checked with α-Smad1 and α-TFII-I antibodies. This assay is representative for two independent experiments. IP, immunoprecipitation; IB, immunoblot.

It was found that Smad1/TFII-I binding is induced by BMP-2 (**Figure 4.47**, upper panel, lanes 2 and 3). Notable, also the interaction between cGKI and the Smad proteins is increased upon BMP-2 stimulation as demonstrated in **Figure 4.21**, **Figure 4.23** and **Figure 4.25**.

4.6.2 Subcellular distribution and co-localization of TFII-I and R-Smad1

Isoform-specific conformation as well as serum starvation, respectively growth factor stimulation regulates the subcellular localization of TFII-I [832]. Immunofluorescence microscopy using an α-pan-TFII-I antibody was performed to locate TFII-I in these cells. For that, C2C12 cells were stimulated with BMP-2 and stained for endogenous TFII-I and Smad1 (**Figure 4.48**).

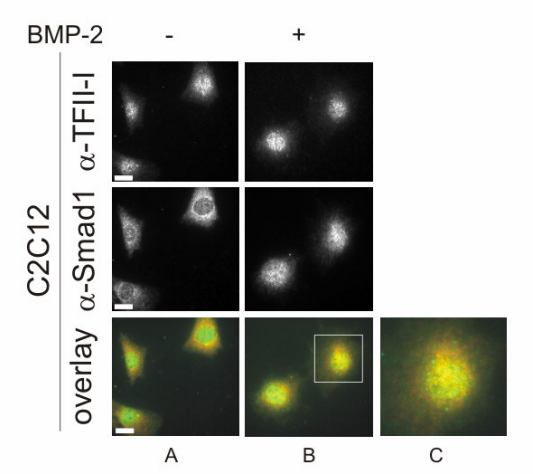

Figure 4.48 Co-localization of TFII-I and Smad1 in BMP-2-induced C2C12 cells. Starved (2 hr, panels A) and BMP-2-stimulated (10 nM, 30 min, panels B) C2C12 cells were immunostained with α-TFII-I (upper panels) and α-Smad1 (middle panels) antibodies. Lower panels show the respective overlay of both stainings with a magnification (panel C). A representative result is shown (n=3). 63-fold magnification. Bar 20 µm.

Figure 4.48 gives evidence for the cellular distribution of TFII-I and Smad1 upon BMP-2 in C2C12 cells. Smad1 translocated into the nucleus upon BMP-2 stimulation (middle panels A and B), whereas TFII-I was predominantly in the nucleus independent of BMP-2 treatment (upper panels A and B). Upon BMP-2 stimulation, TFII-I co-localized with Smad1 in the nucleus (lower panel B) indicating that the interaction detected in **Figure 4.47** between the cGKI/Smad complexes and TFII-I most likely takes place in the nucleus.

Having established that cGKI binds with Smad1 to the promoter of the BMP-2 target gene *Id1* in a BMP-dependent manner, it was suspected that TFII-I is also a component of this complex. Therefore, in collaboration with J. Weiske and O. Huber (Charité, Germany), the ChIP and two-step ChIP experiments from chapter **4.3.5** were repeated using α-Smad1 and α-TFII-I antibodies. C2C12 cells were treated with the indicated stimuli and subjected to ChIP analysis (**Figure 4.49**).

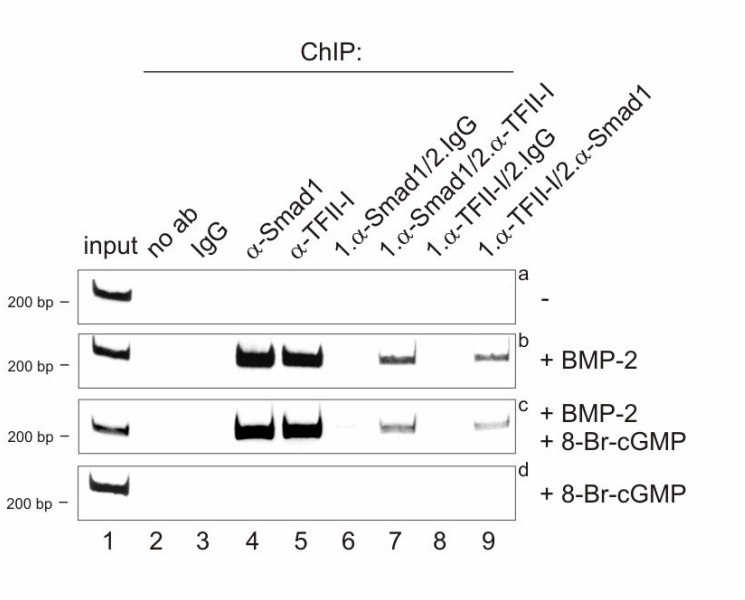

Figure 4.49 Co-localization of endogenous TFII-I and Smad1 at the *Id1* promoter C2C12 cells after BMP-2 stimulation. C2C12 cells were starved for 24 hrs and stimulated for 4 hrs with 10 nM BMP-2 (panel b) and/or 1 µM 8-Br-cGMP (panels c and d) or left unstimulated (panel a), and were analyzed by two-step ChIP using α-Smad1 followed by α-TFII-I antibody (lanes 6 and 7) or *vice versa* (lanes 8 and 9). Subsequent PCR analysis with *Id1* promoter-specific primers revealed the protein binding, respectively. As control for unspecific binding, antibody was left out (lane 2) in the ChIP experiment, or IgG was included (lane 3). Lane 1 monitors the DNA input for each ChIP analysis. This result is representative for two independent experiments. ChIP, chromatin immunoprecipitation. In collaboration with J. Weiske and O. Huber, Charité, Germany.

As demonstrated in **Figure 4.49**, TFII-I bound to the *Id1* promoter depending on BMP-2 stimulation (panels b and c, lane 5). Furthermore, the transcription factor formed a complex with Smad1 at *Id1* promoter sites in BMP-2- and BMP-2/8-Br-cGMP-treated C2C12 cells (panel b and c, lanes 7 and 9), but not in unstimulated cells (panel a).

Summing up the results from **Figure 4.27** and **Figure 4.28**, it is concluded that cGKI and TFII-I associate with Smad1 at the *Id1* promoter in a BMP-2-dependent manner.

4.6.3 Effect of TFII-I expression on the activity of a BMP-2-responsive reporter gene

Since TFII-I complexes with cGKIβ [673] (**Figure 4.46)** and BMP R-Smads (**Figure 4.46** and **Figure 4.47**), and even binds with these proteins to the *Id1* promoter (**Figure 4.49**), the impact of this interaction on BMP-2 signaling was investigated. In order to

do that, TFII-I together with the *BRE* reporter plasmid was transiently transfected into C2C12 cells (**Figure 4.50**).

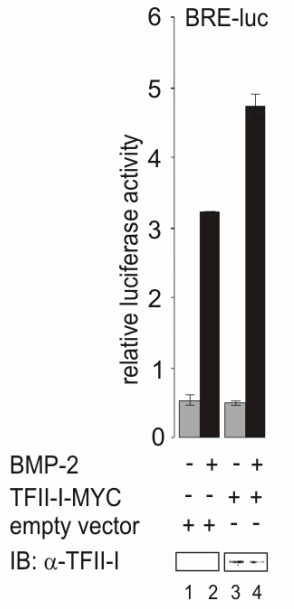

Figure 4.50 Effect of TFII-I on the BMP-2-induced transcriptional activity in C2C12 cells using the *BRE*-luciferase reporter gene. C2C12 cells co-transfected with *BRE*-luc, RL-TK, and TFII-I or empty vector, were starved for 5 hrs and stimulated with 1nM BMP-2 for 24 hrs (black columns) or left untreated (grey columns). Luciferase reporter gene activity was measured, error bars represent the standard error of the mean. TFII-I expresession was checked after SDS-PAGE via immunoblotting using α-TFII-I antibody. This result is representative for two independent experiments. IB, immunoblot.

Figure 4.50 shows that TFII-I modulated BMP signaling. TFII-I overexpression upregulated the *BRE* response 1.6-fold compared to empty vector-transfected cells (columns 2 and 4). This points towards that the cooperation of TFII-I with the transcriptional Smad complex is important for the regulation of BMP-induced gene transcription. Two serines, Ser371 and Ser734, within TFII-I were identified to be phosphorylated by cGKIβ *in vitro* and *in vivo*. Phosphorylation of these serines leads to enhanced transcriptional activity of TFII-I [673]. The serine double mutant of TFII-I (TFII-I-S371A/S734A, [673]) tested in *BRE*-luc assays during this study, behaved very divergent; once it showed the same upregulation than the wildtype, and once it reflected the control level (data not shown). Thus, a definite conclusion about the importance of cGKI-phosphorylated TFII-I couldn´t be drawn.

The next question was whether the BMP-2-induced interaction of TFII-I, cGKI and Smads (**Figure 4.49**, **Figure 4.48**, **Figure 4.47**, **Figure 4.28**, **Figure 4.26** and **Figure 4.25**) in the nucleus has a functional outcome in BMP signaling. During this study it

was furthermore found that a proper nuclear localization of cGKIβ is important for the function of the kinase in BMP signaling (**Figure 4.43**). Thus, the question came up if cGKI has besides its cytoplasmic function a nuclear role in BMP signaling which involves TFII-I. For that, a *BRE* reporter gene assay was done in C2C12 cells transfected with the indicated constructs and the reporter plasmids (**Figure 4.51**).

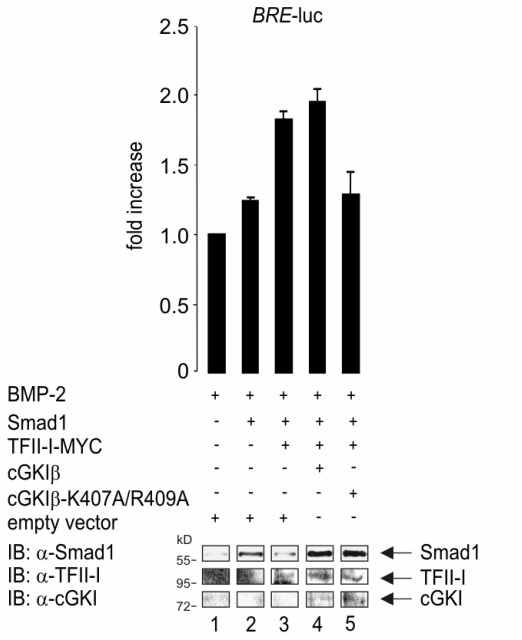

Figure 4.51 Effect of TFII-I and cGKIβ variants on the BMP-2-induced transcriptional activity in C2C12 cells using the *BRE*-luciferase reporter gene. C2C12 cells co-transfected with *BRE*-luc, RL-TK, and the indicated constructs were starved (5 hrs), stimulated with 1 nM BMP-2 for 24 hrs (black columns) or left untreated (grey columns). The activities of the luciferase reporter gene were measured and are presented as fold increase relative to the activity in empty vector, + BMP-2 samples. The error bars are the standard error of the mean. This result was reproduced in three independent experiments. The expression of Smad1, TFII-I, and cGKIβ or cGKIβ-K407A/R409A was controlled after SDS-PAGE and immunoblotting of the samples with the respective antibody. IB, immunoblot.

The graph in **Figure 4.51** shows again that TFII-I overexpression enhanced the *BRE* response 1.5-fold in TFII-I/Smad1-transfected cells compared to Smad1-transfected cells (columns 1 and 3). Furthermore, co-expression of the cGKIβ NLS mutant completely reversed the positive effect of TFII-I (columns 2, 3 and 5) whereas co-expression of wildtype cGKIβ was additive, albeit weak (columns, 2, 3 and 4). This indicates that cGKI and TFII-I cooperate in the nucleus to induce BMP-dependent target gene transcription.

In summary, these data presented in chapter 4.6 propose that (a) the Smad complexes bind the basal transcription factor TFII-I. (b) This occurs very likely in the nucleus after BMP-2 stimulation in transcriptional active Smad complexes. (c) Furthermore, inside these nuclear complexes TFII-I cooperates with cGKI to stimulate BMP signaling since TFII-I´s transactivation potential depends on the presence of cGKIβ in the nucleus.

4.7 Impact of BMP-2 signaling on the expression of cGKI and TFII-I

Studying BMP signaling under the influence of cGKI brought light to a novel and complex regulation mechanism. With the intention of analyzing BMP-2 target genes, it was also examined whether cGKI and TFII-I expression itself are regulated by the BMP-2 cascade. To explore this, C2C12 cells were stimulated with BMP-2 and the *cGKI* and *TFII-I* mRNA expression rate was determined (**Figure 4.52**).

Figure 4.52 Effect of BMP-2 signaling on the expression of *cGKI* and *TFII-I* in C2C12 cells. Starved (24 hrs) C2C12 cells were stimulated with 20 nM BMP-2 for 4 hrs or left untreated. Total mRNA was analyzed by RT-PCR for **(left)** endogenous *cGKI* expression using *cGKI*-specific primers (upper panel) and **(right)** endogenous *TFII-I* expression using *TFII-I*-specific primers (upper panel) *β-Actin* (lower panels) and *Id1* (middle panels) were used as a control. A representative result is shown (n=3), respectively.

The transcription of *cGKI* itself was induced upon BMP-2 stimulation (**Figure 4.52**, left) since addition of BMP-2 lead to a 2-fold upregulation of *cGKI* mRNA (upper panel). The concomitantly detected increase of *Id1* mRNA served as a control for BMP-2 stimulation (left, middle panel). The same result was observed for analyzing *TFII-I* mRNA (right, upper panel) which, as *cGKI* mRNA, was upregulated in the same time frame than *Id1* mRNA (right, middle panel).

Therefore, it is supposed that cGKI and TFII-I not only activate BMP signaling, but are also regulated by a BMP-2-induced feed-forward mechanism inside C2C12 cells.

4.8 Integration of cGKI in defective BMP signaling caused by a pulmonary hypertension mutant of BRII

Pulmonary arterial hypertension (PAH) is a vascular disease which is characterized by narrowing of the pulmonary artery caused by vasoconstriction and vascular remodeling through proliferation of vascular smooth muscle cells (VSMCs) and endothelial cells [568]. Genetic studies in PAH (familial and idiopathic) have revealed heterozygous germline mutations in BRII [13]. Intriguingly, NO, cGMP and cGMP-dependent kinases have been implicated in many physiological processes such as vasodilation. Mice deficient for cGKI show impaired NO/cGMP-dependent dilations of arteries, cardiac contractility and remodeling of VSMCs [657]. A multiplicity of studies describes an antiproliferative role of cGMP/cGKI pathway in VSMC differentiation when analyzing VSMCs in culture, although the overall mechanisms of VSMC growth and proliferation are discussed controversial [529].

4.8.1 Effect of cGKI expression on signaling arising from PAH BRII mutants

The fact that specific mutations in BRII cause PAH suggests that receptor-associated proteins might also play a critical role in PAH and related diseases [191, 261, 264, 269]. For instance, receptor for activated C-kinase 1 (Rack1) was reported to associate with BRII and to attenuate proliferation of SMC of pulmonary arteries [269].

In this study, the effect of cGKI on BMP signaling induced by the mutant MYC-BRII-LF-Q657ins16, a loss-of-function BRII-tail mutant found in patients with idiopathic PAH [215] was tested. Therefore, C2C12 cells were transiently transfected with the *BRE* reporter plasmid, cGKI variants, and wildtype BRII-LF or BRII-LF PAH mutant (**Figure 4.53**).

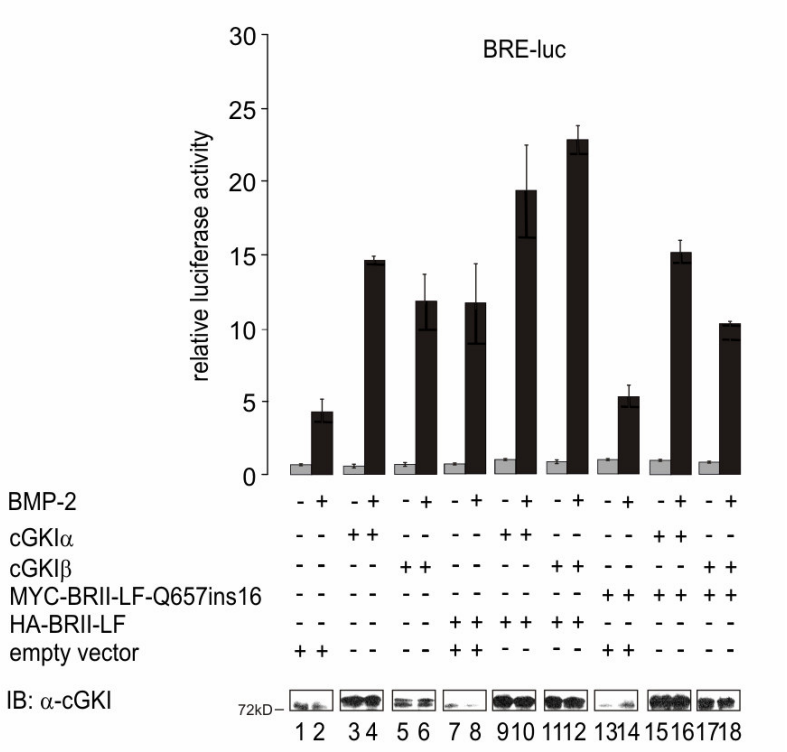

Figure 4.53 Effect of cGKI on the BMP-2-induced transcriptional activity triggered by a PAH BRII mutant using the *BRE*-luciferase reporter gene. C2C12 cells co-transfected with *BRE*-luc, RL-TK and the indicated constructs were starved for 5 hrs and stimulated with 1 nM BMP-2 for 24 hrs (black columns) or left unstimulated (grey columns). *BRE*-driven reporter gene activity was measured and error bars represent standard error of the mean. This result is representative for at least three independent experiments. The expression of cGKIα/β was checked after SDS-PAGE and α-cGKI immunoblotting of the samples. IB, immunoblot.

Interestingly, cGKIα and β isoform rescued the defective BMP signaling originating from the PAH BRII mutant (**Figure 4.53**). The PAH mutant was much less effective in inducing BMP signaling than wildtype BMPRII (black columns 2, 8 and 14). cGKI co-expressed with wildtype BMPRII further enhanced signaling (black columns 2, 8, 10 and 12). *BRE* activity was also upregulated in cells overexpressing both a cGKI variant and the PAH mutant (black columns 16 and 18) when compared to cells expressing the mutant alone (black column 14). Mutant-mediated aberrant BMP signaling was compensated by cGKI to the same degree as BMP signaling was increased on wildtype BRII and cGKI co-expression (black columns 2, 4, 6, 8, 16 and 18). This result suggests an important role for cGKI in stimulating BRII signaling and therefore in compensating the functional loss of BRII-tail caused by this frameshift mutation at position Q657.

Similar results were achieved by using other PAH mutants, MYC-BRII-LF-N764ins47 [542] and MYC-BRII-LF-A796ins7 [215] (**Figure 4.54**).

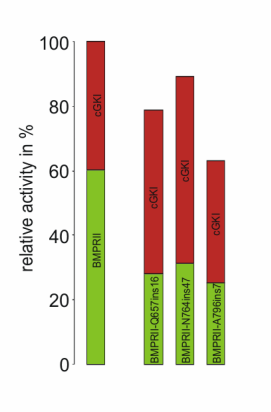

Figure 4.54 Summary of the activating effect of cGKI variant on signaling induced by different BRII PAH mutants. Graph shows the reporter gene activities upon BMPRII mutant and cGKI co-expression relative to the activity measured for wildtype BMPRII and cGKI. The protein effects were calculated separately in order to clarify their impact on the overall *BRE* reporter signal (BMPRII effect, green fraction; cGKI effect, red fraction).

Figure 4.54 demonstrates that these mutants, like BMPRII-Q657ins16, showed decreased signaling ability on the BRE reporter which could be rescued by cGKI co-expression. The graph shows the contribution of each overexpressed protein to the overall BRE reporter activity. cGKI equally and even stronger affects abberant mutant-mediated signal.

4.8.2 Effect of cGKI and PAH BRII mutants on the proliferation of VSMCs

As mentioned above, PAH is associated with vascular remodeling. Both BMP and cGMP/cGKI signaling pathways are implicated in the regulation of vascular smooth muscle cell phenotypes (VSMCs). Therefore, proliferation of human aortic smooth muscle cells in culture was studied under the influence of these pathways. First, VSMC proliferation triggered by PDGF was analyzed. PDGF is a well-known trigger for cell proliferation [529]. In a second experiment, VSMCs were transfected with either the PAH mutant MYC-BRII-LF-Q657ins16 or cGKI or both constructs. After inducing VSMC proliferation with PDGF, cell proliferation rates were measured (**Figure 4.55**).

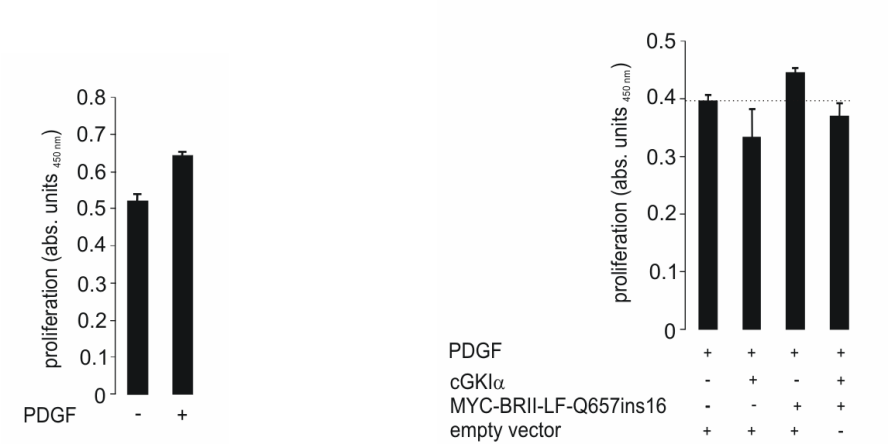

Figure 4.55 Proliferation study of VSMCs expressing a BRII PAH mutant and cGKI upon stimulation with PDGF. (Left) VSMCs were starved for 24 hrs and stimulated with 20 nM PDGF-BB for 24 hrs. Proliferation was measured using the CellTiter 96® AQ_{ueous} One Solution Cell Proliferation Assay according to manufacturer´s instructions. Error bars represent the standard error of the mean. This result is representative for three independent experiments. **(Right)** VSMCs were transfected with MYC-BRII-Q657ins16 or cGKIα or both. Cells were starved (24 hrs) and stimulated with 20 nM PDGF for 24 hrs. Proliferation was measured, and error bars represent the standard error of the mean. This result was reproduced in three independent experiments. abs., absorption.

Figure 4.55 demonstrates that PDGF induced proliferation of VSMCs compared to unstimulated cells (left). Since the induction was less than 1.3-fold in the performed experiments, starvation and stimulation conditions have to be optimized. Additionally, a comparable induction rate of cell proliferation was observed when the VSMCs were treated with serum, i.e. growth medium with 5 % smooth-muscle specific serum (SMGS) after 18 hrs serum starvation (data not shown). The PAH mutant promoted VSMC proliferation (right, lanes 1 and 3), whereas cGKI acted antiproliferative, albeit weak (lanes 1 and 2). Due to low transfection efficiency, the effects were moderate; nevertheless upon co-expression of both proteins, the proproliferative effect of BRII-LF-Q657ins16 was abolished (lanes 1, 3 and 4). The same result was observed using the BRII-LF-A796ins7 (data not shown). These data give the first hints towards a cooperation of cGKI and BRII-mediated signaling in hypertension disease.

To further examine VSMCs in regard to a cooperation of cGMP/cGKI and BMP-2 signaling, Smad phosphorylation and *BRE* reporter gene assays were performed in these cells. These initial studies revealed that the BMP reporter response is synergistically upregulated by co-stimulation with 8-Br-cGMP. Nevertheless, more studies have to be done, also in other VSMC systems, primary as well as cultured, to get a clear picture of a putative cooperation of cGMP/cGKI signaling and the BMP pathway in the vascular system.

Taken together, these results from chapter 4.8 demonstrate that cellular effects caused by PAH BRII mutants can be compensated through expression of cGKI. Therefore, it is proposed that cGKI can modulate signaling originating from defective PAH BRII mutant.

5 Discussion

Stringent control of BMP signaling is very important since this member of the TGFβ superfamily regulates proliferation, differentiation, apoptosis and chemotaxis of cells [833]. Dysfunctions of this pathway cause developmental disorders, fibrosis, vascular diseases and cancer [13]. The pathway is therefore controlled at multiple levels outside the cell, at the plasma membrane and inside the cell [12]. Two isoforms of the BMP type II receptor (BRII) arise from alternative splicing. BRII long form (BRII-LF) in contrast to the short form (BRII-SF) has an unique long cytoplasmic extension (BRII-tail) [75]. Several studies showed equal BMP signaling outputs for BRII-LF and BRII-SF [72, 195], however, specific cellular functions such as regulation of actin dynamics could be attributed to the C-terminal tail of BRII [191, 261, 266, 268]. Still, the importance of the BRII-tail for BMP signaling is unclear, particularly with regard to findings that mutations in BRII, also occuring in the tail, cause the rare autosomal disease pulmonary arterial hypertension (PAH) [13]. In a proteomics-based approach, diverse potential interactors of BRII were found [265]. Among these proteins not published previously was a cGMP-dependent protein kinase, cGKI. In the following, the single findings of the impact of cGKI on BRII, the Smads and on the final signaling output were discussed in detail. At the end, a current model summarizes the dynamic signaling regulation of the Smad pathway of BMP signaling via cGKI.

5.1 Interaction of cGKI with BMP receptors and cGKI-mediated modulation of the receptor complex

In this study it is shown that cGKI is a BRII-associated protein. The kinase was initially identified in a proteomics-based approach for potential interactors of the BMP type II receptor [265]. cGKI was found in BRII-tail protein complexes (Figure 4.1). Two isoforms of cGKI differing in their N-terminal domain exist [658] and the peptides identified by MALDI-TOF mass spectrometry did not allow a differentiation (Figure 4.2). Isoform specificity of an interaction is defined by the binding domain of the interaction partner in the cGKI protein. For instance, the protein IRAG binds

exclusively to the N-terminal domain of cGKIβ isoform [704-706]. On the other hand, the myosin binding subunit of the myosin phosphatase specifically binds cGKIα through the N-terminal leucine zipper [696]. Other proteins such as TRIM39R interact with the catalytical domain of cGKI and thus with both splice variants [723]. In this study it was found that both cGKIα and β interact with BRII-LF (Figure 4.3). Additionally, mapping of the BRII-LF interaction domain on cGKI showed that the receptor probably binds to the kinase domain of cGKI (aa 351-686 (in cGKIβ) or 336-671 (in cGKIα) respectively) (Figure 4.10). Thus, the interaction between cGKI and BRII is not specific for a cGKI isoform. Also the type II receptor exists in two alternative splice variant. BRII-SF ends a few amino acids after the kinase domain and comprises 538 aa. BRII-LF (1038 aa) has an additional exon, exon 12, which encodes for the long cytoplasmic extension, the tail. Mapping experiments of the cGKI binding site on the receptor revealed the following: cGKI binds to BRII when the kinase of BRII is presented, i.e. cGKI precipitated with BRII-SF and all longer truncations (TC4 to TC8) but not with BRII-TC1, which lacks the kinase domain (Figure 4.6). This was puzzling since cGKI was found in the initial pulldown to associate to BRII-tail. Only BRII-LF has the tail domain, while BRII-SF misses this large part C-terminal of the kinase domain. However, it was repeatedly observed that cGKI binds stronger to the recombinant BRII-tail or BRII-LF when compared to BRII-SF. Furthermore, *in vitro* binding studies revealed that cGKI directly binds to the C-terminal tail domain of the receptor (Figure 4.8 and Figure 4.9). As demonstrated, BMP type I and type II receptor complexes exist as homo- and heteromers at the cell surface [195, 219]. Thus, it is suggested that the observed association of cGKI and BRII-SF is indirect via complex formation of BRII-SF and endogenous BRII-LF, which exhibits the tail. Since this scenario of BRII-SF/BRII-LF complex formation can also be assumed for the BRII truncation mutants TC4 to TC8, the interaction domain of cGKI on BRII could not be further narrowed down than to the whole BRII-tail domain. For that purpose, *in vitro* binding with recombinant truncated BRII-tail variants and full length cGKI could be done. Remarkably, these mapping experiments hint towards another interesting finding: since it is suggested that BRII-SF indirectly binds to cGKI through dimerization with BRII-LF, the lack of binding of cGKI to BRII-TC1 supposes no dimerization of TC1 and BRII-LF. Thus, it is possible that the kinase domain of BRII is important for homodimerization of the receptors at the cell surface. Whereas the heterodimerization of BMP type I and type II could be mapped to the kinase

domain [195, 809], this point is of special interest as the homodimerization domain of BRII has not been defined yet.

As described, BMP receptors exist as homo- and heteromeric complexes at the cell surface [219]. Additionally, different oligimerization modes of the receptors were found to initiate different pathways. The preformed complexes (PFCs) reside preassembled in the membrane before ligand binding and activate the Smad pathway [195]. On the other hand, BMP-induced signaling complexes (BISCs) were formed by ligand-dependent recruitment of the type II receptor by the type I receptor; the BISCs mediate non-Smad signaling via the MAPK p38 [195]. Aside from the type II receptor, cGKI also interacts with type I receptors (Figure 4.18 and Figure 4.19). Since cGKI directly binds to BRII via the tail, it is assumed that this association is of indirect character via complex formation between type I and type II receptors. Tctex-1, for example, was also demonstrated to interact with the receptor complex consisting of type I and type II receptors [261]. Additionally, it can be stated that cGKI likely binds to preformed complexes since binding of cGKI to both BRII and BRI appears without ligand, i.e. it is ligand independent (Figure 4.15 and Figure 4.19).

Complex formation of TGFβ receptors is different. The TGFβ type II receptor (TβRII) binds TGFβ-1 with high affinity and recruits the TGFβ type I receptor (TβRI) into a signaling complex [3, 193]. Without ligand, both TβRII and TβRI are present at the cell surface as homodimers [220, 834]. Heterodimeric complex formation however, was strongly increased upon TGFβ-1 stimulation, while in the absence of ligand only a few complexes were observed [221]. The binding of cGKI to TGFβ receptors was also examined (data not shown). These studies appeared to be inconsistent. In 30% of the performed co-IP experiments cGKI interacts with TβRII or TβRI. However, in pulldown assays using the TβRII cytoplasmic domain as bait cGKI did no co-precipitate with this receptor. This hints towards a missing binding of cGKI to TGFβ receptors underscoring the specificity of BRII/cGKI association since the BRII-tail region is not found in TGFβ receptors [75]. Anyhow, interaction studies of cGKI and the TGFβ receptors upon stimulation with TGFβ should be done to draw a final conclusion.

One important step in BMP and TGFβ signaling is the activation of the type I receptor by the respective type II receptor. Upon ligand stimulation and binding of the type II receptor, the type I receptor exhibits two regions, which are predominantly phosphorylated by the type II receptor: the GS-box and a region upstream of the GS-

box [307, 835]. Thus activated type I receptor phosphorylates the R-Smads [193, 306]. It could be demonstrated for TβRII that besides transphosphorylating TβRI, TβRII undergoes autophosphorylation *in vitro* [193]. Until now these phosphorylation events have not been confirmed for BMP receptors. During this work it is shown that BRII-SF as well as BRII-LF indeed is autophosphorylated *in vitro* (Figure 4.12 and Figure 4.13). Furthermore, BRII-associated proteins such as Tctex1 are reported to be phosphorylated by BRII [261]. Inversely, the tyrosine kinase receptor c-kit shows dual kinase activity since it phosphorylates Ser757 in BRII and thus modulates BRII-mediated signaling [266]. Studying cGKI at the receptor complex, it was found that cGKI not only interacts with BRII-tail, but also specifically phosphorylates the tail domain of the receptor *in vitro* and *in vivo* (Figure 4.12, Figure 4.13 and Figure 4.14). This phosphorylation depends on a cGMP-triggered activation of cGKI (**Figure 5.1**).

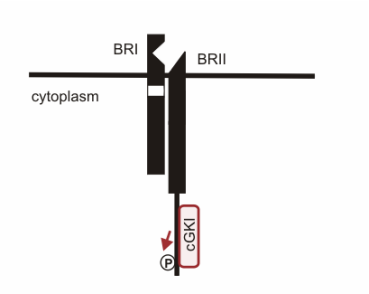

Figure 5.1 Phosphorylation of BRII-tail by cGKI. cGKI interacts with BRII and phosphorylates its tail region.

Database search (NetPhosK 1.0, with filter for evolutionary stable sites; http://www.cbs.dtu.dk/services/NetPhosK) supports this finding since there are two potential phosphorylation sites for cGMP-dependent kinases within BRII-tail, Ser680 and Ser765. These two sites were not analyzed in detail yet. Since cAMP-dependent kinase (PKA) and cGMP-dependent kinases (PKGs) belong to the AGC (PKA, PKG, PKC) kinase family and thus are structurally and functionally related [667], cGKI can also phosphorylate PKA phosphorylation sites as proven for the VASP protein [709]. The consensus sequence for PKA is -R-R/K-X-S/T-. The consensus sequence for cGKI is similar, -R/K_{2-3}-X-S/T-, but it often requires more basic residues in front of the serine or threonine [667]. BRII-tail harbors besides the two cGKI consensus sequences also nine potential PKA substrate sites. In an initial study, two of these putative PKA phosphorylation sites, Ser757 and Ser815 were already tested (data not shown). The serine-to-alanine mutants were checked for cGKI phosphorylation compared to wildtype BRII-LF. Both residues seemed not to be cGKI substrate sites.

It will be interesting to determine the specific phosphorylation site of cGKI in the tail region of BRII.

It is assumed that this cGKI-mediated BRII-tail phosphorylation induces a conformational change, which positively affects BRII transphosphorylation activity. When BMP ligand binds to the receptor complex, BRII is activated and can transphosphorylate BRI mainly at serines in the GS-box. Phosphorylated and thus activated BRI subsequently phosphorylates BMP R-Smads at their C-terminus [3]. Indeed, there is evidence for a regulation of serine phosphorylation on BRIa via cGKI; this phosphorylation on BRIa most likely reflects ligand-induced BRII-mediated transphosphorylation (Figure 4.31). Concomitantly, also Smad phosphorylation at the C-terminus is regulated (Figure 4.30, Figure 4.31 and Figure 4.32). Thus, the data suggest that cGKI modulates BRII activity and, as a consequence also BRIa and R-Smad activity. It is important to note in this aspect, that the phosphatase Dullard was previously reported to dephosphorylate BRIa after stimulation with BMP-4 [230]. Similarily, the phosphatase PP1C, recruited by the FYVE protein Endofin to BRI and the Smads, also dephosphorylates ligand-mediated phospho-BRIa [340]. In both reports, the authors claimed that this contributes to the inhibiting role of Dullard and Endofin/PP1, respectively, on Smad phosphorylation and thus Smad target gene activation.

In the last years, BRII became more important since several reports assigned regulatory functions to this receptor, especially to its unique tail domain [191, 261, 266]. Chan and co-workers recently showed that interaction of Trb3, a positive regulator of BMP signaling, with BRII-tail is disrupted by BMP-4 addition [268]. Consistent with this, c-kit interacts with BRII in the absence of ligand, whereas the interaction is increased when cells are treated with BMP-2, as demonstrated in an overexpression study [266]. These reports already suggest ligand-induced conformational changes within the BMP receptor complex. Similarily, it was found in this study that cGKI associates with BRII in unstimulated cells indicating that the interaction occurs independent from BMP and cGMP. In response to BMP-2, cGKI dissociates from BRII and thus from the activated receptor complex at the cell surface (Figure 4.15). **Figure 5.2** displays this dynamic conjunction:

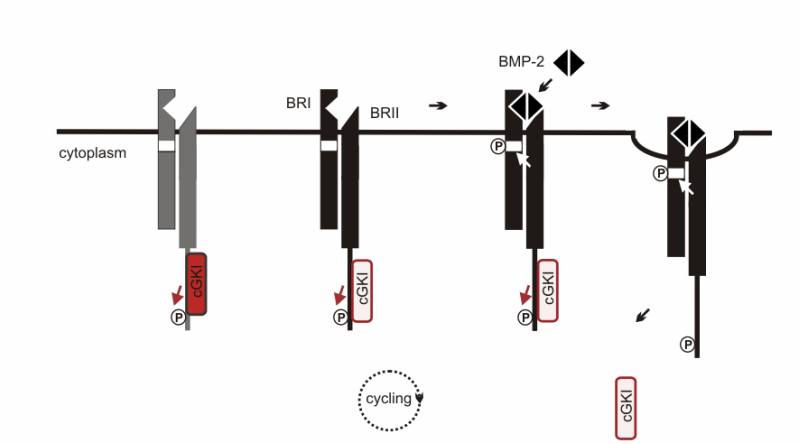

Figure 5.2 Dissociation of cGKI from BRII upon BMP-2 stimulation. It is suggested that cGKI and BRII interaction takes place in a distinct kinetic upon BMP-2 stimulation. When BMP-2 binds to the receptor complex (black), cGKI (light red) dissociates from the receptors within 5-10 min. The receptor complex is probably endocytozed upon BMP stimulation. The recurrence of the interaction might be explained by the interaction of newly synthesized receptors (grey) and cGKI (dark red) molecules at the cell membrane leading to the putative cycling process.

Moreover, it was observed that BMP-2 stimulation led to the release of cGKI from BRII with a distinct time kinetic. Within 60 min of BMP-2 stimulation, cGKI and BMP receptor molecules seem to pass through several interaction states: binding, release and recovery. This dynamic process can occur either through receptor complex activation and induced conformational changes after BMP-2 binding or endocytosis events of the BMP receptor complex or both. Endocytosis via CCPs was reported to be important for the release of activated Smads from the receptors at the cell surface to translocate into the nucleus [12]. It will be interesting to see whether receptor internalization plays a role in the regulation of cGKI and BMP receptors complexes. Initial analysis of BMP-2-activated BRII/cGKI complexes in regard of CCP-mediated endocytosis displayed an inconsistent picture. Inhibition of CCP-mediated endocytosis via chlorpromazine [836], did not give clear information about the need of endocytosis for the BMP-2-induced dissociation of cGKI from the receptor (data not shown).

5.2 Interaction of cGKI with Smad proteins and impact of cGKI on BMP/Smad signaling

TGFβ R-Smads proteins are presented by the FYVE domain protein SARA to the receptor complex to support C-terminal phosphorylation [342]. Upon TGFβ activation,

the receptor complex and R-Smads are endocytozed via SARA-enriched CCPs [225]. The clathrin pathway is also important for continuation of BMP/Smad signaling [227]. Phosphorylation at the C-terminal SSXS motif induces conformational changes within the BMP R-Smads leading to a stronger affinity for co-Smad4 and to the exposure of an NLS [3]. Moreover, it is assumed that the phosphorylated SSXS motif somehow competes with the phosphorylated GS-box at the type I receptor; this results in less binding affinity of the L45 loop in BRI, located near the GS-box, for R-Smad´s L3 loop [3]. Thus, ligand-activated R-Smad/co-Smad complexes translocate into the nucleus for target gene regulation.

An important finding in the study presented here is that cGKI dissociates from BRII upon BMP-2 stimulation (Figure 4.15). What is the destination point of the kinase? Subsequent immunofluorescence studies monitored the intracellular distribution of the kinase and could show that cGKI relocalizes from the cytoplasm to the nucleus in BMP-2-treated cells (Figure 4.16). The described BMP-2-induced nuclear translocation of cGKI represents a novel stimulus for subcellular distribution of cGKI, which is uncoupled from cGMP [672]. This opens new avenues for the function of this kinase. The well described cGMP-induced nuclear translocation of cGKI is mediated by an NLS inside the kinase domain and requires active transport [671]. Since the behaviour of the kinase upon BMP-2 treatment mirrors the ligand-induced shuttling route of R-Smads to the nucleus, it could be suspected that cGKI binds to the Smads while translocating into the nucleus. In several complementary approaches it was found that cGKI interacts with activated Smad complexes in the cytoplasm and in the nucleus in response to BMP-2 (Figure 4.20 - Figure 4.26). Since both, the association of cGKI with BRII and with Smads are regulated by BMP-2, it is suggested that cGKI sequentially binds first to the receptor complex, and after ligand addition to Smads. However, a portion of R-Smads and cGKI already interact in the absence of ligand (Figure 4.21 and Figure 4.25). Since cGKI also associated with BRII in unstimulated cells (Figure 4.15), it is possible that a fraction of R-Smads might already bind to the silent receptor complex at the plasma membrane.

A Smad interaction motif SIM was found in several transcription factors of the Mix and FAST family to be important for Smad binding. SIM is a proline-rich region of 25 aa with a conserved core -P-P-N-K-S/T-I/V- which binds to Smad´s MH2 domain, as demonstrated for Smad2 [837]. This sequence has very high similarity with the well established Smad binding domain (SBD), a proline-rich rigid coil region, in SARA

[343]. *In silico* sequence analysis revealed that a classical SIM, as described above, does not exist in cGKI. A newly identified Smad-interacting domain (SID, aa 1172-1282) in the protein Erbin was shown to specifically interact with the TGFβ Smads2 and 3 [369]. But also with this SID - which rather should be defined as a region than as a domain - the amino acid sequence of cGKI shares no similarity. Mapping of the Smad interaction site within cGKI revealed that the Smads most likely bind to the C-terminal part of cGKI, to the kinase region (aa 351-686 of cGKIβ or aa 335-671 of cGKIα respectively) (Figure 4.22). Thus, fine mapping of this Smad interaction site in cGKI might reveal further interesting insights. Up to now it is not clear which region of the Smad protein is necessary for interaction with cGKI. This is of special interest since cGKI binds to both, R-Smads and co-Smads. Smads can form homodimers, homotrimers or heterotrimers [309, 311, 314, 315, 838]. Oligomerization of Smads depends on phosphorylation of R-Smad at their C-terminus; the phosphorylated SSXS motif of one Smad molecule can bind to a basic binding pocket near the L3 loop of the adjacent Smad molecule [3]. Complex formation of R-/co-Smads is still discussed controversially, but the preferred model is the ligand-induced heteromer of two R-Smad molecules and one Smad4 molecules [2]. From the data presented here it is assumed that cGKI interacts first with R-Smad proteins, which after ligand application get phosphorylated and in contact with Smad4; thus, the R-Smad-bound Smad4 also interacts with cGKI within the activated Smad complex. But direct binding studies will gain more insight into these processes.

cGKI not only binds the activated R-Smads. Concomitantly with cGKI-mediated BRII-tail phosphorylation, it was found that the C-terminal phosphorylation of R-Smad1/5/8 is regulated by cGKI; overexpression of cGKI resulted in enhancement of Smad phosphorylation (Figure 4.32) and subsequently enhancement of Smad target gene expression (Figure 4.39). Analogous, the BMP-2-induced Smad phosphorylation is significantly decreased in C2C12 cells when cGKI is downregulated (Figure 4.30). Furthermore, complex formation of Smad1/Smad4 is reduced (Figure 4.37) and BMP-2-mediated Smad translocation to the nucleus is heavily disturbed in cGKI-knockdown cells (Figure 4.36). This alterations in Smad1 nuclear translocation upon cGKI silencing nicely reflects the behavior of C-terminally mutated Smad1 [306]. Loss of cGKI attenuates Smad C-terminal phosphorylation which downregulates Smad activation, Smad nuclear accumulation and transcriptional activation through Smads. As already described in chapter 5.1, it is

assumed that the cGKI-mediated BRII-tail phosphorylation induces an active BRII conformation leading to enhanced BRI activation and thus R-Smad phosphorylation. Consistent with this are data that an active kinase of cGKI is necessary to induce both BRII-tail phosphorylation (Figure 4.14) and C-terminal Smad phosphorylation (Figure 4.32). Additionally, the very C-terminal SSXS motif of Smad1 (-S^{456}-P-H-N-P-I-S-S*-V-S^{465}*) is improbably a direct cGKI phosphorylation site since cGKI belongs to the family of arginine-directed kinases (AGC kinase family) [667] Moreover, Smad1 does not show a cGKI-specific phosphorylation site according to database search (NetPhosK 1.0, with filter for evolutionary stable sites). However, cross phosphorylation of PKA sites through cGKI, which were found in Smad1, is possible. Therefore, it also a regulatory phosphorylation of BMP Smads by cGKI besides the SSXS motif can be considered.

It is plausible that the binding dynamics of cGKI and BRII or the Smads are controlled by conformational changes within either BRII or the R-Smads or both [3]. These changes can be caused by: (1) ligand binding to the receptor complex; it is known that ligand binding to the receptor complex activates the type II receptor which in turn transphosphorylates the type I receptor at the GS-box. (2) Phosphorylation of R-Smads at the C-terminal SSXS motif by the ligand-activated type I receptor; this induces binding of R-Smads to co-Smad4 which already suggests intramolecular rearrangements within the R-Smad molecules upon ligand stimulation. (3) Endocytosis of the ligand-activated receptor complex; as demonstrated, release of phosphorylated R-Smad1 from the activated receptor complex to accumulate in the nucleus and continuation of Smad signaling requires CCP-mediated endocytosis [227].

Several complementary assays in this work demonstrate that cGKI most likely migrates to the nucleus upon BMP-2 stimulation while bound to Smad complexes. The most crucial point underscoring this proposal is the BMP dependence of the event. cGKI has not yet been reported to be regulated by a ligand of the TGFβ superfamily. However, it was asked whether BMP-2 stimulation might regulate the cGMP level inside the cell; this could be invalidated. VASP phosphorylation on Ser239 does not occur upon BMP-2 stimulation, neither in a short-term (30 min) nor in a long-term measurement (3-5 hrs) (data not shown). Since this assay monitores cGKI activity, it indirectly indicates that BMP-2 does not affect the intracellular cGMP level. Therefore, the BMP-2-mediated regulation of cGKI´s subcellular distribution is

induced by BMP-2-sensitive molecules, such as Smads. This assumption is supported by Casteel et al who claimed that the cell-type-specific nuclear translocation of cGKI might depent on specific cGKI-anchoring proteins [673]. To analyze this in more detail, a cGKI mutant, cGKI-K407A/R409A, which is defective in cGMP-mediated nuclear translocation [671], was investigated. This mutant was created by introducing two mutations, K407A and R409A, into the putative NLS (-K^{404}-I-L-K-K-R-H-I^{411}-) inside the kinase domain of cGKIβ [671]. The NLS mutant is able to interact with BRII (data not shown) and to enhance Smad phosphorylation as wildtype cGKI (Figure 4.42). The latter is plausible since the mutant has an active kinase [671]. On the other hand this NLS mutant is inactive in enhancing the *BRE* reporter gene in contrast to wildtype cGKI (Figure 4.43). This suggests that the mutant still can promote Smad phosphorylation in the cytoplasm, but a proper localization of cGKI in the nucleus is required for its enhancing effect on BMP-dependent target gene transcription. Furthermore, since the mutant does not act dominant-negative on Smad signaling, it can be excluded that cGKI nuclear translocation is necessary for Smad translocation by itself and thus for propagation of signaling. Lastly, the analysis of this mutant again hints towards that cGKI relocalizes to the nucleus after stimulation with BMP-2 as a "backpack" of the R-Smads. But one question remains. Why shows the NLS mutant instead of reduced upregulation of reporter gene activity no effect on the final signaling output? The still occurring enhancement of Smad phosphorylation by the cGKI mutant should be reflected by increased *BRE* reporter activity.

The fine-tuning of these interaction dynamics of cGKI and the Smads is not established yet. Nuclear import of BMP R-Smads depends on several processes. As already mentioned, R-Smads need to be phosphorylated at the C-terminus by the activated BRI [306]. This induces conformational changes which lead to both the exposure of regions inside the R-Smads required for nuclear import and complex formation with co-Smad4 [3]. The FYVE domain protein Endofin not only acts positive on Smad activation through enhancement of phosphorylation at the SSXS motif, but also negatively regulates BMP signaling by facilitating dephosphorylation of BRIa through recruitment of the phosphatase PP1C [340]. Furthermore, phosphorylation of R-Smad1 in the linker region by the MAPK Erk2 at Ser187, Ser195, Ser206 and Ser214 inhibits Smad1 activation through recruitment of the Smad E3 ubiquitin ligase Smurf1 and subsequently ubiquitination and degradation of Smad1 [332]. Also

glycogen synthase kinase 3 (GSK-3) was shown to phosphorylate the Smad1 linker at Ser210 to target Smad1 for proteasomal degradation [333]. In this context, the BRII-associated phosphatase PP2A is shown to control R-Smad activation through acting as a R-Smad linker phosphatase (see chapter 7). The I-Smads 6 and 7 can recruit Smurfs for R-Smad and type I receptor ubiquitination [317, 375]. Moreover, Smurf1 binding to Smad1 interferes with nuclear accumulation of Smad1 since the interaction of Smad1 with the nucleoporin Nup214, which is essential for nuclear import [393, 399], is inhibited [306, 332]. Other proteins of the nuclear envelope, importin7 and 8 and its *Drosophila* ortholog Moleskin were recently shown to be important for the nuclear import of BMP Smads [396]. In the last years, the search for a Smad C-terminal phosphatases resulted in the discovery of several nuclear BMP Smad phosphatases such as PPM1A [335], small C-terminal domain phosphatases (SCPs) [337, 338] and pyruvate dehydrogenase phosphatase (PDP) [334], which attenuate BMP signaling by reduction of C-terminal Smad phosphorylation in the nucleus. It will be interesting to see how these factors may influence cGKI/Smad interaction as well as nuclear translocation of cGKI upon BMP treatment.

Entry of Smads into the nucleus is followed by binding of the signal transducers Smads to DNA to assemble a transcriptional complex at specific target gene sequences to regulate gene expression. All R-Smads except Smad2 as well as co-Smad4 bind to DNA in a sequence-specific manner. The β-hairpin in the MH1 domain of the Smad protein binds to the minimal sequence of 5'-G-T-C-T-3', the Smad binding element (SBE) [3]. At these sequences Smads cooperate with a multitude of transcription factors, which by themselves are further regulated by other signaling pathway. Components of such transcriptional complexes initiated by BMP Smads are for example Runx2 (Cbfa1) or OAZ. Additional co-factors as the CREB-binding protein (CBP) and the histone deacetylase (HDAC) p300 are recruited [2]. A well known target gene of BMP-activated Smads is *Id1* [806, 839]. Inhibitors of differentiation (Id) proteins act as cell growth stimulators by blocking other basic helix-loop-helix (bHLH) transcription factors such as MyoD family members [840]. In this study it could be demonstrated that cGKI binds with Smad1 to the promoter of *Id1* using ChIP analysis (**Figure 5.3**).

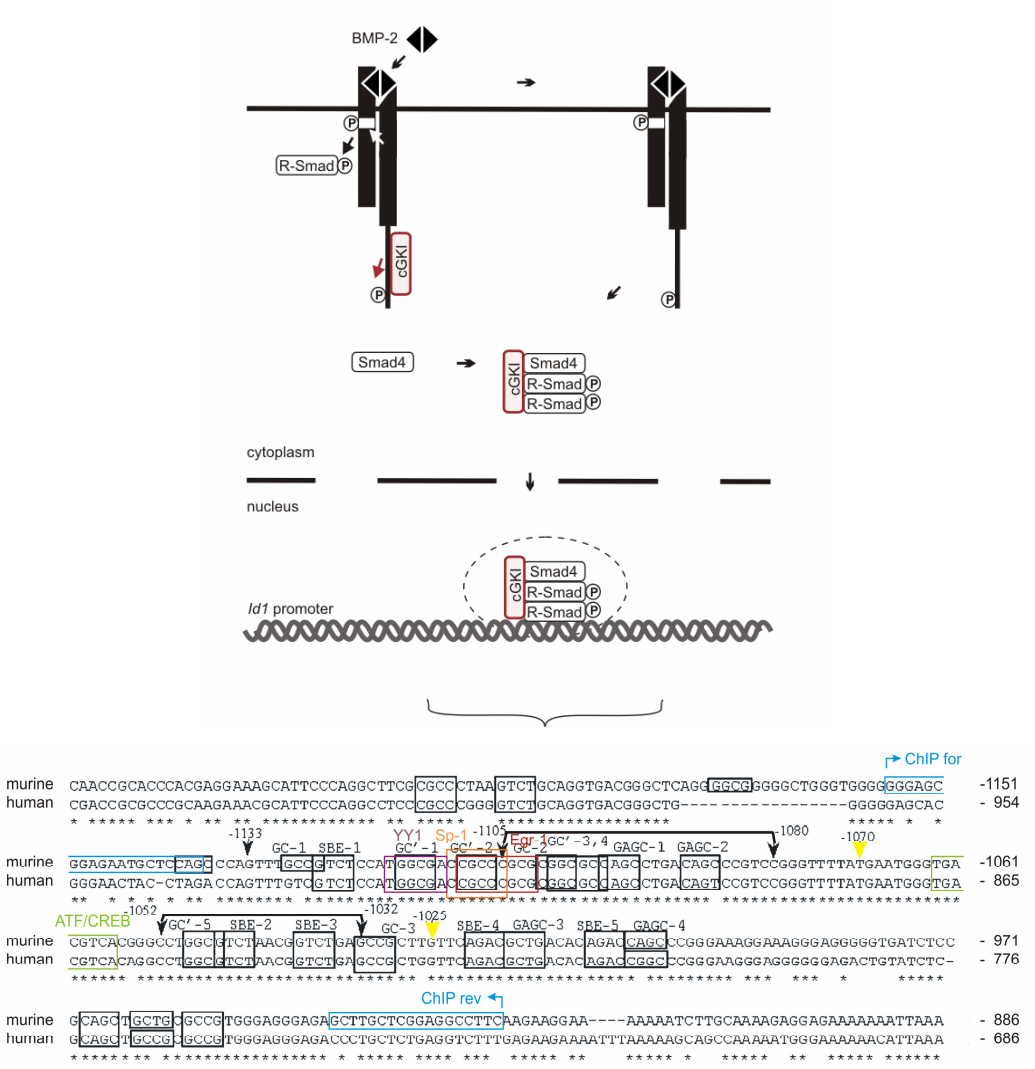

Figure 5.3 Redistribution of cGKI/Smad complexes to the nucleus and binding of cGKI and Smad1 to the promoter region of the BMP target gene *Id1* after BMP-2 stimulation. The analyzed sequence within the *Id1* promoter is magnified in the picture below with sequences for the murine and the human *Id1* promoter aligned. The drawing was adapted from [806]. Distinct regions in the promoter are coloured (oligonucleotides for ChIP analysis (blue), YY1 binding site (margenta), Sp-1 binding site (orange), Egr-1 binding site (red), R-Smad/Smad4 binding site (defined with yellow arrowheads) and ATF/CREB binding site (green)).

This finding is very interesting since it is the first example for a cGMP-dependent kinase to be recruited to a specific DNA sequence in a ligand-dependent manner. Furthermore, it suggests a regulatory role for cGKI in gene transactivation induced by BMP-2. Indeed, several complementary approaches demonstrated that cGKI enhances Smad-dependent transcription of the *Id1* target gene. The *Id1* promoter region is well established. Korchynskyi and ten Dijke showed that a distinct fragment of the murine *Id1* promoter, -1070/-1025 (**Figure 5.3**, lower scheme, defined with yellow arrow heads), binds transcriptional complexes upon BMP-6 stimulation, which

very likely contain Smad5 and Smad4 [806]. This sequence lies inside the amplified and thus examined region of the ChIP analysis (**Figure 5.3**, lower scheme, oligonucleotide sequences, blue coloured). Furthermore, the region -985/-957 inside the human *Id1* promoter was identified as Smad1 and Smad4 binding region [841]. Moreover, Smad1 or Smad4, alone or complexed, were able to bind to the region -985/-863 of the human *Id1* promoter [403]. Due to these reports, it is very likely that Smad1 within the cGKI/Smad complex binds directly to the tested *Id1* promoter site. Analysis whether cGKI also directly binds to *Id1* promoter sequences should be done, although, considering all the data presented here and the literature, it is not assumed that cGKI gets directly in contact with the DNA. Furthermore, co-Smad4 might also be a part of the found cGKI/Smad1 complex at the *Id1* promoter although binding studies of cGKI and Smad4 in the nucleus revealed contrary results (data not shown).

cGKI, as assumed, is involved in regulating gene transcription, but was until now not shown to bind to DNA when relocalized to the nucleus. Frequently, transcription factors as FoxO1a [842] and TFII-I [673] are controlled by the kinase. Regulation of the transcription factor cAMP response element binding protein CREB by cGKI is another illustrative example. CREB is phosphorylated by cGKI on Ser133. This CREB phosphorylation as well as nuclear accumulation of cGKI is required for CREB-mediated induction of the *c-fos* promoter upon NO stimulation [671]. Interestingly, CREB interference with the Smad pathway is reported. The Smad3/co-Smad4/CBP/p300 transcripional response can be inhibited through competition of CREB for CBP/p300 after CREB phosphorylation on Ser133 [843]. Furthermore, it was demonstrated that the interactions of Smad3 with the transcription co-activators CBP/p300 is abolished in a PKA- and CREB-dependent manner [844]. Another factor belonging to the ATF/CREB family of transcription factors, ATF-2 was shown to act cooperatively with Smad1/co-Smad4 on cardiac-specific genes [427]. This finding is very interesting since also a ATF/CREB consensus site was identified inside the promoter region of the *Id1* gene [403] (**Figure 5.3**, lower scheme, ATF/CREB site, green coloured). Whether there is also a crosstalk on *Id1* transcription via cGKI-mediated regulation of CREB or ATF-2 is still unexplored. The main focus in this study, however, was set on another cGKI-modulated transcription factor, TFII-I; these results are addressed in detail in chapter 5.3.

At this point, another interesting finding will be discussed. cGMP is the natural ligand for cGKI. In its inactive state, the N-terminal pseudo-substrate site blocks the kinase domain of cGKI. When cGMP gets in contact with the two cGMP-binding sites, conformational changes within the protein are induced and lead to the release of the pseudo-substrate site; now, the kinase domain can phosphorylate its substrates [664, 669, 845, 846]. In this study it was found that on the one hand cGMP activation is necessary for cGKI to phosphorylate BRII-tail *in vitro* (Figure 4.12). On the other hand, several complementary approaches showed that cGMP stimulation does neither alter Smad phosphorylation (Figure 4.33) nor Smad target gene expression (Figure 4.41) suggesting that cGKI kinase activity is not necessary for Smad activation. But, cGKI action on Smad phosphorylation does depend on an active kinase since cGKIβ-D516A, a kinase-deficient mutant, can not enhance Smad phosphorylation (Figure 4.32) and Smad target gene activation (Figure 4.39) as the wildtype. The cGMP dependency occurs when the kinase is examined *in vitro* suggesting that the kinase in the *in vivo* situation has a higher basal activity. Furthermore, it hints towards that the physiological conditions do influence cGKI activity. Thus, it can be assumed that cGKI in BMP signaling already has an active conformation while bound to the Smad complex. More puzzling in this aspect is the finding that cGMP stimulation results in a synergistical upregulation of endogenous *Id1* when co-stimulated with BMP-2 (Figure 4.41). This is in contrast to the cGMP independence of the *BRE*-luc reporter (Figure 4.41); therefore, the cGMP/cGKI pathway influences the artificial BMP reporter, controlled by a minimal promoter cloned from the *Id1* gene, and the endogenous *Id1* promoter differently. This furthermore suggests that besides the Smad-bound cGKI fraction, which does not need its ligand cGMP for stimulating Smad phosphorylation, there is a second pool of cGKI in the cytoplasm of C2C12 cells, which upon stimulation with 8-Br-cGMP gets activated. This was nicely shown by induction of VASP phosphorylation on Ser239 upon stimualtion with cGMP (Figure 4.33). Another explanation for this might be the following: it was reported by others that activation of cGMP/cGKI pathway increases the expression of the transcription factor early growth response factor 1 (Egr-1) and Egr-1-dependent gene response in neuronal cells [672]. The endogenous *Id1* promoter contains an Egr-1 binding site and expression of *Id1* mRNA is enhanced by Egr-1 [847]. The *BRE* reporter lacks the Egr-1 site [806], which may account for the discrepancy in the studies with the endogenous *Id1* promoter *versus* the *BRE* minimal promoter. However, a comparative study of the

BRE-luc reporter (minimal promoter) and the *Id1*-luc reporter (full promoter) upon cGMP application did not reveal a difference between the reporter gene responses (data not shown); both activities were not affected by cGMP which is contradictory to this Egr-1 theory. Finally, chromatin assembly present at the endogenous *Id1* gene but absent in the artificial reporter might cause the observed differences seen by stimulating cells with 8-Br-cGMP.

R-Smads rapidly get dephosphorylated in the nucleus by putative nuclear phosphatases. TGFβ R-Smads re-shuttle into the cytoplasm after dephosphorylation. News about these phosphatases were recently published. The nuclear phosphatases SCP1, 2 and 3 and PPM1A were shown to dephosphorylate BMP and TGFβ R-Smads C-terminally which attenuated signaling [334-336, 339]. Furthermore, the inner nuclear membrane protein MAN1 is suggested to sequester R-Smads for dephosphorylation [346, 347, 349]. In this work it is explored that Smad1 and Smad4 together with cGKI translocate into the nucleus within 15-30 min. After 60 min, however, the proteins start to redistribute into the cytoplasm again (Figure 4.26). This in general hints towards that the overall BMP signal slowly runs out after 1 hrs of BMP-2 stimulation. As known for TGFβ Smads, the Smad molecule passes through several cycling steps: phosphorylation and activation through the type I receptor in the cytoplasm, nuclear translocation and binding to DNA and lastly, dephosphorylation and export from the nucleus to see the receptors again for *de novo* phosphorylation [1]. Up to now it is not clear what happens with the cGKI/Smad complex after dissociation from the *Id1* promoter and what is the trigger for this event, respectively. According to the presented data, cGKI generally has a lower affinity for the unphosphorylated Smad (Figure 4.21 and Figure 4.25) suggesting that dephosphorylation of R-Smads breaks the complex. Dephosphorylated R-Smad and cGKI are supposed to leave the nucleus separately.

The TGFβ superfamily ligands BMP and TGFβ often counteract their cellular responses, for instance in the regulation of epithelial-to-mesenchymal transition (EMT) in the adult kidney [848]. Furthermore, in C2C12 cells both TGFβ-1 and BMP-2 inhibit myogenesis, but TGFβ-1 effectively suppresses the osteogenic effect of BMP-2 [210]. As described before, the binding of cGKI to TGFβ receptors is rather unlikely. However, both overexpression of cGKI wildtype alone or co-expression with the TGFβ type II receptor resulted in attenuation of TGFβ-1 signaling tested on a Smad3 responsive reporter gene ([808]; see 3.3.6.2). What is the mechanism behind

the cGKI-mediated inhibition of TGFβ signaling? It is assumed that cGKI in BMP signaling competes for factors which are utilized by both signaling pathways; co-Smad4 can be one candidate. cGKI knockdown strongly inhibits C-terminal Smad phosphorylation (Figure 4.30) and consequently, complex formation of Smad1 and Smad4 (Figure 4.37). Since cGKI increases Smad phosphorylation at the C-terminus (Figure 4.32), it is very likely that overexpression of the kinase promotes complex formation of Smad4 with Smad1. Then, cGKI expression would inhibit TGFβ signaling since Smad4 is stronger recruited by BMP Smads due to enhanced phosphorylation of these molecules at the SSXS motif. Another possibility is the cGKI-triggered competition for shared nuclear transcription factors. For instance, Smad3/Smad4/CBP/p300 complexes are inhibited by competition of CREB for CBP/p300 after CREB phosphorylation at Ser133 [843]; this serine is a substrate site for cGKI [738].

Also interesting is that the positive stimulator for BMP signaling, cGKI, itself is induced by BMP-2. BMP-2 target gene analysis revealed that *cGKI* mRNA is upregulated in C2C12 cells when stimulated with BMP-2 (Figure 4.52), suggesting a feed-forward mechanism. *In silico* analysis revealed that there are several minimal sequences for Smad binding (SBEs) inside the cGKI promoter which require further investigation. Furthermore, binding sites for the zinc finger transcription factor Sp-1 were found in the *cGKI* promoter region [672]; these sites are important for basal *cgk1* promoter activity. The Smad-dependent *Id1* promoter also harbors such a Sp-1 binding site (**Figure 5.3**, lower picture, Sp-1 binding site, orange coloured). Furthermore, Sp-1 cooperates with Smad2 and 4 on the activation of TGFβ target genes as p15, p21 Smad7 and PAI [2]. Therefore, it is possible that the BMP-2-induced induction of *cGKI* mRNA might occur through the putative SBEs or the cooperation between Sp-1 and BMP Smads on the *cGKI* promoter.

5.3 Evidence for cGKI/TFII-I cooperation in BMP-2-induced Smad pathway

cGKI is a known regulator of transcription factors [672]. For instance, Casteel and co-workers demonstrated an interaction of cGKIβ with TFII-I. TFII-I is a general transcription factor which commonly binds initiator (Inr) elements and regulatory elements of promoters, mainly TATA-box less promoters [740]. The transcription

factor has a unique character since it functions both as a basal transcription factor at the core promoter and as an activator for transcription at upstream regulatory sites. Both serine and tyrosine phosphoryation is necessary for transcriptional activation [740]. TFII-I is associated with the Bruton´s tyrosine kinase (BTK) in B cells. BTK is required for normal B cell development and mutations within this kinase cause X-linked immunodeficiency in mice and X-linked agammaglobulinemia in humans. Expression of wildtype BTK increased the TFII-I-mediated transcriptional activation and its tyrosine phosphorylation [849]. Furthermore, TFII-I undergoes a c-Src-dependent tyrosine phosphorylation on Tyr248 and 611 and migrates to the nucleus in response to growth factor signaling. Tyrosine-phosphorylated nuclear TFII-I activates *c-fos* gene transcription [850]. The *c-fos* promoter is a well studied one. TFII-I is known to regulate this gene through affecting regulatory sites upstream of its TATA-box [851]. The following drawing illustrates the action of TFII-I inside the cell (**Figure 5.4**):

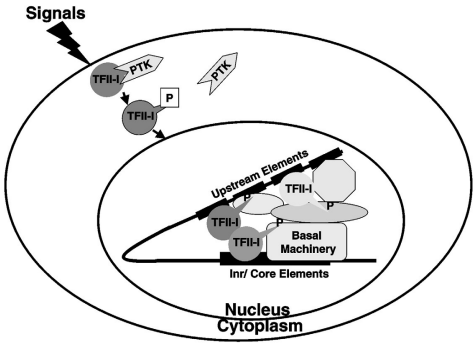

Figure 5.4 Scheme of TFII-I action in a resting cell [740]. TFII-I remains sequestered in the cytoplasm with a non-receptor protein tyrosine kinase (PTK, e.g. BTK or c-Src). In response to extracellular signals (e.g. growth factor stimulation), TFII-I is Tyr-phosphorylated and is released from the cytoplasmic kinase. Subsequently, Tyr-phosphorylated TFII-I translocates to the nucleus to activate gene transcription.

TFII-I has four spliced isoforms, α, β, γ and Δ. Only the β and Δ isoform are expressed in murine fibroblasts [852]. The subcellular localization of TFII-I is regulated by its isoform-specific conformation as well as serum starvation and growth factor stimulation, respectively. Upon serum starvation, TFII-Iβ is nuclear, whereas growth factor stimulation led to export of TFII-Iβ into the cytoplasm. For TFII-IΔ it is different: in resting cells, TFII-IΔ is mainly cytoplasmic; however, growth factor signaling induces nuclear re-localization of the factor [832]. In the cell system studied

here, the murine C2C12 cells, TFII-I is predominantly localized in the nucleus, independently of serum starvation and growth factor, i.e. BMP-2 stimulation, as demonstrated by immunofluorescence using an α-pan-TFII-I antibody (Figure 4.48).

The serines 371 and 743 in TFII-IΔ are phosphorylated by cGKIβ and are required for the induction of *c-fos* promoter response [673]. Recently published data described both serines to be phosphorylated after TGFβ-1 stimulation. Moreover, both residues are important for Smad3/TFII-I complex formation and TGFβ-1-dependent reporter gene response [831]. TFII-I also regulates TGFβ-mediated induction of the *gooesecoid* (*gsc*) gene in P19 cells by interacting with Smad2 and by recruitment to the *gsc* promoter after stimulation with TGFβ [830]. It is shown in this work that after activation of BMP signaling TFII-I and cGKI co-localize with Smad1 at the same *Id1* promoter site, suggesting that these proteins form a ternary complex there (**Figure 5.5**):

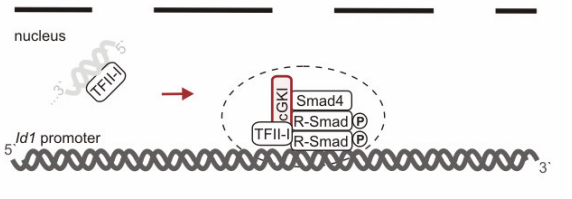

Figure 5.5 BMP-induced complex formation of activated Smads, cGKI and TFII-I at the *Id1* promoter. It is proposed that TFII-I, bound to upstream regulatory sequences, is recruited and/or regulated within the transcriptional Smad complex by cGKI.

The promoter of the murine *Id1* gene has a TATA-box (-T-A-T-A-A-A-A-) at position -119 upstream of the ATG (Ensemble genome browser, http://www.ensembl.org/index.html). Usually, TFII-I regulates TATA-box-less promoters [740]. However, it is reported that the long terminal repeat (LTR) promoter of the Rous sarcoma virus is regulated by TFII-I [853]. The LTR promoter contains a TATA-box and Inr-like sequence which is the transcription start site core. It could be demonstrated that the transcription factors TFII-I and YY1 not only bind to this site, but that both factors are required for efficient transcription of the LTR of the Rous sarcoma virus. An interesting side aspect is that the transcription factor YY1 was shown to interact with Smad1 and Smad4 and to participate in the control of BMP target genes [422, 423]. The finding that TFII-I together with cGKI and Smads binds to the *Id1* promoter suggests that TFII-I participate in the regulation of *Id1*

transcriptional activity. Indeed, it was found that TFII-I modulates BMP signaling; ectopic expression of TFII-I increases the *BRE*-luc reporter response (Figure 4.50 and Figure 4.51). But is TFII-I also regulated within the Smad transcriptional complex? Initial studies established that a cGKI mutant defective in nuclear translocation still promotes Smad phosphorylation but failed to activate Smad transcriptional response (see chapter 5.2, Figure 4.42 and Figure 4.43). This proposes that a proper nuclear redistribution of cGKI is necessary to induce target gene transcription. Interestingly, a cooperation between wildtype cGKI and TFII-I is cumulative on BMP signaling modestly increasing BMP target gene activation, whereas this cGKI NLS mutant significantly represses the activating effect of TFII-I (Figure 4.51). This points towards that the presence of TFII-I in the nucleus is not sufficient to induce Smad signaling; it is necessary that cGKI redistributes to the nucleus upon BMP-2 stimulation enabling TFII-I to affect Smad target gene activation. This pivotal finding proves that cGKI has besides its cytoplasmic function also a nuclear role in BMP signaling which involves TFII-I. cGKI not only modulates BMP receptors and Smad activity in the cytoplasm, but also translocates with the Smads into the nucleus to support transcriptional activation of Smad target genes through cooperation with the transcription factor TFII-I.

The detailed mechanism behind this cooperation is not known yet. TFII-I comprises six I-repeats and each repeat has a potential protein-protein interaction surface due to a putative helix-loop-helix (HLH) motif [740, 854]. TFII-I isoforms are able to form homo- and heterodimers. The N-terminal region including a leucine zipper motif as well as the I-repeats are required for TFII-I dimerization and are thus important for protein-protein interaction [855]. **Figure 5.6** illustrates the structure of TFII-I:

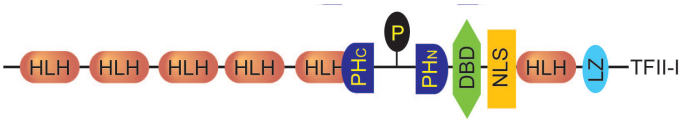

Figure 5.6 Scheme of the structure of TFII-I [854]. HLH, helix-loop-helix motif domain (= I-repeats); PH, pleckstrin homology domain; DBD, DNA-binding domain; NLS, nuclear localization sequence; LZ, leucine zipper motif.

Considering this, it is likely that TFII-I has scaffold function for cGKI and thus for the Smads at promoter sites of BMP target genes. Within the TFII-I protein, the N-terminus and a site near the NLS are important for DNA binding [855]. Hence, DNA

linking of the transcriptional complex assembled by Smads might be strengthened by recruitment of TFII-I which subsequently by itself binds to DNA. Whether TFII-I is regulated by cGKI within the Smad transcription complex needs to be further investigated. Evidence for this is already given, since it was found that TFII-I, co-precipitating with Smad1 and Smad4, reveals higher molecular weight bands suggesting a protein modification in TFII-I protein (Figure 4.46). Although TFII-I co-precipitated with cGKI did not exhibit this modification, it still fits into the model: due to the studies examining the cGMP effect on BMP signaling it is assumed that cGKI is in its active form when bound to the Smads. Thus, a TFII-I modification through phosphorylation would only occur inside a TFII-I/Smad/cGKI complex, and not inside a TFII-I/cGKI complex. Still, other modifications as acetylation or sumoylation of TFII-I must be considered which only take place when TFII-I is complexed with Smads.

In sum, these data indicate that TFII-I is recruited by cGKI to the Smad transcription complex and/or is regulated by the kinase within this complex to activate gene transcription.

5.4 The impact of cGKI in the non-Smad pathway

Non-Smad signaling initiated by the BMP ligand can occur via several alternative pathways. Upon BMP stimulation, several phosphorylation events can be observed. While the p38-MAPK pathway probably is the most examined one [467], other intracellular messenger molecules such as ERK [470], PI3K/Akt [481] and JNK [475] are described to be activated by BMP. Still, all these pathways are under extensive investigation. In 2002, Nohe and co-workers demonstrated that different oligomerization modes of BMP type I and type II receptors induce two divergent routes of BMP signaling. The preformed complex (PFC) resides preassembled in the plasma membrane and triggers the Smad pathway, whereas in the BMP-induced signaling complex (BISC) BRI recruits BRII after ligand binding and the non-Smad pathway via the MAPK p38 is initiated [195]. The p38 pathway is involved in ALP signaling [476] and was assumed to be Smad-independent [195]. However, Hartung et al. could show that BMP-mediated Smad signaling is also needed for ALP induction [227]. As an osteogenetic marker, ALP is still discussed controversially since little is known about the detailed activation mechanism. Since it is a long-term read-out (72 hrs), it is difficult to isolate single factors which influence ALP

expression. However, other osteoblastic target genes of p38 signaling which are induced by BMP-2, are type I collagen, fibronectin, osteocalcin and osteopontin [476]. Interestingly, cGMP/cGKI signaling has been implicated in the regulation of p38. In T-lymphocytes and neutrophils cGMP stimulation increases p38 phosphorylation [681] [856]. Also in HEK/293 and Cos7 cells, p38 undergoes phosphorylation when treated with cGMP [730]. In both cases this effect was additionally enhanced by expression of cGKI. In cardiomyocytes different effects were observed: on the one hand it is reported that in adult cardiomyocytes, p38 phosphorylation is enhanced upon cGMP stimulation [731]. On the other hand p38 activation and p38-induced apoptosis of these cells is inhibited by the interaction with cGKIα and cGMP-triggered activation of the kinase [732]. In this work, neither an effect of cGKI overexpression nor a cGMP effect on the BMP-2-induced p38 phosphorylation were observed (Figure 4.44). Furthermore, the induction and activation of the BMP target gene *ALP* is not significantly affected by cGKI or cGMP stimulation (Figure 4.45). Both was observed in the myoblastic C2C12 cells which still can differentiate into myotubes and, upon BMP-2 treatment, into osteoblasts [210]. However, in rat and murine osteoblasts *ALP* mRNA expression was upregulated by cGMP [857, 858]. In these cells a similar effect on *osteocalcin* mRNA was detected [857, 858]. Also *collagen type I* mRNA expression was cGMP-dependently increased in murine osteoblasts [857]. This implies that the myoblastic C2C12 cell system reacts different on cGMP/cGKI signaling than differentiated osteoblasts. Notably in this aspect, the cGMP/cGKI pathway can induce the BMP target gene *Id1*, which is a known inhibitor for myogenetic differentiation marker such as MyoD family members [840]. Thus, in C2C12 cells cGMP/cGKI signaling more likely inhibits myogenesis than induces osteogenesis. In this context, the finding that the transcription factor FoxO1a is a substrate for cGKIα is of special interest. cGKIα negatively regulates FoxO1a by abolishing its ability to bind DNA which leads to reduced myoblast cell fusion of C2C12 cells, and thus inhibition of myogenesis [842]. In view of both the data presented in this work and data indicating that cGMP analogues can regulate proliferation and differentiation of osteoblastic cells [672], C2C12 cells become an interesting model system to study cGKI-regulated osteogenic *versus* myogenic differentiation.

However, apart from MAPK p38, the BMP-2-mediated induction of fibronectin or osteopontin via the MAPK ERK might be affected through cGKI since the

cGMP/cGKI pathway can also modulate ERK signaling. This modulation was not reported in osteoblasts or other bone-related cells, but in a variety of other cells. For instance, in endothelial cells, fibroblasts and cardiomyocytes, the ERK-MAPK was positively influenced by cGMP stimulation [672]. Thus, it will be very interesting to investigate non-Smad BMP signaling and cGMP/cGKI signaling on C2C12 cells as well as differentiated osteoblasts.

In sum, these results indicate that the BMP pathway in C2C12 cells via ligand-dependent BISCs initiating p38 signaling is not affected by cGMP/cGKI action.

5.5 Integration of cGMP/cGKI signaling into pulmonary arterial hypertension caused by BRII mutants

Pulmonary arterial hypertension (PAH) is characterized by thickening of pulmonary arteries due to abnormal proliferation and apoptosis of cells and remodeling of the small arteries. Accompanied with vasoconstriction, PAH patients suffer from elevated pressure in the pulmonary artery and from heart failure [568]. PAH (idiopathic and familial) has been shown to be associated with heterozygous germline mutations in BRII [13]. Still the cause of the pathogenicity of these mutated receptors is unclear. It is known from several reports that BMP-mediated Smad signaling as well as non-Smad signaling via MAPK p38 is affected by PAH-related mutations in BRII [231]. Smooth muscle-specific expression of mutant BRII in transgenic mice results in increased medial thickness of pulmonary arteries and increased muscularization of small pulmonary arteries. This suggests that loss of BRII function in smooth muscle cells is sufficient to cause a PAH phenotype [539]. Crosstalk to other signaling pathways increases the complexity of the BMP signaling system, and thus, BRII-mediated crosstalk mechanisms are assumed to influence pulmonary hypertension diseases [191, 261, 264, 268, 269, 539].

The here reported modulator of BMP signaling, cGKI, is itself a key regulator of vasodilation [657]. Furthermore, the PDE5 inhibitor Sildenafil is a known treatment of PAH. It supports pulmonary vasodilation through increasing the intracellular cGMP level [794, 859]. cGMP/cGKI signaling in VSMC is an extensively examined issue which is very complex and still discussed controversially. Signaling via cGMP/cGKI in these cells not only regulates intracellular messenger molecules such as MAPKs (ERK, p38 or JNK), but also controls several transcription factors either by direct

modulation through phosphorylation as reported for CREB, or by transcriptional regulation of genes such as the *c-fos* gene [672]. Furthermore, cGMP stimulation affects the transcriptional activity of genes involved in cGMP signaling as cGKs, genes involved in controlling cell proliferation as p21 and genes associated with VSMC differentiation and function as smooth muscle α-actin [672].

During this study, experiments in C2C12 cells and VSMCs demonstrated that cGMP synergistically upregulates the BMP-2-induced transcription of *Id1* mRNA (Figure 4.41) or the *BRE* reporter (data not shown), respectively. Using reporter gene assays in C2C12 cells, it was found that the presence of cGKI can rescue the loss of signaling capacity, i.e. transcriptional activation, of the PAH mutant receptors BRII-LF-Q657ins16 [215], BRII-LF-N764ins47 [261] and BRII-LF-A796ins7 [215] (Figure 4.53 and Figure 4.54). That means that the presence of cGKI restores normal BMP signaling although BRII is defective due to PAH-specific mutations. Since familiar and idiopathic PAH caused by mutant BRII receptors severely affects proliferation of VSMCs and endothelial cells of the pulmonary artery, the data presented here point to a cooperation of BRII and cGKI signaling in vascular diseases. Indeed, initial studies revealed that cGKI expression can compensate enhanced proliferation of VSMCs caused by the expression of the BRII mutant BRII-LF-Q657ins16 (Figure 4.55). What is the mechanism behind this compensating effect (**Figure 5.7**)?

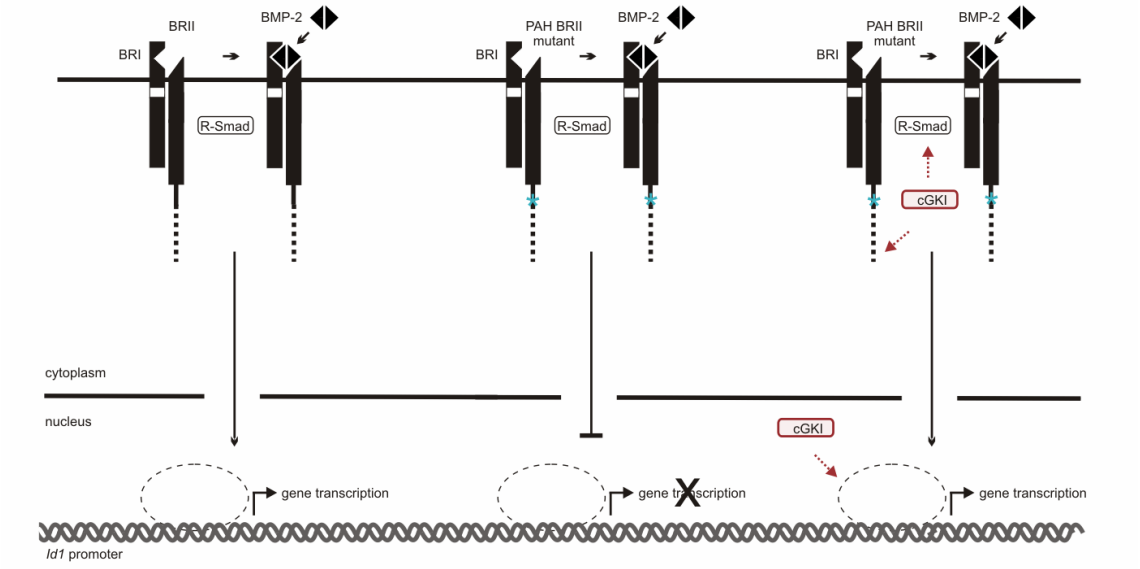

Figure 5.7 Possible effects of cGKI on BMP signaling caused by PAH BRII mutants. PAH BRII mutants inhibit BMP/Smad signaling in C2C12 cells. The presence of cGKI restores deficient BMP signaling caused by these mutants. The blue asterisk marks the PAH mutation in BRII, the red arrows depict the potential regulatory targets of cGKI inside defective BMP signaling caused by PAH BRII receptors.

Due to complementary assays shown in this thesis, it is probably that cGKI regulates Smad phosphorylation as a consequence of receptor complex modulation after cGKI-mediated BRII-tail phosphorylation. As discussed in chapter 5.1, *in silico* analysis yielded two potential phosphorylation sites for cGMP-dependent kinases within BRII-tail, Ser680 and Ser765. Both sites are lost in the three PAH mutant receptors. This is contrary to the proposed model. However, since the definite phosphorylation site of cGKI inside BRII-tail is not known yet, also PKA phosphorylation sites within BRII-tail upstream of the mutations must be considered. Furthermore, the compensating effect of cGKI on Smad-dependent transcription might derive from facilitating BMP gene transcription in cooperation with the Smads and TFII-I. Moreover, cGMP/cGKI-mediated control of gene expression (see chapter 1.11.3) independent of BMP signaling might also play a regulatory role in this context. In VSMCs it is known that genes involved in VSMC differentiation and function such as smooth muscle α-actin or smooth muscle myosin heavy chain are induced by cGKI; these proteins are expressed in differentiated, non-proliferating VSMCs. De-differentiated VSMCs gain the ability to proliferate and have a very low level of cGKI protein [672].

In sum, these findings suggest a crosstalk of cGKI and BMP signaling with impact in vascular biology. Until now both pathways were described separately with high importance in hypertension diseases. In this work for the first time an integration of both is demonstrated. The characterized cGMP/cGKI crosstalk with BMP signaling represents a complex and very important regulatory mechanism with impact in cell signaling and differentiation events and even in vascular diseases.

5.6 Current model of the impact of cGKI on Smad BMP signaling

Novel crosstalk to BMP signaling: cGKI modulates BMP receptor and Smad activity (Schwappacher et al., submitted)

In this thesis it is demonstrated how cGKI modulates BMP receptors and Smads, providing a novel mechanism of enhancing BMP signaling. cGKI, a key mediator of vasodilation and thus development of hypertension diseases, interacts with and phosphorylates the tail region of BRII. The kinase also controls ligand-induced R-Smad shuttling through regulation of C-terminal Smad phosphorylation. In response

to BMP-2, cGKI dissociates from the receptors to associate with activated Smad complexes and to undergo nuclear translocation. In the nucleus, cGKI binds with Smad1 and TFII-I to the promoter of the BMP target gene *Id1* and enhances its transcription in cooperation with TFII-I. Accordingly, cGKI has dual functionality in BMP signaling: it modulates BMP receptor/Smad activity at the plasma membrane, and after redistribution to the nucleus, regulates transcription as a nuclear co-factor for Smads. Cellular defects expressed by BRII mutants causing pulmonary arterial hypertension were compensated through cGKI, supporting cGKI´s positive action on BMP/Smad signaling downstream of the receptors.

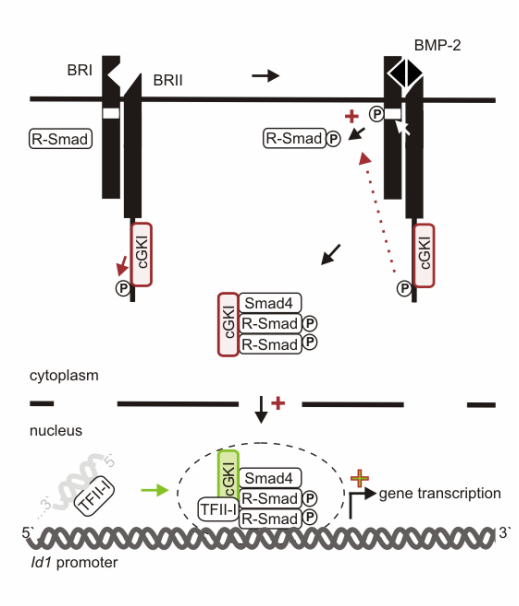

Figure 5.8 The dual role of cGKI in BMP signaling. cGKI interacts with and phosphorylates BRII in its tail region; upon BMP-2 stimulation, cGKI is released from the receptor to bind in association with R-Smads to co-Smad4. These complexes translocate into the nucleus, recruit TFII-I and bind to the promoter of the BMP target gene *Id1*. The cell compartment-specific function of the kinase in BMP signaling is illustrated through colouring of the cGKI molecule. cGKI fine-tunes BMP signaling by (1, red) regulating BMP receptor and R-Smad activation at the plasma membrane, and by (2, green) regulating expression of BMP target genes in the nucleus. “+” means enhancement/upregulation.

6 Summary - Zusammenfassung

Summary

Bone Morphogenetic Proteins (BMPs) regulate a plethora of cellular processes as proliferation, differentiation, chemotaxis and apoptosis in embryonic and mature tissue. The transduction of BMP signals is strictly regulated at each step of the signaling cascade. The importance of this precise regulation is reflected by developmental disorders and dysfunctions in humans such as bone and cartilage diseases or cancer, which appear when specific components of the BMP pathway are defective.

BMP ligands bind to a set of two specific transmembrane serine/threonine kinase receptors, the BMP type I receptor (BRI) and the BMP type II receptor (BRII). These receptors prior to ligand binding either reside preassembled in heteromeric preformed complexes (PFCs) in the cell membrane or exist as monomers or homodimers. Ligand binding to PFCs triggers transphosphorylation of BRI by BRII and propagation of the signal by phosphorylation and concomitant activation of R-Smad1/5/8. The signal is then transduced via heteromeric complexes of R-Smad1/5/8 and co-Smad4 and subsequent translocation into the nucleus to regulate BMP-specific target gene expression. Non-Smad signaling, however, is initiated by binding of BMP-2 to the high affinity receptor BRI, which subsequently recruites BRII into a BMP-induced signaling complex (BISC) to activate MAPK pathways.

Mutations within BRII are implicated in the development of pulmonary arterial hypertension (PAH). PAH is characterized by narrowing of the pulmonary artery due to abnormal cell proliferation resulting in elevated blood preassure and heart failure. Several proteins have been shown to bind to BRII regulating BMP signaling initiated by the receptor complex. Although some of these interaction partners seem to interfere with the pathogenesis of PAH, the role of BRII and its crosstalk mechanisms inside PAH are still unclear.

In the presented work, the impact of the cGMP-dependent kinase I (cGKI) on BRII and thus on BMP signaling was investigated. Using a proteomics-based approach, cGKI was identified to bind to BRII. So far, no function has been assigned to cGKI in BMP signaling. cGKI is a soluble cytoplasmic serine/threonine kinase and one of the major mediators in nitric oxide (NO)/cyclic guanosine 3',5'- monophosphate (cGMP)-triggered signal transduction. The kinase plays a pivotal role in many physiological processes such as vascular tone control, platelet activation and synaptic plasticity. It is highly expressed in vascular smooth muscle cells (VSMCs), where it regulates gene expression, morphology and proliferation. Alterations of cGKI expression and activity are involved in the pathogenesis of hypertension, atherosclerosis, restenosis, and hyperlipemia.

In this thesis, it is shown that cGKI directly interacts with and phosphorylates BRII which likely results in activation of the receptor complex. Consistent with this, cGKI enhances the BMP-2-mediated Smad1/5/8 phosphorylation at the C-terminus and thus R-Smad function. Upon BMP-2 stimulation, cGKI is released from the receptor to bind to R-Smad1/5/8 as well as to co-Smad4. BMP-2-dependently, these complexes translocate into the nucleus, and bind to the promoter of the BMP target gene *Id1*. At the promoter, the general transcription factor TFII-I, which is a known substrate for cGKI, is recruited by the kinase to further enhance BMP signaling. In sum, this thesis demonstrates a dual role for cGKI in BMP signaling through (1) regulating BMP receptor and R-Smad activation at the plasma membrane, and through (2) regulating expression of BMP target genes in the nucleus. In addition, this study supposes that defective cellular responses induced by mutant BRII underlying in patients with PAH can be compensated by cGKI expression. Thus, the characterized cGKI crosstalk with BMP signaling not only expands the functional flexibility of the cGMP/cGKI pathway, but also opens new prospects for investigation of a BMP/cGKI/Smad pathway and treatment of vascular diseases.

Zusammenfassung

Bone morphogenetic proteins (BMPs) regulieren sowohl in embryonalen als auch adulten Geweben eine Vielzahl von zellulären Prozessen wie Proliferation, Differenzierung, Chemotaxis und Apoptose. Jeder einzelne Schritt der Weiterleitung von BMP-Signalen unterliegt einer strengen Kontrolle. Im Menschen können Mutationen einzelner Komponenten dieses Signalweges unter anderem fehlerhafte Knochen- und Knorpelentwicklung oder Krebs induzieren, wodurch sich die Wichtigkeit dieser genauen Regulation widerspiegelt. Der BMP-Ligand bindet an zwei spezifische, transmembrane Serin/Threonin Kinase-Rezeptoren, den BMP Typ I Rezeptor (BRI) und Typ II Rezeptor (BRII). Vor Ligandenbindung sind diese membranständigen Rezeptoren entweder bereits komplexiert (präformierte Komplexe, PFCs) oder liegen als Monomere oder Homodimere vor. Ligandenbindung an den präformierten Komplex löst die BRI-Transphosphorylierung durch BRII aus und führt zur Signalweitergabe durch Phosphorylierung und Aktivierung der Rezeptor-regulierten R-Smads1/5/8. Durch Komplexbildung zwischen phosphorylierten R-Smads und co-Smad4 und anschliessender nukleärer Migration, wird das Signal zur Regulierung von BMP-spezifischen Zielgenen in den Zellkern weitergeleitet. Smad-unabhängige BMP-Signaltransduktion hingegen wird durch BMP-2-Bindung an den hochaffinen BRI eingeleitet, der darauffolgend BRII in den BMP-induzierten Signalkomplex (BISC) rekrutiert, um MAPK-Signalwege zu aktivieren.

Mutationen in BRII können pulmonäre arterielle Hypertonie (PAH) auslösen. PAH zeichnet sich durch Verengung der pulmonalen Arterie durch Hyperproliferation von Zellen aus. Dies resultiert in Bluthochdruck und Herzinsuffizienz. Für mehrere Proteine wurde bereits eine Assoziation mit BRII identifiziert, die die Rezeptor-induzierte BMP-Signaltransduktion regulieren. Obwohl einige dieser Interaktionspartner die Pathogenese von PAH scheinbar beeinflussen, ist die Rolle von BRII und BRII-initiiertem Crosstalk bezüglich PAH dennoch unklar.

In der vorliegenden Arbeit wurde der Einfluss der cGMP-abhängigen Porteinkinase I (cGKI) auf BRII und somit auf die BMP-Signalgebung untersucht. Mit Hilfe eines experimentellen Ansatzes, der auf Proteom-Analyse basiert, konnte cGKI als ein BRII-assoziiertes Protein identifiziert werden. Bis dato wurde keine Funktion von cGKI innerhalb der BMP-Signaltransduktion beschrieben. Die Serin/Threonin-spezifische Kinase ist einer der wichtigsten Mediatoren der durch Stickstoffmonoxid (NO) und zyklischem Guanosin 3',5'-Monophosphat (cGMP) ausgelösten Signalkaskade. cGKI spielt eine zentrale Rolle in vielen physiologischen Prozessen wie Kontrolle des Gefässtonus und der synaptischen Plastizität sowie in der Regulation der Aggregation von Blutplättchen. Die Kinase wird stark in Zellen der glatten vaskulären Muskulatur exprimiert, in denen sie Genexpression, Zellmorphologie und Proliferation reguliert. Veränderung der cGKI-Expression und -Aktivität werden mit der Pathogenese von Hypertonie, Atherosklerose, Restenose und Hyperlipemie in Verbindung gebracht.

Durch dieser Promotionsarbeit kann gezeigt werden, dass cGKI direkt mit BRII assoziiert und den Rezeptor phosphoryliert. Diese Modifikation führt sehr wahrscheinlich zur Aktivierung des Rezeptorkomplexes. Mit diesem Ergebnis vereinbar ist die cGKI-vermittelte Steigerung der Smad1/5/8-Phosphorylierung nach BMP-2-Stimulation. Behandlung mit dem BMP-2-Liganden führt desweiteren zur Dissoziation von cGKI von BRII. Gleichzeitig kommt es zur verstärkten Komplexbildung von cGKI mit R-Smads und co-Smad4. In Abhängigkeit von BMP-2 wandert dieser Proteinkomplex in den Zellkern, um an spezifische Genpromotoren zu binden. Der Transkriptionsfaktor TFII-I, der ein bekanntes cGKI-Substrat darstellt, wird durch die Kinase an den *Id1*-Promotor rekrutiert, um eine weitere Steigerung der BMP-Genantwort zu erzielen. Zusammenfassend wird innerhalb dieser Promotionsschrift eine duale Rolle von cGKI innerhalb der BMP-Signaltransduktion demonstriert: cGKI reguliert (1) die Aktivierung von BMP-Rezeptoren und R-Smads an der Plasmamembran und (2) die Expression von BMP-Zielgenen im Zellkern. Zusätzlich lassen die Ergebnisse der vorliegenden Studie die Schlussfolgerung zu, dass fehlerhafte zelluläre Antworten, die durch PAH-BRII-Mutanten ausgelöst werden, durch Expression von cGKI kompensiert werden können. Somit erweitert der beschriebene Crosstalk von cGKI zur BMP-Signaltransduktion nicht nur die funktionelle Flexibilität des cGMP/cGKI-Signalweges, sondern eröffnet auch neue Perspektiven zur Erfoschung einer BMP/cGKI/Smad-Kaskade und für die Behandlung von Gefässkrankheiten.

7 Other projects

7.1 Impact of different GDF-5 mutants on GDF-5-induced signaling

Activating and deactivating mutations in the receptor interaction site of GDF-5 cause symphalangism and brachydaktyly type A2 [860]

Here we describe two mutations in growth and differentiation factor 5 (GDF-5) that alter receptor-binding affinities. They cause brachydactyly type A2 (L441P) and symphalangism (R438L), conditions previously associated with mutations in the GDF-5 receptor bone morphogenetic protein receptor type 1b (BRIb) and the BMP antagonist Noggin, respectively. We expressed the mutant proteins in limb bud micromass culture and treated ATDC5 and C2C12 cells with recombinant GDF-5. Our results indicated that the L441P mutant is almost inactive. The R438L mutant, in contrast, showed increased biological activity when compared with wildtype GDF-5. Biosensor interaction analyses revealed loss of binding to BRIa and BRIb ectodomains for the L441P mutant, whereas the R438L mutant showed normal binding to BRIb but increased binding to BRIb, the receptor normally activated by BMP-2. The binding to Noggin was normal for both mutants. Thus, the brachydactyly type A2 phenotype (L441P) is caused by inhibition of the ligand-receptor interaction, whereas the symphalangism phenotype (R438L) is caused by a loss of receptor-binding specificity, resulting in a gain of function by the acquisition of BMP-2-like properties. The presented experiments have identified some of the main determinants of GDF-5 receptor-binding specificity in vivo and open new prospects for generating antagonists and superagonists of GDF-5.

Monomeric and dimeric GDF-5 show equal type I receptor binding and oligomerization capability and have the same biological activity [861]

Growth and differentiation factor 5 (GDF-5) is a homodimeric protein stabilized by a single disulfide bridge between cysteine 465 in the respective monomers, as well as by three intramolecular cysteine bridges within each subunit. A mature recombinant human GDF-5 variant with cysteine 465 replaced by alanine (rhGDF-5 C465A) was expressed in E. coli, purified to homogeneity, and chemically renatured. Biochemical analysis showed that this procedure eliminated the sole interchain disulfide bond. Surprisingly, the monomeric variant of rhGDF-5 is as potent in vitro as the dimeric form. This could be confirmed by alkaline phosphatase assays and Smad reporter gene activation. Furthermore, dimeric and monomeric rhGDF-5 show comparable binding to their specific type I receptor, BRIb. Studies on living cells showed that both the dimeric and monomeric rhGDF-5 induce homomeric BRIb and heteromeric BRIb/BRII oligomers. Our results suggest that rhGDF-5 C465A has the same biological activity as rhGDF-5 with respect to binding to, oligomerization of and signaling through the BMP receptor type Ib.

7.2 Impact of the phosphatase PP2A as a Smad linker phosphatase on BMP-2-induced signaling pathways

PP2A regulates BMP signaling by interacting with BMP receptor complexes and by dephosphorylating linker region of Smad1/5/8 (Bengtsson, Schwappacher et al., in revision)

Phosphorylation of Smads is a crucial regulatory step in signal transduction pathway initiated by bone morphogenic factors. While the dephosphorylation events terminating the pathway in the nucleus have been characterized, little is known about the dephosphorylation of Smads in the cytoplasm. In a proteomic screen for interactors of the BMP type II receptor, we found the Bβ subunit of PP2A. PP2A is one of the major serine/threonine phosphatases involved in cell cycle regulation and signal transduction. Here, we present data showing that the Bβ subunit of PP2A interacts with both BMP type I and type II receptors. Furthermore, we demonstrate that several B subunits can associate with the BMP type II receptor, independent of the receptors kinase activity and the catalytic subunit of PP2A. In contrast, the PP2A catalytic subunit is required for PP2A function at the receptor complex, which is to dephosphorylate BMP Smads, mainly in the linker region. PP2A-mediated dephosphorylation of the BMP-Smad linker region leads to increased nuclear translocation of Smads and overall amplification of the BMP-signal. While other phosphatases identified within the TGFβ/BMP-pathway are all shown to inhibit signaling, PP2A resembles the first example for a signaling stimulatory phosphatase within this pathway.

8 References

Ensemble Genome Browser (http://www.ensembl.org/index.html)

NCBI database (http://www.ncbi.nlm.nih.gov/)

NetPhosK 1.0 (http://www.cbs.dtu.dk/services/NetPhosK/)

OMIM (Online Mendelian Inheritance in Man; http://www.ncbi.nlm.nih.gov/sites/entrez?db=omim)

Wikipedia (http://en.wikipedia.org)

1. Schmierer, B. and C.S. Hill, *TGFbeta-SMAD signal transduction: molecular specificity and functional flexibility.* Nat Rev Mol Cell Biol, 2007. **8**(12): p. 970-82.
2. Feng, X.H. and R. Derynck, *Specificity and versatility in tgf-beta signaling through Smads.* Annu Rev Cell Dev Biol, 2005. **21**: p. 659-93.
3. Shi, Y. and J. Massague, *Mechanisms of TGF-beta signaling from cell membrane to the nucleus.* Cell, 2003. **113**(6): p. 685-700.
4. Derynck, R. and Y.E. Zhang, *Smad-dependent and Smad-independent pathways in TGF-beta family signalling.* Nature, 2003. **425**(6958): p. 577-84.
5. Urist, M.R., *Bone: formation by autoinduction.* Science, 1965. **150**(698): p. 893-9.
6. Wozney, J.M., et al., *Novel regulators of bone formation: molecular clones and activities.* Science, 1988. **242**(4885): p. 1528-34.
7. Canalis, E., A.N. Economides, and E. Gazzerro, *Bone morphogenetic proteins, their antagonists, and the skeleton.* Endocr Rev, 2003. **24**(2): p. 218-35.
8. Lories, R.J. and F.P. Luyten, *Bone morphogenetic protein signaling in joint homeostasis and disease.* Cytokine Growth Factor Rev, 2005. **16**(3): p. 287-98.
9. Varga, A.C. and J.L. Wrana, *The disparate role of BMP in stem cell biology.* Oncogene, 2005. **24**(37): p. 5713-21.
10. Schier, A.F. and W.S. Talbot, *Molecular genetics of axis formation in zebrafish.* Annu Rev Genet, 2005. **39**: p. 561-613.
11. Harradine, K.A. and R.J. Akhurst, *Mutations of TGFbeta signaling molecules in human disease.* Ann Med, 2006. **38**(6): p. 403-14.
12. Hartung, A., C. Sieber, and P. Knaus, *Yin and Yang in BMP signaling: Impact on the pathology of diseases and potential for tissue regeneration.* Signal transduction, 2006. **6**(5): p. 314-328.
13. Waite, K.A. and C. Eng, *From developmental disorder to heritable cancer: it's all in the BMP/TGF-beta family.* Nat Rev Genet, 2003. **4**(10): p. 763-73.
14. Constam, D.B. and E.J. Robertson, *Regulation of bone morphogenetic protein activity by pro domains and proprotein convertases.* J Cell Biol, 1999. **144**(1): p. 139-49.
15. Cui, Y., et al., *BMP-4 is proteolytically activated by furin and/or PC6 during vertebrate embryonic development.* Embo J, 1998. **17**(16): p. 4735-43.
16. Cui, Y., et al., *The activity and signaling range of mature BMP-4 is regulated by sequential cleavage at two sites within the prodomain of the precursor.* Genes Dev, 2001. **15**(21): p. 2797-802.
17. Degnin, C., et al., *Cleavages within the prodomain direct intracellular trafficking and degradation of mature bone morphogenetic protein-4.* Mol Biol Cell, 2004. **15**(11): p. 5012-20.
18. Aono, A., et al., *Potent ectopic bone-inducing activity of bone morphogenetic protein-4/7 heterodimer.* Biochem Biophys Res Commun, 1995. **210**(3): p. 670-7.
19. Israel, D.I., et al., *Heterodimeric bone morphogenetic proteins show enhanced activity in vitro and in vivo.* Growth Factors, 1996. **13**(3-4): p. 291-300.
20. Nishimatsu, S. and G.H. Thomsen, *Ventral mesoderm induction and patterning by bone morphogenetic protein heterodimers in Xenopus embryos.* Mech Dev, 1998. **74**(1-2): p. 75-88.
21. Suzuki, A., et al., *Mesoderm induction by BMP-4 and -7 heterodimers.* Biochem Biophys Res Commun, 1997. **232**(1): p. 153-6.
22. Butler, S.J. and J. Dodd, *A role for BMP heterodimers in roof plate-mediated repulsion of commissural axons.* Neuron, 2003. **38**(3): p. 389-401.
23. Knaus, P. and W. Sebald, *Cooperativity of binding epitopes and receptor chains in the BMP/TGFbeta superfamily.* Biol Chem, 2001. **382**(8): p. 1189-95.
24. Scheufler, C., W. Sebald, and M. Hulsmeyer, *Crystal structure of human bone morphogenetic protein-2 at 2.7 A resolution.* J Mol Biol, 1999. **287**(1): p. 103-15.
25. Murray-Rust, J., et al., *Topological similarities in TGF-beta 2, PDGF-BB and NGF define a superfamily of polypeptide growth factors.* Structure, 1993. **1**(2): p. 153-9.
26. Zhang, H. and A. Bradley, *Mice deficient for BMP2 are nonviable and have defects in amnion/chorion and cardiac development.* Development, 1996. **122**(10): p. 2977-86.
27. Winnier, G., et al., *Bone morphogenetic protein-4 is required for mesoderm formation and patterning in the mouse.* Genes Dev, 1995. **9**(17): p. 2105-16.
28. Dudley, A.T., K.M. Lyons, and E.J. Robertson, *A requirement for bone morphogenetic protein-7 during development of the mammalian kidney and eye.* Genes Dev, 1995. **9**(22): p. 2795-807.
29. Luo, G., et al., *BMP-7 is an inducer of nephrogenesis, and is also required for eye development and skeletal patterning.* Genes Dev, 1995. **9**(22): p. 2808-20.
30. Lyons, K.M., R.W. Pelton, and B.L. Hogan, *Patterns of expression of murine Vgr-1 and BMP-2a RNA suggest that transforming growth factor-beta-like genes coordinately regulate aspects of embryonic development.* Genes Dev, 1989. **3**(11): p. 1657-68.

31. Lyons, K.M., R.W. Pelton, and B.L. Hogan, *Organogenesis and pattern formation in the mouse: RNA distribution patterns suggest a role for bone morphogenetic protein-2A (BMP-2A).* Development, 1990. **109**(4): p. 833-44.
32. Wang, E.A., et al., *Recombinant human bone morphogenetic protein induces bone formation.* Proc Natl Acad Sci U S A, 1990. **87**(6): p. 2220-4.
33. Luyten, F.P., et al., *Purification and partial amino acid sequence of osteogenin, a protein initiating bone differentiation.* J Biol Chem, 1989. **264**(23): p. 13377-80.
34. Vukicevic, S., M.N. Helder, and F.P. Luyten, *Developing human lung and kidney are major sites for synthesis of bone morphogenetic protein-3 (osteogenin).* J Histochem Cytochem, 1994. **42**(7): p. 869-75.
35. Vukicevic, S., F.P. Luyten, and A.H. Reddi, *Stimulation of the expression of osteogenic and chondrogenic phenotypes in vitro by osteogenin.* Proc Natl Acad Sci U S A, 1989. **86**(22): p. 8793-7.
36. Bahamonde, M.E. and K.M. Lyons, *BMP3: to be or not to be a BMP.* J Bone Joint Surg Am, 2001. **83-A Suppl 1**(Pt 1): p. S56-62.
37. Gamer, L.W., et al., *BMP-3 is a novel inhibitor of both activin and BMP-4 signaling in Xenopus embryos.* Dev Biol, 2005. **285**(1): p. 156-68.
38. Daluiski, A., et al., *Bone morphogenetic protein-3 is a negative regulator of bone density.* Nat Genet, 2001. **27**(1): p. 84-8.
39. Chen, D., et al., *Cloning and sequence of bone morphogenetic protein 4 cDNA from fetal rat calvarial cell.* Biochim Biophys Acta, 1993. **1174**(3): p. 289-92.
40. Dale, L. and F.C. Wardle, *A gradient of BMP activity specifies dorsal-ventral fates in early Xenopus embryos.* Semin Cell Dev Biol, 1999. **10**(3): p. 319-26.
41. Jones, C.M., et al., *Bone morphogenetic protein-4 (BMP-4) acts during gastrula stages to cause ventralization of Xenopus embryos.* Development, 1996. **122**(5): p. 1545-54.
42. Jones, C.M., K.M. Lyons, and B.L. Hogan, *Involvement of Bone Morphogenetic Protein-4 (BMP-4) and Vgr-1 in morphogenesis and neurogenesis in the mouse.* Development, 1991. **111**(2): p. 531-42.
43. Dunn, N.R., et al., *Haploinsufficient phenotypes in Bmp4 heterozygous null mice and modification by mutations in Gli3 and Alx4.* Dev Biol, 1997. **188**(2): p. 235-47.
44. Katagiri, T., et al., *Skeletal abnormalities in doubly heterozygous Bmp4 and Bmp7 mice.* Dev Genet, 1998. **22**(4): p. 340-8.
45. DiLeone, R.J., L.B. Russell, and D.M. Kingsley, *An extensive 3' regulatory region controls expression of Bmp5 in specific anatomical structures of the mouse embryo.* Genetics, 1998. **148**(1): p. 401-8.
46. King, J.A., et al., *BMP5 and the molecular, skeletal, and soft-tissue alterations in short ear mice.* Dev Biol, 1994. **166**(1): p. 112-22.
47. Green, E.L., *Quantitative genetics of skeletal variations in the mouse. I. Crosses between three short-ear strains (P, NB, SEC/2).* J Natl Cancer Inst, 1954. **15**(3): p. 609-27.
48. Kingsley, D.M., et al., *The mouse short ear skeletal morphogenesis locus is associated with defects in a bone morphogenetic member of the TGF beta superfamily.* Cell, 1992. **71**(3): p. 399-410.
49. Storm, E.E. and D.M. Kingsley, *Joint patterning defects caused by single and double mutations in members of the bone morphogenetic protein (BMP) family.* Development, 1996. **122**(12): p. 3969-79.
50. Ebisawa, T., et al., *Characterization of bone morphogenetic protein-6 signaling pathways in osteoblast differentiation.* J Cell Sci, 1999. **112 (Pt 20)**: p. 3519-27.
51. Solloway, M.J., et al., *Mice lacking Bmp6 function.* Dev Genet, 1998. **22**(4): p. 321-39.
52. Perry, M.J., et al., *Impaired growth plate function in bmp-6 null mice.* Bone, 2008. **42**(1): p. 216-25.
53. Blessing, M., P. Schirmacher, and S. Kaiser, *Overexpression of bone morphogenetic protein-6 (BMP-6) in the epidermis of transgenic mice: inhibition or stimulation of proliferation depending on the pattern of transgene expression and formation of psoriatic lesions.* J Cell Biol, 1996. **135**(1): p. 227-39.
54. Dick, A., et al., *Essential role of Bmp7 (snailhouse) and its prodomain in dorsoventral patterning of the zebrafish embryo.* Development, 2000. **127**(2): p. 343-54.
55. Ozkaynak, E., et al., *OP-1 cDNA encodes an osteogenic protein in the TGF-beta family.* Embo J, 1990. **9**(7): p. 2085-93.
56. Yamashita, H., et al., *Osteogenic protein-1 binds to activin type II receptors and induces certain activin-like effects.* J Cell Biol, 1995. **130**(1): p. 217-26.
57. Jena, N., et al., *BMP7 null mutation in mice: developmental defects in skeleton, kidney, and eye.* Exp Cell Res, 1997. **230**(1): p. 28-37.
58. Ozkaynak, E., et al., *Osteogenic protein-2. A new member of the transforming growth factor-beta superfamily expressed early in embryogenesis.* J Biol Chem, 1992. **267**(35): p. 25220-7.
59. Zhao, G.Q., L. Liaw, and B.L. Hogan, *Bone morphogenetic protein 8A plays a role in the maintenance of spermatogenesis and the integrity of the epididymis.* Development, 1998. **125**(6): p. 1103-12.
60. Zhao, G.Q., et al., *The gene encoding bone morphogenetic protein 8B is required for the initiation and maintenance of spermatogenesis in the mouse.* Genes Dev, 1996. **10**(13): p. 1657-69.
61. David, L., et al., *Identification of BMP9 and BMP10 as functional activators of the orphan activin receptor-like kinase 1 (ALK1) in endothelial cells.* Blood, 2007. **109**(5): p. 1953-61.
62. Neuhaus, H., V. Rosen, and R.S. Thies, *Heart specific expression of mouse BMP-10 a novel member of the TGF-beta superfamily.* Mech Dev, 1999. **80**(2): p. 181-4.
63. Chen, H., et al., *BMP10 is essential for maintaining cardiac growth during murine cardiogenesis.* Development, 2004. **131**(9): p. 2219-31.
64. Dube, J.L., et al., *The bone morphogenetic protein 15 gene is X-linked and expressed in oocytes.* Mol Endocrinol, 1998. **12**(12): p. 1809-17.
65. Edwards, S.J., et al., *The cooperative effect of growth and differentiation factor-9 and bone morphogenetic protein (BMP)-15 on granulosa cell function is modulated primarily through BMP receptor II.* Endocrinology, 2008. **149**(3): p. 1026-30.
66. Moore, R.K., F. Otsuka, and S. Shimasaki, *Molecular basis of bone morphogenetic protein-15 signaling in granulosa cells.* J Biol Chem, 2003. **278**(1): p. 304-10.
67. Yan, C., et al., *Synergistic roles of bone morphogenetic protein 15 and growth differentiation factor 9 in ovarian function.* Mol Endocrinol, 2001. **15**(6): p. 854-66.
68. Balemans, W. and W. Van Hul, *Extracellular regulation of BMP signaling in vertebrates: a cocktail of modulators.* Dev Biol, 2002. **250**(2): p. 231-50.

69. Botchkarev, V.A. and A.A. Sharov, *BMP signaling in the control of skin development and hair follicle growth.* Differentiation, 2004. **72**(9-10): p. 512-26.
70. De Robertis, E.M., *Spemann's organizer and self-regulation in amphibian embryos.* Nat Rev Mol Cell Biol, 2006. **7**(4): p. 296-302.
71. Koenig, B.B., et al., *Characterization and cloning of a receptor for BMP-2 and BMP-4 from NIH 3T3 cells.* Mol Cell Biol, 1994. **14**(9): p. 5961-74.
72. Liu, F., et al., *Human type II receptor for bone morphogenic proteins (BMPs): extension of the two-kinase receptor model to the BMPs.* Mol Cell Biol, 1995. **15**(7): p. 3479-86.
73. Nishitoh, H., et al., *Identification of type I and type II serine/threonine kinase receptors for growth/differentiation factor-5.* J Biol Chem, 1996. **271**(35): p. 21345-52.
74. Nohno, T., et al., *Identification of a human type II receptor for bone morphogenetic protein-4 that forms differential heteromeric complexes with bone morphogenetic protein type I receptors.* J Biol Chem, 1995. **270**(38): p. 22522-6.
75. Rosenzweig, B.L., et al., *Cloning and characterization of a human type II receptor for bone morphogenetic proteins.* Proc Natl Acad Sci U S A, 1995. **92**(17): p. 7632-6.
76. ten Dijke, P., et al., *Identification of type I receptors for osteogenic protein-1 and bone morphogenetic protein-4.* J Biol Chem, 1994. **269**(25): p. 16985-8.
77. Kirsch, T., W. Sebald, and M.K. Dreyer, *Crystal structure of the BMP-2-BRIA ectodomain complex.* Nat Struct Biol, 2000. **7**(6): p. 492-6.
78. Kirsch, T., J. Nickel, and W. Sebald, *BMP-2 antagonists emerge from alterations in the low-affinity binding epitope for receptor BMPR-II.* Embo J, 2000. **19**(13): p. 3314-24.
79. Allendorph, G.P., W.W. Vale, and S. Choe, *Structure of the ternary signaling complex of a TGF-beta superfamily member.* Proc Natl Acad Sci U S A, 2006. **103**(20): p. 7643-8.
80. Griffith, D.L., et al., *Three-dimensional structure of recombinant human osteogenic protein 1: structural paradigm for the transforming growth factor beta superfamily.* Proc Natl Acad Sci U S A, 1996. **93**(2): p. 878-83.
81. Keller, S., et al., *Molecular recognition of BMP-2 and BMP receptor IA.* Nat Struct Mol Biol, 2004. **11**(5): p. 481-8.
82. Weber, D., et al., *A silent H-bond can be mutationally activated for high-affinity interaction of BMP-2 and activin type IIB receptor.* BMC Struct Biol, 2007. **7**: p. 6.
83. Zimmerman, L.B., J.M. De Jesus-Escobar, and R.M. Harland, *The Spemann organizer signal noggin binds and inactivates bone morphogenetic protein 4.* Cell, 1996. **86**(4): p. 599-606.
84. Avsian-Kretchmer, O. and A.J. Hsueh, *Comparative genomic analysis of the eight-membered ring cystine knot-containing bone morphogenetic protein antagonists.* Mol Endocrinol, 2004. **18**(1): p. 1-12.
85. Smith, W.C. and R.M. Harland, *Expression cloning of noggin, a new dorsalizing factor localized to the Spemann organizer in Xenopus embryos.* Cell, 1992. **70**(5): p. 829-40.
86. Valenzuela, D.M., et al., *Identification of mammalian noggin and its expression in the adult nervous system.* J Neurosci, 1995. **15**(9): p. 6077-84.
87. Brunet, L.J., et al., *Noggin, cartilage morphogenesis, and joint formation in the mammalian skeleton.* Science, 1998. **280**(5368): p. 1455-7.
88. McMahon, J.A., et al., *Noggin-mediated antagonism of BMP signaling is required for growth and patterning of the neural tube and somite.* Genes Dev, 1998. **12**(10): p. 1438-52.
89. Botchkarev, V.A., et al., *Noggin is a mesenchymally derived stimulator of hair-follicle induction.* Nat Cell Biol, 1999. **1**(3): p. 158-64.
90. Kulessa, H., G. Turk, and B.L. Hogan, *Inhibition of Bmp signaling affects growth and differentiation in the anagen hair follicle.* Embo J, 2000. **19**(24): p. 6664-74.
91. Bachiller, D., et al., *The organizer factors Chordin and Noggin are required for mouse forebrain development.* Nature, 2000. **403**(6770): p. 658-61.
92. Nakayama, N., et al., *A novel chordin-like protein inhibitor for bone morphogenetic proteins expressed preferentially in mesenchymal cell lineages.* Dev Biol, 2001. **232**(2): p. 372-87.
93. Sakuta, H., et al., *Ventroptin: a BMP-4 antagonist expressed in a double-gradient pattern in the retina.* Science, 2001. **293**(5527): p. 111-5.
94. Nakayama, N., et al., *A novel chordin-like BMP inhibitor, CHL2, expressed preferentially in chondrocytes of developing cartilage and osteoarthritic joint cartilage.* Development, 2004. **131**(1): p. 229-40.
95. Oren, A., et al., *hCHL2, a novel chordin-related gene, displays differential expression and complex alternative splicing in human tissues and during myoblast and osteoblast maturation.* Gene, 2004. **331**: p. 17-31.
96. Hemmati-Brivanlou, A., O.G. Kelly, and D.A. Melton, *Follistatin, an antagonist of activin, is expressed in the Spemann organizer and displays direct neuralizing activity.* Cell, 1994. **77**(2): p. 283-95.
97. Matzuk, M.M., et al., *Multiple defects and perinatal death in mice deficient in follistatin.* Nature, 1995. **374**(6520): p. 360-3.
98. Schneyer, A., et al., *Follistatin-related protein (FSRP): a new member of the follistatin gene family.* Mol Cell Endocrinol, 2001. **180**(1-2): p. 33-8.
99. Tsuchida, K., et al., *Identification and characterization of a novel follistatin-like protein as a binding protein for the TGF-beta family.* J Biol Chem, 2000. **275**(52): p. 40788-96.
100. Xia, Y., Y. Sidis, and A. Schneyer, *Overexpression of follistatin-like 3 in gonads causes defects in gonadal development and function in transgenic mice.* Mol Endocrinol, 2004. **18**(4): p. 979-94.
101. Rentzsch, F., et al., *Crossveinless 2 is an essential positive feedback regulator of Bmp signaling during zebrafish gastrulation.* Development, 2006. **133**(5): p. 801-11.
102. Shimmi, O., et al., *The crossveinless gene encodes a new member of the Twisted gastrulation family of BMP-binding proteins which, with Short gastrulation, promotes BMP signaling in the crossveins of the Drosophila wing.* Dev Biol, 2005. **282**(1): p. 70-83.
103. Koike, N., et al., *Brorin, a novel secreted bone morphogenetic protein antagonist, promotes neurogenesis in mouse neural precursor cells.* J Biol Chem, 2007. **282**(21): p. 15843-50.
104. Rydziel, S., et al., *Nephroblastoma overexpressed (Nov) inhibits osteoblastogenesis and causes osteopenia.* J Biol Chem, 2007. **282**(27): p. 19762-72.
105. Abreu, J.G., et al., *Connective-tissue growth factor (CTGF) modulates cell signalling by BMP and TGF-beta.* Nat Cell Biol, 2002. **4**(8): p. 599-604.
106. Baguma-Nibasheka, M. and B. Kablar, *Pulmonary hypoplasia in the connective tissue growth factor (Ctgf) null mouse.* Dev Dyn, 2008. **237**(2): p. 485-93.

107. Wilkinson, L., et al., *CRIM1 regulates the rate of processing and delivery of bone morphogenetic proteins to the cell surface.* J Biol Chem, 2003. **278**(36): p. 34181-8.
108. Pennisi, D.J., et al., *Crim1KST264/KST264 mice display a disruption of the Crim1 gene resulting in perinatal lethality with defects in multiple organ systems.* Dev Dyn, 2007. **236**(2): p. 502-11.
109. Moser, M., et al., *BMPER, a novel endothelial cell precursor-derived protein, antagonizes bone morphogenetic protein signaling and endothelial cell differentiation.* Mol Cell Biol, 2003. **23**(16): p. 5664-79.
110. Lin, J., et al., *Kielin/chordin-like protein, a novel enhancer of BMP signaling, attenuates renal fibrotic disease.* Nat Med, 2005. **11**(4): p. 387-93.
111. Chang, C., et al., *Twisted gastrulation can function as a BMP antagonist.* Nature, 2001. **410**(6827): p. 483-7.
112. Ross, J.J., et al., *Twisted gastrulation is a conserved extracellular BMP antagonist.* Nature, 2001. **410**(6827): p. 479-83.
113. Scott, I.C., et al., *Homologues of Twisted gastrulation are extracellular cofactors in antagonism of BMP signalling.* Nature, 2001. **410**(6827): p. 475-8.
114. Nosaka, T., et al., *Mammalian twisted gastrulation is essential for skeleto-lymphogenesis.* Mol Cell Biol, 2003. **23**(8): p. 2969-80.
115. Zakin, L. and E.M. De Robertis, *Inactivation of mouse Twisted gastrulation reveals its role in promoting Bmp4 activity during forebrain development.* Development, 2004. **131**(2): p. 413-24.
116. Dionne, M.S., W.C. Skarnes, and R.M. Harland, *Mutation and analysis of Dan, the founding member of the Dan family of transforming growth factor beta antagonists.* Mol Cell Biol, 2001. **21**(2): p. 636-43.
117. Yokouchi, Y., et al., *Antagonistic signaling by Caronte, a novel Cerberus-related gene, establishes left-right asymmetric gene expression.* Cell, 1999. **98**(5): p. 573-83.
118. Simpson, E.H., et al., *The mouse Cer1 (Cerberus related or homologue) gene is not required for anterior pattern formation.* Dev Biol, 1999. **213**(1): p. 202-6.
119. Belo, J.A., et al., *Cerberus-like is a secreted BMP and nodal antagonist not essential for mouse development.* Genesis, 2000. **26**(4): p. 265-70.
120. Khokha, M.K., et al., *Gremlin is the BMP antagonist required for maintenance of Shh and Fgf signals during limb patterning.* Nat Genet, 2003. **34**(3): p. 303-7.
121. Michos, O., et al., *Reduction of BMP4 activity by gremlin 1 enables ureteric bud outgrowth and GDNF/WNT11 feedback signalling during kidney branching morphogenesis.* Development, 2007. **134**(13): p. 2397-405.
122. Gazzerro, E., et al., *Conditional deletion of gremlin causes a transient increase in bone formation and bone mass.* J Biol Chem, 2007. **282**(43): p. 31549-57.
123. Minabe-Saegusa, C., et al., *Sequence and expression of a novel mouse gene PRDC (protein related to DAN and cerberus) identified by a gene trap approach.* Dev Growth Differ, 1998. **40**(3): p. 343-53.
124. Pearce, J.J., G. Penny, and J. Rossant, *A mouse cerberus/Dan-related gene family.* Dev Biol, 1999. **209**(1): p. 98-110.
125. Eimon, P.M. and R.M. Harland, *Xenopus Dan, a member of the Dan gene family of BMP antagonists, is expressed in derivatives of the cranial and trunk neural crest.* Mech Dev, 2001. **107**(1-2): p. 187-9.
126. Bell, E., et al., *Cell fate specification and competence by Coco, a maternal BMP, TGFbeta and Wnt inhibitor.* Development, 2003. **130**(7): p. 1381-9.
127. van Bezooijen, R.L., et al., *Wnt but not BMP signaling is involved in the inhibitory action of sclerostin on BMP-stimulated bone formation.* J Bone Miner Res, 2007. **22**(1): p. 19-28.
128. van Bezooijen, R.L., et al., *SOST/sclerostin, an osteocyte-derived negative regulator of bone formation.* Cytokine Growth Factor Rev, 2005. **16**(3): p. 319-27.
129. Kusu, N., et al., *Sclerostin is a novel secreted osteoclast-derived bone morphogenetic protein antagonist with unique ligand specificity.* J Biol Chem, 2003. **278**(26): p. 24113-7.
130. Li, X., et al., *Sclerostin binds to LRP5/6 and antagonizes canonical Wnt signaling.* J Biol Chem, 2005. **280**(20): p. 19883-7.
131. Li, X., et al., *Targeted deletion of the sclerostin gene in mice results in increased bone formation and bone strength.* J Bone Miner Res, 2008. **23**(6): p. 860-9.
132. Blish, K.R., et al., *A Human Bone Morphogenetic Protein Antagonist Is Down-Regulated in Renal Cancer.* Mol Biol Cell, 2008. **19**(2): p. 457-464.
133. Laurikkala, J., et al., *Identification of a secreted BMP antagonist, ectodin, integrating BMP, FGF, and SHH signals from the tooth enamel knot.* Dev Biol, 2003. **264**(1): p. 91-105.
134. Tanaka, M., et al., *Expression of BMP-7 and USAG-1 (a BMP antagonist) in kidney development and injury.* Kidney Int, 2008. **73**(2): p. 181-91.
135. Marques, G., et al., *Production of a DPP activity gradient in the early Drosophila embryo through the opposing actions of the SOG and TLD proteins.* Cell, 1997. **91**(3): p. 417-26.
136. Piccolo, S., et al., *Cleavage of Chordin by Xolloid metalloprotease suggests a role for proteolytic processing in the regulation of Spemann organizer activity.* Cell, 1997. **91**(3): p. 407-16.
137. Scott, I.C., et al., *Mammalian BMP-1/Tolloid-related metalloproteinases, including novel family member mammalian Tolloid-like 2, have differential enzymatic activities and distributions of expression relevant to patterning and skeletogenesis.* Dev Biol, 1999. **213**(2): p. 283-300.
138. Takahara, K., et al., *Characterization of a novel gene product (mammalian tolloid-like) with high sequence similarity to mammalian tolloid/bone morphogenetic protein-1.* Genomics, 1996. **34**(2): p. 157-65.
139. Suzuki, N., et al., *Failure of ventral body wall closure in mouse embryos lacking a procollagen C-proteinase encoded by Bmp1, a mammalian gene related to Drosophila tolloid.* Development, 1996. **122**(11): p. 3587-95.
140. Clark, T.G., et al., *The mammalian Tolloid-like 1 gene, Tll1, is necessary for normal septation and positioning of the heart.* Development, 1999. **126**(12): p. 2631-42.
141. Groppe, J., et al., *Structural basis of BMP signalling inhibition by the cystine knot protein Noggin.* Nature, 2002. **420**(6916): p. 636-42.
142. Gong, Y., et al., *Heterozygous mutations in the gene encoding noggin affect human joint morphogenesis.* Nat Genet, 1999. **21**(3): p. 302-4.
143. Polymeropoulos, M.H., et al., *Localization of the gene (SYM1) for proximal symphalangism to human chromosome 17q21-q22.* Genomics, 1995. **27**(2): p. 225-9.
144. Krakow, D., et al., *Localization of a multiple synostoses-syndrome disease gene to chromosome 17q21-22.* Am J Hum Genet, 1998. **63**(1): p. 120-4.

145. Connor, J.M. and D.A. Evans, *Genetic aspects of fibrodysplasia ossificans progressiva.* J Med Genet, 1982. **19**(1): p. 35-9.
146. Fontaine, K., et al., *A new mutation of the noggin gene in a French Fibrodysplasia ossificans progressiva (FOP) family.* Genet Couns, 2005. **16**(2): p. 149-54.
147. Lucotte, G. and J.P. Lagarde, *Mutations of the noggin and of the activin A type I receptor genes in fibrodysplasia ossificans progressiva (FOP).* Genet Couns, 2007. **18**(3): p. 349-52.
148. Lucotte, G., O. Semonin, and P. Lutz, *A de novo heterozygous deletion of 42 base-pairs in the noggin gene of a fibrodysplasia ossificans progressiva patient.* Clin Genet, 1999. **56**(6): p. 469-70.
149. Semonin, O., et al., *Identification of three novel mutations of the noggin gene in patients with fibrodysplasia ossificans progressiva.* Am J Med Genet, 2001. **102**(4): p. 314-7.
150. Sasai, Y., et al., *Xenopus chordin: a novel dorsalizing factor activated by organizer-specific homeobox genes.* Cell, 1994. **79**(5): p. 779-90.
151. Schmidl, M., et al., *Twisted gastrulation modulates bone morphogenetic protein-induced collagen II and X expression in chondrocytes in vitro and in vivo.* J Biol Chem, 2006. **281**(42): p. 31790-800.
152. Oelgeschlager, M., et al., *The evolutionarily conserved BMP-binding protein Twisted gastrulation promotes BMP signalling.* Nature, 2000. **405**(6788): p. 757-63.
153. Blader, P., et al., *Cleavage of the BMP-4 antagonist chordin by zebrafish tolloid.* Science, 1997. **278**(5345): p. 1937-40.
154. Brunkow, M.E., et al., *Bone dysplasia sclerosteosis results from loss of the SOST gene product, a novel cystine knot-containing protein.* Am J Hum Genet, 2001. **68**(3): p. 577-89.
155. Balemans, W., et al., *Increased bone density in sclerosteosis is due to the deficiency of a novel secreted protein (SOST).* Hum Mol Genet, 2001. **10**(5): p. 537-43.
156. Balemans, W., et al., *Localization of the gene for sclerosteosis to the van Buchem disease-gene region on chromosome 17q12-q21.* Am J Hum Genet, 1999. **64**(6): p. 1661-9.
157. Van Hul, W., et al., *Van Buchem disease (hyperostosis corticalis generalisata) maps to chromosome 17q12-q21.* Am J Hum Genet, 1998. **62**(2): p. 391-9.
158. Winkler, D.G., et al., *Osteocyte control of bone formation via sclerostin, a novel BMP antagonist.* Embo J, 2003. **22**(23): p. 6267-76.
159. Ruppert, R., E. Hoffmann, and W. Sebald, *Human bone morphogenetic protein 2 contains a heparin-binding site which modifies its biological activity.* Eur J Biochem, 1996. **237**(1): p. 295-302.
160. Jiao, X., et al., *Heparan sulfate proteoglycans (HSPGs) modulate BMP2 osteogenic bioactivity in C2C12 cells.* J Biol Chem, 2007. **282**(2): p. 1080-6.
161. Takada, T., et al., *Sulfated polysaccharides enhance the biological activities of bone morphogenetic proteins.* J Biol Chem, 2003. **278**(44): p. 43229-35.
162. Zhao, B., et al., *Heparin potentiates the in vivo ectopic bone formation induced by bone morphogenetic protein-2.* J Biol Chem, 2006. **281**(32): p. 23246-53.
163. Kanzaki, S., et al., *Heparin inhibits BMP-2 osteogenic bioactivity by binding to both BMP-2 and BMP receptor.* J Cell Physiol, 2008. **216**(3): p. 844-50.
164. Ohkawara, B., et al., *Action range of BMP is defined by its N-terminal basic amino acid core.* Curr Biol, 2002. **12**(3): p. 205-9.
165. Jasuja, R., et al., *Cell-surface heparan sulfate proteoglycans potentiate chordin antagonism of bone morphogenetic protein signaling and are necessary for cellular uptake of chordin.* J Biol Chem, 2004. **279**(49): p. 51289-97.
166. Paine-Saunders, S., et al., *Heparan sulfate proteoglycans retain Noggin at the cell surface: a potential mechanism for shaping bone morphogenetic protein gradients.* J Biol Chem, 2002. **277**(3): p. 2089-96.
167. Irie, A., et al., *Heparan sulfate is required for bone morphogenetic protein-7 signaling.* Biochem Biophys Res Commun, 2003. **308**(4): p. 858-65.
168. Gutierrez, J., N. Osses, and E. Brandan, *Changes in secreted and cell associated proteoglycan synthesis during conversion of myoblasts to osteoblasts in response to bone morphogenetic protein-2: role of decorin in cell response to BMP-2.* J Cell Physiol, 2006. **206**(1): p. 58-67.
169. Chen, X.D., et al., *The small leucine-rich proteoglycan biglycan modulates BMP-4-induced osteoblast differentiation.* Faseb J, 2004. **18**(9): p. 948-58.
170. Macias-Silva, M., et al., *Specific activation of Smad1 signaling pathways by the BMP7 type I receptor, ALK2.* J Biol Chem, 1998. **273**(40): p. 25628-36.
171. Mathews, L.S. and W.W. Vale, *Expression cloning of an activin receptor, a predicted transmembrane serine kinase.* Cell, 1991. **65**(6): p. 973-82.
172. Attisano, L., et al., *Novel activin receptors: distinct genes and alternative mRNA splicing generate a repertoire of serine/threonine kinase receptors.* Cell, 1992. **68**(1): p. 97-108.
173. Greenwald, J., et al., *The BMP7/ActRII extracellular domain complex provides new insights into the cooperative nature of receptor assembly.* Mol Cell, 2003. **11**(3): p. 605-17.
174. Ahn, K., et al., *BMPR-IA signaling is required for the formation of the apical ectodermal ridge and dorsal-ventral patterning of the limb.* Development, 2001. **128**(22): p. 4449-61.
175. Chen, D., et al., *Differential roles for bone morphogenetic protein (BMP) receptor type IB and IA in differentiation and specification of mesenchymal precursor cells to osteoblast and adipocyte lineages.* J Cell Biol, 1998. **142**(1): p. 295-305.
176. Dewulf, N., et al., *Distinct spatial and temporal expression patterns of two type I receptors for bone morphogenetic proteins during mouse embryogenesis.* Endocrinology, 1995. **136**(6): p. 2652-63.
177. Mishina, Y., et al., *Bmpr encodes a type I bone morphogenetic protein receptor that is essential for gastrulation during mouse embryogenesis.* Genes Dev, 1995. **9**(24): p. 3027-37.
178. Yoon, B.S., et al., *Bmpr1a and Bmpr1b have overlapping functions and are essential for chondrogenesis in vivo.* Proc Natl Acad Sci U S A, 2005. **102**(14): p. 5062-7.
179. Baur, S.T., J.J. Mai, and S.M. Dymecki, *Combinatorial signaling through BMP receptor IB and GDF5: shaping of the distal mouse limb and the genetics of distal limb diversity.* Development, 2000. **127**(3): p. 605-19.
180. Yi, S.E., et al., *The type I BMP receptor BMPRIB is required for chondrogenesis in the mouse limb.* Development, 2000. **127**(3): p. 621-30.
181. Yi, S.E., et al., *The type I BMP receptor BmprIB is essential for female reproductive function.* Proc Natl Acad Sci U S A, 2001. **98**(14): p. 7994-9.

182. Gu, Z., et al., *The type I serine/threonine kinase receptor ActRIA (ALK2) is required for gastrulation of the mouse embryo.* Development, 1999. **126**(11): p. 2551-61.
183. Tsuchida, K., L.S. Mathews, and W.W. Vale, *Cloning and characterization of a transmembrane serine kinase that acts as an activin type I receptor.* Proc Natl Acad Sci U S A, 1993. **90**(23): p. 11242-6.
184. Verschueren, K., et al., *Expression of type I and type IB receptors for activin in midgestation mouse embryos suggests distinct functions in organogenesis.* Mech Dev, 1995. **52**(1): p. 109-23.
185. Dudas, M., et al., *Craniofacial defects in mice lacking BMP type I receptor Alk2 in neural crest cells.* Mech Dev, 2004. **121**(2): p. 173-82.
186. Kaartinen, V., et al., *Cardiac outflow tract defects in mice lacking ALK2 in neural crest cells.* Development, 2004. **131**(14): p. 3481-90.
187. Beppu, H., et al., *BMP type II receptor is required for gastrulation and early development of mouse embryos.* Dev Biol, 2000. **221**(1): p. 249-58.
188. Feijen, A., M.J. Goumans, and A.J. van den Eijnden-van Raaij, *Expression of activin subunits, activin receptors and follistatin in postimplantation mouse embryos suggests specific developmental functions for different activins.* Development, 1994. **120**(12): p. 3621-37.
189. Song, J., et al., *The type II activin receptors are essential for egg cylinder growth, gastrulation, and rostral head development in mice.* Dev Biol, 1999. **213**(1): p. 157-69.
190. Garamszegi, N., et al., *Transforming growth factor beta receptor signaling and endocytosis are linked through a COOH terminal activation motif in the type I receptor.* Mol Biol Cell, 2001. **12**(9): p. 2881-93.
191. Foletta, V.C., et al., *Direct signaling by the BMP type II receptor via the cytoskeletal regulator LIMK1.* J Cell Biol, 2003. **162**(6): p. 1089-98.
192. Chen, F. and R.A. Weinberg, *Biochemical evidence for the autophosphorylation and transphosphorylation of transforming growth factor beta receptor kinases.* Proc Natl Acad Sci U S A, 1995. **92**(5): p. 1565-9.
193. Wrana, J.L., et al., *Mechanism of activation of the TGF-beta receptor.* Nature, 1994. **370**(6488): p. 341-7.
194. Wieser, R., J.L. Wrana, and J. Massague, *GS domain mutations that constitutively activate T beta R-I, the downstream signaling component in the TGF-beta receptor complex.* Embo J, 1995. **14**(10): p. 2199-208.
195. Nohe, A., et al., *The mode of bone morphogenetic protein (BMP) receptor oligomerization determines different BMP-2 signaling pathways.* J Biol Chem, 2002. **277**(7): p. 5330-8.
196. Huse, M., et al., *Crystal structure of the cytoplasmic domain of the type I TGF beta receptor in complex with FKBP12.* Cell, 1999. **96**(3): p. 425-36.
197. Akiyama, S., et al., *Constitutively active BMP type I receptors transduce BMP-2 signals without the ligand in C2C12 myoblasts.* Exp Cell Res, 1997. **235**(2): p. 362-9.
198. Fujii, M., et al., *Roles of bone morphogenetic protein type I receptors and Smad proteins in osteoblast and chondroblast differentiation.* Mol Biol Cell, 1999. **10**(11): p. 3801-13.
199. Imamura, T., et al., *Smad6 inhibits signalling by the TGF-beta superfamily.* Nature, 1997. **389**(6651): p. 622-6.
200. Wang, T., et al., *The immunophilin FKBP12 functions as a common inhibitor of the TGF beta family type I receptors.* Cell, 1996. **86**(3): p. 435-44.
201. Feng, X.H. and R. Derynck, *A kinase subdomain of transforming growth factor-beta (TGF-beta) type I receptor determines the TGF-beta intracellular signaling specificity.* Embo J, 1997. **16**(13): p. 3912-23.
202. Chen, Y.G., et al., *Determinants of specificity in TGF-beta signal transduction.* Genes Dev, 1998. **12**(14): p. 2144-52.
203. Lo, R.S., et al., *The L3 loop: a structural motif determining specific interactions between SMAD proteins and TGF-beta receptors.* Embo J, 1998. **17**(4): p. 996-1005.
204. Kawakami, Y., et al., *BMP signaling during bone pattern determination in the developing limb.* Development, 1996. **122**(11): p. 3557-66.
205. Zou, H., et al., *Distinct roles of type I bone morphogenetic protein receptors in the formation and differentiation of cartilage.* Genes Dev, 1997. **11**(17): p. 2191-203.
206. Stottmann, R.W., et al., *BMP receptor IA is required in mammalian neural crest cells for development of the cardiac outflow tract and ventricular myocardium.* Development, 2004. **131**(9): p. 2205-18.
207. Araya, R., et al., *BMP signaling through BMPRIA in astrocytes is essential for proper cerebral angiogenesis and formation of the blood-brain-barrier.* Mol Cell Neurosci, 2008. **38**(3): p. 417-30.
208. Maeno, M., et al., *A truncated bone morphogenetic protein 4 receptor alters the fate of ventral mesoderm to dorsal mesoderm: roles of animal pole tissue in the development of ventral mesoderm.* Proc Natl Acad Sci U S A, 1994. **91**(22): p. 10260-4.
209. Suzuki, A., et al., *A truncated bone morphogenetic protein receptor affects dorsal-ventral patterning in the early Xenopus embryo.* Proc Natl Acad Sci U S A, 1994. **91**(22): p. 10255-9.
210. Katagiri, T., et al., *Bone morphogenetic protein-2 converts the differentiation pathway of C2C12 myoblasts into the osteoblast lineage.* J Cell Biol, 1994. **127**(6 Pt 1): p. 1755-66.
211. Namiki, M., et al., *A kinase domain-truncated type I receptor blocks bone morphogenetic protein-2-induced signal transduction in C2C12 myoblasts.* J Biol Chem, 1997. **272**(35): p. 22046-52.
212. Ishikawa, T., et al., *Truncated type II receptor for BMP-4 induces secondary axial structures in Xenopus embryos.* Biochem Biophys Res Commun, 1995. **216**(1): p. 26-33.
213. Deng, Z., et al., *Familial primary pulmonary hypertension (gene PPH1) is caused by mutations in the bone morphogenetic protein receptor-II gene.* Am J Hum Genet, 2000. **67**(3): p. 737-44.
214. Lane, K.B., et al., *Heterozygous germline mutations in BMPR2, encoding a TGF-beta receptor, cause familial primary pulmonary hypertension. The International PPH Consortium.* Nat Genet, 2000. **26**(1): p. 81-4.
215. Thomson, J.R., et al., *Sporadic primary pulmonary hypertension is associated with germline mutations of the gene encoding BMPR-II, a receptor member of the TGF-beta family.* J Med Genet, 2000. **37**(10): p. 741-5.
216. Nishihara, A., et al., *Functional heterogeneity of bone morphogenetic protein receptor-II mutants found in patients with primary pulmonary hypertension.* Mol Biol Cell, 2002. **13**(9): p. 3055-63.
217. Yang, J., et al., *Mutations in bone morphogenetic protein type II receptor cause dysregulation of Id gene expression in pulmonary artery smooth muscle cells: implications for familial pulmonary arterial hypertension.* Circ Res, 2008. **102**(10): p. 1212-21.
218. Yu, P.B., et al., *Bone morphogenetic protein (BMP) type II receptor deletion reveals BMP ligand-specific gain of signaling in pulmonary artery smooth muscle cells.* J Biol Chem, 2005. **280**(26): p. 24443-50.
219. Gilboa, L., et al., *Bone morphogenetic protein receptor complexes on the surface of live cells: a new oligomerization mode for serine/threonine kinase receptors.* Mol Biol Cell, 2000. **11**(3): p. 1023-35.

220. Henis, Y.I., et al., *The types II and III transforming growth factor-beta receptors form homo-oligomers.* J Cell Biol, 1994. **126**(1): p. 139-54.
221. Wells, R.G., et al., *Transforming growth factor-beta induces formation of a dithiothreitol-resistant type I/Type II receptor complex in live cells.* J Biol Chem, 1999. **274**(9): p. 5716-22.
222. Nohe, A., et al., *Effect of the distribution and clustering of the type I A BMP receptor (ALK3) with the type II BMP receptor on the activation of signalling pathways.* J Cell Sci, 2003. **116**(Pt 16): p. 3277-84.
223. Simons, K. and E. Ikonen, *Functional rafts in cell membranes.* Nature, 1997. **387**(6633): p. 569-72.
224. Simons, K. and D. Toomre, *Lipid rafts and signal transduction.* Nat Rev Mol Cell Biol, 2000. **1**(1): p. 31-9.
225. Di Guglielmo, G.M., et al., *Distinct endocytic pathways regulate TGF-beta receptor signalling and turnover.* Nat Cell Biol, 2003. **5**(5): p. 410-21.
226. Mitchell, H., et al., *Ligand-dependent and -independent transforming growth factor-beta receptor recycling regulated by clathrin-mediated endocytosis and Rab11.* Mol Biol Cell, 2004. **15**(9): p. 4166-78.
227. Hartung, A., et al., *Different routes of bone morphogenic protein (BMP) receptor endocytosis influence BMP signaling.* Mol Cell Biol, 2006. **26**(20): p. 7791-805.
228. Nohe, A., et al., *Dynamics and interaction of caveolin-1 isoforms with BMP-receptors.* J Cell Sci, 2005. **118**(Pt 3): p. 643-50.
229. Ramos, M., et al., *The BMP type II receptor is located in lipid rafts, including caveolae, of pulmonary endothelium in vivo and in vitro.* Vascul Pharmacol, 2006. **44**(1): p. 50-9.
230. Satow, R., et al., *Dullard promotes degradation and dephosphorylation of BMP receptors and is required for neural induction.* Dev Cell, 2006. **11**(6): p. 763-74.
231. Rudarakanchana, N., et al., *Functional analysis of bone morphogenetic protein type II receptor mutations underlying primary pulmonary hypertension.* Hum Mol Genet, 2002. **11**(13): p. 1517-25.
232. Andres, J.L., et al., *Membrane-anchored and soluble forms of betaglycan, a polymorphic proteoglycan that binds transforming growth factor-beta.* J Cell Biol, 1989. **109**(6 Pt 1): p. 3137-45.
233. Lopez-Casillas, F., et al., *Structure and expression of the membrane proteoglycan betaglycan, a component of the TGF-beta receptor system.* Cell, 1991. **67**(4): p. 785-95.
234. Wang, X.F., et al., *Expression cloning and characterization of the TGF-beta type III receptor.* Cell, 1991. **67**(4): p. 797-805.
235. Lopez-Casillas, F., et al., *Betaglycan can act as a dual modulator of TGF-beta access to signaling receptors: mapping of ligand binding and GAG attachment sites.* J Cell Biol, 1994. **124**(4): p. 557-68.
236. Lopez-Casillas, F., J.L. Wrana, and J. Massague, *Betaglycan presents ligand to the TGF beta signaling receptor.* Cell, 1993. **73**(7): p. 1435-44.
237. Kirkbride, K.C., et al., *Bone morphogenetic proteins signal through the transforming growth factor-beta type III receptor.* J Biol Chem, 2008. **283**(12): p. 7628-37.
238. Cheifetz, S., et al., *Endoglin is a component of the transforming growth factor-beta receptor system in human endothelial cells.* J Biol Chem, 1992. **267**(27): p. 19027-30.
239. Barbara, N.P., J.L. Wrana, and M. Letarte, *Endoglin is an accessory protein that interacts with the signaling receptor complex of multiple members of the transforming growth factor-beta superfamily.* J Biol Chem, 1999. **274**(2): p. 584-94.
240. Scherner, O., et al., *Endoglin differentially modulates antagonistic transforming growth factor-beta1 and BMP-7 signaling.* J Biol Chem, 2007. **282**(19): p. 13934-43.
241. Onichtchouk, D., et al., *Silencing of TGF-beta signalling by the pseudoreceptor BAMBI.* Nature, 1999. **401**(6752): p. 480-5.
242. Grotewold, L., et al., *Bambi is coexpressed with Bmp-4 during mouse embryogenesis.* Mech Dev, 2001. **100**(2): p. 327-30.
243. Chen, J., et al., *The TGF-beta pseudoreceptor gene Bambi is dispensable for mouse embryonic development and postnatal survival.* Genesis, 2007. **45**(8): p. 482-6.
244. Halbrooks, P.J., et al., *Role of RGM coreceptors in bone morphogenetic protein signaling.* J Mol Signal, 2007. **2**: p. 4.
245. Samad, T.A., et al., *DRAGON, a bone morphogenetic protein co-receptor.* J Biol Chem, 2005. **280**(14): p. 14122-9.
246. Babitt, J.L., et al., *Repulsive guidance molecule (RGMa), a DRAGON homologue, is a bone morphogenetic protein co-receptor.* J Biol Chem, 2005. **280**(33): p. 29820-7.
247. Xia, Y., et al., *Repulsive guidance molecule RGMa alters utilization of bone morphogenetic protein (BMP) type II receptors by BMP2 and BMP4.* J Biol Chem, 2007. **282**(25): p. 18129-40.
248. Babitt, J.L., et al., *Bone morphogenetic protein signaling by hemojuvelin regulates hepcidin expression.* Nat Genet, 2006. **38**(5): p. 531-9.
249. Xia, Y., et al., *Hemojuvelin regulates hepcidin expression via a selective subset of BMP ligands and receptors independently of neogenin.* Blood, 2008. **111**(10): p. 5195-204.
250. Babitt, J.L., et al., *Modulation of bone morphogenetic protein signaling in vivo regulates systemic iron balance.* J Clin Invest, 2007. **117**(7): p. 1933-9.
251. Yu, P.B., et al., *Dorsomorphin inhibits BMP signals required for embryogenesis and iron metabolism.* Nat Chem Biol, 2008. **4**(1): p. 33-41.
252. Sammar, M., et al., *Modulation of GDF5/BRI-b signalling through interaction with the tyrosine kinase receptor Ror2.* Genes Cells, 2004. **9**(12): p. 1227-38.
253. Kurozumi, K., et al., *BRAM1, a BMP receptor-associated molecule involved in BMP signalling.* Genes Cells, 1998. **3**(4): p. 257-64.
254. Shibuya, H., et al., *Role of TAK1 and TAB1 in BMP signaling in early Xenopus development.* Embo J, 1998. **17**(4): p. 1019-28.
255. Yamaguchi, K., et al., *XIAP, a cellular member of the inhibitor of apoptosis protein family, links the receptors to TAB1-TAK1 in the BMP signaling pathway.* Embo J, 1999. **18**(1): p. 179-87.
256. Watanabe, H., et al., *Splicing factor 3b subunit 4 binds BMPR-IA and inhibits osteochondral cell differentiation.* J Biol Chem, 2007. **282**(28): p. 20728-38.
257. Lee-Hoeflich, S.T., et al., *Activation of LIMK1 by binding to the BMP receptor, BMPRII, regulates BMP-dependent dendritogenesis.* Embo J, 2004. **23**(24): p. 4792-801.
258. Matsuura, I., et al., *BMP inhibits neurite growth by a mechanism dependent on LIM-kinase.* Biochem Biophys Res Commun, 2007. **360**(4): p. 868-73.
259. Wen, Z., et al., *BMP gradients steer nerve growth cones by a balancing act of LIM kinase and Slingshot phosphatase on ADF/cofilin.* J Cell Biol, 2007. **178**(1): p. 107-19.

260. Eaton, B.A. and G.W. Davis, *LIM Kinase1 controls synaptic stability downstream of the type II BMP receptor.* Neuron, 2005. **47**(5): p. 695-708.
261. Machado, R.D., et al., *Functional interaction between BMPR-II and Tctex-1, a light chain of Dynein, is isoform-specific and disrupted by mutations underlying primary pulmonary hypertension.* Hum Mol Genet, 2003. **12**(24): p. 3277-86.
262. Meng, Q., et al., *Identification of Tctex2beta, a novel dynein light chain family member that interacts with different transforming growth factor-beta receptors.* J Biol Chem, 2006. **281**(48): p. 37069-80.
263. Tang, Q., et al., *A novel transforming growth factor-beta receptor-interacting protein that is also a light chain of the motor protein dynein.* Mol Biol Cell, 2002. **13**(12): p. 4484-96.
264. Wong, W.K., J.A. Knowles, and J.H. Morse, *Bone morphogenetic protein receptor type II C-terminus interacts with c-Src: implication for a role in pulmonary arterial hypertension.* Am J Respir Cell Mol Biol, 2005. **33**(5): p. 438-46.
265. Hassel, S., et al., *Proteins associated with type II bone morphogenetic protein receptor (BMPR-II) and identified by two-dimensional gel electrophoresis and mass spectrometry.* Proteomics, 2004. **4**(5): p. 1346-58.
266. Hassel, S., et al., *Interaction and functional cooperation between the serine/threonine kinase bone morphogenetic protein type II receptor with the tyrosine kinase stem cell factor receptor.* J Cell Physiol, 2006. **206**(2): p. 457-67.
267. Marshall, C.J., et al., *Bone morphogenetic protein 4 modulates c-Kit expression and differentiation potential in murine embryonic aorta-gonad-mesonephros haematopoiesis in vitro.* Br J Haematol, 2007. **139**(2): p. 321-30.
268. Chan, M.C., et al., *A novel regulatory mechanism of the bone morphogenetic protein (BMP) signaling pathway Involving the carboxyl-terminal tail domain of BMP type II receptor.* Mol Cell Biol, 2007. **27**(16): p. 5776-89.
269. Zakrzewicz, A., et al., *Receptor for activated C-kinase 1, a novel interaction partner of type II bone morphogenetic protein receptor, regulates smooth muscle cell proliferation in pulmonary arterial hypertension.* Circulation, 2007. **115**(23): p. 2957-68.
270. Jin, W., et al., *TrkC binds to the bone morphogenetic protein type II receptor to suppress bone morphogenetic protein signaling.* Cancer Res, 2007. **67**(20): p. 9869-77.
271. Jin, W., et al., *TrkC binds to the type II TGF-beta receptor to suppress TGF-beta signaling.* Oncogene, 2007. **26**(55): p. 7684-91.
272. Liu, F., et al., *A human Mad protein acting as a BMP-regulated transcriptional activator.* Nature, 1996. **381**(6583): p. 620-3.
273. Lechleider, R.J., et al., *Targeted mutagenesis of Smad1 reveals an essential role in chorioallantoic fusion.* Dev Biol, 2001. **240**(1): p. 157-67.
274. Tremblay, K.D., N.R. Dunn, and E.J. Robertson, *Mouse embryos lacking Smad1 signals display defects in extra-embryonic tissues and germ cell formation.* Development, 2001. **128**(18): p. 3609-21.
275. Pangas, S.A., et al., *Conditional deletion of Smad1 and Smad5 in somatic cells of male and female gonads leads to metastatic tumor development in mice.* Mol Cell Biol, 2008. **28**(1): p. 248-57.
276. Hild, M., et al., *The smad5 mutation somitabun blocks Bmp2b signaling during early dorsoventral patterning of the zebrafish embryo.* Development, 1999. **126**(10): p. 2149-59.
277. Suzuki, A., et al., *Smad5 induces ventral fates in Xenopus embryo.* Dev Biol, 1997. **184**(2): p. 402-5.
278. Chang, H., et al., *Smad5 knockout mice die at mid-gestation due to multiple embryonic and extraembryonic defects.* Development, 1999. **126**(8): p. 1631-42.
279. Yang, X., et al., *Angiogenesis defects and mesenchymal apoptosis in mice lacking SMAD5.* Development, 1999. **126**(8): p. 1571-80.
280. Hester, M., et al., *Smad1 and Smad8 function similarly in mammalian central nervous system development.* Mol Cell Biol, 2005. **25**(11): p. 4683-92.
281. Watanabe, T.K., et al., *Cloning and characterization of a novel member of the human Mad gene family (MADH6).* Genomics, 1997. **42**(3): p. 446-51.
282. Hahn, S.A., et al., *DPC4, a candidate tumor suppressor gene at human chromosome 18q21.1.* Science, 1996. **271**(5247): p. 350-3.
283. Lagna, G., et al., *Partnership between DPC4 and SMAD proteins in TGF-beta signalling pathways.* Nature, 1996. **383**(6603): p. 832-6.
284. Zhang, Y., T. Musci, and R. Derynck, *The tumor suppressor Smad4/DPC 4 as a central mediator of Smad function.* Curr Biol, 1997. **7**(4): p. 270-6.
285. Sirard, C., et al., *The tumor suppressor gene Smad4/Dpc4 is required for gastrulation and later for anterior development of the mouse embryo.* Genes Dev, 1998. **12**(1): p. 107-19.
286. Yang, X., et al., *The tumor suppressor SMAD4/DPC4 is essential for epiblast proliferation and mesoderm induction in mice.* Proc Natl Acad Sci U S A, 1998. **95**(7): p. 3667-72.
287. Takaku, K., et al., *Intestinal tumorigenesis in compound mutant mice of both Dpc4 (Smad4) and Apc genes.* Cell, 1998. **92**(5): p. 645-56.
288. Takaku, K., et al., *Gastric and duodenal polyps in Smad4 (Dpc4) knockout mice.* Cancer Res, 1999. **59**(24): p. 6113-7.
289. Hata, A., et al., *Smad6 inhibits BMP/Smad1 signaling by specifically competing with the Smad4 tumor suppressor.* Genes Dev, 1998. **12**(2): p. 186-97.
290. Nakayama, T., et al., *Smad6 functions as an intracellular antagonist of some TGF-beta family members during Xenopus embryogenesis.* Genes Cells, 1998. **3**(6): p. 387-94.
291. Galvin, K.M., et al., *A role for smad6 in development and homeostasis of the cardiovascular system.* Nat Genet, 2000. **24**(2): p. 171-4.
292. Casellas, R. and A.H. Brivanlou, *Xenopus Smad7 inhibits both the activin and BMP pathways and acts as a neural inducer.* Dev Biol, 1998. **198**(1): p. 1-12.
293. Li, R., et al., *Deletion of exon I of SMAD7 in mice results in altered B cell responses.* J Immunol, 2006. **176**(11): p. 6777-84.
294. Hoodless, P.A., et al., *MADR1, a MAD-related protein that functions in BMP2 signaling pathways.* Cell, 1996. **85**(4): p. 489-500.
295. Kawai, S., et al., *Mouse smad8 phosphorylation downstream of BMP receptors ALK-2, ALK-3, and ALK-6 induces its association with Smad4 and transcriptional activity.* Biochem Biophys Res Commun, 2000. **271**(3): p. 682-7.
296. Yamamoto, N., et al., *Smad1 and smad5 act downstream of intracellular signalings of BMP-2 that inhibits myogenic differentiation and induces osteoblast differentiation in C2C12 myoblasts.* Biochem Biophys Res Commun, 1997. **238**(2): p. 574-80.
297. Hayashi, K., et al., *SMAD1 signaling is critical for initial commitment of germ cell lineage from mouse epiblast.* Mech Dev, 2002. **118**(1-2): p. 99-109.

298. Umans, L., et al., *Inactivation of Smad5 in endothelial cells and smooth muscle cells demonstrates that Smad5 is required for cardiac homeostasis.* Am J Pathol, 2007. **170**(5): p. 1460-72.
299. Liu, X., et al., *Transforming growth factor beta signaling through Smad1 in human breast cancer cells.* Cancer Res, 1998. **58**(20): p. 4752-7.
300. Yue, J., R.S. Frey, and K.M. Mulder, *Cross-talk between the Smad1 and Ras/MEK signaling pathways for TGFbeta.* Oncogene, 1999. **18**(11): p. 2033-7.
301. Katsuno, Y., et al., *Bone morphogenetic protein signaling enhances invasion and bone metastasis of breast cancer cells through Smad pathway.* Oncogene, 2008.
302. McReynolds, L.J., et al., *Smad1 and Smad5 differentially regulate embryonic hematopoiesis.* Blood, 2007. **110**(12): p. 3881-90.
303. Bruno, E., et al., *The Smad5 gene is involved in the intracellular signaling pathways that mediate the inhibitory effects of transforming growth factor-beta on human hematopoiesis.* Blood, 1998. **91**(6): p. 1917-23.
304. Liu, B., et al., *Disruption of Smad5 gene leads to enhanced proliferation of high-proliferative potential precursors during embryonic hematopoiesis.* Blood, 2003. **101**(1): p. 124-33.
305. Nishimura, R., et al., *Smad5 and DPC4 are key molecules in mediating BMP-2-induced osteoblastic differentiation of the pluripotent mesenchymal precursor cell line C2C12.* J Biol Chem, 1998. **273**(4): p. 1872-9.
306. Kretzschmar, M., et al., *The TGF-beta family mediator Smad1 is phosphorylated directly and activated functionally by the BMP receptor kinase.* Genes Dev, 1997. **11**(8): p. 984-95.
307. Souchelnytskyi, S., et al., *Phosphorylation of Ser465 and Ser467 in the C terminus of Smad2 mediates interaction with Smad4 and is required for transforming growth factor-beta signaling.* J Biol Chem, 1997. **272**(44): p. 28107-15.
308. Qin, B.Y., et al., *Structural basis of Smad1 activation by receptor kinase phosphorylation.* Mol Cell, 2001. **8**(6): p. 1303-12.
309. Wu, J.W., et al., *Formation of a stable heterodimer between Smad2 and Smad4.* J Biol Chem, 2001. **276**(23): p. 20688-94.
310. Wu, J.W., et al., *Crystal structure of a phosphorylated Smad2. Recognition of phosphoserine by the MH2 domain and insights on Smad function in TGF-beta signaling.* Mol Cell, 2001. **8**(6): p. 1277-89.
311. Chacko, B.M., et al., *The L3 loop and C-terminal phosphorylation jointly define Smad protein trimerization.* Nat Struct Biol, 2001. **8**(3): p. 248-53.
312. Chacko, B.M., et al., *Structural basis of heteromeric smad protein assembly in TGF-beta signaling.* Mol Cell, 2004. **15**(5): p. 813-23.
313. Kawabata, M., et al., *Smad proteins exist as monomers in vivo and undergo homo- and hetero-oligomerization upon activation by serine/threonine kinase receptors.* Embo J, 1998. **17**(14): p. 4056-65.
314. Jayaraman, L. and J. Massague, *Distinct oligomeric states of SMAD proteins in the transforming growth factor-beta pathway.* J Biol Chem, 2000. **275**(52): p. 40710-7.
315. Inman, G.J. and C.S. Hill, *Stoichiometry of active smad-transcription factor complexes on DNA.* J Biol Chem, 2002. **277**(52): p. 51008-16.
316. Hata, A., et al., *Mutations increasing autoinhibition inactivate tumour suppressors Smad2 and Smad4.* Nature, 1997. **388**(6637): p. 82-7.
317. Zhu, H., et al., *A SMAD ubiquitin ligase targets the BMP pathway and affects embryonic pattern formation.* Nature, 1999. **400**(6745): p. 687-93.
318. Sangadala, S., R.P. Metpally, and B.V. Reddy, *Molecular interaction between Smurf1 WW2 domain and PPXY motifs of Smad1, Smad5, and Smad6--modeling and analysis.* J Biomol Struct Dyn, 2007. **25**(1): p. 11-23.
319. Ying, S.X., Z.J. Hussain, and Y.E. Zhang, *Smurf1 facilitates myogenic differentiation and antagonizes the bone morphogenetic protein-2-induced osteoblast conversion by targeting Smad5 for degradation.* J Biol Chem, 2003. **278**(40): p. 39029-36.
320. Lin, X., M. Liang, and X.H. Feng, *Smurf2 is a ubiquitin E3 ligase mediating proteasome-dependent degradation of Smad2 in transforming growth factor-beta signaling.* J Biol Chem, 2000. **275**(47): p. 36818-22.
321. Zhang, Y., et al., *Regulation of Smad degradation and activity by Smurf2, an E3 ubiquitin ligase.* Proc Natl Acad Sci U S A, 2001. **98**(3): p. 974-9.
322. Zhao, M., et al., *Smurf1 inhibits osteoblast differentiation and bone formation in vitro and in vivo.* J Biol Chem, 2004. **279**(13): p. 12854-9.
323. Li, L., et al., *CHIP mediates degradation of Smad proteins and potentially regulates Smad-induced transcription.* Mol Cell Biol, 2004. **24**(2): p. 856-64.
324. Li, R.F., et al., *Differential ubiquitination of Smad1 mediated by CHIP: implications in the regulation of the bone morphogenetic protein signaling pathway.* J Mol Biol, 2007. **374**(3): p. 777-90.
325. Li, J. and W.X. Li, *A novel function of Drosophila eIF4A as a negative regulator of Dpp/BMP signalling that mediates SMAD degradation.* Nat Cell Biol, 2006. **8**(12): p. 1407-14.
326. Inoue, Y., et al., *Smad3 is acetylated by p300/CBP to regulate its transactivation activity.* Oncogene, 2007. **26**(4): p. 500-8.
327. Simonsson, M., et al., *The DNA binding activities of Smad2 and Smad3 are regulated by coactivator-mediated acetylation.* J Biol Chem, 2006. **281**(52): p. 39870-80.
328. Tu, A.W. and K. Luo, *Acetylation of Smad2 by the co-activator p300 regulates activin and transforming growth factor beta response.* J Biol Chem, 2007. **282**(29): p. 21187-96.
329. Hidetoshi, H., *Smad1 is Acetylated by p300/CBP to Regulate its Stability.* Seikagaku, 2006.
330. Kretzschmar, M., J. Doody, and J. Massague, *Opposing BMP and EGF signalling pathways converge on the TGF-beta family mediator Smad1.* Nature, 1997. **389**(6651): p. 618-22.
331. Pera, E.M., et al., *Integration of IGF, FGF, and anti-BMP signals via Smad1 phosphorylation in neural induction.* Genes Dev, 2003. **17**(24): p. 3023-8.
332. Sapkota, G., et al., *Balancing BMP signaling through integrated inputs into the Smad1 linker.* Mol Cell, 2007. **25**(3): p. 441-54.
333. Fuentealba, L.C., et al., *Integrating patterning signals: Wnt/GSK3 regulates the duration of the BMP/Smad1 signal.* Cell, 2007. **131**(5): p. 980-93.
334. Chen, H.B., et al., *Identification of phosphatases for Smad in the BMP/DPP pathway.* Genes Dev, 2006. **20**(6): p. 648-53.
335. Duan, X., et al., *Protein serine/threonine phosphatase PPM1A dephosphorylates Smad1 in the bone morphogenetic protein signaling pathway.* J Biol Chem, 2006. **281**(48): p. 36526-32.

336. Lin, X., et al., *PPM1A functions as a Smad phosphatase to terminate TGFbeta signaling.* Cell, 2006. **125**(5): p. 915-28.
337. Sapkota, G., et al., *Dephosphorylation of the linker regions of Smad1 and Smad2/3 by small C-terminal domain phosphatases has distinct outcomes for bone morphogenetic protein and transforming growth factor-beta pathways.* J Biol Chem, 2006. **281**(52): p. 40412-9.
338. Wrighton, K.H., et al., *Small C-terminal domain phosphatases dephosphorylate the regulatory linker regions of Smad2 and Smad3 to enhance transforming growth factor-beta signaling.* J Biol Chem, 2006. **281**(50): p. 38365-75.
339. Knockaert, M., et al., *Unique players in the BMP pathway: small C-terminal domain phosphatases dephosphorylate Smad1 to attenuate BMP signaling.* Proc Natl Acad Sci U S A, 2006. **103**(32): p. 11940-5.
340. Shi, W., et al., *Endofin acts as a Smad anchor for receptor activation in BMP signaling.* J Cell Sci, 2007. **120**(Pt 7): p. 1216-24.
341. Chen, Y.G., et al., *Endofin, a FYVE domain protein, interacts with Smad4 and facilitates transforming growth factor-beta signaling.* J Biol Chem, 2007. **282**(13): p. 9688-95.
342. Tsukazaki, T., et al., *SARA, a FYVE domain protein that recruits Smad2 to the TGFbeta receptor.* Cell, 1998. **95**(6): p. 779-91.
343. Wu, G., et al., *Structural basis of Smad2 recognition by the Smad anchor for receptor activation.* Science, 2000. **287**(5450): p. 92-7.
344. Miura, S., et al., *Hgs (Hrs), a FYVE domain protein, is involved in Smad signaling through cooperation with SARA.* Mol Cell Biol, 2000. **20**(24): p. 9346-55.
345. Peterson, R.S., et al., *CD44 modulates Smad1 activation in the BMP-7 signaling pathway.* J Cell Biol, 2004. **166**(7): p. 1081-91.
346. Osada, S., S.Y. Ohmori, and M. Taira, *XMAN1, an inner nuclear membrane protein, antagonizes BMP signaling by interacting with Smad1 in Xenopus embryos.* Development, 2003. **130**(9): p. 1783-94.
347. Pan, D., et al., *The integral inner nuclear membrane protein MAN1 physically interacts with the R-Smad proteins to repress signaling by the transforming growth factor-{beta} superfamily of cytokines.* J Biol Chem, 2005. **280**(16): p. 15992-6001.
348. Raju, G.P., et al., *SANE, a novel LEM domain protein, regulates bone morphogenetic protein signaling through interaction with Smad1.* J Biol Chem, 2003. **278**(1): p. 428-37.
349. Bengtsson, L., *What MAN1 does to the Smads. TGFbeta/BMP signaling and the nuclear envelope.* Febs J, 2007. **274**(6): p. 1374-82.
350. Cohen, T.V., O. Kosti, and C.L. Stewart, *The nuclear envelope protein MAN1 regulates TGFbeta signaling and vasculogenesis in the embryonic yolk sac.* Development, 2007. **134**(7): p. 1385-95.
351. Ishimura, A., et al., *Man1, an inner nuclear membrane protein, regulates vascular remodeling by modulating transforming growth factor beta signaling.* Development, 2006. **133**(19): p. 3919-28.
352. Van Berlo, J.H., et al., *A-type lamins are essential for TGF-beta1 induced PP2A to dephosphorylate transcription factors.* Hum Mol Genet, 2005. **14**(19): p. 2839-49.
353. Schutte, M., et al., *DPC4 gene in various tumor types.* Cancer Res, 1996. **56**(11): p. 2527-30.
354. Howell, M., et al., *Xenopus Smad4beta is the co-Smad component of developmentally regulated transcription factor complexes responsible for induction of early mesodermal genes.* Dev Biol, 1999. **214**(2): p. 354-69.
355. Masuyama, N., et al., *Identification of two Smad4 proteins in Xenopus. Their common and distinct properties.* J Biol Chem, 1999. **274**(17): p. 12163-70.
356. de Caestecker, M.P., et al., *Characterization of functional domains within Smad4/DPC4.* J Biol Chem, 1997. **272**(21): p. 13690-6.
357. Qin, B., S.S. Lam, and K. Lin, *Crystal structure of a transcriptionally active Smad4 fragment.* Structure, 1999. **7**(12): p. 1493-503.
358. Tada, K., et al., *Region between alpha-helices 3 and 4 of the mad homology 2 domain of Smad4: functional roles in oligomer formation and transcriptional activation.* Genes Cells, 1999. **4**(12): p. 731-41.
359. Roelen, B.A., et al., *Phosphorylation of threonine 276 in Smad4 is involved in transforming growth factor-beta-induced nuclear accumulation.* Am J Physiol Cell Physiol, 2003. **285**(4): p. C823-30.
360. Moren, A., et al., *Degradation of the tumor suppressor Smad4 by WW and HECT domain ubiquitin ligases.* J Biol Chem, 2005. **280**(23): p. 22115-23.
361. Moren, A., et al., *Differential ubiquitination defines the functional status of the tumor suppressor Smad4.* J Biol Chem, 2003. **278**(35): p. 33571-82.
362. Xu, J. and L. Attisano, *Mutations in the tumor suppressors Smad2 and Smad4 inactivate transforming growth factor beta signaling by targeting Smads to the ubiquitin-proteasome pathway.* Proc Natl Acad Sci U S A, 2000. **97**(9): p. 4820-5.
363. Lee, P.S., et al., *Sumoylation of Smad4, the common Smad mediator of transforming growth factor-beta family signaling.* J Biol Chem, 2003. **278**(30): p. 27853-63.
364. Lin, X., et al., *SUMO-1/Ubc9 promotes nuclear accumulation and metabolic stability of tumor suppressor Smad4.* J Biol Chem, 2003. **278**(33): p. 31043-8.
365. Lin, X., et al., *Activation of transforming growth factor-beta signaling by SUMO-1 modification of tumor suppressor Smad4/DPC4.* J Biol Chem, 2003. **278**(21): p. 18714-9.
366. Shimada, K., et al., *Ubc9 promotes the stability of Smad4 and the nuclear accumulation of Smad1 in osteoblast-like Saos-2 cells.* Bone, 2008. **42**(5): p. 886-93.
367. Chang, C.C., et al., *Daxx mediates the small ubiquitin-like modifier-dependent transcriptional repression of Smad4.* J Biol Chem, 2005. **280**(11): p. 10164-73.
368. Long, J., et al., *Repression of Smad4 transcriptional activity by SUMO modification.* Biochem J, 2004. **379**(Pt 1): p. 23-9.
369. Dai, F., et al., *Erbin inhibits transforming growth factor beta signaling through a novel Smad-interacting domain.* Mol Cell Biol, 2007. **27**(17): p. 6183-94.
370. Afrakhte, M., et al., *Induction of inhibitory Smad6 and Smad7 mRNA by TGF-beta family members.* Biochem Biophys Res Commun, 1998. **249**(2): p. 505-11.
371. Ishida, W., et al., *Smad6 is a Smad1/5-induced smad inhibitor. Characterization of bone morphogenetic protein-responsive element in the mouse Smad6 promoter.* J Biol Chem, 2000. **275**(9): p. 6075-9.
372. Takase, M., et al., *Induction of Smad6 mRNA by bone morphogenetic proteins.* Biochem Biophys Res Commun, 1998. **244**(1): p. 26-9.

373. Wang, Q., et al., *Bone morphogenetic protein 2 activates Smad6 gene transcription through bone-specific transcription factor Runx2.* J Biol Chem, 2007. **282**(14): p. 10742-8.
374. Hanyu, A., et al., *The N domain of Smad7 is essential for specific inhibition of transforming growth factor-beta signaling.* J Cell Biol, 2001. **155**(6): p. 1017-27.
375. Murakami, G., et al., *Cooperative inhibition of bone morphogenetic protein signaling by Smurf1 and inhibitory Smads.* Mol Biol Cell, 2003. **14**(7): p. 2809-17.
376. Horiki, M., et al., *Smad6/Smurf1 overexpression in cartilage delays chondrocyte hypertrophy and causes dwarfism with osteopenia.* J Cell Biol, 2004. **165**(3): p. 433-45.
377. Bai, S., et al., *Smad6 as a transcriptional corepressor.* J Biol Chem, 2000. **275**(12): p. 8267-70.
378. Lin, X., et al., *Smad6 recruits transcription corepressor CtBP to repress bone morphogenetic protein-induced transcription.* Mol Cell Biol, 2003. **23**(24): p. 9081-93.
379. Nakao, A., et al., *Identification of Smad7, a TGFbeta-inducible antagonist of TGF-beta signalling.* Nature, 1997. **389**(6651): p. 631-5.
380. Ebisawa, T., et al., *Smurf1 interacts with transforming growth factor-beta type I receptor through Smad7 and induces receptor degradation.* J Biol Chem, 2001. **276**(16): p. 12477-80.
381. Kavsak, P., et al., *Smad7 binds to Smurf2 to form an E3 ubiquitin ligase that targets the TGF beta receptor for degradation.* Mol Cell, 2000. **6**(6): p. 1365-75.
382. Souchelnytskyi, S., et al., *Physical and functional interaction of murine and Xenopus Smad7 with bone morphogenetic protein receptors and transforming growth factor-beta receptors.* J Biol Chem, 1998. **273**(39): p. 25364-70.
383. Shi, W., et al., *GADD34-PP1C recruited by Smad7 dephosphorylates TGF{beta} type I receptor.* J Cell Biol, 2004. **164**(2): p. 291-300.
384. Koinuma, D., et al., *Arkadia amplifies TGF-beta superfamily signalling through degradation of Smad7.* Embo J, 2003. **22**(24): p. 6458-70.
385. Fukasawa, H., et al., *Down-regulation of Smad7 expression by ubiquitin-dependent degradation contributes to renal fibrosis in obstructive nephropathy in mice.* Proc Natl Acad Sci U S A, 2004. **101**(23): p. 8687-92.
386. Gronroos, E., et al., *Control of Smad7 stability by competition between acetylation and ubiquitination.* Mol Cell, 2002. **10**(3): p. 483-93.
387. Simonsson, M., et al., *The balance between acetylation and deacetylation controls Smad7 stability.* J Biol Chem, 2005. **280**(23): p. 21797-803.
388. Itoh, F., et al., *Promoting bone morphogenetic protein signaling through negative regulation of inhibitory Smads.* Embo J, 2001. **20**(15): p. 4132-42.
389. Torregroza, I. and T. Evans, *Tid1 is a Smad-binding protein that can modulate Smad7 activity in developing embryos.* Biochem J, 2006. **393**(Pt 1): p. 311-20.
390. Nicolas, F.J., et al., *Analysis of Smad nucleocytoplasmic shuttling in living cells.* J Cell Sci, 2004. **117**(Pt 18): p. 4113-25.
391. Pierreux, C.E., F.J. Nicolas, and C.S. Hill, *Transforming growth factor beta-independent shuttling of Smad4 between the cytoplasm and nucleus.* Mol Cell Biol, 2000. **20**(23): p. 9041-54.
392. Schmierer, B. and C.S. Hill, *Kinetic analysis of Smad nucleocytoplasmic shuttling reveals a mechanism for transforming growth factor beta-dependent nuclear accumulation of Smads.* Mol Cell Biol, 2005. **25**(22): p. 9845-58.
393. Xu, L., et al., *Smad2 nucleocytoplasmic shuttling by nucleoporins CAN/Nup214 and Nup153 feeds TGFbeta signaling complexes in the cytoplasm and nucleus.* Mol Cell, 2002. **10**(2): p. 271-82.
394. Watanabe, M., et al., *Regulation of intracellular dynamics of Smad4 by its leucine-rich nuclear export signal.* EMBO Rep, 2000. **1**(2): p. 176-82.
395. Xiao, Z., et al., *Nucleocytoplasmic shuttling of Smad1 conferred by its nuclear localization and nuclear export signals.* J Biol Chem, 2001. **276**(42): p. 39404-10.
396. Xu, L., et al., *Msk is required for nuclear import of TGF-beta/BMP-activated Smads.* J Cell Biol, 2007. **178**(6): p. 981-94.
397. Kurisaki, A., et al., *Transforming growth factor-beta induces nuclear import of Smad3 in an importin-beta1 and Ran-dependent manner.* Mol Biol Cell, 2001. **12**(4): p. 1079-91.
398. Xiao, Z., X. Liu, and H.F. Lodish, *Importin beta mediates nuclear translocation of Smad 3.* J Biol Chem, 2000. **275**(31): p. 23425-8.
399. Xu, L., et al., *Distinct domain utilization by Smad3 and Smad4 for nucleoporin interaction and nuclear import.* J Biol Chem, 2003. **278**(43): p. 42569-77.
400. Kurisaki, A., et al., *The mechanism of nuclear export of Smad3 involves exportin 4 and Ran.* Mol Cell Biol, 2006. **26**(4): p. 1318-32.
401. Xiao, Z., R. Latek, and H.F. Lodish, *An extended bipartite nuclear localization signal in Smad4 is required for its nuclear import and transcriptional activity.* Oncogene, 2003. **22**(7): p. 1057-69.
402. Itoh, S., et al., *Transforming growth factor beta1 induces nuclear export of inhibitory Smad7.* J Biol Chem, 1998. **273**(44): p. 29195-201.
403. Lopez-Rovira, T., et al., *Direct binding of Smad1 and Smad4 to two distinct motifs mediates bone morphogenetic protein-specific transcriptional activation of Id1 gene.* J Biol Chem, 2002. **277**(5): p. 3176-85.
404. Henningfeld, K.A., et al., *Autoregulation of Xvent-2B; direct interaction and functional cooperation of Xvent-2 and Smad1.* J Biol Chem, 2002. **277**(3): p. 2097-103.
405. Henningfeld, K.A., et al., *Smad1 and Smad4 are components of the bone morphogenetic protein-4 (BMP-4)-induced transcription complex of the Xvent-2B promoter.* J Biol Chem, 2000. **275**(29): p. 21827-35.
406. Graham, A., et al., *The signalling molecule BMP4 mediates apoptosis in the rhombencephalic neural crest.* Nature, 1994. **372**(6507): p. 684-6.
407. Vainio, S., et al., *Identification of BMP-4 as a signal mediating secondary induction between epithelial and mesenchymal tissues during early tooth development.* Cell, 1993. **75**(1): p. 45-58.
408. Hata, K., et al., *Differential roles of Smad1 and p38 kinase in regulation of peroxisome proliferator-activating receptor gamma during bone morphogenetic protein 2-induced adipogenesis.* Mol Biol Cell, 2003. **14**(2): p. 545-55.
409. Shi, Y., et al., *Crystal structure of a Smad MH1 domain bound to DNA: insights on DNA binding in TGF-beta signaling.* Cell, 1998. **94**(5): p. 585-94.
410. Zawel, L., et al., *Human Smad3 and Smad4 are sequence-specific transcription activators.* Mol Cell, 1998. **1**(4): p. 611-7.
411. Zhang, Y.W., et al., *A RUNX2/PEBP2alpha A/CBFA1 mutation displaying impaired transactivation and Smad interaction in cleidocranial dysplasia.* Proc Natl Acad Sci U S A, 2000. **97**(19): p. 10549-54.

412. Shi, X., et al., *Smad1 interacts with homeobox DNA-binding proteins in bone morphogenetic protein signaling.* J Biol Chem, 1999. **274**(19): p. 13711-7.
413. Wan, M., et al., *Transcriptional mechanisms of bone morphogenetic protein-induced osteoprotegrin gene expression.* J Biol Chem, 2001. **276**(13): p. 10119-25.
414. Zhou, B., et al., *MH1 domain of SMAD4 binds N-terminal residues of the homeodomain of Hoxc9.* Biochim Biophys Acta, 2008. **1784**(5): p. 747-52.
415. Chiba, S., et al., *Homeoprotein DLX-1 interacts with Smad4 and blocks a signaling pathway from activin A in hematopoietic cells.* Proc Natl Acad Sci U S A, 2003. **100**(26): p. 15577-82.
416. Berghorn, K.A., et al., *Smad6 represses Dlx3 transcriptional activity through inhibition of DNA binding.* J Biol Chem, 2006. **281**(29): p. 20357-67.
417. Hata, A., et al., *OAZ uses distinct DNA- and protein-binding zinc fingers in separate BMP-Smad and Olf signaling pathways.* Cell, 2000. **100**(2): p. 229-40.
418. Ku, M., et al., *OAZ regulates bone morphogenetic protein signaling through Smad6 activation.* J Biol Chem, 2006. **281**(8): p. 5277-87.
419. Ku, M.C., S. Stewart, and A. Hata, *Poly(ADP-ribose) polymerase 1 interacts with OAZ and regulates BMP-target genes.* Biochem Biophys Res Commun, 2003. **311**(3): p. 702-7.
420. Benchabane, H. and J.L. Wrana, *GATA- and Smad1-dependent enhancers in the Smad7 gene differentially interpret bone morphogenetic protein concentrations.* Mol Cell Biol, 2003. **23**(18): p. 6646-61.
421. Brown, C.O., 3rd, et al., *The cardiac determination factor, Nkx2-5, is activated by mutual cofactors GATA-4 and Smad1/4 via a novel upstream enhancer.* J Biol Chem, 2004. **279**(11): p. 10659-69.
422. Lee, K.H., et al., *SMAD-mediated modulation of YY1 activity regulates the BMP response and cardiac-specific expression of a GATA4/5/6-dependent chick Nkx2.5 enhancer.* Development, 2004. **131**(19): p. 4709-23.
423. Kurisaki, K., et al., *Nuclear factor YY1 inhibits transforming growth factor beta- and bone morphogenetic protein-induced cell differentiation.* Mol Cell Biol, 2003. **23**(13): p. 4494-510.
424. Jin, W., et al., *Schnurri-2 controls BMP-dependent adipogenesis via interaction with Smad proteins.* Dev Cell, 2006. **10**(4): p. 461-71.
425. Saita, Y., et al., *Lack of Schnurri-2 expression associates with reduced bone remodeling and osteopenia.* J Biol Chem, 2007. **282**(17): p. 12907-15.
426. Yao, L.C., et al., *Schnurri transcription factors from Drosophila and vertebrates can mediate Bmp signaling through a phylogenetically conserved mechanism.* Development, 2006. **133**(20): p. 4025-34.
427. Monzen, K., et al., *Smads, TAK1, and their common target ATF-2 play a critical role in cardiomyocyte differentiation.* J Cell Biol, 2001. **153**(4): p. 687-98.
428. Sano, Y., et al., *ATF-2 is a common nuclear target of Smad and TAK1 pathways in transforming growth factor-beta signaling.* J Biol Chem, 1999. **274**(13): p. 8949-57.
429. Suzuki, A., et al., *Nanog binds to Smad1 and blocks bone morphogenetic protein-induced differentiation of embryonic stem cells.* Proc Natl Acad Sci U S A, 2006. **103**(27): p. 10294-9.
430. Hu, M.C., T.D. Piscione, and N.D. Rosenblum, *Elevated SMAD1/beta-catenin molecular complexes and renal medullary cystic dysplasia in ALK3 transgenic mice.* Development, 2003. **130**(12): p. 2753-66.
431. Hu, M.C. and N.D. Rosenblum, *Smad1, beta-catenin and Tcf4 associate in a molecular complex with the Myc promoter in dysplastic renal tissue and cooperate to control Myc transcription.* Development, 2005. **132**(1): p. 215-25.
432. Yamamoto, T., F. Saatcioglu, and T. Matsuda, *Cross-talk between bone morphogenic proteins and estrogen receptor signaling.* Endocrinology, 2002. **143**(7): p. 2635-42.
433. Wu, L., et al., *Smad4 as a transcription corepressor for estrogen receptor alpha.* J Biol Chem, 2003. **278**(17): p. 15192-200.
434. Dahlqvist, C., et al., *Functional Notch signaling is required for BMP4-induced inhibition of myogenic differentiation.* Development, 2003. **130**(24): p. 6089-99.
435. Itoh, F., et al., *Synergy and antagonism between Notch and BMP receptor signaling pathways in endothelial cells.* Embo J, 2004. **23**(3): p. 541-51.
436. Xiao, C., et al., *Ecsit is required for Bmp signaling and mesoderm formation during mouse embryogenesis.* Genes Dev, 2003. **17**(23): p. 2933-49.
437. Feng, X.H., et al., *The tumor suppressor Smad4/DPC4 and transcriptional adaptor CBP/p300 are coactivators for smad3 in TGF-beta-induced transcriptional activation.* Genes Dev, 1998. **12**(14): p. 2153-63.
438. de Caestecker, M.P., et al., *The Smad4 activation domain (SAD) is a proline-rich, p300-dependent transcriptional activation domain.* J Biol Chem, 2000. **275**(3): p. 2115-22.
439. Ghosh-Choudhury, N., et al., *Concerted action of Smad and CREB-binding protein regulates bone morphogenetic protein-2-stimulated osteoblastic colony-stimulating factor-1 expression.* J Biol Chem, 2006. **281**(29): p. 20160-70.
440. Kahata, K., et al., *Regulation of transforming growth factor-beta and bone morphogenetic protein signalling by transcriptional coactivator GCN5.* Genes Cells, 2004. **9**(2): p. 143-51.
441. Shioda, T., et al., *Transcriptional activating activity of Smad4: roles of SMAD hetero-oligomerization and enhancement by an associating transactivator.* Proc Natl Acad Sci U S A, 1998. **95**(17): p. 9785-90.
442. Postigo, A.A., *Opposing functions of ZEB proteins in the regulation of the TGFbeta/BMP signaling pathway.* Embo J, 2003. **22**(10): p. 2443-52.
443. Postigo, A.A., et al., *Regulation of Smad signaling through a differential recruitment of coactivators and corepressors by ZEB proteins.* Embo J, 2003. **22**(10): p. 2453-62.
444. Verschueren, K., et al., *SIP1, a novel zinc finger/homeodomain repressor, interacts with Smad proteins and binds to 5'-CACCT sequences in candidate target genes.* J Biol Chem, 1999. **274**(29): p. 20489-98.
445. Bond, H.M., et al., *Early hematopoietic zinc finger protein (EHZF), the human homolog to mouse Evi3, is highly expressed in primitive human hematopoietic cells.* Blood, 2004. **103**(6): p. 2062-70.
446. Bai, R.Y., et al., *SMIF, a Smad4-interacting protein that functions as a co-activator in TGFbeta signalling.* Nat Cell Biol, 2002. **4**(3): p. 181-90.
447. Cho, G., et al., *Sizn1 is a novel protein that functions as a transcriptional coactivator of bone morphogenic protein signaling.* Mol Cell Biol, 2008. **28**(5): p. 1565-72.
448. Yoshida, Y., et al., *Negative regulation of BMP/Smad signaling by Tob in osteoblasts.* Cell, 2000. **103**(7): p. 1085-97.
449. Tzachanis, D., et al., *Tob is a negative regulator of activation that is expressed in anergic and quiescent T cells.* Nat Immunol, 2001. **2**(12): p. 1174-82.
450. Yoshida, Y., et al., *Tob proteins enhance inhibitory Smad-receptor interactions to repress BMP signaling.* Mech Dev, 2003. **120**(5): p. 629-37.

451. Jiao, K., Y. Zhou, and B.L. Hogan, *Identification of mZnf8, a mouse Kruppel-like transcriptional repressor, as a novel nuclear interaction partner of Smad1.* Mol Cell Biol, 2002. **22**(21): p. 7633-44.
452. Kim, R.H., et al., *A novel smad nuclear interacting protein, SNIP1, suppresses p300-dependent TGF-beta signal transduction.* Genes Dev, 2000. **14**(13): p. 1605-16.
453. Alliston, T., et al., *Repression of bone morphogenetic protein and activin-inducible transcription by Evi-1.* J Biol Chem, 2005. **280**(25): p. 24227-37.
454. Kurokawa, M., et al., *The oncoprotein Evi-1 represses TGF-beta signalling by inhibiting Smad3.* Nature, 1998. **394**(6688): p. 92-6.
455. Takeda, M., et al., *Interaction with Smad4 is indispensable for suppression of BMP signaling by c-Ski.* Mol Biol Cell, 2004. **15**(3): p. 963-72.
456. Wang, W., et al., *Ski represses bone morphogenic protein signaling in Xenopus and mammalian cells.* Proc Natl Acad Sci U S A, 2000. **97**(26): p. 14394-9.
457. Wu, J.W., et al., *Structural mechanism of Smad4 recognition by the nuclear oncoprotein Ski: insights on Ski-mediated repression of TGF-beta signaling.* Cell, 2002. **111**(3): p. 357-67.
458. Luo, K., et al., *The Ski oncoprotein interacts with the Smad proteins to repress TGFbeta signaling.* Genes Dev, 1999. **13**(17): p. 2196-206.
459. Barrio, R., et al., *Characterization of dSnoN and its relationship to Decapentaplegic signaling in Drosophila.* Dev Biol, 2007. **306**(1): p. 66-81.
460. Arndt, S., et al., *Fussel-15, a novel Ski/Sno homolog protein, antagonizes BMP signaling.* Mol Cell Neurosci, 2007. **34**(4): p. 603-11.
461. Chen, Z., et al., *MAP kinases.* Chem Rev, 2001. **101**(8): p. 2449-76.
462. Kendall, S.E., et al., *NRAGE mediates p38 activation and neural progenitor apoptosis via the bone morphogenetic protein signaling cascade.* Mol Cell Biol, 2005. **25**(17): p. 7711-24.
463. Yamaguchi, K., et al., *Identification of a member of the MAPKKK family as a potential mediator of TGF-beta signal transduction.* Science, 1995. **270**(5244): p. 2008-11.
464. Shirakabe, K., et al., *TAK1 mediates the ceramide signaling to stress-activated protein kinase/c-Jun N-terminal kinase.* J Biol Chem, 1997. **272**(13): p. 8141-4.
465. Ge, B., et al., *MAPKK-independent activation of p38alpha mediated by TAB1-dependent autophosphorylation of p38alpha.* Science, 2002. **295**(5558): p. 1291-4.
466. Lu, G., et al., *TAB-1 modulates intracellular localization of p38 MAP kinase and downstream signaling.* J Biol Chem, 2006. **281**(9): p. 6087-95.
467. Iwasaki, S., et al., *Specific activation of the p38 mitogen-activated protein kinase signaling pathway and induction of neurite outgrowth in PC12 cells by bone morphogenetic protein-2.* J Biol Chem, 1999. **274**(37): p. 26503-10.
468. Kimura, N., et al., *BMP2-induced apoptosis is mediated by activation of the TAK1-p38 kinase pathway that is negatively regulated by Smad6.* J Biol Chem, 2000. **275**(23): p. 17647-52.
469. Xu, R.H., et al., *Involvement of Ras/Raf/AP-1 in BMP-4 signaling during Xenopus embryonic development.* Proc Natl Acad Sci U S A, 1996. **93**(2): p. 834-8.
470. Palcy, S. and D. Goltzman, *Protein kinase signalling pathways involved in the up-regulation of the rat alpha1(I) collagen gene by transforming growth factor beta1 and bone morphogenetic protein 2 in osteoblastic cells.* Biochem J, 1999. **343 Pt 1**: p. 21-7.
471. Lou, J., et al., *Involvement of ERK in BMP-2 induced osteoblastic differentiation of mesenchymal progenitor cell line C3H10T1/2.* Biochem Biophys Res Commun, 2000. **268**(3): p. 757-62.
472. Gallea, S., et al., *Activation of mitogen-activated protein kinase cascades is involved in regulation of bone morphogenetic protein-2-induced osteoblast differentiation in pluripotent C2C12 cells.* Bone, 2001. **28**(5): p. 491-8.
473. Nakamura, K., et al., *p38 mitogen-activated protein kinase functionally contributes to chondrogenesis induced by growth/differentiation factor-5 in ATDC5 cells.* Exp Cell Res, 1999. **250**(2): p. 351-63.
474. Vinals, F., et al., *Inhibition of PI3K/p70 S6K and p38 MAPK cascades increases osteoblastic differentiation induced by BMP-2.* FEBS Lett, 2002. **510**(1-2): p. 99-104.
475. Guicheux, J., et al., *Activation of p38 mitogen-activated protein kinase and c-Jun-NH2-terminal kinase by BMP-2 and their implication in the stimulation of osteoblastic cell differentiation.* J Bone Miner Res, 2003. **18**(11): p. 2060-8.
476. Lai, C.F. and S.L. Cheng, *Signal transductions induced by bone morphogenetic protein-2 and transforming growth factor-beta in normal human osteoblastic cells.* J Biol Chem, 2002. **277**(18): p. 15514-22.
477. Goswami, M., A.R. Uzgare, and A.K. Sater, *Regulation of MAP kinase by the BMP-4/TAK1 pathway in Xenopus ectoderm.* Dev Biol, 2001. **236**(2): p. 259-70.
478. Lee, Y.S. and C.M. Chuong, *Activation of protein kinase A is a pivotal step involved in both BMP-2- and cyclic AMP-induced chondrogenesis.* J Cell Physiol, 1997. **170**(2): p. 153-65.
479. Hay, E., et al., *Bone morphogenetic protein-2 promotes osteoblast apoptosis through a Smad-independent, protein kinase C-dependent signaling pathway.* J Biol Chem, 2001. **276**(31): p. 29028-36.
480. Lemonnier, J., et al., *Protein kinase C-independent activation of protein kinase D is involved in BMP-2-induced activation of stress mitogen-activated protein kinases JNK and p38 and osteoblastic cell differentiation.* J Biol Chem, 2004. **279**(1): p. 259-64.
481. Ghosh-Choudhury, N., et al., *Requirement of BMP-2-induced phosphatidylinositol 3-kinase and Akt serine/threonine kinase in osteoblast differentiation and Smad-dependent BMP-2 gene transcription.* J Biol Chem, 2002. **277**(36): p. 33361-8.
482. Osyczka, A.M. and P.S. Leboy, *Bone morphogenetic protein regulation of early osteoblast genes in human marrow stromal cells is mediated by extracellular signal-regulated kinase and phosphatidylinositol 3-kinase signaling.* Endocrinology, 2005. **146**(8): p. 3428-37.
483. Tokuda, H., et al., *p38 MAP kinase regulates BMP-4-stimulated VEGF synthesis via p70 S6 kinase in osteoblasts.* Am J Physiol Endocrinol Metab, 2003. **284**(6): p. E1202-9.
484. Langenfeld, E.M., Y. Kong, and J. Langenfeld, *Bone morphogenetic protein-2-induced transformation involves the activation of mammalian target of rapamycin.* Mol Cancer Res, 2005. **3**(12): p. 679-84.
485. Hu, M.C., et al., *p38MAPK acts in the BMP7-dependent stimulatory pathway during epithelial cell morphogenesis and is regulated by Smad1.* J Biol Chem, 2004. **279**(13): p. 12051-9.
486. Nakayama, K., et al., *Receptor tyrosine kinases inhibit bone morphogenetic protein-Smad responsive promoter activity and differentiation of murine MC3T3-E1 osteoblast-like cells.* J Bone Miner Res, 2003. **18**(5): p. 827-35.
487. Suzawa, M., et al., *Stimulation of Smad1 transcriptional activity by Ras-extracellular signal-regulated kinase pathway: a possible mechanism for collagen-dependent osteoblastic differentiation.* J Bone Miner Res, 2002. **17**(2): p. 240-8.

488. Feng, J.Q., et al., *The mouse bone morphogenetic protein-4 gene. Analysis of promoter utilization in fetal rat calvarial osteoblasts and regulation by COUP-TFI orphan receptor.* J Biol Chem, 1995. **270**(47): p. 28364-73.
489. Helvering, L.M., et al., *Regulation of the promoters for the human bone morphogenetic protein 2 and 4 genes.* Gene, 2000. **256**(1-2): p. 123-38.
490. Ghosh-Choudhury, N., et al., *Autoregulation of mouse BMP-2 gene transcription is directed by the proximal promoter element.* Biochem Biophys Res Commun, 2001. **286**(1): p. 101-8.
491. Spinella-Jaegle, S., et al., *Opposite effects of bone morphogenetic protein-2 and transforming growth factor-beta1 on osteoblast differentiation.* Bone, 2001. **29**(4): p. 323-30.
492. Singhatanadgit, W., V. Salih, and I. Olsen, *Up-regulation of bone morphogenetic protein receptor IB by growth factors enhances BMP-2-induced human bone cell functions.* J Cell Physiol, 2006. **209**(3): p. 912-22.
493. Standal, T., et al., *HGF inhibits BMP-induced osteoblastogenesis: possible implications for the bone disease of multiple myeloma.* Blood, 2007. **109**(7): p. 3024-30.
494. Ducy, P., et al., *Osf2/Cbfa1: a transcriptional activator of osteoblast differentiation.* Cell, 1997. **89**(5): p. 747-54.
495. Komori, T., *Requisite roles of Runx2 and Cbfb in skeletal development.* J Bone Miner Metab, 2003. **21**(4): p. 193-7.
496. Banerjee, C., et al., *Differential regulation of the two principal Runx2/Cbfa1 n-terminal isoforms in response to bone morphogenetic protein-2 during development of the osteoblast phenotype.* Endocrinology, 2001. **142**(9): p. 4026-39.
497. Lee, K.S., et al., *Runx2 is a common target of transforming growth factor beta1 and bone morphogenetic protein 2, and cooperation between Runx2 and Smad5 induces osteoblast-specific gene expression in the pluripotent mesenchymal precursor cell line C2C12.* Mol Cell Biol, 2000. **20**(23): p. 8783-92.
498. Takazawa, Y., et al., *An osteogenesis-related transcription factor, core-binding factor A1, is constitutively expressed in the chondrocytic cell line TC6, and its expression is upregulated by bone morphogenetic protein-2.* J Endocrinol, 2000. **165**(3): p. 579-86.
499. Wu, X.B., et al., *Impaired osteoblastic differentiation, reduced bone formation, and severe osteoporosis in noggin-overexpressing mice.* J Clin Invest, 2003. **112**(6): p. 924-34.
500. Nakashima, K., et al., *The novel zinc finger-containing transcription factor osterix is required for osteoblast differentiation and bone formation.* Cell, 2002. **108**(1): p. 17-29.
501. Celil, A.B. and P.G. Campbell, *BMP-2 and insulin-like growth factor-I mediate Osterix (Osx) expression in human mesenchymal stem cells via the MAPK and protein kinase D signaling pathways.* J Biol Chem, 2005. **280**(36): p. 31353-9.
502. Celil, A.B., J.O. Hollinger, and P.G. Campbell, *Osx transcriptional regulation is mediated by additional pathways to BMP2/Smad signaling.* J Cell Biochem, 2005. **95**(3): p. 518-28.
503. Ulsamer, A., et al., *BMP-2 induces Osterix expression through up-regulation of Dlx5 and its phosphorylation by p38.* J Biol Chem, 2008. **283**(7): p. 3816-26.
504. Yagi, K., et al., *Bone morphogenetic protein-2 enhances osterix gene expression in chondrocytes.* J Cell Biochem, 2003. **88**(6): p. 1077-83.
505. Robledo, R.F., et al., *The Dlx5 and Dlx6 homeobox genes are essential for craniofacial, axial, and appendicular skeletal development.* Genes Dev, 2002. **16**(9): p. 1089-101.
506. Miyama, K., et al., *A BMP-inducible gene, dlx5, regulates osteoblast differentiation and mesoderm induction.* Dev Biol, 1999. **208**(1): p. 123-33.
507. Kim, Y.J., et al., *Bone morphogenetic protein-2-induced alkaline phosphatase expression is stimulated by Dlx5 and repressed by Msx2.* J Biol Chem, 2004. **279**(49): p. 50773-80.
508. Lee, M.H., et al., *BMP-2-induced Runx2 expression is mediated by Dlx5, and TGF-beta 1 opposes the BMP-2-induced osteoblast differentiation by suppression of Dlx5 expression.* J Biol Chem, 2003. **278**(36): p. 34387-94.
509. Lee, M.H., et al., *Dlx5 specifically regulates Runx2 type II expression by binding to homeodomain-response elements in the Runx2 distal promoter.* J Biol Chem, 2005. **280**(42): p. 35579-87.
510. Lee, M.H., et al., *BMP-2-induced Osterix expression is mediated by Dlx5 but is independent of Runx2.* Biochem Biophys Res Commun, 2003. **309**(3): p. 689-94.
511. Satokata, I., et al., *Msx2 deficiency in mice causes pleiotropic defects in bone growth and ectodermal organ formation.* Nat Genet, 2000. **24**(4): p. 391-5.
512. Wilkie, A.O., et al., *Functional haploinsufficiency of the human homeobox gene MSX2 causes defects in skull ossification.* Nat Genet, 2000. **24**(4): p. 387-90.
513. Brugger, S.M., et al., *A phylogenetically conserved cis-regulatory module in the Msx2 promoter is sufficient for BMP-dependent transcription in murine and Drosophila embryos.* Development, 2004. **131**(20): p. 5153-65.
514. Abdelmagid, S.M., et al., *Osteoactivin acts as downstream mediator of BMP-2 effects on osteoblast function.* J Cell Physiol, 2007. **210**(1): p. 26-37.
515. Selim, A.A., et al., *Anti-osteoactivin antibody inhibits osteoblast differentiation and function in vitro.* Crit Rev Eukaryot Gene Expr, 2003. **13**(2-4): p. 265-75.
516. Sammons, J., et al., *The role of BMP-6, IL-6, and BMP-4 in mesenchymal stem cell-dependent bone development: effects on osteoblastic differentiation induced by parathyroid hormone and vitamin D(3).* Stem Cells Dev, 2004. **13**(3): p. 273-80.
517. Tamura, Y., et al., *Focal adhesion kinase activity is required for bone morphogenetic protein--Smad1 signaling and osteoblastic differentiation in murine MC3T3-E1 cells.* J Bone Miner Res, 2001. **16**(10): p. 1772-9.
518. Yang, X.L., et al., *MFH-1 is required for bone morphogenetic protein-2-induced osteoblastic differentiation of C2C12 myoblasts.* FEBS Lett, 2000. **470**(1): p. 29-34.
519. Lengner, C.J., et al., *Nkx3.2-mediated repression of Runx2 promotes chondrogenic differentiation.* J Biol Chem, 2005. **280**(16): p. 15872-9.
520. Provot, S., et al., *Nkx3.2/Bapx1 acts as a negative regulator of chondrocyte maturation.* Development, 2006. **133**(4): p. 651-62.
521. Shirakawa, K., et al., *CCAAT/enhancer-binding protein homologous protein (CHOP) regulates osteoblast differentiation.* Mol Cell Biol, 2006. **26**(16): p. 6105-16.
522. Hayashi, M., et al., *Pitx2 prevents osteoblastic transdifferentiation of myoblasts by bone morphogenetic proteins.* J Biol Chem, 2008. **283**(1): p. 565-71.
523. Morinobu, M., et al., *The nucleocytoplasmic shuttling protein CIZ reduces adult bone mass by inhibiting bone morphogenetic protein-induced bone formation.* J Exp Med, 2005. **201**(6): p. 961-70.
524. Shen, Z.J., et al., *Negative regulation of bone morphogenetic protein/Smad signaling by Cas-interacting zinc finger protein in osteoblasts.* J Biol Chem, 2002. **277**(33): p. 29840-6.

525. Canalis, E. and B. Gabbitas, *Bone morphogenetic protein 2 increases insulin-like growth factor I and II transcripts and polypeptide levels in bone cell cultures.* J Bone Miner Res, 1994. **9**(12): p. 1999-2005.
526. Gong, Y., et al., *LDL receptor-related protein 5 (LRP5) affects bone accrual and eye development.* Cell, 2001. **107**(4): p. 513-23.
527. Hay, E., et al., *N- and E-cadherin mediate early human calvaria osteoblast differentiation promoted by bone morphogenetic protein-2.* J Cell Physiol, 2000. **183**(1): p. 117-28.
528. Varghese, S. and E. Canalis, *Regulation of collagenase-3 by bone morphogenetic protein-2 in bone cell cultures.* Endocrinology, 1997. **138**(3): p. 1035-40.
529. Lincoln, T.M., et al., *Regulation of vascular smooth muscle cell phenotype by cyclic GMP and cyclic GMP-dependent protein kinase.* Front Biosci, 2006. **11**: p. 356-67.
530. Dorai, H., S. Vukicevic, and T.K. Sampath, *Bone morphogenetic protein-7 (osteogenic protein-1) inhibits smooth muscle cell proliferation and stimulates the expression of markers that are characteristic of SMC phenotype in vitro.* J Cell Physiol, 2000. **184**(1): p. 37-45.
531. Nakaoka, T., et al., *Inhibition of rat vascular smooth muscle proliferation in vitro and in vivo by bone morphogenetic protein-2.* J Clin Invest, 1997. **100**(11): p. 2824-32.
532. Maciel, T.T., et al., *Gremlin promotes vascular smooth muscle cell proliferation and migration.* J Mol Cell Cardiol, 2008. **44**(2): p. 370-9.
533. Yang, X., et al., *Dysfunctional Smad signaling contributes to abnormal smooth muscle cell proliferation in familial pulmonary arterial hypertension.* Circ Res, 2005. **96**(10): p. 1053-63.
534. Lagna, G., et al., *BMP-dependent activation of caspase-9 and caspase-8 mediates apoptosis in pulmonary artery smooth muscle cells.* Am J Physiol Lung Cell Mol Physiol, 2006. **291**(5): p. L1059-67.
535. Zhang, S., et al., *Bone morphogenetic proteins induce apoptosis in human pulmonary vascular smooth muscle cells.* Am J Physiol Lung Cell Mol Physiol, 2003. **285**(3): p. L740-54.
536. Fantozzi, I., et al., *Bone morphogenetic protein-2 upregulates expression and function of voltage-gated K+ channels in human pulmonary artery smooth muscle cells.* Am J Physiol Lung Cell Mol Physiol, 2006. **291**(5): p. L993-1004.
537. Yang, X., et al., *BMP4 induces HO-1 via a Smad-independent, p38MAPK-dependent pathway in pulmonary artery myocytes.* Am J Respir Cell Mol Biol, 2007. **37**(5): p. 598-605.
538. Fantozzi, I., et al., *Divergent effects of BMP-2 on gene expression in pulmonary artery smooth muscle cells from normal subjects and patients with idiopathic pulmonary arterial hypertension.* Exp Lung Res, 2005. **31**(8): p. 783-806.
539. West, J., et al., *Pulmonary hypertension in transgenic mice expressing a dominant-negative BMPRII gene in smooth muscle.* Circ Res, 2004. **94**(8): p. 1109-14.
540. West, J., et al., *Suppression of type II bone morphogenic protein receptor in vascular smooth muscle induces pulmonary arterial hypertension in transgenic mice.* Chest, 2005. **128**(6 Suppl): p. 553S.
541. Davis, B.N., et al., *SMAD proteins control DROSHA-mediated microRNA maturation.* Nature, 2008. **454**(7200): p. 56-61.
542. Machado, R.D., et al., *BMPR2 haploinsufficiency as the inherited molecular mechanism for primary pulmonary hypertension.* Am J Hum Genet, 2001. **68**(1): p. 92-102.
543. Upton, P.D., et al., *Functional characterization of bone morphogenetic protein binding sites and Smad1/5 activation in human vascular cells.* Mol Pharmacol, 2008. **73**(2): p. 539-52.
544. Morrell, N.W. and M.R. Wilkins, *Genetic and molecular mechanisms of pulmonary hypertension.* Clin Med, 2001. **1**(2): p. 138-45.
545. Ihida-Stansbury, K., et al., *Tenascin-C is induced by mutated BMP type II receptors in familial forms of pulmonary arterial hypertension.* Am J Physiol Lung Cell Mol Physiol, 2006. **291**(4): p. L694-702.
546. Eddahibi, S., et al., *Serotonin transporter overexpression is responsible for pulmonary artery smooth muscle hyperplasia in primary pulmonary hypertension.* J Clin Invest, 2001. **108**(8): p. 1141-50.
547. Long, L., et al., *Serotonin increases susceptibility to pulmonary hypertension in BMPR2-deficient mice.* Circ Res, 2006. **98**(6): p. 818-27.
548. Hagen, M., et al., *Interaction of interleukin-6 and the BMP pathway in pulmonary smooth muscle.* Am J Physiol Lung Cell Mol Physiol, 2007. **292**(6): p. L1473-9.
549. Lawrie, A., et al., *Evidence of a role for osteoprotegerin in the pathogenesis of pulmonary arterial hypertension.* Am J Pathol, 2008. **172**(1): p. 256-64.
550. Zhang, J. and L. Li, *BMP signaling and stem cell regulation.* Dev Biol, 2005. **284**(1): p. 1-11.
551. James, D., et al., *TGFbeta/activin/nodal signaling is necessary for the maintenance of pluripotency in human embryonic stem cells.* Development, 2005. **132**(6): p. 1273-82.
552. Labbe, E., A. Letamendia, and L. Attisano, *Association of Smads with lymphoid enhancer binding factor 1/T cell-specific factor mediates cooperative signaling by the transforming growth factor-beta and wnt pathways.* Proc Natl Acad Sci U S A, 2000. **97**(15): p. 8358-63.
553. Sato, N., et al., *Maintenance of pluripotency in human and mouse embryonic stem cells through activation of Wnt signaling by a pharmacological GSK-3-specific inhibitor.* Nat Med, 2004. **10**(1): p. 55-63.
554. Gough, N.M. and R.L. Williams, *The pleiotropic actions of leukemia inhibitory factor.* Cancer Cells, 1989. **1**(3): p. 77-80.
555. Williams, R.L., et al., *Myeloid leukaemia inhibitory factor maintains the developmental potential of embryonic stem cells.* Nature, 1988. **336**(6200): p. 684-7.
556. Munoz-Sanjuan, I. and A.H. Brivanlou, *Neural induction, the default model and embryonic stem cells.* Nat Rev Neurosci, 2002. **3**(4): p. 271-80.
557. Ying, Q.L., et al., *BMP induction of Id proteins suppresses differentiation and sustains embryonic stem cell self-renewal in collaboration with STAT3.* Cell, 2003. **115**(3): p. 281-92.
558. Qi, X., et al., *BMP4 supports self-renewal of embryonic stem cells by inhibiting mitogen-activated protein kinase pathways.* Proc Natl Acad Sci U S A, 2004. **101**(16): p. 6027-32.
559. Amit, M., et al., *Clonally derived human embryonic stem cell lines maintain pluripotency and proliferative potential for prolonged periods of culture.* Dev Biol, 2000. **227**(2): p. 271-8.
560. Thomson, J.A., et al., *Embryonic stem cell lines derived from human blastocysts.* Science, 1998. **282**(5391): p. 1145-7.
561. Xu, R.H., et al., *Basic FGF and suppression of BMP signaling sustain undifferentiated proliferation of human ES cells.* Nat Methods, 2005. **2**(3): p. 185-90.
562. Xiao, L., X. Yuan, and S.J. Sharkis, *Activin A maintains self-renewal and regulates fibroblast growth factor, Wnt, and bone morphogenic protein pathways in human embryonic stem cells.* Stem Cells, 2006. **24**(6): p. 1476-86.

563. Yuasa, S., et al., *Transient inhibition of BMP signaling by Noggin induces cardiomyocyte differentiation of mouse embryonic stem cells.* Nat Biotechnol, 2005. **23**(5): p. 607-11.
564. Gouon-Evans, V., et al., *BMP-4 is required for hepatic specification of mouse embryonic stem cell-derived definitive endoderm.* Nat Biotechnol, 2006. **24**(11): p. 1402-11.
565. Koay, E.J., G.M. Hoben, and K.A. Athanasiou, *Tissue engineering with chondrogenically differentiated human embryonic stem cells.* Stem Cells, 2007. **25**(9): p. 2183-90.
566. Schofield, R., *The relationship between the spleen colony-forming cell and the haemopoietic stem cell.* Blood Cells, 1978. **4**(1-2): p. 7-25.
567. Zhang, J., et al., *Identification of the haematopoietic stem cell niche and control of the niche size.* Nature, 2003. **425**(6960): p. 836-41.
568. Puri, A., M.D. McGoon, and S.S. Kushwaha, *Pulmonary arterial hypertension: current therapeutic strategies.* Nat Clin Pract Cardiovasc Med, 2007. **4**(6): p. 319-29.
569. Atkinson, C., et al., *Primary pulmonary hypertension is associated with reduced pulmonary vascular expression of type II bone morphogenetic protein receptor.* Circulation, 2002. **105**(14): p. 1672-8.
570. Takeda, M., et al., *Characterization of the bone morphogenetic protein (BMP) system in human pulmonary arterial smooth muscle cells isolated from a sporadic case of primary pulmonary hypertension: roles of BMP type IB receptor (activin receptor-like kinase-6) in the mitotic action.* Endocrinology, 2004. **145**(9): p. 4344-54.
571. Reynolds, A.M., et al., *Bone morphogenetic protein type 2 receptor gene therapy attenuates hypoxic pulmonary hypertension.* Am J Physiol Lung Cell Mol Physiol, 2007. **292**(5): p. L1182-92.
572. Shore, E.M., et al., *A recurrent mutation in the BMP type I receptor ACVR1 causes inherited and sporadic fibrodysplasia ossificans progressiva.* Nat Genet, 2006. **38**(5): p. 525-7.
573. Glaser, D.L., et al., *In vivo somatic cell gene transfer of an engineered Noggin mutein prevents BMP4-induced heterotopic ossification.* J Bone Joint Surg Am, 2003. **85-A**(12): p. 2332-42.
574. Kaplan, F.S., et al., *Dysregulation of the BMP-4 signaling pathway in fibrodysplasia ossificans progressiva.* Ann N Y Acad Sci, 2006. **1068**: p. 54-65.
575. Gannon, F.H., et al., *Bone morphogenetic protein 2/4 in early fibromatous lesions of fibrodysplasia ossificans progressiva.* Hum Pathol, 1997. **28**(3): p. 339-43.
576. Shafritz, A.B., et al., *Overexpression of an osteogenic morphogen in fibrodysplasia ossificans progressiva.* N Engl J Med, 1996. **335**(8): p. 555-61.
577. Kan, L., et al., *Transgenic mice overexpressing BMP4 develop a fibrodysplasia ossificans progressiva (FOP)-like phenotype.* Am J Pathol, 2004. **165**(4): p. 1107-15.
578. O'Connell, M.P., et al., *HSPG modulation of BMP signaling in fibrodysplasia ossificans progressiva cells.* J Cell Biochem, 2007. **102**(6): p. 1493-503.
579. de la Pena, L.S., et al., *Fibrodysplasia ossificans progressiva (FOP), a disorder of ectopic osteogenesis, misregulates cell surface expression and trafficking of BMPRIA.* J Bone Miner Res, 2005. **20**(7): p. 1168-76.
580. Fiori, J.L., et al., *Dysregulation of the BMP-p38 MAPK signaling pathway in cells from patients with fibrodysplasia ossificans progressiva (FOP).* J Bone Miner Res, 2006. **21**(6): p. 902-9.
581. Shovlin, C.L., et al., *A gene for hereditary haemorrhagic telangiectasia maps to chromosome 9q3.* Nat Genet, 1994. **6**(2): p. 205-9.
582. Bobik, A., *Transforming growth factor-betas and vascular disorders.* Arterioscler Thromb Vasc Biol, 2006. **26**(8): p. 1712-20.
583. Johnson, D.W., et al., *A second locus for hereditary hemorrhagic telangiectasia maps to chromosome 12.* Genome Res, 1995. **5**(1): p. 21-8.
584. Vincent, P., et al., *A third locus for hereditary haemorrhagic telangiectasia maps to chromosome 12q.* Hum Mol Genet, 1995. **4**(5): p. 945-9.
585. Gallione, C.J., et al., *A combined syndrome of juvenile polyposis and hereditary haemorrhagic telangiectasia associated with mutations in MADH4 (SMAD4).* Lancet, 2004. **363**(9412): p. 852-9.
586. Harrison, R.E., et al., *Molecular and functional analysis identifies ALK-1 as the predominant cause of pulmonary hypertension related to hereditary haemorrhagic telangiectasia.* J Med Genet, 2003. **40**(12): p. 865-71.
587. Trembath, R.C., et al., *Clinical and molecular genetic features of pulmonary hypertension in patients with hereditary hemorrhagic telangiectasia.* N Engl J Med, 2001. **345**(5): p. 325-34.
588. Howe, J.R., et al., *Germline mutations of the gene encoding bone morphogenetic protein receptor 1A in juvenile polyposis.* Nat Genet, 2001. **28**(2): p. 184-7.
589. Kotzsch, A., et al., *Structure analysis of bone morphogenetic protein-2 type I receptor complexes reveals a mechanism of receptor inactivation in juvenile polyposis syndrome.* J Biol Chem, 2008. **283**(9): p. 5876-87.
590. Zhou, X.P., et al., *Germline mutations in BMPR1A/ALK3 cause a subset of cases of juvenile polyposis syndrome and of Cowden and Bannayan-Riley-Ruvalcaba syndromes.* Am J Hum Genet, 2001. **69**(4): p. 704-11.
591. Howe, J.R., et al., *Mutations in the SMAD4/DPC4 gene in juvenile polyposis.* Science, 1998. **280**(5366): p. 1086-8.
592. Haramis, A.P., et al., *De novo crypt formation and juvenile polyposis on BMP inhibition in mouse intestine.* Science, 2004. **303**(5664): p. 1684-6.
593. He, X.C., et al., *BMP signaling inhibits intestinal stem cell self-renewal through suppression of Wnt-beta-catenin signaling.* Nat Genet, 2004. **36**(10): p. 1117-21.
594. Huang, H.C. and P.S. Klein, *Interactions between BMP and Wnt signaling pathways in mammalian cancers.* Cancer Biol Ther, 2004. **3**(7): p. 676-8.
595. Bailey, J.M., P.K. Singh, and M.A. Hollingsworth, *Cancer metastasis facilitated by developmental pathways: Sonic hedgehog, Notch, and bone morphogenic proteins.* J Cell Biochem, 2007. **102**(4): p. 829-39.
596. Qiao, W., et al., *Hair follicle defects and squamous cell carcinoma formation in Smad4 conditional knockout mouse skin.* Oncogene, 2006. **25**(2): p. 207-17.
597. He, W., et al., *Smads mediate signaling of the TGFbeta superfamily in normal keratinocytes but are lost during skin chemical carcinogenesis.* Oncogene, 2001. **20**(4): p. 471-83.
598. Sneddon, J.B., et al., *Bone morphogenetic protein antagonist gremlin 1 is widely expressed by cancer-associated stromal cells and can promote tumor cell proliferation.* Proc Natl Acad Sci U S A, 2006. **103**(40): p. 14842-7.
599. Ming Kwan, K., et al., *Essential roles of BMPR-IA signaling in differentiation and growth of hair follicles and in skin tumorigenesis.* Genesis, 2004. **39**(1): p. 10-25.
600. Wen, X.Z., et al., *Frequent epigenetic silencing of the bone morphogenetic protein 2 gene through methylation in gastric carcinomas.* Oncogene, 2006. **25**(18): p. 2666-73.

601. Beck, S.E., et al., *Bone morphogenetic protein signaling and growth suppression in colon cancer.* Am J Physiol Gastrointest Liver Physiol, 2006. **291**(1): p. G135-45.
602. Grijelmo, C., et al., *Proinvasive activity of BMP-7 through SMAD4/src-independent and ERK/Rac/JNK-dependent signaling pathways in colon cancer cells.* Cell Signal, 2007. **19**(8): p. 1722-32.
603. Kodach, L.L., et al., *The bone morphogenetic protein pathway is active in human colon adenomas and inactivated in colorectal cancer.* Cancer, 2008. **112**(2): p. 300-6.
604. Mancino, M., et al., *Regulation of human Cripto-1 gene expression by TGF-beta1 and BMP-4 in embryonal and colon cancer cells.* J Cell Physiol, 2008. **215**(1): p. 192-203.
605. Yamada, N., et al., *Bone morphogenetic protein type IB receptor is progressively expressed in malignant glioma tumours.* Br J Cancer, 1996. **73**(5): p. 624-9.
606. Piccirillo, S.G., et al., *Bone morphogenetic proteins inhibit the tumorigenic potential of human brain tumour-initiating cells.* Nature, 2006. **444**(7120): p. 761-5.
607. Hallahan, A.R., et al., *BMP-2 mediates retinoid-induced apoptosis in medulloblastoma cells through a paracrine effect.* Nat Med, 2003. **9**(8): p. 1033-8.
608. Gobbi, G., et al., *Seven BMPs and all their receptors are simultaneously expressed in osteosarcoma cells.* Int J Oncol, 2002. **20**(1): p. 143-7.
609. Miyazaki, H., et al., *BMP signals inhibit proliferation and in vivo tumor growth of androgen-insensitive prostate carcinoma cells.* Oncogene, 2004. **23**(58): p. 9326-35.
610. Jin, Y., et al., *Overexpression of BMP-2/4, -5 and BMPR-IA associated with malignancy of oral epithelium.* Oral Oncol, 2001. **37**(3): p. 225-33.
611. Styrkarsdottir, U., et al., *Linkage of osteoporosis to chromosome 20p12 and association to BMP2.* PLoS Biol, 2003. **1**(3): p. E69.
612. Bogdan, C., *Nitric oxide and the regulation of gene expression.* Trends Cell Biol, 2001. **11**(2): p. 66-75.
613. Kone, B.C., et al., *Protein interactions with nitric oxide synthases: controlling the right time, the right place, and the right amount of nitric oxide.* Am J Physiol Renal Physiol, 2003. **285**(2): p. F178-90.
614. Mori, M., *Regulation of nitric oxide synthesis and apoptosis by arginase and arginine recycling.* J Nutr, 2007. **137**(6 Suppl 2): p. 1616S-1620S.
615. Kuncewicz, T., et al., *Specific association of nitric oxide synthase-2 with Rac isoforms in activated murine macrophages.* Am J Physiol Renal Physiol, 2001. **281**(2): p. F326-36.
616. Kaluski, E., et al., *Nitric oxide synthase inhibitors in post-myocardial infarction cardiogenic shock--an update.* Clin Cardiol, 2006. **29**(11): p. 482-8.
617. Ashman, D.F., et al., *Isolation of adenosine 3', 5'-monophosphate and guanosine 3', 5'-monophosphate from rat urine.* Biochem Biophys Res Commun, 1963. **11**: p. 330-4.
618. Lucas, K.A., et al., *Guanylyl cyclases and signaling by cyclic GMP.* Pharmacol Rev, 2000. **52**(3): p. 375-414.
619. Pyriochou, A. and A. Papapetropoulos, *Soluble guanylyl cyclase: more secrets revealed.* Cell Signal, 2005. **17**(4): p. 407-13.
620. Behrends, S. and K. Vehse, *The beta(2) subunit of soluble guanylyl cyclase contains a human-specific frameshift and is expressed in gastric carcinoma.* Biochem Biophys Res Commun, 2000. **271**(1): p. 64-9.
621. Zabel, U., et al., *Homodimerization of soluble guanylyl cyclase subunits. Dimerization analysis using a glutathione s-transferase affinity tag.* J Biol Chem, 1999. **274**(26): p. 18149-52.
622. Nighorn, A., K.A. Byrnes, and D.B. Morton, *Identification and characterization of a novel beta subunit of soluble guanylyl cyclase that is active in the absence of a second subunit and is relatively insensitive to nitric oxide.* J Biol Chem, 1999. **274**(4): p. 2525-31.
623. Wedel, B., et al., *Mutation of His-105 in the beta 1 subunit yields a nitric oxide-insensitive form of soluble guanylyl cyclase.* Proc Natl Acad Sci U S A, 1994. **91**(7): p. 2592-6.
624. Stone, J.R. and M.A. Marletta, *Soluble guanylate cyclase from bovine lung: activation with nitric oxide and carbon monoxide and spectral characterization of the ferrous and ferric states.* Biochemistry, 1994. **33**(18): p. 5636-40.
625. Zhou, Z., et al., *Structural and functional characterization of the dimerization region of soluble guanylyl cyclase.* J Biol Chem, 2004. **279**(24): p. 24935-43.
626. Schmidt, P.M., et al., *Identification of residues crucially involved in the binding of the heme moiety of soluble guanylate cyclase.* J Biol Chem, 2004. **279**(4): p. 3025-32.
627. Friebe, A., G. Schultz, and D. Koesling, *Sensitizing soluble guanylyl cyclase to become a highly CO-sensitive enzyme.* Embo J, 1996. **15**(24): p. 6863-8.
628. Garthwaite, J., et al., *Potent and selective inhibition of nitric oxide-sensitive guanylyl cyclase by 1H-[1,2,4]oxadiazolo[4,3-a]quinoxalin-1-one.* Mol Pharmacol, 1995. **48**(2): p. 184-8.
629. Murthy, K.S., *Activation of phosphodiesterase 5 and inhibition of guanylate cyclase by cGMP-dependent protein kinase in smooth muscle.* Biochem J, 2001. **360**(Pt 1): p. 199-208.
630. Ferrero, R., et al., *Nitric oxide-sensitive guanylyl cyclase activity inhibition through cyclic GMP-dependent dephosphorylation.* J Neurochem, 2000. **75**(5): p. 2029-39.
631. Zabel, U., et al., *Calcium-dependent membrane association sensitizes soluble guanylyl cyclase to nitric oxide.* Nat Cell Biol, 2002. **4**(4): p. 307-11.
632. Venema, R.C., et al., *Novel complexes of guanylate cyclase with heat shock protein 90 and nitric oxide synthase.* Am J Physiol Heart Circ Physiol, 2003. **285**(2): p. H669-78.
633. de Bold, A.J., *Atrial natriuretic factor: a hormone produced by the heart.* Science, 1985. **230**(4727): p. 767-70.
634. Aburaya, M., et al., *Distribution and molecular forms of brain natriuretic peptide in the central nervous system, heart and peripheral tissue of rat.* Biochem Biophys Res Commun, 1989. **165**(2): p. 880-7.
635. Sudoh, T., et al., *A new natriuretic peptide in porcine brain.* Nature, 1988. **332**(6159): p. 78-81.
636. Sudoh, T., et al., *C-type natriuretic peptide (CNP): a new member of natriuretic peptide family identified in porcine brain.* Biochem Biophys Res Commun, 1990. **168**(2): p. 863-70.
637. Chusho, H., et al., *Dwarfism and early death in mice lacking C-type natriuretic peptide.* Proc Natl Acad Sci U S A, 2001. **98**(7): p. 4016-21.
638. Suda, M., et al., *Skeletal overgrowth in transgenic mice that overexpress brain natriuretic peptide.* Proc Natl Acad Sci U S A, 1998. **95**(5): p. 2337-42.
639. Yasoda, A., et al., *Natriuretic peptide regulation of endochondral ossification. Evidence for possible roles of the C-type natriuretic peptide/guanylyl cyclase-B pathway.* J Biol Chem, 1998. **273**(19): p. 11695-700.
640. Chinkers, M. and E.M. Wilson, *Ligand-independent oligomerization of natriuretic peptide receptors. Identification of heteromeric receptors and a dominant negative mutant.* J Biol Chem, 1992. **267**(26): p. 18589-97.

641. Sunahara, R.K., et al., *Exchange of substrate and inhibitor specificities between adenylyl and guanylyl cyclases.* J Biol Chem, 1998. **273**(26): p. 16332-8.
642. Omori, K. and J. Kotera, *Overview of PDEs and their regulation.* Circ Res, 2007. **100**(3): p. 309-27.
643. Kass, D.A., et al., *Phosphodiesterase regulation of nitric oxide signaling.* Cardiovasc Res, 2007. **75**(2): p. 303-14.
644. Corbin, J.D., et al., *Phosphorylation of phosphodiesterase-5 by cyclic nucleotide-dependent protein kinase alters its catalytic and allosteric cGMP-binding activities.* Eur J Biochem, 2000. **267**(9): p. 2760-7.
645. Corbin, J.D., S.H. Francis, and D.J. Webb, *Phosphodiesterase type 5 as a pharmacologic target in erectile dysfunction.* Urology, 2002. **60**(2 Suppl 2): p. 4-11.
646. Turko, I.V., et al., *Inhibition of cyclic GMP-binding cyclic GMP-specific phosphodiesterase (Type 5) by sildenafil and related compounds.* Mol Pharmacol, 1999. **56**(1): p. 124-30.
647. Corbin, J.D. and S.H. Francis, *Cyclic GMP phosphodiesterase-5: target of sildenafil.* J Biol Chem, 1999. **274**(20): p. 13729-32.
648. Castro, L.R., et al., *Cyclic guanosine monophosphate compartmentation in rat cardiac myocytes.* Circulation, 2006. **113**(18): p. 2221-8.
649. Reed, T.M., et al., *Phosphodiesterase 1B knock-out mice exhibit exaggerated locomotor hyperactivity and DARPP-32 phosphorylation in response to dopamine agonists and display impaired spatial learning.* J Neurosci, 2002. **22**(12): p. 5188-97.
650. Fesenko, E.E., S.S. Kolesnikov, and A.L. Lyubarsky, *Induction by cyclic GMP of cationic conductance in plasma membrane of retinal rod outer segment.* Nature, 1985. **313**(6000): p. 310-3.
651. Kaupp, U.B. and R. Seifert, *Cyclic nucleotide-gated ion channels.* Physiol Rev, 2002. **82**(3): p. 769-824.
652. Weber, I.T., J.B. Shabb, and J.D. Corbin, *Predicted structures of the cGMP binding domains of the cGMP-dependent protein kinase: a key alanine/threonine difference in evolutionary divergence of cAMP and cGMP binding sites.* Biochemistry, 1989. **28**(14): p. 6122-7.
653. Shabb, J.B., et al., *Mutating protein kinase cAMP-binding sites into cGMP-binding sites. Mechanism of cGMP selectivity.* J Biol Chem, 1991. **266**(36): p. 24320-6.
654. Kuo, J.F. and P. Greengard, *An assay method for cyclic AMP and cyclic GMP based upon their abilities to activate cyclic AMP-dependent and cyclic GMP-dependent protein kinases.* Adv Cyclic Nucleotide Res, 1972. **2**: p. 41-50.
655. de Jonge, H.R., *Cyclic GMP-dependent protein kinase in intestinal brushborders.* Adv Cyclic Nucleotide Res, 1981. **14**: p. 315-33.
656. Vaandrager, A.B., B.M. Hogema, and H.R. de Jonge, *Molecular properties and biological functions of cGMP-dependent protein kinase II.* Front Biosci, 2005. **10**: p. 2150-64.
657. Hofmann, F., et al., *Function of cGMP-dependent protein kinases as revealed by gene deletion.* Physiol Rev, 2006. **86**(1): p. 1-23.
658. Feil, R., S. Feil, and F. Hofmann, *A heretical view on the role of NO and cGMP in vascular proliferative diseases.* Trends Mol Med, 2005. **11**(2): p. 71-5.
659. Yuasa, K., et al., *Identification of a conserved residue responsible for the autoinhibition of cGMP-dependent protein kinase Ialpha and beta.* FEBS Lett, 2000. **466**(1): p. 175-8.
660. Richie-Jannetta, R., S.H. Francis, and J.D. Corbin, *Dimerization of cGMP-dependent protein kinase Ibeta is mediated by an extensive amino-terminal leucine zipper motif, and dimerization modulates enzyme function.* J Biol Chem, 2003. **278**(50): p. 50070-9.
661. Yuasa, K., K. Omori, and N. Yanaka, *Specific domain of cGMP-dependent protein kinase Ibeta but not Ialpha functions as a transcriptional activator in yeast.* IUBMB Life, 2000. **49**(1): p. 17-22.
662. Ruth, P., et al., *Identification of the amino acid sequences responsible for high affinity activation of cGMP kinase Ialpha.* J Biol Chem, 1997. **272**(16): p. 10522-8.
663. Reed, R.B., et al., *Fast and slow cyclic nucleotide-dissociation sites in cAMP-dependent protein kinase are transposed in type Ibeta cGMP-dependent protein kinase.* J Biol Chem, 1996. **271**(29): p. 17570-5.
664. Zhao, J., et al., *Progressive cyclic nucleotide-induced conformational changes in the cGMP-dependent protein kinase studied by small angle X-ray scattering in solution.* J Biol Chem, 1997. **272**(50): p. 31929-36.
665. Smith, J.A., et al., *Autophosphorylation of type Ibeta cGMP-dependent protein kinase increases basal catalytic activity and enhances allosteric activation by cGMP or cAMP.* J Biol Chem, 1996. **271**(34): p. 20756-62.
666. Lohmann, S.M. and U. Walter, *Tracking functions of cGMP-dependent protein kinases (cGK).* Front Biosci, 2005. **10**: p. 1313-28.
667. Wang, X. and P.J. Robinson, *Cyclic GMP-dependent protein kinase and cellular signaling in the nervous system.* J Neurochem, 1997. **68**(2): p. 443-56.
668. Chu, D.M., et al., *Activation by cyclic GMP binding causes an apparent conformational change in cGMP-dependent protein kinase.* J Biol Chem, 1997. **272**(50): p. 31922-8.
669. Wall, M.E., et al., *Mechanisms associated with cGMP binding and activation of cGMP-dependent protein kinase.* Proc Natl Acad Sci U S A, 2003. **100**(5): p. 2380-5.
670. Alverdi, V., et al., *cGMP-binding prepares PKG for substrate binding by disclosing the C-terminal domain.* J Mol Biol, 2008. **375**(5): p. 1380-93.
671. Gudi, T., S.M. Lohmann, and R.B. Pilz, *Regulation of gene expression by cyclic GMP-dependent protein kinase requires nuclear translocation of the kinase: identification of a nuclear localization signal.* Mol Cell Biol, 1997. **17**(9): p. 5244-54.
672. Pilz, R.B. and K.E. Broderick, *Role of cyclic GMP in gene regulation.* Front Biosci, 2005. **10**: p. 1239-68.
673. Casteel, D.E., et al., *cGMP-dependent protein kinase I beta physically and functionally interacts with the transcriptional regulator TFII-I.* J Biol Chem, 2002. **277**(35): p. 32003-14.
674. Browning, D.D., et al., *Functional analysis of type 1alpha cGMP-dependent protein kinase using green fluorescent fusion proteins.* J Biol Chem, 2001. **276**(16): p. 13039-48.
675. Dey, N.B., et al., *Cyclic GMP-dependent protein kinase inhibits osteopontin and thrombospondin production in rat aortic smooth muscle cells.* Circ Res, 1998. **82**(2): p. 139-46.
676. Sinnaeve, P., et al., *Overexpression of a constitutively active protein kinase G mutant reduces neointima formation and in-stent restenosis.* Circulation, 2002. **105**(24): p. 2911-6.
677. Wang, S., et al., *Expression of constitutively active cGMP-dependent protein kinase prevents glucose stimulation of thrombospondin 1 expression and TGF-beta activity.* Diabetes, 2003. **52**(8): p. 2144-50.
678. Busch, J.L., et al., *A conserved serine juxtaposed to the pseudosubstrate site of type I cGMP-dependent protein kinase contributes strongly to autoinhibition and lower cGMP affinity.* J Biol Chem, 2002. **277**(37): p. 34048-54.

679. Chu, D.M., et al., *Activation by autophosphorylation or cGMP binding produces a similar apparent conformational change in cGMP-dependent protein kinase.* J Biol Chem, 1998. **273**(23): p. 14649-56.
680. Hou, Y., et al., *Activation of cGMP-dependent protein kinase by protein kinase C.* J Biol Chem, 2003. **278**(19): p. 16706-12.
681. Fischer, T.A., et al., *Activation of cGMP-dependent protein kinase Ibeta inhibits interleukin 2 release and proliferation of T cell receptor-stimulated human peripheral T cells.* J Biol Chem, 2001. **276**(8): p. 5967-74.
682. Smolenski, A., et al., *Regulation of human endothelial cell focal adhesion sites and migration by cGMP-dependent protein kinase I.* J Biol Chem, 2000. **275**(33): p. 25723-32.
683. Koeppen, M., et al., *cGMP-dependent protein kinase mediates NO- but not acetylcholine-induced dilations in resistance vessels in vivo.* Hypertension, 2004. **44**(6): p. 952-5.
684. Pfeifer, A., et al., *Defective smooth muscle regulation in cGMP kinase I-deficient mice.* Embo J, 1998. **17**(11): p. 3045-51.
685. Sausbier, M., et al., *Mechanisms of NO/cGMP-dependent vasorelaxation.* Circ Res, 2000. **87**(9): p. 825-30.
686. Massberg, S., et al., *Increased adhesion and aggregation of platelets lacking cyclic guanosine 3',5'-monophosphate kinase I.* J Exp Med, 1999. **189**(8): p. 1255-64.
687. Schmidt, H., et al., *cGMP-mediated signaling via cGKIalpha is required for the guidance and connectivity of sensory axons.* J Cell Biol, 2002. **159**(3): p. 489-98.
688. Tegeder, I., et al., *Reduced inflammatory hyperalgesia with preservation of acute thermal nociception in mice lacking cGMP-dependent protein kinase I.* Proc Natl Acad Sci U S A, 2004. **101**(9): p. 3253-7.
689. Yamahara, K., et al., *Significance and therapeutic potential of the natriuretic peptides/cGMP/cGMP-dependent protein kinase pathway in vascular regeneration.* Proc Natl Acad Sci U S A, 2003. **100**(6): p. 3404-9.
690. Wolfsgruber, W., et al., *A proatherogenic role for cGMP-dependent protein kinase in vascular smooth muscle cells.* Proc Natl Acad Sci U S A, 2003. **100**(23): p. 13519-24.
691. Wegener, J.W., et al., *cGMP-dependent protein kinase I mediates the negative inotropic effect of cGMP in the murine myocardium.* Circ Res, 2002. **90**(1): p. 18-20.
692. Kleppisch, T., et al., *Hippocampal cGMP-dependent protein kinase I supports an age- and protein synthesis-dependent component of long-term potentiation but is not essential for spatial reference and contextual memory.* J Neurosci, 2003. **23**(14): p. 6005-12.
693. Feil, R., et al., *Impairment of LTD and cerebellar learning by Purkinje cell-specific ablation of cGMP-dependent protein kinase I.* J Cell Biol, 2003. **163**(2): p. 295-302.
694. Huang, Q.Q., S.A. Fisher, and F.V. Brozovich, *Unzipping the role of myosin light chain phosphatase in smooth muscle cell relaxation.* J Biol Chem, 2004. **279**(1): p. 597-603.
695. Surks, H.K. and M.E. Mendelsohn, *Dimerization of cGMP-dependent protein kinase 1alpha and the myosin-binding subunit of myosin phosphatase: role of leucine zipper domains.* Cell Signal, 2003. **15**(10): p. 937-44.
696. Surks, H.K., et al., *Regulation of myosin phosphatase by a specific interaction with cGMP- dependent protein kinase Ialpha.* Science, 1999. **286**(5444): p. 1583-7.
697. Wooldridge, A.A., et al., *Smooth muscle phosphatase is regulated in vivo by exclusion of phosphorylation of threonine 696 of MYPT1 by phosphorylation of Serine 695 in response to cyclic nucleotides.* J Biol Chem, 2004. **279**(33): p. 34496-504.
698. Ellerbroek, S.M., K. Wennerberg, and K. Burridge, *Serine phosphorylation negatively regulates RhoA in vivo.* J Biol Chem, 2003. **278**(21): p. 19023-31.
699. Sauzeau, V., et al., *Cyclic GMP-dependent protein kinase signaling pathway inhibits RhoA-induced Ca2+ sensitization of contraction in vascular smooth muscle.* J Biol Chem, 2000. **275**(28): p. 21722-9.
700. Walker, L.A., et al., *Site-specific phosphorylation and point mutations of telokin modulate its Ca2+-desensitizing effect in smooth muscle.* J Biol Chem, 2001. **276**(27): p. 24519-24.
701. Yuasa, K., et al., *A novel interaction of cGMP-dependent protein kinase I with troponin T.* J Biol Chem, 1999. **274**(52): p. 37429-34.
702. Koller, A., et al., *Association of phospholamban with a cGMP kinase signaling complex.* Biochem Biophys Res Commun, 2003. **300**(1): p. 155-60.
703. Lalli, M.J., et al., *[Ca2+]i homeostasis and cyclic nucleotide relaxation in aorta of phospholamban-deficient mice.* Am J Physiol, 1999. **277**(3 Pt 2): p. H963-70.
704. Ammendola, A., et al., *Molecular determinants of the interaction between the inositol 1,4,5-trisphosphate receptor-associated cGMP kinase substrate (IRAG) and cGMP kinase Ibeta.* J Biol Chem, 2001. **276**(26): p. 24153-9.
705. Casteel, D.E., G.R. Boss, and R.B. Pilz, *Identification of the interface between cGMP-dependent protein kinase Ibeta and its interaction partners TFII-I and IRAG reveals a common interaction motif.* J Biol Chem, 2005. **280**(46): p. 38211-8.
706. Schlossmann, J., et al., *Regulation of intracellular calcium by a signalling complex of IRAG, IP3 receptor and cGMP kinase Ibeta.* Nature, 2000. **404**(6774): p. 197-201.
707. Tang, K.M., et al., *Regulator of G-protein signaling-2 mediates vascular smooth muscle relaxation and blood pressure.* Nat Med, 2003. **9**(12): p. 1506-12.
708. Butt, E., et al., *cAMP- and cGMP-dependent protein kinase phosphorylation sites of the focal adhesion vasodilator-stimulated phosphoprotein (VASP) in vitro and in intact human platelets.* J Biol Chem, 1994. **269**(20): p. 14509-17.
709. Smolenski, A., et al., *Analysis and regulation of vasodilator-stimulated phosphoprotein serine 239 phosphorylation in vitro and in intact cells using a phosphospecific monoclonal antibody.* J Biol Chem, 1998. **273**(32): p. 20029-35.
710. MacMillan-Crow, L.A. and T.M. Lincoln, *High-affinity binding and localization of the cyclic GMP-dependent protein kinase with the intermediate filament protein vimentin.* Biochemistry, 1994. **33**(26): p. 8035-43.
711. Mullershausen, F., et al., *Direct activation of PDE5 by cGMP: long-term effects within NO/cGMP signaling.* J Cell Biol, 2003. **160**(5): p. 719-27.
712. Rybalkin, S.D., et al., *Regulation of cGMP-specific phosphodiesterase (PDE5) phosphorylation in smooth muscle cells.* J Biol Chem, 2002. **277**(5): p. 3310-7.
713. Rybalkin, S.D., et al., *Cyclic GMP phosphodiesterases and regulation of smooth muscle function.* Circ Res, 2003. **93**(4): p. 280-91.
714. Huber, A., et al., *Cysteine-rich protein 2, a novel substrate for cGMP kinase I in enteric neurons and intestinal smooth muscle.* J Biol Chem, 2000. **275**(8): p. 5504-11.
715. Schmidtko, A., et al., *Cysteine-rich protein 2, a novel downstream effector of cGMP/cGMP-dependent protein kinase I-mediated persistent inflammatory pain.* J Neurosci, 2008. **28**(6): p. 1320-30.

716. Xue, J., et al., *Phosphorylation of septin 3 on Ser-91 by cGMP-dependent protein kinase-I in nerve terminals.* Biochem J, 2004. **381**(Pt 3): p. 753-60.
717. Endo, S., et al., *Molecular identification of human G-substrate, a possible downstream component of the cGMP-dependent protein kinase cascade in cerebellar Purkinje cells.* Proc Natl Acad Sci U S A, 1999. **96**(5): p. 2467-72.
718. Snyder, G.L., et al., *Phosphorylation of DARPP-32 and protein phosphatase inhibitor-1 in rat choroid plexus: regulation by factors other than dopamine.* J Neurosci, 1992. **12**(8): p. 3071-83.
719. Tsou, K., G.L. Snyder, and P. Greengard, *Nitric oxide/cGMP pathway stimulates phosphorylation of DARPP-32, a dopamine- and cAMP-regulated phosphoprotein, in the substantia nigra.* Proc Natl Acad Sci U S A, 1993. **90**(8): p. 3462-5.
720. Zhou, X.B., et al., *A molecular switch for specific stimulation of the BKCa channel by cGMP and cAMP kinase.* J Biol Chem, 2001. **276**(46): p. 43239-45.
721. Yuasa, K., K. Omori, and N. Yanaka, *Binding and phosphorylation of a novel male germ cell-specific cGMP-dependent protein kinase-anchoring protein by cGMP-dependent protein kinase Ialpha.* J Biol Chem, 2000. **275**(7): p. 4897-905.
722. Fryer, B.H., et al., *cGMP-dependent protein kinase phosphorylates p21-activated kinase (Pak) 1, inhibiting Pak/Nck binding and stimulating Pak/vasodilator-stimulated phosphoprotein association.* J Biol Chem, 2006. **281**(17): p. 11487-95.
723. Roberts, J.D., Jr., et al., *cGMP-dependent protein kinase I interacts with TRIM39R, a novel Rpp21 domain-containing TRIM protein.* Am J Physiol Lung Cell Mol Physiol, 2007. **293**(4): p. L903-12.
724. Hood, J. and H.J. Granger, *Protein kinase G mediates vascular endothelial growth factor-induced Raf-1 activation and proliferation in human endothelial cells.* J Biol Chem, 1998. **273**(36): p. 23504-8.
725. Parenti, A., et al., *Nitric oxide is an upstream signal of vascular endothelial growth factor-induced extracellular signal-regulated kinase1/2 activation in postcapillary endothelium.* J Biol Chem, 1998. **273**(7): p. 4220-6.
726. Zaragoza, C., et al., *Activation of the mitogen activated protein kinase extracellular signal-regulated kinase 1 and 2 by the nitric oxide-cGMP-cGMP-dependent protein kinase axis regulates the expression of matrix metalloproteinase 13 in vascular endothelial cells.* Mol Pharmacol, 2002. **62**(4): p. 927-35.
727. Komalavilas, P., et al., *Activation of mitogen-activated protein kinase pathways by cyclic GMP and cyclic GMP-dependent protein kinase in contractile vascular smooth muscle cells.* J Biol Chem, 1999. **274**(48): p. 34301-9.
728. Silberbach, M., et al., *Extracellular signal-regulated protein kinase activation is required for the anti-hypertrophic effect of atrial natriuretic factor in neonatal rat ventricular myocytes.* J Biol Chem, 1999. **274**(35): p. 24858-64.
729. Suhasini, M., et al., *Cyclic-GMP-dependent protein kinase inhibits the Ras/Mitogen-activated protein kinase pathway.* Mol Cell Biol, 1998. **18**(12): p. 6983-94.
730. Browning, D.D., et al., *Nitric oxide activation of p38 mitogen-activated protein kinase in 293T fibroblasts requires cGMP-dependent protein kinase.* J Biol Chem, 2000. **275**(4): p. 2811-6.
731. Kim, S.O., et al., *Cyclic GMP-dependent and -independent regulation of MAP kinases by sodium nitroprusside in isolated cardiomyocytes.* Biochim Biophys Acta, 2000. **1496**(2-3): p. 277-84.
732. Fiedler, B., et al., *cGMP-dependent protein kinase type I inhibits TAB1-p38 mitogen-activated protein kinase apoptosis signaling in cardiac myocytes.* J Biol Chem, 2006. **281**(43): p. 32831-40.
733. Soh, J.W., et al., *Cyclic GMP mediates apoptosis induced by sulindac derivatives via activation of c-Jun NH2-terminal kinase 1.* Clin Cancer Res, 2000. **6**(10): p. 4136-41.
734. Wang, X., et al., *Phosphorylation of splicing factor SF1 on Ser20 by cGMP-dependent protein kinase regulates spliceosome assembly.* Embo J, 1999. **18**(16): p. 4549-59.
735. De La Vega, L.A. and R.J. Stockert, *Regulation of the insulin and asialoglycoprotein receptors via cGMP-dependent protein kinase.* Am J Physiol Cell Physiol, 2000. **279**(6): p. C2037-42.
736. Stockert, R.J., et al., *Posttranscriptional regulation of the asialoglycoprotein receptor by cGMP.* J Biol Chem, 1992. **267**(1): p. 56-9.
737. Shaywitz, A.J. and M.E. Greenberg, *CREB: a stimulus-induced transcription factor activated by a diverse array of extracellular signals.* Annu Rev Biochem, 1999. **68**: p. 821-61.
738. Gudi, T., et al., *NO activation of fos promoter elements requires nuclear translocation of G-kinase I and CREB phosphorylation but is independent of MAP kinase activation.* Oncogene, 2000. **19**(54): p. 6324-33.
739. Gudi, T., et al., *cGMP-dependent protein kinase inhibits serum-response element-dependent transcription by inhibiting rho activation and functions.* J Biol Chem, 2002. **277**(40): p. 37382-93.
740. Roy, A.L., *Biochemistry and biology of the inducible multifunctional transcription factor TFII-I.* Gene, 2001. **274**(1-2): p. 1-13.
741. Kalra, D., et al., *Nitric oxide provokes tumor necrosis factor-alpha expression in adult feline myocardium through a cGMP-dependent pathway.* Circulation, 2000. **102**(11): p. 1302-7.
742. He, B. and G.F. Weber, *Phosphorylation of NF-kappaB proteins by cyclic GMP-dependent kinase. A noncanonical pathway to NF-kappaB activation.* Eur J Biochem, 2003. **270**(10): p. 2174-85.
743. Simpson, C.S. and B.J. Morris, *Activation of nuclear factor kappaB by nitric oxide in rat striatal neurones: differential inhibition of the p50 and p65 subunits by dexamethasone.* J Neurochem, 1999. **73**(1): p. 353-61.
744. Browner, N.C., et al., *Regulation of cGMP-dependent protein kinase expression by soluble guanylyl cyclase in vascular smooth muscle cells.* J Biol Chem, 2004. **279**(45): p. 46631-6.
745. Soff, G.A., et al., *Smooth muscle cell expression of type I cyclic GMP-dependent protein kinase is suppressed by continuous exposure to nitrovasodilators, theophylline, cyclic GMP, and cyclic AMP.* J Clin Invest, 1997. **100**(10): p. 2580-7.
746. Sellak, H., et al., *Sp1 transcription factor as a molecular target for nitric oxide-- and cyclic nucleotide--mediated suppression of cGMP-dependent protein kinase-Ialpha expression in vascular smooth muscle cells.* Circ Res, 2002. **90**(4): p. 405-12.
747. Filippov, G., D.B. Bloch, and K.D. Bloch, *Nitric oxide decreases stability of mRNAs encoding soluble guanylate cyclase subunits in rat pulmonary artery smooth muscle cells.* J Clin Invest, 1997. **100**(4): p. 942-8.
748. Hussain, M.B., A.J. Hobbs, and R.J. MacAllister, *Autoregulation of nitric oxide-soluble guanylate cyclase-cyclic GMP signalling in mouse thoracic aorta.* Br J Pharmacol, 1999. **128**(5): p. 1082-8.
749. Inoue, T., et al., *cGMP upregulates nitric oxide synthase expression in vascular smooth muscle cells.* Hypertension, 1995. **25**(4 Pt 2): p. 711-4.
750. Jacob, A., et al., *Insulin inhibits PDGF-directed VSMC migration via NO/ cGMP increase of MKP-1 and its inactivation of MAPKs.* Am J Physiol Cell Physiol, 2002. **283**(3): p. C704-13.

751. Pervin, S., et al., *MKP-1-induced dephosphorylation of extracellular signal-regulated kinase is essential for triggering nitric oxide-induced apoptosis in human breast cancer cell lines: implications in breast cancer.* Cancer Res, 2003. **63**(24): p. 8853-60.
752. Sugimoto, T., et al., *Atrial natriuretic peptide induces the expression of MKP-1, a mitogen-activated protein kinase phosphatase, in glomerular mesangial cells.* J Biol Chem, 1996. **271**(1): p. 544-7.
753. Gu, M. and P. Brecher, *Nitric oxide-induced increase in p21(Sdi1/Cip1/Waf1) expression during the cell cycle in aortic adventitial fibroblasts.* Arterioscler Thromb Vasc Biol, 2000. **20**(1): p. 27-34.
754. Hanada, S., et al., *Overexpression of protein kinase G using adenovirus inhibits cyclin E transcription and mesangial cell cycle.* Am J Physiol Renal Physiol, 2001. **280**(5): p. F851-9.
755. Kronemann, N., et al., *Growth-inhibitory effect of cyclic GMP- and cyclic AMP-dependent vasodilators on rat vascular smooth muscle cells: effect on cell cycle and cyclin expression.* Br J Pharmacol, 1999. **126**(1): p. 349-57.
756. Chiche, J.D., et al., *Adenovirus-mediated gene transfer of cGMP-dependent protein kinase increases the sensitivity of cultured vascular smooth muscle cells to the antiproliferative and pro-apoptotic effects of nitric oxide/cGMP.* J Biol Chem, 1998. **273**(51): p. 34263-71.
757. Cornwell, T.L., et al., *Regulation of the expression of cyclic GMP-dependent protein kinase by cell density in vascular smooth muscle cells.* J Vasc Res, 1994. **31**(6): p. 330-7.
758. Osinski, M.T., B.H. Rauch, and K. Schror, *Antimitogenic actions of organic nitrates are potentiated by sildenafil and mediated via activation of protein kinase A.* Mol Pharmacol, 2001. **59**(5): p. 1044-50.
759. Yu, S.M., L.M. Hung, and C.C. Lin, *cGMP-elevating agents suppress proliferation of vascular smooth muscle cells by inhibiting the activation of epidermal growth factor signaling pathway.* Circulation, 1997. **95**(5): p. 1269-77.
760. Boerth, N.J., et al., *Cyclic GMP-dependent protein kinase regulates vascular smooth muscle cell phenotype.* J Vasc Res, 1997. **34**(4): p. 245-59.
761. Lincoln, T.M., N. Dey, and H. Sellak, *Invited review: cGMP-dependent protein kinase signaling mechanisms in smooth muscle: from the regulation of tone to gene expression.* J Appl Physiol, 2001. **91**(3): p. 1421-30.
762. Soh, J.W., et al., *Protein kinase G activates the JNK1 pathway via phosphorylation of MEKK1.* J Biol Chem, 2001. **276**(19): p. 16406-10.
763. Shaulian, E. and M. Karin, *AP-1 as a regulator of cell life and death.* Nat Cell Biol, 2002. **4**(5): p. E131-6.
764. Andoh, T., C.C. Chiueh, and P.B. Chock, *Cyclic GMP-dependent protein kinase regulates the expression of thioredoxin and thioredoxin peroxidase-1 during hormesis in response to oxidative stress-induced apoptosis.* J Biol Chem, 2003. **278**(2): p. 885-90.
765. Ciani, E., et al., *Nitric oxide regulates cGMP-dependent cAMP-responsive element binding protein phosphorylation and Bcl-2 expression in cerebellar neurons: implication for a survival role of nitric oxide.* J Neurochem, 2002. **82**(5): p. 1282-9.
766. Ciani, E., M. Virgili, and A. Contestabile, *Akt pathway mediates a cGMP-dependent survival role of nitric oxide in cerebellar granule neurones.* J Neurochem, 2002. **81**(2): p. 218-28.
767. Ha, K.S., et al., *Nitric oxide prevents 6-hydroxydopamine-induced apoptosis in PC12 cells through cGMP-dependent PI3 kinase/Akt activation.* Faseb J, 2003. **17**(9): p. 1036-47.
768. Kim, N.N., et al., *Regulation of cardiac fibroblast extracellular matrix production by bradykinin and nitric oxide.* J Mol Cell Cardiol, 1999. **31**(2): p. 457-66.
769. Lee, S.Y., et al., *17beta-estradiol activates ICI 182,780-sensitive estrogen receptors and cyclic GMP-dependent thioredoxin expression for neuroprotection.* Faseb J, 2003. **17**(8): p. 947-8.
770. Park, D.S., et al., *Ordering the cell death pathway. Differential effects of BCL2, an interleukin-1-converting enzyme family protease inhibitor, and other survival agents on JNK activation in serum/nerve growth factor-deprived PC12 cells.* J Biol Chem, 1996. **271**(36): p. 21898-905.
771. Kawasaki, K., et al., *Activation of the phosphatidylinositol 3-kinase/protein kinase Akt pathway mediates nitric oxide-induced endothelial cell migration and angiogenesis.* Mol Cell Biol, 2003. **23**(16): p. 5726-37.
772. Wang, S., et al., *Nitric oxide and cGMP-dependent protein kinase regulation of glucose-mediated thrombospondin 1-dependent transforming growth factor-beta activation in mesangial cells.* J Biol Chem, 2002. **277**(12): p. 9880-8.
773. Haby, C., et al., *Stimulation of the cyclic GMP pathway by NO induces expression of the immediate early genes c-fos and junB in PC12 cells.* J Neurochem, 1994. **62**(2): p. 496-501.
774. Pawliczak, R., et al., *p11 expression in human bronchial epithelial cells is increased by nitric oxide in a cGMP-dependent pathway involving protein kinase G activation.* J Biol Chem, 2001. **276**(48): p. 44613-21.
775. Pilz, R.B., et al., *Nitric oxide and cGMP analogs activate transcription from AP-1-responsive promoters in mammalian cells.* Faseb J, 1995. **9**(7): p. 552-8.
776. Thiriet, N., et al., *Immediate early gene induction by natriuretic peptides in PC12 phaeochromocytoma and C6 glioma cells.* Neuroreport, 1997. **8**(2): p. 399-402.
777. Cibelli, G., et al., *Nitric oxide-induced programmed cell death in human neuroblastoma cells is accompanied by the synthesis of Egr-1, a zinc finger transcription factor.* J Neurosci Res, 2002. **67**(4): p. 450-60.
778. Esteve, L., et al., *Cyclic GMP-dependent protein kinase potentiates serotonin-induced Egr-1 binding activity in PC12 cells.* Cell Signal, 2001. **13**(6): p. 425-32.
779. Nisoli, E., et al., *Mitochondrial biogenesis in mammals: the role of endogenous nitric oxide.* Science, 2003. **299**(5608): p. 896-9.
780. Saura, M., et al., *Nitric oxide regulates transforming growth factor-beta signaling in endothelial cells.* Circ Res, 2005. **97**(11): p. 1115-23.
781. Gamm, D.M., et al., *The type II isoform of cGMP-dependent protein kinase is dimeric and possesses regulatory and catalytic properties distinct from the type I isoforms.* J Biol Chem, 1995. **270**(45): p. 27380-8.
782. Vaandrager, A.B., et al., *Endogenous type II cGMP-dependent protein kinase exists as a dimer in membranes and can Be functionally distinguished from the type I isoforms.* J Biol Chem, 1997. **272**(18): p. 11816-23.
783. Vaandrager, A.B., et al., *N-terminal myristoylation is required for membrane localization of cGMP-dependent protein kinase type II.* J Biol Chem, 1996. **271**(12): p. 7025-9.
784. Taylor, M.K. and M.D. Uhler, *The amino-terminal cyclic nucleotide binding site of the type II cGMP-dependent protein kinase is essential for full cyclic nucleotide-dependent activation.* J Biol Chem, 2000. **275**(36): p. 28053-62.
785. Gambaryan, S., et al., *cGMP-dependent protein kinase type II regulates basal level of aldosterone production by zona glomerulosa cells without increasing expression of the steroidogenic acute regulatory protein gene.* J Biol Chem, 2003. **278**(32): p. 29640-8.
786. Vo, N.K., J.M. Gettemy, and V.M. Coghlan, *Identification of cGMP-dependent protein kinase anchoring proteins (GKAPs).* Biochem Biophys Res Commun, 1998. **246**(3): p. 831-5.

787. Pfeifer, A., et al., *Intestinal secretory defects and dwarfism in mice lacking cGMP-dependent protein kinase II.* Science, 1996. **274**(5295): p. 2082-6.
788. Chikuda, H., et al., *Cyclic GMP-dependent protein kinase II is a molecular switch from proliferation to hypertrophic differentiation of chondrocytes.* Genes Dev, 2004. **18**(19): p. 2418-29.
789. Schlossmann, J., R. Feil, and F. Hofmann, *Signaling through NO and cGMP-dependent protein kinases.* Ann Med, 2003. **35**(1): p. 21-7.
790. Eigenthaler, M., et al., *Defective nitrovasodilator-stimulated protein phosphorylation and calcium regulation in cGMP-dependent protein kinase-deficient human platelets of chronic myelocytic leukemia.* J Biol Chem, 1993. **268**(18): p. 13526-31.
791. Parker, J.O., *Nitrates and angina pectoris.* Am J Cardiol, 1993. **72**(8): p. 3C-6C; discussion 6C-8C.
792. Malinski, T., *Nitric oxide and nitroxidative stress in Alzheimer's disease.* J Alzheimers Dis, 2007. **11**(2): p. 207-18.
793. Brenman, J.E., et al., *Nitric oxide synthase complexed with dystrophin and absent from skeletal muscle sarcolemma in Duchenne muscular dystrophy.* Cell, 1995. **82**(5): p. 743-52.
794. Ghofrani, H.A., I.H. Osterloh, and F. Grimminger, *Sildenafil: from angina to erectile dysfunction to pulmonary hypertension and beyond.* Nat Rev Drug Discov, 2006. **5**(8): p. 689-702.
795. Browning, D.D., *Protein kinase G as a therapeutic target for the treatment of metastatic colorectal cancer.* Expert Opin Ther Targets, 2008. **12**(3): p. 367-76.
796. Madhusoodanan, K.S. and F. Murad, *NO-cGMP signaling and regenerative medicine involving stem cells.* Neurochem Res, 2007. **32**(4-5): p. 681-94.
797. Hanahan, D., *Studies on transformation of Escherichia coli with plasmids.* J Mol Biol, 1983. **166**(4): p. 557-80.
798. Young, K.A., et al., *BMP signaling controls PASMC KV channel expression in vitro and in vivo.* Am J Physiol Lung Cell Mol Physiol, 2006. **290**(5): p. L841-8.
799. Studier, F.W. and B.A. Moffatt, *Use of bacteriophage T7 RNA polymerase to direct selective high-level expression of cloned genes.* J Mol Biol, 1986. **189**(1): p. 113-30.
800. Goldman, L.A., et al., *Modifications of vectors pEF-BOS, pcDNA1 and pcDNA3 result in improved convenience and expression.* Biotechniques, 1996. **21**(6): p. 1013-5.
801. Andersson, S., et al., *Cloning, structure, and expression of the mitochondrial cytochrome P-450 sterol 26-hydroxylase, a bile acid biosynthetic enzyme.* J Biol Chem, 1989. **264**(14): p. 8222-9.
802. Tsai, R.Y. and R.R. Reed, *Using a eukaryotic GST fusion vector for proteins difficult to express in E. coli.* Biotechniques, 1997. **23**(5): p. 794-6, 798, 800.
803. Hsu, D.R., et al., *The Xenopus dorsalizing factor Gremlin identifies a novel family of secreted proteins that antagonize BMP activities.* Mol Cell, 1998. **1**(5): p. 673-83.
804. Meinecke, M., et al., *Human cyclic GMP-dependent protein kinase I beta overexpression increases phosphorylation of an endogenous focal contact-associated vasodilator-stimulated phosphoprotein without altering the thrombin-evoked calcium response.* Mol Pharmacol, 1994. **46**(2): p. 283-90.
805. Akiyoshi, S., et al., *c-Ski acts as a transcriptional co-repressor in transforming growth factor-beta signaling through interaction with smads.* J Biol Chem, 1999. **274**(49): p. 35269-77.
806. Korchynskyi, O. and P. ten Dijke, *Identification and functional characterization of distinct critically important bone morphogenetic protein-specific response elements in the Id1 promoter.* J Biol Chem, 2002. **277**(7): p. 4883-91.
807. Jonk, L.J., et al., *Identification and functional characterization of a Smad binding element (SBE) in the JunB promoter that acts as a transforming growth factor-beta, activin, and bone morphogenetic protein-inducible enhancer.* J Biol Chem, 1998. **273**(33): p. 21145-52.
808. Chen, S.J., et al., *Interaction of smad3 with a proximal smad-binding element of the human alpha2(I) procollagen gene promoter required for transcriptional activation by TGF-beta.* J Cell Physiol, 2000. **183**(3): p. 381-92.
809. Hassel, S., et al., *Initiation of Smad-dependent and Smad-independent signaling via distinct BMP-receptor complexes.* J Bone Joint Surg Am, 2003. **85-A Suppl 3**: p. 44-51.
810. Kolodziej, P.A. and R.A. Young, *Epitope tagging and protein surveillance.* Methods Enzymol, 1991. **194**: p. 508-19.
811. Loewinger, L. and F. McKeon, *Mutations in the nuclear lamin proteins resulting in their aberrant assembly in the cytoplasm.* Embo J, 1988. **7**(8): p. 2301-9.
812. Persson, U., et al., *The L45 loop in type I receptors for TGF-beta family members is a critical determinant in specifying Smad isoform activation.* FEBS Lett, 1998. **434**(1-2): p. 83-7.
813. Moustakas, A., et al., *The transforming growth factor beta receptors types I, II, and III form hetero-oligomeric complexes in the presence of ligand.* J Biol Chem, 1993. **268**(30): p. 22215-8.
814. Moustakas, A., et al., *GH3 pituitary tumor cells contain heteromeric type I and type II receptor complexes for transforming growth factor beta and activin-A.* J Biol Chem, 1995. **270**(2): p. 765-9.
815. Fire, A., et al., *Potent and specific genetic interference by double-stranded RNA in Caenorhabditis elegans.* Nature, 1998. **391**(6669): p. 806-11.
816. Hammond, S.M., A.A. Caudy, and G.J. Hannon, *Post-transcriptional gene silencing by double-stranded RNA.* Nat Rev Genet, 2001. **2**(2): p. 110-9.
817. Elbashir, S.M., et al., *Duplexes of 21-nucleotide RNAs mediate RNA interference in cultured mammalian cells.* Nature, 2001. **411**(6836): p. 494-8.
818. Tuschl, T. and A. Borkhardt, *Small interfering RNAs: a revolutionary tool for the analysis of gene function and gene therapy.* Mol Interv, 2002. **2**(3): p. 158-67.
819. Weiske, J. and O. Huber, *The histidine triad protein Hint1 triggers apoptosis independent of its enzymatic activity.* J Biol Chem, 2006. **281**(37): p. 27356-66.
820. Boussif, O., et al., *A versatile vector for gene and oligonucleotide transfer into cells in culture and in vivo: polyethylenimine.* Proc Natl Acad Sci U S A, 1995. **92**(16): p. 7297-301.
821. Ogata, T., et al., *Bone morphogenetic protein 2 transiently enhances expression of a gene, Id (inhibitor of differentiation), encoding a helix-loop-helix molecule in osteoblast-like cells.* Proc Natl Acad Sci U S A, 1993. **90**(19): p. 9219-22.
822. Bengtsson, L. and K.L. Wilson, *Barrier-to-autointegration factor phosphorylation on Ser-4 regulates emerin binding to lamin A in vitro and emerin localization in vivo.* Mol Biol Cell, 2006. **17**(3): p. 1154-63.
823. Klotz, U., K.H. Antonin, and P. Bieck, *Cyclic nucleotide phosphodiesterases of human and rat gastric mucosa.* Naunyn Schmiedebergs Arch Pharmacol, 1977. **296**(2): p. 187-90.
824. Redinbaugh, M.G. and R.B. Turley, *Adaptation of the bicinchoninic acid protein assay for use with microtiter plates and sucrose gradient fractions.* Anal Biochem, 1986. **153**(2): p. 267-71.

825. Laemmli, U.K., *Cleavage of structural proteins during the assembly of the head of bacteriophage T4.* Nature, 1970. **227**(5259): p. 680-5.
826. Burnette, W.N., *"Western blotting": electrophoretic transfer of proteins from sodium dodecyl sulfate--polyacrylamide gels to unmodified nitrocellulose and radiographic detection with antibody and radioiodinated protein A.* Anal Biochem, 1981. **112**(2): p. 195-203.
827. Aberle, H., et al., *wishful thinking encodes a BMP type II receptor that regulates synaptic growth in Drosophila.* Neuron, 2002. **33**(4): p. 545-58.
828. Ruth, P., et al., *The activation of expressed cGMP-dependent protein kinase isozymes I alpha and I beta is determined by the different amino-termini.* Eur J Biochem, 1991. **202**(3): p. 1339-44.
829. Nickel, J., et al., *A single residue of GDF-5 defines binding specificity to BMP receptor IB.* J Mol Biol, 2005. **349**(5): p. 933-47.
830. Ku, M., et al., *Positive and negative regulation of the transforming growth factor beta/activin target gene goosecoid by the TFII-I family of transcription factors.* Mol Cell Biol, 2005. **25**(16): p. 7144-57.
831. Stasyk, T., et al., *Phosphoproteome profiling of transforming growth factor (TGF)-beta signaling: abrogation of TGFbeta1-dependent phosphorylation of transcription factor-II-I (TFII-I) enhances cooperation of TFII-I and Smad3 in transcription.* Mol Biol Cell, 2005. **16**(10): p. 4765-80.
832. Hakre, S., et al., *Opposing functions of TFII-I spliced isoforms in growth factor-induced gene expression.* Mol Cell, 2006. **24**(2): p. 301-8.
833. Massague, J. and Y.G. Chen, *Controlling TGF-beta signaling.* Genes Dev, 2000. **14**(6): p. 627-44.
834. Gilboa, L., et al., *Oligomeric structure of type I and type II transforming growth factor beta receptors: homodimers form in the ER and persist at the plasma membrane.* J Cell Biol, 1998. **140**(4): p. 767-77.
835. Saitoh, M., et al., *Identification of important regions in the cytoplasmic juxtamembrane domain of type I receptor that separate signaling pathways of transforming growth factor-beta.* J Biol Chem, 1996. **271**(5): p. 2769-75.
836. Wang, L.H., K.G. Rothberg, and R.G. Anderson, *Mis-assembly of clathrin lattices on endosomes reveals a regulatory switch for coated pit formation.* J Cell Biol, 1993. **123**(5): p. 1107-17.
837. Randall, R.A., et al., *Different Smad2 partners bind a common hydrophobic pocket in Smad2 via a defined proline-rich motif.* Embo J, 2002. **21**(1-2): p. 145-56.
838. Shi, Y., et al., *A structural basis for mutational inactivation of the tumour suppressor Smad4.* Nature, 1997. **388**(6637): p. 87-93.
839. Hollnagel, A., et al., *Id genes are direct targets of bone morphogenetic protein induction in embryonic stem cells.* J Biol Chem, 1999. **274**(28): p. 19838-45.
840. Benezra, R., et al., *The protein Id: a negative regulator of helix-loop-helix DNA binding proteins.* Cell, 1990. **61**(1): p. 49-59.
841. Katagiri, T., et al., *Identification of a BMP-responsive element in Id1, the gene for inhibition of myogenesis.* Genes Cells, 2002. **7**(9): p. 949-60.
842. Bois, P.R., et al., *FoxO1a-cyclic GMP-dependent kinase I interactions orchestrate myoblast fusion.* Mol Cell Biol, 2005. **25**(17): p. 7645-56.
843. Liang, M.H., J.R. Wendland, and D.M. Chuang, *Lithium inhibits Smad3/4 transactivation via increased CREB activity induced by enhanced PKA and AKT signaling.* Mol Cell Neurosci, 2008. **37**(3): p. 440-53.
844. Schiller, M., F. Verrecchia, and A. Mauviel, *Cyclic adenosine 3',5'-monophosphate-elevating agents inhibit transforming growth factor-beta-induced SMAD3/4-dependent transcription via a protein kinase A-dependent mechanism.* Oncogene, 2003. **22**(55): p. 8881-90.
845. Francis, S.H., et al., *Mechanisms of autoinhibition in cyclic nucleotide-dependent protein kinases.* Front Biosci, 2002. **7**: p. d580-92.
846. Orstavik, S., et al., *Characterization of the human gene encoding the type I alpha and type I beta cGMP-dependent protein kinase (PRKG1).* Genomics, 1997. **42**(2): p. 311-8.
847. Tournay, O. and R. Benezra, *Transcription of the dominant-negative helix-loop-helix protein Id1 is regulated by a protein complex containing the immediate-early response gene Egr-1.* Mol Cell Biol, 1996. **16**(5): p. 2418-30.
848. Wahab, N.A. and R.M. Mason, *A critical look at growth factors and epithelial-to-mesenchymal transition in the adult kidney. Interrelationships between growth factors that regulate EMT in the adult kidney.* Nephron Exp Nephrol, 2006. **104**(4): p. e129-34.
849. Novina, C.D., V. Cheriyath, and A.L. Roy, *Regulation of TFII-I activity by phosphorylation.* J Biol Chem, 1998. **273**(50): p. 33443-8.
850. Cheriyath, V., Z.P. Desgranges, and A.L. Roy, *c-Src-dependent transcriptional activation of TFII-I.* J Biol Chem, 2002. **277**(25): p. 22798-805.
851. Kim, D.W., et al., *TFII-I enhances activation of the c-fos promoter through interactions with upstream elements.* Mol Cell Biol, 1998. **18**(6): p. 3310-20.
852. Cheriyath, V. and A.L. Roy, *Alternatively spliced isoforms of TFII-I. Complex formation, nuclear translocation, and differential gene regulation.* J Biol Chem, 2000. **275**(34): p. 26300-8.
853. Mobley, C.M. and L. Sealy, *The Rous sarcoma virus long terminal repeat promoter is regulated by TFII-I.* J Virol, 2000. **74**(14): p. 6511-9.
854. Roy, A.L., *Transcription factor TFII-I conducts a cytoplasmic orchestra.* ACS Chem Biol, 2006. **1**(10): p. 619-22.
855. Cheriyath, V. and A.L. Roy, *Structure-function analysis of TFII-I. Roles of the N-terminal end, basic region, and I-repeats.* J Biol Chem, 2001. **276**(11): p. 8377-83.
856. Browning, D.D., N.D. Windes, and R.D. Ye, *Activation of p38 mitogen-activated protein kinase by lipopolysaccharide in human neutrophils requires nitric oxide-dependent cGMP accumulation.* J Biol Chem, 1999. **274**(1): p. 537-42.
857. Inoue, A., et al., *Stimulation by C-type natriuretic peptide of the differentiation of clonal osteoblastic MC3T3-E1 cells.* Biochem Biophys Res Commun, 1996. **221**(3): p. 703-7.
858. Inoue, A., et al., *Reciprocal regulation by cyclic nucleotides of the differentiation of rat osteoblast-like cells and mineralization of nodules.* Biochem Biophys Res Commun, 1995. **215**(3): p. 1104-10.
859. Hemnes, A.R. and H.C. Champion, *Sildenafil, a PDE5 inhibitor, in the treatment of pulmonary hypertension.* Expert Rev Cardiovasc Ther, 2006. **4**(3): p. 293-300.
860. Seemann, P., et al., *Activating and deactivating mutations in the receptor interaction site of GDF5 cause symphalangism or brachydactyly type A2.* J Clin Invest, 2005. **115**(9): p. 2373-81.
861. Sieber, C., et al., *Monomeric and dimeric GDF-5 show equal type I receptor binding and oligomerization capability and have the same biological activity.* Biol Chem, 2006. **387**(4): p. 451-60.

9 Appendix

Abbreviations

Terms

ab	antibody
abs	absorption
ActRI	Activin receptor I
ActRII	Activin receptor II
ALK	Activin-like kinase
ALP	alkaline phosphatase
AMH	anti-Muellerian hormone
ANP	atrial natriuretic peptide
ATP	adenosine-5`-triphosphate
BAMBI	BMP and activin membrane-bound inhibitor
β-gal	β-galactosidase
BISC	BMP-induced signaling complex
BMP	bone morphogenetic protein
BNP	brain natriuretic peptide
BRAM-1	BMP receptor-associated molecule 1
BRE	BMP response element
BRI	BMP receptor I
BRII	BMP receptor II
BTK	Brutons tyrosine kinase
c	cytoplasm
Cam	calmodulin
CamKII	calmodulin-dependent kinase II
cAMP	cyclic adenosine 3', 5'-monophosphate
Cav-1	Caveolin-1
CBP	CREB binding protein
CCP	clathrin-coated pits
CDK	cyclin-dependent kinase
C. elegans	*Caenorhabditis elegans*
cGKI	cGMP-dependent kinase I
cGKII	cGMP-dependent kinase II
cGMP	cyclic guanosine 3', 5'-monophosphate
CHIP	Hsc70 interacting protein
CNP	C-type natriuretic peptide
co-Smad	common-mediator Smad
CR	chordin-like region
I-Smad	inhibitory Smad
IRAG	inositol 1,4,5-trisphosphate receptor (IP_3R)-associated cGMP kinase substrate
IP_3	inositol 1,4,5-trisphosphate
IP_3R	inositol 1,4,5-trisphosphate receptor
JNK	c-jun N-terminal kinase
JPS	juvenile polyposis syndrome
LIF	leukemia inhibitory factor
LIMK-1	LIM kinase 1
LF	long form
MAPK	mitogen-activated protein kinase
MAPKK	MAPK kinase
MAPKKK	MAPK kinase kinase
MBP	maltose binding protein
MEK	MAP Erk kinase
mES cell	mouse embryonic stem cell
MH domain	MAD homology domain
MLC	myosin light chain
MLCK	myosin light chain kinase
MLCP	myosin light chain phosphatase
MW	molecular weight
n	nucleus
NES	nuclear export signal
NF-κB	nuclear factor κ B
NGF	nerve growth factor
NLS	nuclear localization sequence
NOS	nitric oxide synthase
NO	nitric oxide
PAH	pulmonary arterial hypertension
PAVSMC	pulmonary arterial vascular smooth muscle cell
PDE	phosphodiesterase
PDGF	platelet-derived growth factor
PDP	pyruvate dehydrogenase phosphatase
PFC	preformed complex
pGS	particulate guanylyl cyclase
PKA	protein kinase A

CRE	cAMP response element
CREB	CRE binding protein
CtBP	C-terminal binding protein
Dlx	distal-less
D. melanogaster	*Drosophila melanogaster*
DNA	2-deoxyribonucleic acid
DPP	decapentaplegic
DRM	detergent-resistance membrane
ds	double strand
ECM	extracellular matrix
E. coli	*Escherichia coli*
EGF	epidermal growth factor
eGFP	enhanced green fluorescence protein
Egr-1	early growth response gene 1
Erk	extracellular signal-regulated kinase
ES cell	embryonic stem cell
FGF	fibroblast growth factor
Fig	figure
FOP	fibrodysplasia ossificans progressive
GADD-34	growth arrest and DNA damage-inducible protein
GC	guanylyl cyclase
sGC	soluble guanylyl cyclase
pGC	particulate guanylyl cyclase
GDF	growth and differentiation factor
GFP	green fluorescence protein
GS-box	glycine/serine -rich box
GSK-3	glycogen synthase kinase 3
GST	glutathione S transferase
HA	haemagglutinin
HAT	histone acetylase
HDAC	histone deacetylase
hES cell	human embryonic stem cell
HGF	hepatocyte growth factor
HHT	hereditary hemorrhagic telangiectasia
Id1	inhibitor of differentiation 1
IGF	insulin-like growth factor
IL	interleukin
INM	inner nuclear membrane
PKB	protein kinase B
PKC	protein kinase C
PKD	protein kinase D
PKG	protein kinase G
PP1	protein phosphatase
PP2A	protein phosphatase 2A
Rack-1	receptor for activated C-kinase
RGM	repulsive guidance molecule
RISC	RNA-induced silencing complex
RNA	ribonucleic acid
RNAi	RNA interference
R-Smad	receptor-regulated Smad
SAD	Smad activation domain
SARA	Smad anchor for receptor activation
SBE	Smad binding element
SCP	small C-terminal domain phosphatase
SF	short form
sGC	soluble guanylyl cyclase
shRNA	short-hairpin RNA
SID	Smad interaction domain
SIM	Smad interacting motif
siRNA	small interfering RNA
SMC	smooth muscle cell
Smurf	Smad ubiquitin regulatory factor
SOST	sclerostin
ss	single strand
SUMO-1	small ubiquitin-like modifier
TAB-1	TAK binding protein 1
TAK-1	TGFβ activated kinase 1
TC	truncation
TGFβ	transforming growth factor β
TNFα	tumor necrosis factor α
Trb-3	tribbles-like protein 3
Trk	tropomyosin-related kinase
Tsg	twisted gastrulation
VASP	vasodilator-stimulated phospho-protein
VSMC	vascular smooth muscle cell
XIAP	X-linked inhibitor of apoptosis

Chemicals/Material/Methods

8-Br-cGMP	8-bromo-cyclic guanosine monophosphate
A	adenine
ATP	adenosintriphosphate
BCA	bichinonic acid
BSA	bovine serum albumin
C	cytosine
cDNA	copy DNA
ChIP	chromatin immunoprecipitation
CMV	cytomegali virus
co-IP	co-immunoprecipitation
DMEM	Dulbecco´s modified Eagle medium
DMS	dimethyl suberimidate
DMSO	dimethylsulfoxide
dNTP	desoxyribonucleotide triphosphate
DTT	dithiothreitol
ECL	enhanced chemiluminescence
EDTA	ethylenediaminetetraacetic acid
EtBr	ethidium bromide
FBS	fetal bovine serum
G	guanine
HAoSMC	human aortic smooth muscle cell
HRP	horseradish peroxidase
IB	immunoblot
IBMX	isobutylmethylxanthine
IF	immunofluorescence
IgG	immunoglobuline G
IP	immunoprecipitation
IPTG	isopropyl β-D-1-thiogalactopyranoside
LB	Luria-Bertani
luc	luciferase
MMLV	Moloney murine leukemia virus
mRNA	messenger RNA
OD	optical density
PAGE	polyacrylamide gelelectrophoresis
PBS	phosphate-buffered saline
PCR	polymerase chain reaction
PEI	polyethylenimine
pI	isoelectric point
PI	protease inhibitor
PPI	protein phosphatase inhibitor
PMSF	phenylmethylsulfonylfluoride
^{32}P	radioactively-labelled P
SDS	sodium dodecyl sulfate
SOB	super optimal broth
SOC	super optimal broth, catabolit repression
SV40	simian virus 40
T	thymin
TBS	Tris-buffered saline
TCA	trichloric acid
v/v	volume per volume
w/v	weight per volume

Units

aa	amino acid
bp	base pair
℃	degree Celsius
d	day
fg	femtogram
g	gram
hr	hour
kb	kilobase
kD	kiloDalton
kV	kiloVolt
l	liter
µg	microgram
µCi	microCurie
mg	milligram
msec	millisecond
ml	milliliter
mM	millimolar
min	minute
M	molar
nM	nanomolar
%	percent
pM	picomolar
RLU	relative light units
rpm	rounds per minute
RT	room temperature
sec	second
U	unit
V	volt

Sequences

Protein sequences of the human proteins analyzed in this study and their accession numbers according to the National Center for Biotechnology Information (NCBI, http://www.ncbi.nlm.nih.gov).

BRIa; NP 004320

```
   1 mpqlyiyirl lgaylfiisr vqgqnldsml hgtgmksdsd qkksengvtl apedtlpflk
  61 cycsghcpdd ainntcitng hcfaiieedd qgettlasgc mkyegsdfqc kdspkaqlrr
 121 tieccrtnlc nqylqptlpp vvigpffdgs irwlvllism avciiamiif sscfcykhyc
 181 ksissrrryn rdleqdeafi pvgeslkdli dqsqssgsgs glpllvqrti akqiqmvrqv
 241 gkgrygevwm gkwrgekvav kvfftteeas wfreteiyqt vlmrhenilg fiaadikgtg
 301 swtqlylitd yhengslydf lkcatldtra llklaysaac glchlhteiy gtqgkpaiah
 361 rdlksknili kkngscciad lglavkfnsd tnevdvplnt rvgtkrymap evldeslnkn
 421 hfqpyimadi ysfgliiwem arrcitggiv eeyqlpyynm vpsdpsyedm revvcvkrlr
 481 pivsnrwnsd eclravlklm secwahnpas rltalrikkt lakmvesqdv ki
```

BRIb; NP 001194

```
   1 mllrsagkln vgtkkedges taptprpkvl rckchhhcpe dsvnnicstd gycftmieed
  61 dsglpvvtsg clglegsdfq crdtpiphqr rsiecctern ecnkdlhptl pplknrdfvd
 121 gpihhralli svtvcslllv liilfcyfry krqetrprys igleqdetyi ppgeslrdli
 181 eqsqssgsgs glpllvqrti akqiqmvkqi gkgrygevwm gkwrgekvav kvfftteeas
 241 wfreteiyqt vlmrhenilg fiaadikgtg swtqlylitd yhengslydy lksttldaks
 301 mlklayssvs glchlhteif stqgkpaiah rdlksknilv kkngtcciad lglavkfisd
 361 tnevdippnt rvgtkrympp evldeslnrn hfqsyimadm ysfglilwev arrcvsggiv
 421 eeyqlpyhdl vpsdpsyedm reivcikklr psfpnrwssd eclrqmgklm tecwahnpas
 481 rltalrvkkt lakmsesqdi kl
```

BRII; NP 001195

```
   1 mtsslqrpwr vpwlpwtill vstaaasqnq erlcafkdpy qqdlgigesr ishengtilc
  61 skgstcyglw ekskgdinlv kqgcwshigd pqechyeecv vtttppsiqn gtyrfcccst
 121 dlcnvnften fpppdttpls pphsfnrdet iiialasvsv lavlivalcf gyrmltgdrk
 181 qglhsmnmme aaasepsldl dnlkllelig rgrygavykg slderpvavk vfsfanrqnf
 241 inekniyrvp lmehdniarf ivgdervtad grmeyllvme yypngslcky lslhtsdwvs
 301 scrlahsvtr glaylhtelp rgdhykpais hrdlnsrnvl vkndgtcvis dfglsmrltg
 361 nrlvrpgeed naaisevgti rymapevleg avnlrdcesa lkqvdmyalg liyweifmrc
 421 tdlfpgesvp eyqmafqtev gnhptfedmq vlvsrekqrp kfpeawkens lavrslketi
 481 edcwdqdaea rltaqcaeer maelmmiwer nksvsptvnp mstamqnern lshnrrvpki
 541 gpypdyssss yiedsihhtd sivknisseh smsstpltig eknrnsinye rqqaqarips
 601 petsvtslst nttttnttgl tpstgmttis empypdetnl httnvaqsig ptpvclqlte
 661 edletnkldp kevdknlkes sdenlmehsl kqfsgpdpls stsssllypl iklaveatgq
 721 qdftqtangq aclipdvlpt qiyplpkqqn lpkrptslpl ntknstkepr lkfgskhksn
 781 lkqvetgvak mntinaaeph vvtvtmngva grnhsvnsha attqyangtv lsgqttnivt
 841 hraqemlqnq figedtrlni nsspdehepl lrreqqaghd egvldrlvdr rerpleggrt
 901 nsnnnnsnpc seqdvlaqgv pstaadpgps kprraqrpns ldlsatnvld gssiqigest
 961 qdgksgsgek ikkrvktpys lkrwrpstwv istesldcev nnngsnravh sksstavyla
1021 eggtattmvs kdigmncl
```

Smad1; NP 005891

```
   1 mnvtslfsft spavkrllgw kqgdeeekwa ekavdalvkk lkkkkgamee lekalscpgq
  61 psncvtiprs ldgrlqvshr kglphviycr vwrwpdlqsh helkplecce fpfgskqkev
 121 cinpyhykrv espvlppvlv prhseynpqh sllaqfrnlg qnephmplna tfpdsfqqpn
 181 shpfphspns sypnspgsss styphsptss dpgspfqmpa dtpppaylpp edpmtqdgsq
 241 pmdtnmmapp lpseinrgdv qavayeepkh wcsivyyeln nrvgeafhas stsvlvdgft
 301 dpsnnknrfc lgllsnvnrn stientrrhi gkgvhlyyvg gevyaeclsd ssifvqsrnc
 361 nyhhgfhptt vckipsgcsl kifnnqefaq llaqsvnhgf etvyeltkmc tirmsfvkgw
 421 gaeyhrqdvt stpcwieihl hgplqwldkv ltqmgsphnp issvs
```

Smad5; NP 005894

```
   1 mtsmaslfsf tspavkrllg wkqgdeeekw aekavdalvk klkkkkgame elekalsspg
  61 qpskcvtipr sldgrlqvsh rkglphviyc rvwrwpdlqs hhelkpldic efpfgskqke
 121 vcinpyhykr vespvlppvl vprhnefnpq hsllvqfrnl shnephmpqn atfpdsfhqp
 181 nntpfplspn spyppspass typnspassg pgspfqlpad tpppaymppd dqmgqdnsqp
```

```
241 mdtsnnmipq impsissrdv qpvayeepkh wcsivyyeln nrvgeafhas stsvlvdgft
301 dpsnnksrfc lgllsnvnrn stientrrhi gkgvhlyyvg gevyaeclsd ssifvqsrnc
361 nfhhgfhptt vckipsscsl kifnnqefaq llaqsvnhgf eavyeltkmc tirmsfvkgw
421 gaeyhrqdvt stpcwieihl hgplqwldkv ltqmgsplnp issvs
```

Smad4; NP 005350

```
  1 mdnmsitntp tsndaclsiv hslmchrqgg esetfakrai eslvkklkek kdeldslita
 61 ittngahpsk cvtiqrtldg rlqvagrkgf phviyarlwr wpdlhknelk hvkycqyafd
121 lkcdsvcvnp yhyervvspg idlsgltlqs napssmmvkd eyvhdfegqp slsteghsiq
181 tiqhppsnra stetystpal lapsesnats tanfpnipva stsqpasilg gshsegllqi
241 asgpqpgqqq ngftgqpaty hhnstttwtg srtapytpnl phhqnghlqh hppmpphpgh
301 ywpvhnelaf qppisnhpap eywcsiayfe mdvqvgetfk vpsscpivtv dgyvdpsggd
361 rfclgqlsnv hrteaierar lhigkgvqle ckgegdvwvr clsdhavfvq syyldreagr
421 apgdavhkiy psayikvfdl rqchrqmqqq aataqaaaaa qaaavagnip gpgsvggiap
481 aislsaaagi gvddlrrlci lrmsfvkgwg pdyprqsike tpcwieihlh ralqlldevl
541 htmpiadpqp ld
```

cGKIα; NP 001091082

```
  1 mseleedfak ilmlkeerik elekrlseke eeiqelkrkl hkcqsvlpvp sthigprttr
 61 aqgisaepqt yrsfhdlrqa frkftksers kdlikeaild ndfmknlels qiqeivdcmy
121 pveygkdsci ikegdvgslv yvmedgkvev tkegvklctm gpgkvfgela ilynctrtat
181 vktlvnvklw aidrqcfqti mmrtglikht eymeflksvp tfqslpeeil skladvleet
241 hyengeyiir qgargdtffi iskgtvnvtr edspsedpvf lrtlgkgdwf gekalqgedv
301 rtanviaaea vtclvidrds fkhliggldd vsnkayedae akakyeaeaa ffanlklsdf
361 niidtlgvgg fgrvelvqlk seesktfamk ilkkrhivdt rqqehirsek qimqgahsdf
421 ivrlyrtfkd skylymlmea clggelwtil rdrgsfedst trfytacvve afaylhskgi
481 iyrdlkpenl ildhrgyakl vdfgfakkig fgkktwtfcg tpeyvapeii lnkghdisad
541 ywslgilmye lltgsppfsg pdpmktynii lrgidmiefp kkiaknaanl ikklcrdnps
601 erlgnlkngv kdiqkhkwfe gfnweglrkg tltppiipsv asptdtsnfd sfpedndepp
661 pddnsgwdid f
```

cGKIβ; NP 006249

```
  1 mgtlrdlqya lqekieelrq rdalidelel eldqkdeliq klqneldkyr svirpatqqa
 61 qkqsastlqg eprtkrqais aeptafdiqd lshvtlpfyp kspqskdlik eaildndfmk
121 nlelsqiqei vdcmypveyg kdsciikegd vgslvyvmed gkvevtkegv klctmgpgkv
181 fgelailync trtatvktlv nvklwaidrq cfqtimmrtg likhteymef lksvptfqsl
241 peeilsklad vleethyeng eyiirqgarg dtffiiskgt vnvtredsps edpvflrtlg
301 kgdwfgekal qgedvrtanv iaaeavtclv idrdsfkhli ggldvsnka yedaeakaky
361 eaeaaffanl klsdfniidt lgvggfgrve lvqlkseesk tfamkilkkr hivdtrqqeh
421 irsekqimqg ahsdfivrly rtfkdskyly mlmeaclgge lwtilrdrgs fedsttrfyt
481 acvveafayl hskgiiyrdl kpenlildhr gyaklvdfgf akkigfgkkt wtfcgtpeyv
541 apeiilnkgh disadywslg ilmyelltgs ppfsgpdpmk tyniilrgid miefpkkiak
601 naanlikklc rdnpserlgn lkngvkdiqk hkwfegfnwe glrkgtltpp iipsvasptd
661 tsnfdsfped ndepppddns gwdidf
```

TFII-IΔ; NP 001509

```
  1 maqvamstlp vedeessesr mvvtflmsal esmckelaks kaevaciavy etdvfvvgte
 61 rgrafvntrk dfqkdfvkyc veeeekaaem hkmksttqan rmsvdaveie tlrktvedyf
121 cfcygkalgk stvvpvpyek mlrdqsavvv qglpegvafk hpenydlatl kwilenkagi
181 sfiikrpfle pkkhvggrvm vtdadrsils pggscgpikv kteptedsgi slemaavtvk
241 eesedpdyyq yniqgshhss egnegtemev paedddyspp skrpkanelp qppvpepana
301 gkrkvrefnf ekwnaritdl rkqveelfer kyaqaikakg pvtipyplfq shvedlyveg
361 lpegipfrrp stygiprler illakerirf vikkhellns tredlqldkp asgvkeewya
421 ritklrkmvd qlfckkfaea lgsteakavp yqkfeahpnd lyveglpeni pfrspswygi
481 prlekiiqvg nrikfvikrp ellthsttev tqprtntpvk edwnvritkl rkqveeifnl
541 kfaqalglte avkvpypvfe snpeflyveg lpegipfrsp twfgiprler ivrgsnkikf
601 vvkkpelvis ylppgmaski ntkalqspkr prspgsnskv peievtvegp nnnnpqtsav
661 rtptqtngsn vpfkprgref sfeawnakit dlkqkvenlf nekcgealgl kqavkvpfal
721 fesfpedfyv eglpegvpfr rpstfgiprl ekilrnkaki kfiikkpemf etaikestss
781 kspprkinss pnvnttasgv edlniiqvti pdddnerlsk vekarqlreq vndlfsrkfg
841 eaigmgfpvk vpyrkitinp gcvvvdgmpp gvsfkapsyl eissmrrild saefikftvi
901 rpfpglvinn qlvdqseseg pviqesaeps qlevpateei ketdgssqik qepdptw
```

Nucleotide sequences of the used mouse-specific oligonucleotides and sh/siRNAs.

Id1

forward: 5′-AGGTGAAGCTCCTGCTCTACGA-3′

reverse: 5′-CAGGATCTCCACCTTGCTCACT-3′

ALP

forward: 5′-AATCGGAACAACCTGACTGACC-3′

reverse: 5′-TCCTTCCACCAGCAAGAAGAA-3′

cGKI

forward: 5′-GGGGTTCGTTTGAAGACTCA-3′

reverse: 5′-AGGATGAGATTCTCCGGCTT-3′

TFII-I

forward: 5´-CCTGCCGAAGATGAAGAGTC-3´

reverse: 5´-CCTCTTTCGGTTCCAACAAC-3´

β-actin

forward: 5′-CGGAACGCGTCATTGCC-3′

reverse: 5′-ACCCACACTGTGCCCATCTA-3′

Id1 promoter

forward: 5′-GGAGCGGAGAATGCTCCAG-3′

reverse: 5′-GAAGGCCTCCGAGCAAGC-3′

sh-cGKI

5′-CACCGGGACGATGTTTCTAACAAACGAATTTGTTAGAAACATCGTCC-3′

sh-nt

5′-AGACGTTTCACGTCGGAGA-3′

si-cGKI

forward: 5´-AAGCCGGAGAATCTCATCCTACCTGTCTC-3´

reverse: 5´-AATAGGATGAGATTCTCCGGCCCTGTCTC-3´

si-GFP

purchased from Ambion, SilencerTM siRNA construction kit

cGKIβ cloning

forward: 5'-CGCGGATCCGCCGCCATGGGCACCTTGCGGGATTTAC-3'

reverse: 5'-CGCGGATCCTTAGAAGTCTATATCCCATCC-3'

Acknowledgement - Danksagung

Ich möchte Prof. Dr. Petra Knaus sehr danken für die Möglichkeit, diese Arbeit anfertigen zu können. Besonders danken möchte ich Dir für den Freiraum in Forschung und Laboralltag, durch den ich wachsen konnte, sowie für Deine stete Motivation, gerade in Situationen, in denen es erforderlich war, positiv in die Zukunft zu blicken. Die Zusammenarbeit mir Dir ist etwas Besonderes gewesen!

Prof. Dr. Otmar Huber möchte ich sehr herzlich für die Übernahme des Zweitgutachtens danken, obgleich doch alles sehr plötzlich geschehen musste, sowie für die gute und erfolgreiche Kollaboration.

Ebenfalls herzlich danken möchte ich Prof. Dr. Walter Sebald für die gute Zeit am Lehrstuhl für Physiologische Chemie II in Würzburg und für die interessanten Diskussionen.

I like to thank Dr. Renate Pilz for many fruitful discussions. I´m especially thankful for your support during the last months and I´m really looking forward to our collaboration during the next years!

Many thanks also to Prof. Dr. Yoav Henis and Barak Marom for a good collaboration and helpful comments about my work.

Ebenfalls möchte ich Prof. Dr. Oliver Eickelberg danken für die gute Zusammenarbeit sowie für viele gute Ratschläge.

Desweiteren gilt mein Dank allen ehemaligen Würzburger Kollegen. Gesondert bedanken möchte ich mich bei Prof. Dr. Thomas Müller, Dr. Joachim Nickel, Dr. Sylke Hassel, Dr. Martin Roth, Dr. Marei Sammar, Wolfgang Hädelt und Uli Borst, die stets ein offenes Ohr für mich hatten/haben sowie den einen oder anderen guten Ratschlag.

Ein Dankeschön geht ebenfalls an die Kollegen des Berliner Labors sowie des gesamten Otto-Hahn-Baus. Katharina Hoffmann, Gisela Wendel und Gerburg Schwärzer möchte ich besonders danken dafür, dass ihr mir fast immer mit Rat und Tat zur Seite standet. Ein herzliches Danke!

Dr. Jörg Weiske gilt grosser Dank für die grossartige Zusammenarbeit und die damit verbundenen interessanten Diskussionen und Hilfestellungen.

Im Speziellen danken möchte ich ehemaligen Kollegen und jetzt sehr guten Freunden. Ohne Dr. Anke Hartung, Dr. Luiza Bengtsson, Dr. Claudia Keil, Valeska Wenzel, Simone Hillgärtner, Manuel Bauer, Johannes Schnitzer und Verena Ezerski wäre ich nicht das, was ich jetzt bin! Viele Gespräche wissenschaftlicher und privater Natur waren mir stets eine unschätzbare Hilfe und haben mich in meinen Vorhaben unterstützt. Keine dieser Freundschaften möchte ich je missen! DANKE!

Auch meinen Freunden Dr. Nadja Kroha, Robin Kroha und Steffen Reichert muss ich von Herzen danken, für all die guten und aufmunternden Gespräche und die vielen gemeinsamen Unternehmungen, die mir nach manchen frustrierenden Labortagen wieder klare Sicht aufs Wesentliche gegeben haben.

Der grösste Dank gilt meinem Mann Hendrik Montag-Schwappacher, meinen Eltern Erika und Heinz Schwappacher und meinen Schwestern Ulla Schwappacher-Korn und Britta Schwappacher-Göttge und deren Familien. Die grossartigsten Menschen der Welt um sich zu haben, erleichtert so manche Hürde. Danke für alles und ich bin sehr, sehr froh, dass es Euch gibt.

Curriculum vitae - Lebenslauf

Der Lebenslauf ist in der Online-Version aus Gründen des Datenschutzes nicht enthalten.

Publication list - Schriftenverzeichnis

Publications

Schwappacher R., Weiske J., Ezerski V., Huber O., Knaus P.: *Novel crosstalk to BMP signaling: cGMP-dependent protein kinase I modulates BMP receptor and Smad activity.*
submitted

Bengtsson L.*, Schwappacher R.*, Roth M., Hassel S., Knaus P.: *PP2A regulates BMP signaling by interacting with BMP receptor complexes and by dephosphorylating linker region of Smad1/5/8.*
*authors contributed equally
in revision

Sieber C., Plöger F., Schwappacher R., Bechthold R., Hanke M., Kawai S., Mouler Rechtman M., Henis Y.I., Pohl J., Knaus P.: *Monomeric and dimeric GDF-5 show equal type I receptor binding and oligomerization capability and have the same biological activity.* Biol Chem 2006 Apr; 387:451-460. 2006

Seemann P., Schwappacher, R., Kjaer K. W., Krakow D., Lehmann K., Dawson K., Stricker S., Pohl J., Plöger F., Staub E., Nickel J., Knaus P., Mundlos S.: *Activating and deactivating mutations in the receptor interaction site of GDF5 cause symphalangism or Brachydactyly Type A2.* J Clin Invest 2005 Sep 1;115(9):2373-2381. 2005

Oral presentations

Schwappacher R.: *Characterization of BMP type II receptor-associated proteins*. XX. Paulo Symposium "Targeting and activation of TGFβ Family growth and differentiation factors", **Helsinki**, Finland, 2005

Schwappacher R.: *Characterization of BMP type II receptor-associated proteins* , Annual Retreat of the International Graduate Program „Molecular Biology and Medicine of the Lung", **Rauischholzhausen**/**Giessen**, Germany, 2003

Poster presentations

Heining, E., Schwappacher R., Weiske J., Ezerski V., Huber O, Knaus P.: *cGMP-dependent protein kinase I promotes BMP signaling.* TGFβ Meeting, **Leiden**, The Netherlands, 2008

Schwappacher R., Weiske J., Ezerski V., Huber O, Knaus P.: *cGMP-dependent protein kinase I promotes BMP signaling.* 3rd International Conference on "cGMP Generators, Effectors and Therapeutic Implications", **Dresden**, Germany, 2007

Schwappacher R., Weiske J., Ezerski V., Huber O, Knaus P.: *cGMP-dependent protein kinase I promotes BMP signaling.* TGFβ Meeting, **Uppsala**, Sweden, 2007

Sieber C., Seemann P., Schwappacher R., Plöger F., Henis Y.I., Pohl J., Mundlos S., Knaus P.: *GDF5 signaling and bone formation: Molecular characterization of GDF-5 mutants.* FEBS conference "Molecules in Health and Disease", **Istanbul**, Turkey, 2006

Schwappacher R., Hassel S., Souchelnytskyi S., Knaus P.: *Biochemical characterization of a protein kinase acting along BMP-2 signaling cascade.* Gordon Research Conference „Growth factor signaling", **New London**, Connecticut, USA, 2006

Bengtsson L., Schwappacher R., Roth M., Hassel S., Knaus P.: *PP2A B-subunit attenuates Smad-mediated BMP signaling by interacting with BMP type I and type II receptors.* Gordon Research Conference „Growth factor signaling", **New London**, Connecticut, USA, 2006

Schwappacher R., Hassel S., Krecisz A., Schnitzer J.K., Roth M., Souchelnytskyi S., Eickelberg O., Knaus P.: *Characterization of BMP type II receptor-associated proteins*. Annual Meeting of the German Society for Biochemistry and Molecular Biology, **Berlin**, Germany, 2005

Schwappacher R., Hassel S., Krecisz A., Schnitzer J.K., Roth M., Souchelnytskyi S., Eickelberg O., Knaus P.: *Characterization of BMP type II receptor-associated proteins*. XX. Paulo Symposium "Targeting and activation of TGF-β Family growth and differentiation factors", **Helsinki**, Finland, 2005

Schwappacher R., Hassel S., Krecisz A., Schnitzer J.K., Roth M., Souchelnytskyi S., Eickelberg O., Knaus P.: *Characterization of BMP type II receptor-associated proteins*. Annual Meeting of the German Society for Cell Biology DGZ, **Heidelberg**, Germany, 2005

Schwappacher R., Hassel S., Roth M., Scholz S., Souchelnytskyi S., Knaus P.: *Characterization of BMP type II receptor-associated proteins*. International Conference „Strategies in Tissue Engineering", **Würzburg**, Germany, 2004

Schwappacher R., Hassel S., Roth M., Scholz S., Souchelnytskyi S., Knaus P.: *Characterization of BMP type II receptor-associated proteins*. Annual Meeting of the German Society for Cell Biology DGZ, **Berlin**, Germany, 2004

Hassel S., Hartung A., Schwappacher R., Schmitt S., Nohe A., Souchelnytskyi S., Henis Y.I., Sebald W., Knaus P.: *BMP receptor oligomerization determines the initiation of different signaling cascades.* FASEB conference "The TGFβ Superfamily: Signaling & Development", **Tucson**, Arozona, USA, 2003

Declaration - Erklärung

Hiermit erkläre ich ehrenwörtlich, dass ich die vorliegende Dissertation in allen Teilen selbständig angefertigt und keine anderen als die von mir angegebenen Quellen und Hilfsmittel verwendet habe.

Ich erkläre weiterhin, dass ich diese Dissertation weder in gleicher noch in ähnlicher Form in anderen Prüfungsverfahren vorgelegt habe.

Ich habe ausser den mit dem Zustellungsgesuch urkundlich vorgelegten Graden keine weiteren akademischen Grade erworben oder zu erwerben versucht.

Berlin, im September 2008